RIVER RESPONSE TO LATE QUATERNARY ENVIRONMENTAL CHANGE IN CORSICA

Suzanne Hewitt

Submitted in accordance with the requirements for the degree of Doctor of Philosophy

The University of Leeds
School of Geography

August 2002

The candidate confirms that the work submitted is her own and that appropriate credit has been given where reference has been made to the work of others.

ACKNOWLEDGEMENTS

Many people have helped me to complete this thesis over the last four years by providing laboratory, technical, fieldwork and emotional support. Firstly I would like to thank Jamie Woodward and Mark Macklin for presenting this opportunity to research Mediterranean Quaternary Environments and for their supervision throughout the Ph.D. I am also very grateful to the Natural Environment Research Council for the studentship. A big thanks to Odette Conchon too, who provided me with her thesis at the beginning of the project together with many words of encouragement for working in Corsica.

I am indebted to Susan Ivy-Ochs and Peter Kubik of ETH in Zürich, firstly for accepting my own invitation to prepare samples for cosmogenic nuclide dating in their laboratories, secondly for providing me with so much of their time and thirdly for imparting with so much subject knowledge. I would also like to thank all the other researchers and technicians on the particle physics floor for making me feel so welcome. I must also thank Mark Bateman of the University of Sheffield for allowing me to use the facilities of the SCIDR to prepare my samples for luminescence dating and for all his guidance, patience and analysis. Further sample analysis was conducted at the University of East Anglia under the supervision of Barbara Maher. I thank her kindly for the use of the equipment and help in the Environmental Magnetism laboratory. I also wish to thank the others that occupied the laboratory for their time and help as a result of my almost continuous bombardment of questions. Bill Perkins also conducted several analyses for me at the University of Aberystwyth, so thank you. I must also thank Mark Pegden in the Mining and Mineral Engineering department at the University of Leeds for cutting and crushing all my granite rocks....quite a job! The lab work I have conducted at the School of Geography has been aided by David Ashley, Linda Gregorash, and Rachel Gasior. I am especially grateful to David for all his help, enthusiasm and encouragement over the past few years.

All this lab work would not have been possible without the fieldtrips to Corsica! I thank Jamie and Mark for their help, Vicky Parry for being an all round ab fab fieldtrip buddie and Glenn Maas for giving up his time and assisting with the surveying and mapping and all his jokes! On the technical side, I wish to thank David Appleyard in graphics for all his hard work in producing many of my figures and Mike Kirkby who helped me with the snowpack model. I would also like to thank Sim Reaney for always having the right answer when I had a computer query.

So many academics and fellow postgraduates have enhanced this Ph.D. experience and helped me through those 'not so great' times. I wish to thank Mike Kirkby, Tavi Murray and Chronis Tzedakis for their words of wisdom and encouragement. I owe Rob, Claire, Steve, Gary, Frank, Sim, Lia and Sue a huge thank you for their support. Ruth Schofield and Dave Moreton have both been superstars. Ruth has provided me with her guidance and patience and Dave has been a wonderful editor and a positive thinker. I would also like to say a special thank you to Crewenna for her friendship and support. I wish to thank my friends at home for their continuous encouragement and cheeriness, Laura, Kelly, Becky, Jennie, Steve H., Richard, Ben, Steve S., Nicky, and Martin and also James and Vicky in Leeds.

My mum and dad have helped me in so many ways that I owe a lot of my achievement to them. They are the best and I thank them both so much. I also thank my brother, David for his support and providing me with the opportunity to escape spontaneously to Australia one Christmas! Finally I would like to thank Glenn for all he has done for me over the past two years. His love, help and encouragement has been incessant.

ABSTRACT

Mediterranean river systems are particularly sensitive to environmental change and often provide good archives to reconstruct fluvial histories. This study investigates river response to environmental change in two steepland river catchments in Corsica. Late Pleistocene alluviation and pedogenic weathering is explored within the Tavignano River basin (~775 km^2) and river response to Late Holocene (including Little Ice Age) environmental change is examined in the Figarella catchment (~132 km^2). A range of geochronological controls has been employed including optically stimulated luminescence (OSL) dating, a profile development index (PDI) determined from pedogenic properties, and lichenometry. This study also examines the potential of a relatively new absolute dating technique, terrestrial *in-situ* cosmogenic nuclide dating, for establishing the timing of recent glacial activity in Corsica.

Two cosmogenic ^{10}Be nuclide exposure ages of 14.09 ± 1.04 k and 12.70 ± 0.96 k cal. years suggest that Corsica was glaciated during the Lateglacial period. Although more samples are required to confirm these ages, support for this interpretation is evident from other palaeoenvironmental data in the western Mediterranean and a simple snowpack model simulating Younger Dryas conditions in Corsica. Analysis of the Tavignano alluvial units indicates that Pleistocene glaciation is likely to have had a strong impact on the river regime and sedimentation style. The timing of the major alluviation phases has been estimated using an age model derived from OSL ages and the PDI. Deposition is broadly coeval with the Late Pleistocene cold stages and climate change is therefore considered to be the dominant control on river behaviour during the Late Pleistocene.

Lichenometric dating of coarse flood deposits on the Figarella valley floor has established the timing of flood periods since *ca.* AD 1570. At least ten distinct periods of enhanced flooding are evident over the last five centuries. Flooding was particularly prominent during the 1500s, mid-late 1700s and throughout the 1800s in the Figarella, corresponding to particularly cold and wet periods. The apparent synchrony of flood events across the Mediterranean region during the Little Ice Age suggests that climate variability over the past 500 years has been the overriding control on flood frequency in Corsica. Analyses of twentieth century rainfall records show a strong correlation between heavy precipitation events in the western Mediterranean and a strong negative winter North Atlantic Oscillation.

CONTENTS

LIST OF FIGURES

CHAPTER 1

CHAPTER 2

CHAPTER 3

CHAPTER 4

CHAPTER 5

CHAPTER 6

LIST OF TABLES

CHAPTER 1

CHAPTER 2

CHAPTER 3

CHAPTER 4

CHAPTER 5

CHAPTER 6

LIST OF ABBREVIATIONS

^{14}C	Radiocarbon (dating)
AMS	Accelerator Mass Spectrometry
ARM	Anhysteretic Remanent Magnetization
BADC	British Atmospheric Data Centre
BGSL	Blue Green Stimulate Luminescence
CLIMAP	Climate Long-range Investigation, Mapping and Prediction
CND	Cosmogenic Nuclide Dating
ED	Equivalent Dose
EDM	Electronic Distance Measurer
ELR	Environmental Lapse Rate
ENSO	El Niño Southern Oscillation
ESR	Electron Spin Resonance
ETH	Swiss Federal Institute of Technology
FLAG	Fluvial Archives Group
GCM	General Circulation Model
GSL	Green Stimulated Luminescence
ICP	Inter-coupled Plasma (spectrometry)
INTIMATE	Integration of Ice-core, Marine and Terrestrial Records of the Last Termination
IRM	Isothermal Remanent Magnetization
IRSL	Infra-red Stimulated Luminescence
LGM	Last Glacial Maximum
LIA	Little Ice Age
LR	*Lecanora rupicola spp.*
MAP	Mean Annual Precipitation
MAT	Mean Annual Temperature
MD	Multidomain
MIS	Marine Isotope Stage
MS	Mass Spectrometry
MWP	Medieval Warm Period
NADW	North Atlantic Deep Water
NAO	North Atlantic Oscillation
NSIDC	National Snow and Ice Data Center
OSL	Optically Stimulated Luminescence
PAGES	Past Climate Variability Through Europe and Africa
PDI	Profile Development Index

RCM	Regional Climate Model
RZ	*Rhizocarpon geographicum agg.*
SAR	Single Aliquot Regeneration
SCIDR	Sheffield Centre for International Drylands Research
SD	Standard Deviation
SEM	Scanning Electron Microscopy
SIRM	Saturated Isothermal Remanent Magnetization
SP	Superparamagnetic
SSD	Stable Single Domain
TL	Thermoluminescence
U-Th	Uranium Thorium (dating)
WCD	World Climate Disk
WGMS	World Glacier Monitoring Service

1 INTRODUCTION

1.1 SYNOPSIS

This chapter provides an introduction to the investigation by highlighting the importance of studying river response to environmental change. The selection of Corsica as a study area in the western Mediterranean basin is justified and a brief summary of previous work conducted on the island is presented. The number of international research projects undertaken to improve our understanding of Late Quaternary global and regional environmental change has increased considerably over the past decade, and several of the current investigations of relevance to this thesis are listed with their aims. The aims, spatial and temporal scale and objectives of this project are then outlined. The major controls on river behaviour and catchment processes are briefly discussed and the nomenclature and dating calibration convertions used throughout this study are described. Finally, the thesis structure is presented.

1.2 WHY STUDY RIVER RESPONSE TO ENVIRONMENTAL CHANGE?

Rivers are dynamic systems which can respond rapidly to environmental change in terms of process and form (Schumm, 1977). Rivers are also an important component of the physical landscape and provide an essential resource to humans. For example, navigation and agriculture are two important activities which are heavily dependent on river channels and their water resources (Newson, 1997; Smith & Ward, 1998). The importance of understanding fluvial response to environmental change must therefore not be understated. The continued global increase in population will inevitably intensify the pressure on fresh water supplies in the future and increase the potential to modify catchments and catchment processes. It is important to appreciate the effects of human-induced changes on the fluvial system, such as dam construction, forest clearance, urbanization and river channelisation, all of which greatly modify the sediment yield and hydrology of the river (Knighton, 1998). The current concern for global warming is also a result of increasing population and the increasing greenhouse gas emissions. Forecasts of higher temperatures, sea-level rise and enhanced storm frequencies emphasize the need to improve our understanding of the response of rivers to environmental change. This may lead to more accurate predictions of environmental change.

Climatic change is one extrinsic control which has had a major impact on river behaviour on a variety of timescales. For example, it has been shown that the last glacial stage caused dramatic changes in sediment load and hydrological regime across the northern hemisphere although many studies focus on the mid latitudes (e.g. Lewin *et al.*, 1995a; Knox, 1995). Over shorter timescales (10^0-10^2 years) and on a regional scale it has been illustrated that modest climatic variations (1-2°C change in mean annual temperature (MAT) and $\leq$ 10-20% mean annual

precipitation MAP)) have resulted in major changes in the frequency and magnitude of flooding effecting significant adjustments to fluvial activity and form (Knox, 1993; Ely, 1997). The speed at which climate can change has also recently become clear from high resolution proxy climate records (e.g. Dansgaard *et al.*, 1993; Allen *et al.*, 1999; Cacho *et al.*, 2001). Transitions between fundamentally different climates can occur within decades. In order to understand these variations and their impact we need to investigate different environments over a range of temporal and geographical scales.

1.3 SELECTION OF STUDY AREA

It can be argued that Mediterranean rivers (Figure 1.1) have many characteristics which enhance their sensitivity to environmental change. The high relief of the Mediterranean region promotes steep hillslope and channel gradients which accentuates erosive forces (Woodward, 1995). Young, erodible lithologies are also evident in the Mediterranean (Woodward, 1995). In addition, the basin is especially prone to intense convective storms (Wainwright, 1996) and flashy, high magnitude flood events which can lead to major channel modifications (Poeson & Hooke, 1997). It has also been argued that the Mediterranean basin has been especially sensitive to climatic variations, primarily in response to precipitation related changes in vegetation cover and sediment yield (Macklin *et al.*, 1995). Generally, climate variations over the Pleistocene and Holocene have resulted in alternating periods of sediment production and river alluviation, followed by slope stability and valley floor or fan incision (e.g. Vita-Finzi, 1969; Lewin *et al.*, 1991; Harvey, 1996; Macklin *et al.*, 1997; Maas & Macklin, in press). Detailed fluvial geochronologies of Late Pleistocene river response to environmental change have been established in several areas of the western (e.g. Fuller *et al.*, 1998; Rose *et al.*, 1999) and eastern (e.g. Macklin *et al.*, 1997; Maas *et al.*, 1998; Hamlin *et al.*, 2000) Mediterranean. More recent climatic changes of lower amplitude, for example during the Little Ice Age (LIA) AD 1450-1850, have also led to significant changes in river sedimentation styles (Ballais, 1995; Grove, 2001) and the frequency and magnitude of flood events (Benito *et al.*, 1996; Barriendos-Vallve & Martin-Vide, 1998, Maas, 1998). In addition to the steepland environment, the fragility of the Mediterranean landscape has increased throughout the Holocene due to disturbance of the land from anthropogenic activities, which has in turn, led to further fluvial modifications (e.g. van Andel, 1986). The Mediterranean is also a zone of active tectonics (Dewey *et al.*, 1973), a factor which plays a very important role in river behaviour (Harvey & Wells, 1987; Kuzucuoglu, 1995).

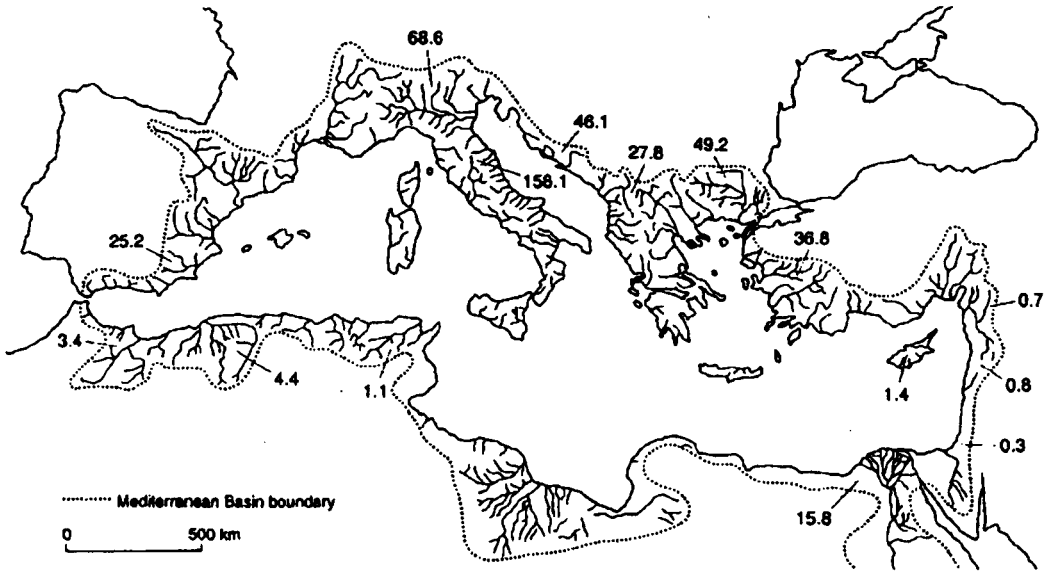

Figure 1.1 The river drainage network of the Mediterranean Basin. Values given on land indicate river runoff and agricultural discharges (after Allen (2001), adapted from Macklin *et al.*, 1995 and Cruzado, 1985 (from 1977 United Nations Environment Programme data)).

The island of Corsica in the western Mediterranean basin was chosen as a study area for a number of reasons. The island provides a suitable location for investigating Late Quaternary fluvial activity to allow comparison with other studies conducted in the Mediterranean including Spain (e.g. Fuller *et al.*, 1998), Mallorca (e.g. Rose *et al.*, 1999) and Greece (Maas *et al.*, 1998; Hamlin *et al.*, 2000) and to test recent ideas on the long term behaviour of Mediterranean rivers (e.g. Macklin *et al.*, 2002). In contrast to many other basins in the Mediterranean which are dominated by sedimentary rocks, namely limestone, flysh and marls, Corsica has a predominant lithology of granite. This difference provides the opportunity to compare the impact geology has on sediment production and river behaviour. Corsica was also glaciated during the Pleistocene period, and as previous studies in the Mediterranean have shown (e.g. Woodward *et al.*, 1995) the effects of glaciation can propagate well beyond the glacier margins influencing wholesale changes in river regimes and sedimentation styles. In Corsica during the Late Pleistocene, the headwater regions of the major rivers are likely to have developed glaciers under conditions close to their climatic limit of viability because of the limited altitude of the mountains (< 3,000 m), the latitudinal position (40-44°N) and the vicinity of the Mediterranean Sea. This provides an ideal area to study environmental change as smaller glaciers react to changes in temperature and precipitation in much shorter timescales than the larger Alpine glaciers, possibly providing a better resolution of climatic events in the associated deposits. The Mediterranean region was also ecologically sensitive during the Late Pleistocene and numerous plant and animal refuges are likely to have been present in Corsica. The combination of factors described suggests that the Mediterranean serves as an important reference point in regional studies of Late Quaternary environmental change.

1.3.1 Mediterranean steepland river systems

The potential for exploring river responses to environmental change in the Mediterranean is well illustrated in the publication of *Mediterranean Quaternary River Environments* (Lewin *et al.*, 1995a). Nineteen case studies are incorporated and concern the identification of controls on Quaternary river development. Each study shows the value and range of fluvial archives in the region for palaeoenvironmental reconstruction. The importance of Quaternary tectonic, climatic and human activity on river behaviour is highlighted repeatedly in a variety of alluvial settings. Such alluvial environments include alluvial fans, basin and range settings and coastal alluvial plains and deltas. The publication, however, stresses the need for further research into Mediterranean steepland river environments (Lewin *et al.*, 1995b). Corsica provides a suitable research location to address this issue as the island comprises many steepland river systems. For example, the highest mountain, Mount Cinto is 2,706 m in altitude and is located less than 30 km from the western coastline.

On a temporal scale, *Mediterranean Quaternary River Environments* emphasizes the need for steepland river studies encompassing the historical period. Evaluation of environmental controls on flood frequency and flood magnitude during the LIA is highlighted as a key research area, whereby the slope-channel linkages and sensitivity to recent climatic changes are manifest (Lewin *et al.*, 1995b). Recent catastrophic flood events in southern France and Sardinia (11-13 November, 1999), Italy (8-10 September, 2000), Corsica (14-16 October, 2000) and Spain (22-24 October, 2000) have illustrated the importance of understanding the detailed mechanisms of river behaviour in these sensitive environments if appropriate flood alleviation and sustainable river management schemes are to be developed.

1.3.2 Previous work in Corsica

There have been no recent glacial and fluvial geomorphological investigations conducted on the island of Corsica. However, in the 1970s Odette Conchon identified and mapped the river terraces preserved along the major rivers (Conchon, 1975). The glacial deposits evident in Corsica have also been mapped by Conchon and correlated to the fluvial sediments on the basis of weathering characteristics (Conchon, 1975, 1986). The terrestrial chronologies proposed by Conchon (1975, 1986) for glaciation and river aggradation in Corsica are, however, extremely tentative. The relative ages are based on broad pedogenic parameters which are linked by analogy to sequences in the Alps (Conchon, 1975, 1978). No robust chronologies were constructed by Conchon principally because of the lack of appropriate absolute dating controls in the 1970s.

1.3.3 Advances on earlier studies in Corsica

Over the last two decades or so, isotopic (cosmogenic nuclide, radiocarbon and uranium-series) and radiometric (luminescence) dating techniques for Quaternary sequences have been developed and/or further refined and offer the potential to provide studies with a firmer chronological base (e.g. Fuller *et al.*, 1998; Hamlin *et al.*, 2000). This study aims to advance Conchon's investigations through the use of absolute and relative dating techniques in an attempt to constrain the age of Late Pleistocene glacial and fluvial activity in Corsica. New and existing dating methods need to be tested and refined to allow for cause and river response to be related with confidence (Lewin *et al.*, 1995b). Well dated mountain moraine and alluvial sequences are necessary to test the notion that climatic variability during the last glaciation was synchronous and worldwide (Broecker, 1997; Mahaney, 1998). There are also new approaches (such as the use of mineral magnetic properties) to quantify weathering patterns and to develop correlation schemes and relative age models (e.g. Harvey *et al.*, 1995; Pope, 2000). Precise age determinations of glacial and fluvial deposits are necessary if terrestrial and marine records are to be linked, and base-line data for regional and global climatic change established.

Several studies within the Mediterranean have recently addressed one future research need outlined in *Mediterranean Quaternary River Environments* which concerns work on historical floods. Coarse flood deposits in steepland river systems on mainland Greece (Hamlin, 2000) and Crete (Maas, 1998) have been mapped and dated by lichenometry. This incremental dating technique has been used in conjunction with local instrumented precipitation data to provide high resolution records of enhanced flood frequency and magnitude over the last 3-400 years. No investigations of this type have been conducted in the western Mediterranean. The steep gradient cobble- and boulder-bed stream channels in Corsica offer ideal environments for the supply, entrainment, deposition and preservation of coarse flood material. Providing that lichens colonise the substrate surface soon after exposure, a detailed flood history can be developed for the local area.

1.4 CURRENT QUATERNARY PALAEOENVIRONMENTAL RESEARCH

Since CLIMAP (Climate Long-range Investigation, Mapping and Prediction) in the 1970's there have been numerous projects set up across the world to study climate variability. Several large-scale international projects currently active include EPILOG (Environmental Processes of the Ice Age: Land, Oceans and Glaciers) (http://www.images.cnrs-gif.fr/epilog.html), INTIMATE (Integration of Ice-core, Marine and Terrestrial Records of the Last Termination) (http://www.uu.nl/fg/INTIMATE) and PAGES (Past Climate Variability Through Europe and Africa) (http://www.pages.unibe.ch/). There are also regional investigations such as the 'Iberia Project'. Their goals are all similar in that they aim to effect more precise, high resolution synthesis of palaeoenvironmental data. Some authors have argued that there is a clear need for

more rigorous stratigraphical, palaeoecological and geochronological procedures than those that have been adopted up to now (Macklin, 1995; Mahaney, 1998; Maddy *et al.*, 2001). The main challenges presently facing the continental and marine palaeo-data communities according to Lowe (2001) are:

i) To improve the precision by which past environmental changes can be reconstructed.

ii) To improve the accuracy by which the inferred environmental changes can be dated.

iii) To provide data at temporal and spatial resolutions that are useful to the climate modelling community.

It is recognized that although it may not be possible to study terrestrial and marine sequences at the temporal resolution of ice core records, significant advances are being made with indications that decadal- to annual- scale resolution may be feasible in certain circumstances (e.g. von Grafenstein *et al.*, 1999; Litt *et al.*, 2001). Projects focusing on river behaviour and environmental change include FLAG (Fluvial Archives Group) which was formed in 1996 due to the increasing interest over the past decade in fluvial systems (http://www.qra.org.uk/FLAG). Two major research themes have been identified. The first addresses long terrestrial records spanning the entire Quaternary and the second examines fluvial environments and processes in relation to external and internal forcing (see Maddy *et al.*, 2001). In essence, one of the key issues for all Late Quaternary palaoenvironmental research projects involves the shift from essentially qualitative investigations to gathering quantitative data in order to validate existing models and develop new and more accurate models.

1.5 PROJECT AIMS, SCALES AND RESEARCH OBJECTIVES

The overall aim of this thesis is to investigate the impact of Late Quaternary environmental change on river behaviour in Corsica over a range of temporal and spatial scales including the Late Holocene period, using a range of absolute and relative age dating methods. It is hoped that this will improve our understanding of river response to environmental change in the western Mediterranean.

1.5.1 Spatial and temporal scale of investigation

Two study areas have been chosen for the fluvial investigations; one focuses on the nature of river response to environmental change on the timescale of 10^3-10^4 years and encompasses the lower half of the Tavignano River catchment (~775km^2), the other explores river response on a decadal and centennial timescale to recent (<500 years) environmental change from a single reach (1.5 km) of the Figarella river basin (~132km^2) (Chapter 3.2). Both timescales incorporate periods of considerable climatic instability and fluvial activity. Several studies have

shown that Mediterranean river catchments witnessed large changes in the storage and flux of water and sediment during the Last glacial to Interglacial transition (Woodward *et al.*, 1995; Fuller *et al.*, 1998; Rose *et al.*, 1999; Hamlin *et al.*, 2000). Glacial activity is believed to have played a major role in river behaviour during this time period (Lewin *et al.*, 1991; Woodward *et al.*, 1995; Hamlin *et al.*, 2000). The hydroclimatic conditions across Europe and the Mediterranean during the sixteenth to nineteenth centuries (Little Ice Age) were also especially changeable (Pfister, 1995) which led to widespread geomorphological adjustments (Maas, 1998; Hamlin, 2000; Grove, 2001, Maas & Macklin, in press).

1.5.2 Research objectives

There are three key objectives for this study in Corsica:

i) To employ terrestrial in-situ cosmogenic nuclide dating (CND) to establish exposure ages for Late Pleistocene glacial deposits in Corsica.

ii) To investigate river response to environmental change over the Late Pleistocene.

iii) To establish the response of a steepland river system to recent (<500 years) environmental change.

The first objective involves a recently developed dating technique that has not been widely applied in Europe. This project therefore acts as a pilot study to explore the potential of ^{10}Be CND in Corsica and indeed in a Mediterranean environment. The second objective builds on the work of Conchon (1975) by employing a combination of relative and absolute dating techniques in addition to sedimentological analysis to develop a fluvial history. Comparisons with regional palaeoenvironmental records and previous Mediterranean studies will also help identify the local, regional and Mediterranean-wide controlling factors. The final objective will combine instrumented data and historical documents from the western Mediterranean region to aid in the interpretation of any hydrological and sedimentological adjustments. Chronological controls over recent timescales (e.g. lichenometry) commonly offer higher resolution records of past river activity, allowing for cause and effect relationships to be explored more effectively. It is essential that historical climate variations and their impacts are understood so that more accurate hydroclimate predictions can be made in the future in the light of global warming.

1.6 RIVER SYSTEMS AND ENVIRONMENTAL CHANGE

This section provides a basic, but important introduction to the controls on river behaviour and catchment processes. The nomenclature used within this study is also outlined in addition to the calibration of radiocarbon dates to calendar years.

1.6.1 Controls on river behaviour

A natural river can be thought of as an open system with inflows and outflows of energy and matter (Leopold and Langbein, 1962). The important characteristics of river behaviour can therefore be described as the external constraints or controls imposed on the system, the internal modifications made in response to those controls and the nature of adjustment. The fluvial system at any particular location reflects the integrated effect of a set of upstream, or independent basin controls, notably climate, geology, land use and basin physiography which together determine the hydrologic regime and the quantity and type of sediment supplied (Knighton, 1998) (Figure 1.2). Climate is of primary significance in that it provides energy for many of the important fluvial processes but also has an indirect control on hydrology and rates of erosion through its impact on vegetation. Geology can have an effect at a variety of scales but it particularly influences drainage pattern (surface and sub-surface) and soil type and hence vegetation. Tectonic activity and downstream controls such as base level change are also very important with regards to longitudinal profile adjustment. In addition to these natural controls, anthropogenic activities presently have a strong influence in terms of land use change and river regulation and management in many countries.

1.6.2 Catchment processes

The river catchment provides a clearly defined unit for fluvial studies and comprises the recognizable elements of an open system with inputs, throughputs and outputs. Schumm (1977) envisaged a simplistic scheme consisting of three zones arranged in a downstream sequence: an upper zone of sediment production, a middle zone of sediment transfer and a lower zone of sediment deposition (Figure 1.3). Although it is known that sediment is eroded, transported and deposited throughout the entire drainage basin, the model underlines how different processes may dominate longitudinally (Knighton, 1998). This model implies the importance of headwaters as source areas and how downstream effects may have upstream causes, emphasizing the need to study the catchment as a whole.

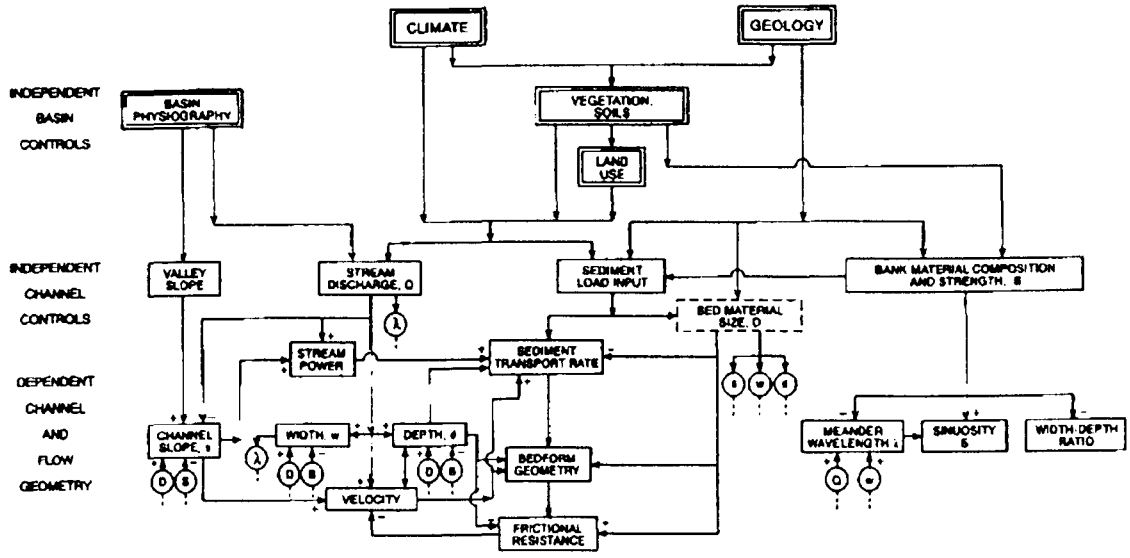

Figure 1.2 Interrelationships in the fluvial system. Relationships are indicated as direct (+) or inverse (-) and arrows indicate the direction of influence (after Knighton, 1998).

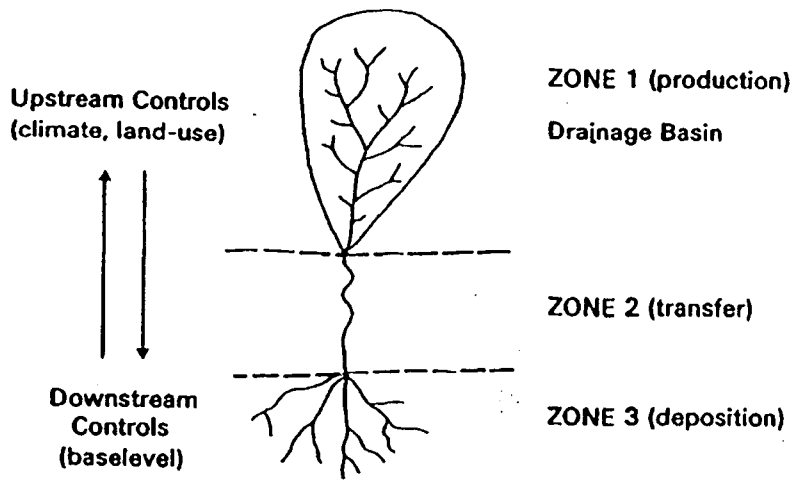

Figure 1.3 Schematic tripartite diagram of catchment processes; sediment production characterizes the upper zone, sediment transfer is associated with the middle zone and sediment deposition is generally related to the lower zone (Schumm, 1977).

Whilst rivers establish a form which is in equilibrium with the prevailing hydrological and sedimentological conditions (Chorley, 1962), numerous disturbances within the catchment could induce a change in form. These interruptions could either be of a 'pulsed' nature, such as flood events, or of a more progressive 'ramped' nature such as variations in climate (Brunsden & Thornes, 1979). Other disturbances to the system may include tectonic, biotic or anthropogenic factors. If thresholds are crossed, adjustments need to be made in response to the induced controls and a certain length of time, namely the 'relaxation time', or the 'recovery period' is required in order for the river to regain its steady state. However, because rivers are

sensitive systems that endure frequent disturbances it has been argued that the state of equilibrium is rarely achieved (Bull, 1979, Ferguson, 1993).

1.6.3 Nomenclature and calibration

Two of the most contentious issues when correlating different climate proxy records (with each other and between regions) are the nomenclature used and the calibration of different dating techniques. The latter is especially important for periods experiencing more abrupt and rapid changes in climate such as the Lateglacial.

One of the first empirical studies of fluvial response to climatic change was by Penck & Brückner (1909) who linked aggradation to glacial period sediment supply, and incision with interglacial intervals. Examination of terraces along tributaries to the Danube in southern Germany yielded the concept of the four Pleistocene glacial-interglacial cycles. The four major ice ages in the Alpine chronology were named Günz, Mindel, Riss and Würm, the latter being the most recent (Table 1.1).

Table 1.1 Quaternary time units (from Ahnert, 1998).

Years before present	Condition	Alps	Northern Europe	United Kingdom	North America
		Postglacial	Holocene	Flandrian	Holocene
10 000	Interglacial				
		Würm	Weichselian	Devensian	Wisconsin
70 000	Glacial				
		Riss/ Würm	Eemian	Ipswichian	Sangamon
120 000	Interglacial				
		Riss	Saalian	Wolstonian	Illinoian
180 000	Glacial				
		Mindel/Riss	Holsteinian	Hoxnian	Yarmouth
260 000	Interglacial				
		Mindel	Elsterian	Anglian	Kansan
420 000	Glacial				
		Günz/Mindel	Cromerian	Cromerian	Aftonian
820 000	Interglacial				
	Glacial			Beestonian	
	Interglacial			Pastonian	
		Günz	Menapian	Baventian	Nebraskan
1.2 million					

This model remained dominant until the development of oxygen isotope records from ocean basins in the 1960s and 1970s and the confirmation of the Milankovitch theory of glaciation (Hays *et al.*, 1976). The evolution of radiocarbon dating (Libby, 1952) provided the opportunity to develop a chronology for climatic change from palaeobiological indicators and independently from alluvial successions (Blum & Törnqvist, 2000). It is now known that the glacial framework is much more complex than a succession of four glacials with intervening interglacials. Moreover, within a glacial stage there are warmer short-lived episodes termed interstadials, contrasting with adjacent colder stadials. Although it is current practice to express

Quaternary time units as marine isotope stages (MIS), authors still employ the four principal stage names. Its transference to non-Alpine regions raises problems of correlation, arising essentially from the discontinuous nature of the geomorphological record. Not only is the record made up from components in different locations of a region but it may be that in some regions evidence of particular phases may be totally lacking, in some cases due to eradication by erosion from a later glaciation of the region.

Reference to the Alpine terminology is made throughout this study, principally due to the closeness of the Alps to the Mediterranean region. Many Mediterranean palaeoclimatic studies use the term Würm to describe the last glacial period, *ca.* 70-10 ka, which incorporates the Quaternary time unit of MIS 2, 3 and 4, the middle phase characterizing a slight warming within the last glacial period. The subdivisions of the Würm are not unanimous and vary from author to author which results in confusion. The Alpine chronology is divided into Würm I, Würm II and Würm III, but in northwest Europe, the broad substages are Early-glacial, Pleniglacial and Lateglacial. The latter nomenclature is employed more widely in the Mediterranean literature than the former, and much more is known about the Lateglacial than the preceding substages (although the long pollen records are now helping to overcome this, see Table 2.1). The Lateglacial can be divided up into Interstadials and Stadials, periods of warmer and cooler climatic conditions respectively (Table 1.2).

Table 1.2 Subdivisions [a] of the Lateglacial and Postglacial phases of northwest Europe.

		Chronozone	Condition	Radiocarbon age [b] (yr BP)	Calendar age (yr BP) Intercepts and range [c]
Postglacial Holocene Flandrian	Late	Sub-Atlantic	Cool and wet		
				2,500	(2,709)-2,581-(2,509)
	Middle	Sub-Boreal	Warm and dry		
				5,000	5,731
		Atlantic	Warm and wet		
				8,000	(8,950)-8,784-(8,767)
	Early	Boreal	Warm and dry		
				9,000	9,979
		Pre-Boreal	Warm and dry		
				10,000	(11,700)-11,500-(11,000)
Lateglacial	Late Würm/ Weichselian	Younger Dryas	Stadial		
				11,000	12,917
		Alleröd	Interstadial		
				11,800	
		Older Dryas	Stadial		
				12,000	13,992
		Bölling	Interstadial		
				13,000	15,437
		Oldest Dryas	cold		
				14,000	16,792

[a] The terminology for the Holocene is based on the Blytt-Sernander sequence.
[b] The ages in conventional radiocarbon years are those used by Mangerud *et al.* (1974) to define chronozones which in the Holocene approximate to the Blytt-Sernander climatic zones.
[c] Calibration to calendar years from Roberts (1998).

The Postglacial which represents the current interglacial is more commonly known as the Holocene and can be divided into chronozones. Both the Lateglacial and the Postglacial periods and their subdivisions are well constrained due to the abundance of suitable organic material which can be radiocarbon dated. This is due mainly to human settlement throughout the Holocene and good preservation of organic deposits in the Lateglacial in comparison to the earlier substages. However, radiocarbon years can not be directly compared to calendar years and a correction must be made when comparing ages which have been determined from different dating techniques (Roberts, 1998) (Table 1.2).

1.7 THESIS STRUCTURE

A review of Late Quaternary palaeoclimates in the Mediterranean is presented in the following chapter. The possible forcing mechanisms of climate cyclicity are reported in addition to the impacts environmental change has on Late Pleistocene and Late Holocene river behaviour. Previous studies that have investigated long term (10^2-10^4 years) and short term (10^0-10^2 years) river development are discussed. Background information on Corsica is described in Chapter 3 where the geological history, tectonic history and physiographic setting of the western Mediterranean island are presented together with the present-day land-use and climate.

The results of this investigation are presented in Chapters 4, 5 and 6. Chapter 4 details the utility of cosmogenic nuclide dating to elucidate the age of glacial deposits in Corsica and discusses the feasibility of the results incorporating a basic snow accumulation model. Chapter 5 documents the work conducted along the Tavignano River with regards to establishing the nature of pedogenic weathering and the timing of major aggradation in the area during the Late Pleistocene. The response of the Figarella river to environmental change over the past 400 years is illustrated in Chapter 6.

A synthesis of the main research findings is provided in Chapter 7 and compares the results of the investigation in Corsica with other Late Quaternary Mediterranean alluvial environments. An evaluation of the absolute, incremental and relative dating techniques employed within this study is also given. Chapter 8 presents the main conclusions of the study and recommendations for future work.

2 LATE QUATERNARY CLIMATE CHANGE AND MEDITERRANEAN RIVER BEHAVIOUR

2.1 SYNOPSIS

This chapter focuses on Mediterranean climate change from the Late Pleistocene through to the Late Holocene period. Palaeoclimates encompassing the period from 140 to 10 ka are largely based on: i) proxy data from terrestrial and marine sources within the western Mediterranean region, and ii) model simulations comprising a number of environmental variables. Climate reconstructions for Corsica are based on pollen sequences from cores extracted from Lake Creno in central Corsica. The palynological records date back to the Lateglacial period and provide the only available climate proxy for the island. Forcing mechanisms of Late Quaternary climate change are addressed in addition to the impact variations in climate have on river behaviour on both a long and short timescale. Other extrinsic influences on Late Pleistocene and Holocene river behaviour are discussed including tectonic and anthropogenic activity.

2.2 INTRODUCTION

Interpretation of European and Mediterranean Quaternary environmental change history has been reconstructed mainly from pollen and plant macrofossil records (e.g. Woillard & Mook, 1982; Ponel & Coope, 1990; Watts *et al.*, 1996) and lake level changes (e.g. Harrison & Digerfeldt, 1993; Roberts & Wright, 1993). Pollen sequences illustrate the shifting vegetation patterns that accompanied the glacial-interglacial cycles and also the lower order climate variations throughout the Quaternary (Table 1.1 & 1.2). Such biological evidence enables palaeoclimates to be inferred, although it is often argued that accurate pollen-based reconstructions are hampered by the lack of modern analogues for many of the pollen assemblages (Huntley & Prentice, 1993; Peñalba *et al.*, 1997). Uncertainties also exist about the resolution of palynological sequences with regards to the lag time between climate change and vegetation response. However, numerous authors have recently demonstrated that Mediterranean pollen records can provide a sensitive and high resolution account of rapid (centennial-millennial) environmental fluctuations comparable to those obtained from marine and ice cores (e.g. Follieri *et al.*, 1998; Allen *et al.*, 1999; Roucoux *et al.*, 2001).

Ice cores from Greenland (e.g. GRIP and GISP2) and sediment sequences from the North Atlantic Ocean (e.g. Duplessy *et al.*, 1992; Waelbroeck *et al.*, 2001) and the Mediterranean Sea (e.g. Paterne, 1999; Cacho *et al.*, 1999, 2001) provide an accurate measure of the timing and amplitude of climatic fluctuations through variations in isotopic ($\delta^{18}O$) and chemical signatures.

Chronological control for the Greenland ice cores has been based on a number of parameters. In the GRIP record, annual cycles in Ca and dust have been counted back to 100 ka in addition to the application of an ice accumulation model (Johnsen et al., 2001). In the GISP2 record, the counting of annual laminations and the correlations with the Vostok core provide the dating control (Meese *et al.*, 1997; Johnsen *et al.*, 2001). One of the main methods of glacial-interglacial ordering has been by marine isotope stages (MIS), which many of the terrestrial sequences are used as a chronostratigraphic framework.

The lack of geochronological control beyond the effective dating range of radiocarbon (^{14}C) has restricted many detailed reconstructions to the Last Glacial to Interglacial transition through to the present day (e.g. Pérez-Obiol & Julià, 1994). The accuracy of ^{14}C dating has been questioned due to the fluctuations in the carbon production rate and the plateau identified at around 12-11 ka BP (Ammann & Lotter, 1989), a time period of considerable environmental change (Table 1.2). Cross correlation with sequences dated by other methods such as cosmogenic or uranium-series techniques must be conducted with caution, although it has been argued that calibration and correction procedures are now more straightforward (e.g. van Andel, 1998). An alternative approach to implementing a numerical dated stratigraphy is to align terrestrial cores to the marine astronomically tuned timescale (Tzedakis, 1997; 2001). Four long continuous pollen sequences from southern Europe have been used to develop a complete stratigraphical scheme of major vegetational events for the past 430 ka (Tzedakis *et al.*, 2001). In a similar manner, Lateglacial and Holocene tree ring chronologies have been constructed throughout central Europe and extended to the Mediterranean region (Friedrich *et al.*, 2001). Absolute dating, however, is crucial for accurate comparisons and correlations between different continental sequences of environmental change. For example, the fluvial record cannot be easily compared to the vegetation records if ages of major events are not established. One exception would be if a common feature such as a tephra layer is identified in both records.

The main aim of this chapter is to outline the major climate changes that have occurred during the Late Pleistocene and Holocene periods and establish the prevalent river behaviour throughout the Mediterranean during these times. The objectives are as follows:

i) Define the main climatic boundaries during the Late Quaternary (from 140 ka onwards) and discuss the dominating climate conditions within each period.

ii) Describe the effects climate change has on fluvial systems and review other controlling mechanisms on river behaviour.

iii) Examine the timing and nature of fluvial activity across the Mediterranean during the Late Quaternary.

2.3 CLIMATE CYCLICITY AND THE INFLUENCE OF THE NORTH ATLANTIC OCEAN

Information on temperature fluctuations in the North Atlantic region over the last 200 kyr have been obtained from oxygen isotope records of marine and ice cores (e.g. Martinson *et al.*, 1987: Dansgaard *et al.*, 1993; Meese *et al.*, 1997). The longest cycle is thought to drive the glacial-interglacial sequences while a combination of the others promotes lower order but higher frequency climatic variations, known as stadials and interstadial phases. The long term fluctuations in temperature are primarily the result of periodic changes in the Earth's orbit and axis which control the amount of radiation received by the earth (Milankovitch forcing). Detailed analysis of ocean core sequences suggests that the climatic oscillations operate over cycles of 43 kyr (obliquity) and 24 kyr (precession) (Hays *et al.*, 1976). A longer cycle of 100 kyr is also evident in the marine and ice core records but the origin is still uncertain. It is argued that the 100 kyr cycle could also be derived by variations in the Earths orbit (eccentricity), but there is still some uncertainty.

Superimposed on these 24, 43 and 100 year cycles are distinct changes in temperature on millennial frequencies. These millennial-scale variations are well illustrated in ice cores, ocean sediment cores and terrestrial records and are named Dansgaard-Oeschger events (Dansgaard *et al.*, 1993). The planktonic record of core MD95-2042 (Shackleton *et al.*, 2000) clearly shows the variation in the concentration of $\delta^{18}O$ which is indicative of changing ice volume, sea surface temperature and salinity and used as a proxy for regional temperature trends (Figure 2.1). The Last Glacial in particular exhibited a number of these rapid climate fluctuations of relatively large magnitude (e.g. Allen *et al.*, 1999). Between 110 and 14 ka, 24 of these warm events are recognized in the marine and ice core record (Bond *et al.*, 1993; Dansgaard *et al.*, 1993; Taylor *et al.*, 1993, 1997). The warmer periods are well defined showing an abrupt beginning and a more gradual termination. The gradual cooling phase often ends with an abrupt final reduction in temperature back to cold conditions. Extensive ice rafting events known as 'Heinrich events' (Heinrich, 1988; Broecker *et al.*, 1992; Bond *et al.*, 1992; 1993), outflows of glacial meltwater (Broecker & Denton, 1989; Bard *et al.*, 1996) and re-routed continental runoff (Manabe & Stouffer, 1997; Clark *et al.*, 2001) into the North Atlantic are believed to have occurred in the intense cold and dry phase of some Dansgaard-Oeschger cycles. The massive input of fresh water into the ocean is thought to disrupt the North Atlantic Deep Water (NADW) formation and the transfer of heat and salt. Weakening of the thermohaline circulation had a strong influence on atmospheric circulation patterns resulting in a southward movement of the polar front and winter storm tracks (Duplessy *et al.*, 1992; Hughen *et al.*, 1996). Low sea surface temperatures (SST) in the Mediterranean basin have also been attributed to Heinrich events from polar water entrance through the Strait of Gibraltar (Cacho *et al.*, 1999; Paterne *et al.*, 1999) and intensification of the wind systems in the northern

hemisphere (Rohling *et al.*, 1998; Bácena *et al.*, 2001). Correlation between Heinrich events and periods of rapid climate changes reconstructed from isotopic and sedimentological records in the western Mediterranean also show a strong link with North Atlantic events (Valero-Garcés *et al.*, 1998; Ramrath *et al.*, 1999; Asioli *et al.*, 2001).

The detailed timescale on which most of these ice-rafting and climate change events began and ended is uncertain, although it cannot have been very much longer than several decades because the events themselves lasted no more than a few centuries (Mayewski *et al.*, 1997). Detailed studies of the Heinrich events suggest that the periodicity was between 7-13 ka during MIS 4, 3 and 2 (Adams *et al.*, 1999). The Dansgaard-Oeschger cycles seem to occur every 1-3 kyr with a mean cycle length of about 1,500 years (Bond *et al.*, 1997). Similar but lower amplitude 1,500 year oscillations also occur during the Holocene interglacial (Campbell *et al.*, 1998). The Little Ice Age (LIA) (AD 1450-1850) is believed to be the latest expression of the 1,500 year cycle (Bond *et al.*, 1997). Chemical composition analysis in the Greenland ice cores suggests that the LIA may have been the largest and most rapid change in polar circulation during the Holocene (O'Brien *et al.*, 1996; Mayewski *et al.*, 1997).

It is uncertain whether the frequent abrupt and severe climatic fluctuations during the Last Glacial and the Holocene were solely the result of internal mechanisms or whether there was an external influence. Coupled atmospheric-oceanic models of global circulation have simulated present day climate conditions without the use of external forcing such as insertions of large amounts of fresh water into the North Atlantic Ocean. Hall & Stouffer (2001) present a model which suggests a drastic cooling event within 3,500 years. Persistent northwesterly winds transport large quantities of cold and fresh water into the northern North Atlantic and oceanic convection shuts down in response. A cooling of 3°C lasting 40 years has been simulated and is qualitatively similar to some abrupt millennial scale North Atlantic cooling events seen in the Holocene record (Bond *et al.*, 1997). Bond *et al.* (2001), however, demonstrate that the Earth's climate system is highly sensitive to even weak perturbations in the Sun's energy output, not just on a decadal scale but also on centennial and millennial timescales. Over the last 12 kyr virtually every centennial time scale increase in drift ice evident in the North Atlantic records was associated with a distinct interval of variable and, overall, reduced solar output (Bond *et al.*, 2001). Such studies highlight the need to further our knowledge of centennial-millennial scale natural variability if the impacts of global warming are to be accurately assessed.

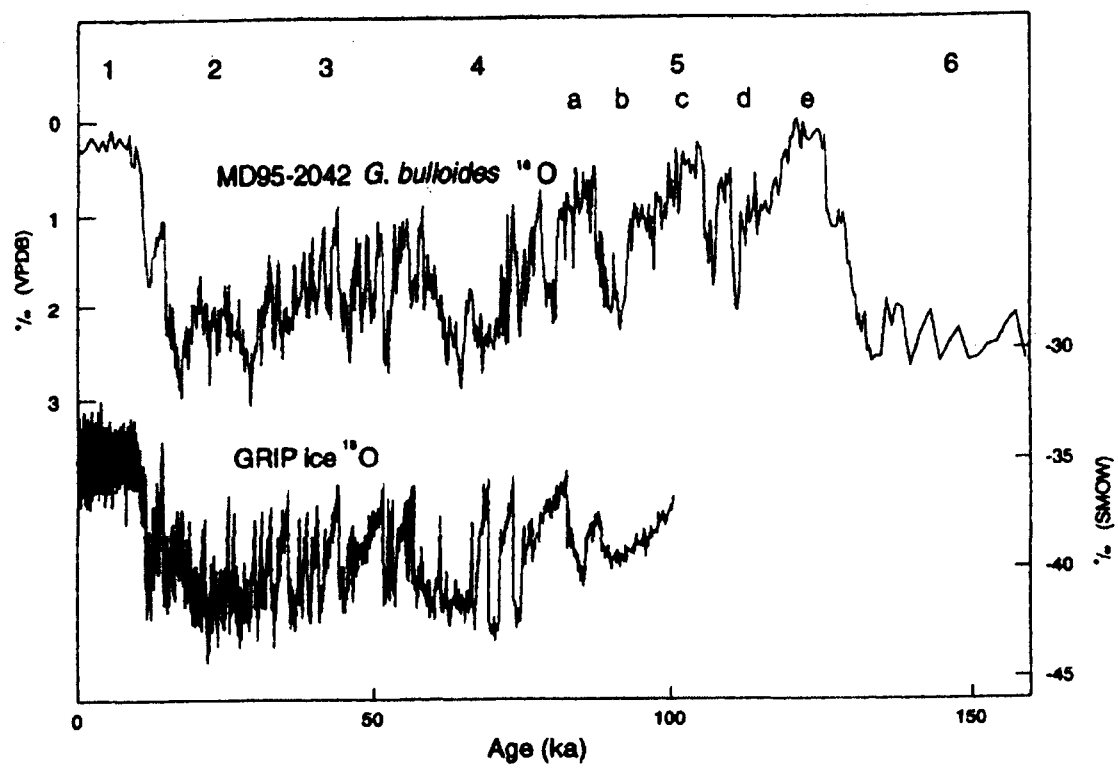

Figure 2.1 Planktonic oxygen isotope stratigraphy of core MD95-2042 identifying isotope stages, timescale of Cayre *et al.* (1999), and Greenland Ice Core Project (GRIP) $\delta^{18}O$ (Johnsen *et al.*, 1992). Taken from Shackleton *et al.*, 2000.

2.4 MEDITERRANEAN QUATERNARY PALAEOCLIMATES

Climate changes in the North Atlantic region inferred from $\delta^{18}O$ records can be linked to the changing vegetation communities in the western and central Mediterranean region. Many of the longest terrestrial pollen sequences originate from sediment cores extracted from maar lakes in Italy (e.g. Lago di Monticchio) and France (Lac du Bouchet) extending up to 450 ka BP and these have been correlated to the deep sea oxygen isotope record (e.g. Narcisi *et al.*, 1992; Allen *et al.*, 1999; Reille *et al.*, 2000). Grande Pile sediment cores from central France also exhibit a long record of vegetation changes and cover the last 140 ka with a chronology tied to the marine oxygen isotope stratigraphy (Woillard, 1978; Woillard & Mook, 1982). Other key sites from which pollen sequences have been widely used to reconstruct climate change in the western Mediterranean are Banyoles lake in northeastern Spain (Pérez-Obiol & Julià, 1994) and Padul in southern Spain (Pons & Reille, 1988) (Table 2.1,Figure 2.2). Recent high resolution marine records from the Mediterranean Sea ((e.g. core MD 95-2043 in the Alboran Sea (Cacho *et al.*, 1999; 2001) and pollen record (Sanchez-Goñi *et al.*, 2002) and core KET 80-03 in the Tyrrhenian Sea (Paterne *et al.*, 1999)) have also revealed climate variability in increasing detail. Table 2.1 and Figure 2.2 give details of the various climate proxies and their locations that have been used in the reconstructions of Middle and late Pleistocene and Holocene climate in the western Mediterranean region.

Table 2.1 Main climate proxy records in the western Mediterranean region (Figure 2.2).

Record	Reference	Site and region	Climate proxy	Length of record (^{14}C ka)
Continental				
Spain				
1	Allen *et al.*, 1996	Lago de Ajo Northwestern Spain	Pollen	14
2	Peñalba *et al.*, 1997	Quintanar de la Sierra North central Spain	Pollen	18.5
3	Pérez-Obiol & Julià, 1994	Banyoles Northeast Spain	Pollen	30
4	Florschütz *et al.*, 1971; Pons & Reille, 1988	Padul Southern Spain	Pollen	*ca.* 200 *ca.* 70
France				
	Jalut *et al.*, 1992	13 sites in the Pyrenees	Pollen	30
5, 6, 7	Andrieu *et al.*, 1993	Le Moura, Biscaye, Barbazan Western Pyrenees	Pollen	*ca.* 15
8, 9	Reille & Lowe, 1993; Pons *et al.*, 1987	Freychinede, La Moulinasse Eastern Pyrenees	Pollen	*ca.* 12
10	Woillard, 1978; Woillard & Mook, 1982	Grande Pile Central France	Pollen	140
11	Beaulieu & Reille, 1984	Les Echets, Southern France	Pollen	
12	Ponel & Coope, 1990	La Taphanel Massif Central	Pollen, macrofossil, coleoptera	*ca.* 15
12, 13, 14	Beaulieu *et al.*, 1985	La Taphanel, Marais de Limagne, La Chaumette-Brameloup Massif Central	Pollen	*ca.* 15
15	Reille *et al.*, 1997, 1999	Lac de Creno Central Corsica	Pollen	15
Italy				
16	Ponel & Lowe, 1992	Prato Spilla Northern Apennines, Italy	Pollen, coleoptera	*ca.* 15
17	Narcisi., 2001	Lago di Vico Central Italy	Pollen, macrofacies and sedimentological data	90
18	Follieri *et al.*, 1988; Narcisi *et al.*, 1992	Valle di Castiglione Central Italy	Pollen, mineralogical and geochemical and biostratigraphical data	250 250
19	Watts 1985; Watts *et al.*, 1996	Lago Grande di Monticchio Southern Italy	Pollen , macrofossil, diatom	15
19	Allen *et al.*, 1999	Lago Grande di Monticchio Southern Italy	Pollen, physical and geochemical data	102
Marine				
20	Cacho *et al.*, 1999, 2001	Alboran Sea Western Mediterranean Sea	Sea surface temperature	25
21, 22	Kallel *et al.*, 1997	Tyrrhenian Sea Central Mediterranean Sea	Sea surface temperature, salinity	18
22	Rossignol-Strick & Planchais, 1989; Paterne *et al.*, 1999	Tyrrhenian Sea Central Mediterranean Sea	Pollen, sea surface temperature, salinity and oxygen isotope composition	15-75

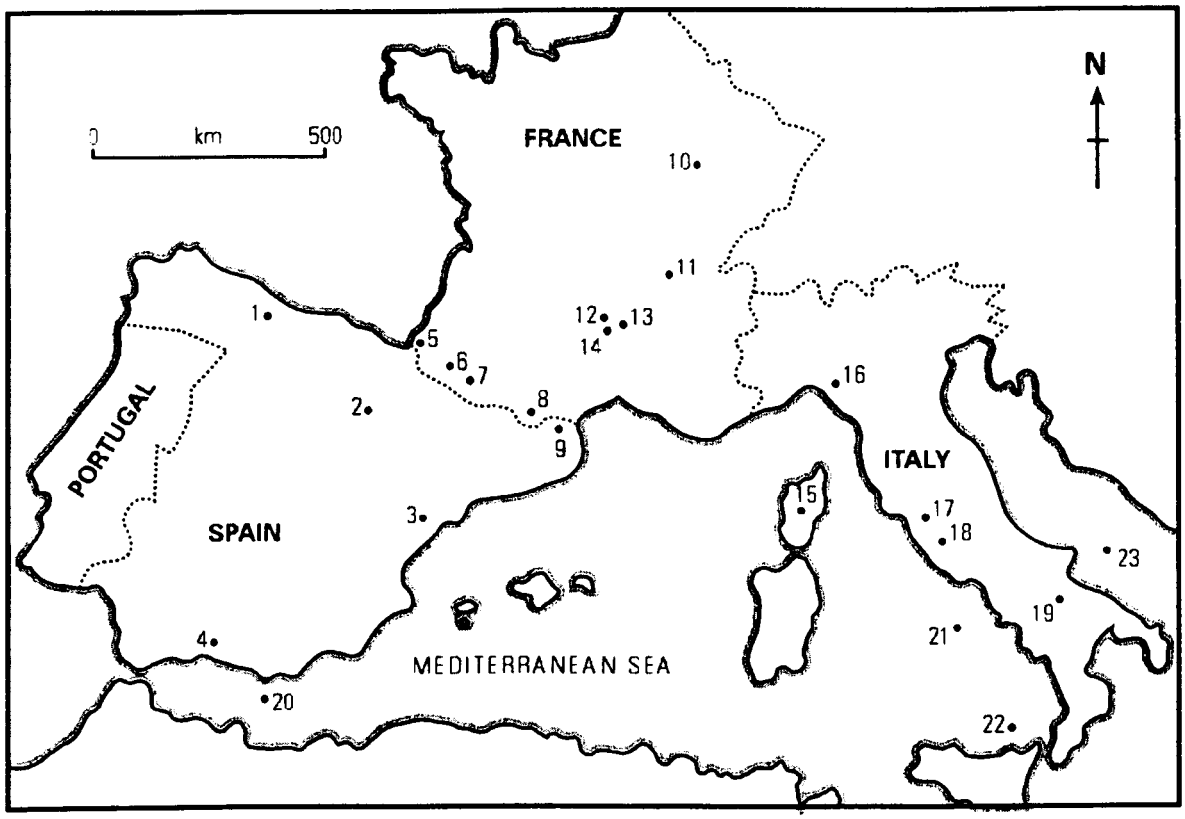

Figure 2.2 Location of the main climate proxy records in the western Mediterranean region (Table 2.1)

1. Lago de Ajo; 2. Quintanar de la Sierra; 3. Banyoles; 4. Padul; 5. Le Moura; 6. Biscaye; 7. Barbazan; 8. Freychinede; 9. La Moulinasse; 10. Grande Pile; 11. Les Eschets; 12. La Taphanel; 13. Marais de Limagne; 14. La Chaumette-Brameloup; 15. Creno; 16. Prato Spilla; 17. Vico; 18. Castiglione; 19. Monticchio; 20. Alboran; 21 & 22. Tyrrhenian; 23. Adriatic.

2.4.1 Late Pleistocene (MIS 6) to Last Glacial Maximum

Alternations between forest and open vegetation communities reflect high order changes of magnitude such as those major climatic shifts from interglacial to glacial modes (Table 1.1). Interglacial vegetation in southern Europe was generally dominated by mixed evergreen and deciduous woodland taxa such as oak (*Quercus*), elm (*Ulnus*), hazel (Corylus). Mediterranean taxa included olive (*Olea*) and pistachio (*Pistacia*) (van Andel & Tzedakis, 1996). The glacial stages in contrast, were synonymous with semi-desert like steppe vegetation with abundant *Artemisia* in addition to chenopods and grasses (Wijmstra, 1969). Superimposed on these oscillations is a lower order variability associated with vegetation changes between stadials and interstadials (Tzedakis, 1993). Often vegetation changes were rapid, frequently occurring in less than 200 years (Allen *et al.*, 1999). A comprehensive review of the European environment from 150 to 25 ka BP is given in van Andel and Tzedakis (1996). The distinct climatic divisions and conditions and associated vegetation for southern Europe throughout the Late Pleistocene from MIS 6 are illustrated in Figure 2.3. In addition, relative sea level is shown as a proxy to global ice volume variations.

The last glacial period (MIS 2) peaked in Europe at around 18 k radiocarbon years BP although the precise timing varies from region to region. Large ice sheets were present over much of northern Europe and ice caps covered the Alps and the Pyrenees. Extensive glaciers also occupied the upland valleys in Corsica (Conchon, 1975, 1986) (Chapter 4.3) during this Last Glacial Maximum (LGM). Severe cold and aridity characterized the LGM and the succeeding millennia up to 14 ka BP and these conditions were clearly reflected in the pollen sequences. However, evidence for high lake levels in the Mediterranean region at the time of the LGM suggest that the climate was wetter than present (Harrison & Digerfeldt, 1993; Roberts & Wright, 1993; Harrison *et al.*, 1996). This apparent contradiction has been explained primarily by the increased seasonality of precipitation when the winters were characterized by cold temperatures and intense precipitation and the summers were mild and dry (Prentice *et al.*, 1992; Peyron *et al.*, 1998; Collier *et al.*, 2000). Ecological modelling of the LGM in the Mediterranean region has estimated a reduction in winter temperature by 18°C and a summer temperature not dissimilar from today (Guiot *et al.*, 2000). The combination of increased precipitation in the winter and drier summers than modern times would generate more 20% more runoff (+100 $mmyr^{-1}$) (Guiot *et al.*, 2000). These climatic conditions are slightly more extreme than those initially established from General Circulation Models by Kutzbach & Guetter (1986) and COHMAP members (1988) that suggest a decrease of around 10°C in the winter and 1-2°C below present temperatures in the summer. The mean annual SST in the western Mediterranean basin during the LGM is estimated to have been 4°C lower than present (Bigg, 1994). However, the small number of sites used for lake level reconstruction at the LGM must be highlighted. For the western Mediterranean basin, only one basin was examined (Harrison & Digerfeldt, 1993). In addition, recent data from Ioannina basin, northwest Greece have shown LGM lake levels to be low, which suggests the models for high seasonal precipitation yet widespread aridity are not necessarily needed (Frogley *et al.*, 2001). More data must be collected and analysed for this controversy to be settled.

In southern Europe, some areas of open pine (*Pinus*) and birch (*Betula*) woodland seem to have existed during the LGM. In sheltered areas, mainly in the western Balkans (Tzedakis, 1993; Willis, 1994; Willis *et al.*, 2000), the mountains of Italy (Bennett *et al.*, 1991), and possibly Corsica (Reille *et al.*, 1997), scattered temperate tree populations survived in refugia where temperature variations were not extreme and precipitation was sufficient. Scattered patches of pine woodland may have also been present in valleys and other sheltered sites in the mountains of Spain (Turner & Hannon, 1988; Ramil-Rego *et al.*, 2000).

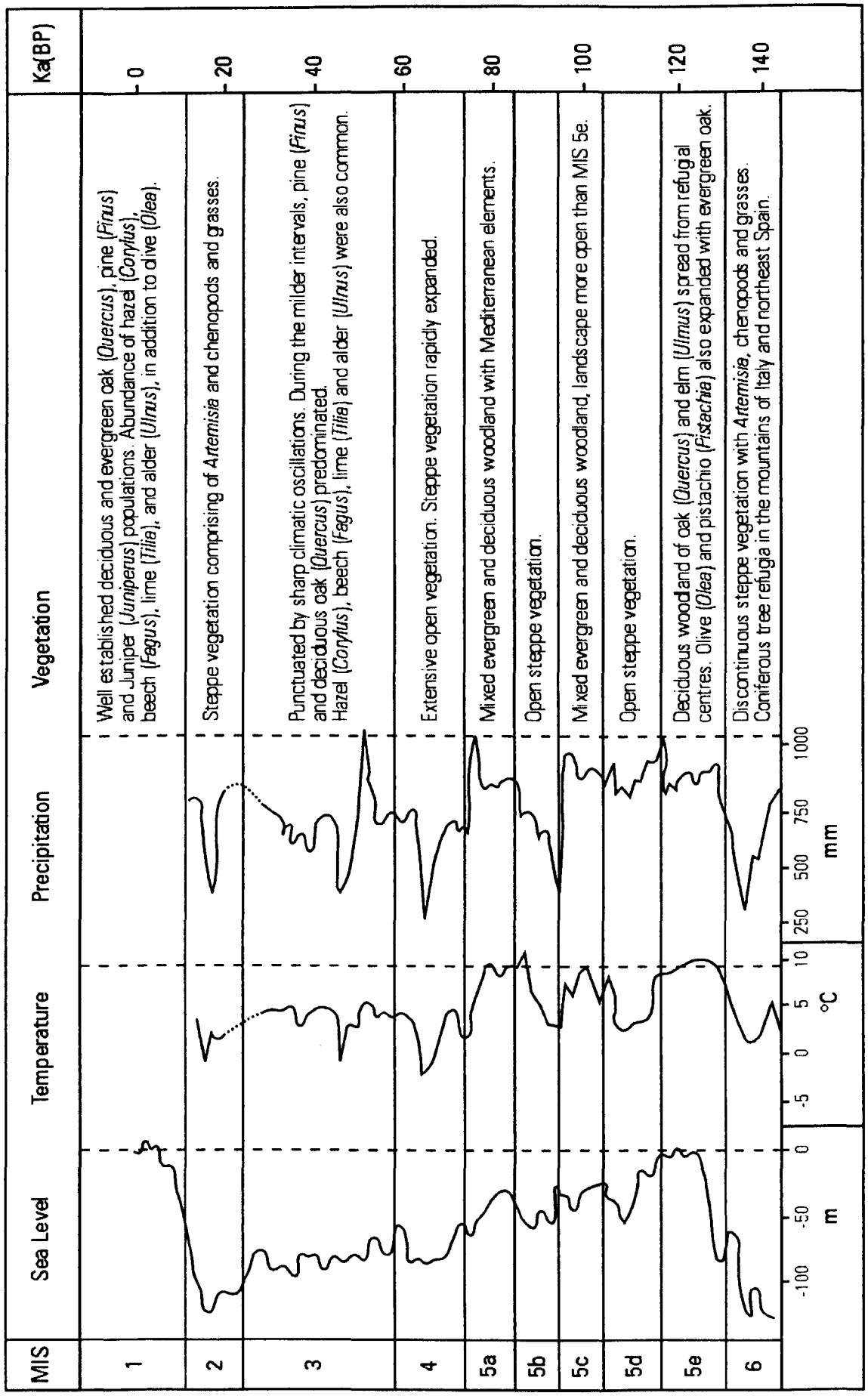

Figure 2.3 Climate and vegetation characteristics of southern Europe throughout the Late Quaternary from MIS 6 (data from van Andel & Tzedakis, 1996). Global sea level changes from Barbados (Bard *et al.*, 1990; Gallup *et al.*, 1994) and the Bahamas (Chen *et al.*, 1991). Mean annual temperature and precipitation after Guiot *et al.* (1989). Dashed vertical lines mark present values.

2.4.2 The Lateglacial to Holocene transition

Recent research on the last glacial period has demonstrated a close correspondence to millennial-centennial climatic and oceanic variability in the North Atlantic (Rohling *et al.*, 1998; Cacho *et al.*, 1999, Paterne *et al.*, 1999). The last deglaciation and Holocene periods were also characterized by short-term climatic variability (Bond *et al.*, 1997). The Lateglacial (*ca.* 15 to 10 k radiocarbon years BP) was particularly marked in the northern hemisphere by conspicuous climate changes which included rapid glacial retreat. The most widely recognized intervals are the Older Dryas cold phase, the Alleröd/Bölling interstadials and the Younger Dryas cold phase (Figure 2.4). Each of these rapid climatic fluctuations is clearly evident in many of terrestrial, deep sea and ice core records in the northern hemisphere. The climate variations during the Lateglacial have probably been studied in most detail due to the excellent preservation of fossil material and the availability and application of dating techniques (e.g. radiocarbon dating).

The rise in global temperatures soon after the Last Glacial Maximum led to an increase in tree cover across the Mediterranean region associated with an overall reduction in *Artemisia* and other steppe like vegetation. However, cooler conditions returned at around 15 k radiocarbon years BP and a subsequent increase in *Artemisia* and other non arboreal pollen marked the beginning of the Lateglacial in Corsica (Reille *et al.*, 1997) (Figure 2.5) and more generally across the whole of southern Europe (Beaulieu & Reille, 1984; Reille & Andrieu, 1995). This stadial is often referred to the Oldest Dryas, and although distinct in some terrestrial (e.g. Pons & Reille, 1988; Watts *et al.*, 1996) and marine pollen sequences (e.g. Combourieu-Nebout *et al.*, 1998) and SST records (e.g. Kallel *et al.*, 1997), it is not recognized in all palaeoenvironmental records. The beginning of this period coincides with a large discharge of icebergs in the North Atlantic, Heinrich event H1 (Bond *et al.*, 1993). Marked aridity also corresponds to the Oldest Dryas event in southern Europe and the Mediterranean. Lake levels in the western Mediterranean were at their lowest around 16 to 15 k radiocarbon years BP (Figure 2.5) due to the periodic poleward movement and strengthening of the subtropical pressure cells and the reduced winter precipitation from the northward migration of the jet stream (Prentice *et al.*, 1992; Harrison & Digerfeldt 1993).

Late Glacial Chronozones	Estimated ages in ^{14}C ka BP	Vegetational characteristic	Climatic characteristics
Younger Dryas	11.0 – 10.0	Expansion of *Artemisia* and Chenopodiceae and decrease of all mesophilous trees (*Quercus, Alnus, Tilia*).	Return of glacial conditions. Very cold and dry.
Alleröd	11.8 – 11. 0	Decline in steppe vegetation and extension of xerophytic shrubland. Increase in birch (*Betula*) and alder (*Alnus*).	Warm and moist conditions. Cooler than the Bölling.
Older Dryas	12.0 – 11.8	Return of steppe vegetation and reduction of arboreal pollen in the mountainous regions of Spain, France and Italy.	Colder conditions during a general cooling trend.
Bölling	13.0 – 12. 0	Expansion of oak (*Quercus*) and pine (*Pinus*) forest. Retraction of steppe vegetation.	Rapid warming.
Oldest Dryas	15.0 – 13.0	High abundance of *Artemisia, Ephedra* and Chenopodiceae pollen. Low arboreal percentages. Retreat of high altitude coniferous trees to refuges.	Cold and very dry.

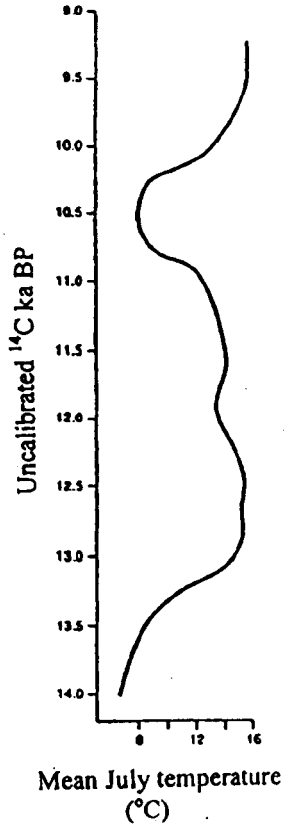

Figure 2.4 Vegetation and climate characteristics during the Late Glacial in southern Europe. Mean July temperatures are reconstructed from palynological and coleopteran evidence from La Taphanel, Massif Central (Guiot *et al.*, 1993, from Beaulieu *et al.*, 1994).

Climatic improvement was widely developed in southwestern Europe by 13 k radiocarbon years BP (Beaulieu *et al.*, 1994) and deglaciation was half complete (Ruddiman & McIntyre, 1981). Climatic conditions continued to warm and moisten which resulted in the growth of open wooded vegetation. This interstadial, known as the Alleröd-Bölling event across Europe, was punctuated by two cooling events, the Older Dryas and the Younger Dryas around 12 k BP and 11 k radiocarbon years BP respectively (Figure 2.4). The earlier event was less emphatic and briefer than the latter and is not as well marked in the palaeoclimatic records, although significant changes in the $\delta^{18}O$ signal are evident in both the Greenland ice core records at this time (Johnsen *et al.*, 1992; Grootes *et al.*, 1993).

In Corsica, the Older Dryas does not appear to have a significant affect on the vegetation cover in the vicinity of Lake Creno (Reille *et al.*, 1997). However, the signal is more clearly identifiable in numerous other palaeoenvironmental records in the western Mediterranean. The Older Dryas cooling led to an increase in steppe-like vegetation and a reduction in tree pollen in northern Spain (Watts, 1986; Pérez-Obiol & Julia, 1994), the Pyrenees (Andrieu *et al.*, 1993; Reille, 1993) and the Massif Central (Beaulieu *et al.*, 1985; Ponel & Coope, 1990). The stadial

is also evident by the reappearance of certain beetle species at La Taphanel (Massif Central) and Prato Spilla (northern Apennines) which are associated with cooler conditions (Beaulieu *et al.*, 1985; Ponel & Coope, 1990; Ponel & Lowe, 1992). These differences in vegetation cover and insect species imply that some sites are clearly more sensitive than others to such abrupt climate variations. It is suggested that the Older Dryas signal was more significant in northern Spain and Pyrenean sites than in southern parts of Spain (Valero-Garcés *et al.*, 1998). The Lake Creno site in central Corsica may also be more sheltered than the other Mediterranean mountain locations which illustrated a more distinct Older Dryas signal. It is interesting to note however, that one of the highest resolution marine palaeoclimatic reconstructions available from the western Mediterranean Sea (Cacho *et al.*, 2001) does not show the Older Dryas signal.

The decline of steppe vegetation and extension of xerophytic shrubland around 11.7 k radiocarbon years BP in the Lake Creno pollen record corresponds to the increased temperatures and slight moistening of the climate before the onset of the Younger Dryas (Reille *et al.*, 1997). This evidence is also supported by the increase in birch (*Betula pendula*) and alder (*Alnus viridis ssp. suaveolens, Alnus glutinosa*). Surprisingly, a marked increase in pine taxa (*Pinus nigra ssp. laricio*) was not recognized during this period of climatic improvement in Corsica unlike other parts of southern Europe at similar altitudes (e.g. Reille & Lowe, 1993). A major expansion of oak (*Quercus*) during the Alleröd (*ca.* 11.7 to 11 k radiocarbon years BP) is also not evident, in contrast to many Italian lacustrine pollen sequences. Perhaps this reinforces the suggestion that the Lake Creno site is sheltered and is not as responsive to small changes in climate as other sites. The vegetation during the Alleröd interstadial in Corsica was similar to that colonising the present slopes between 1,700 m to 2,200 m asl belt on the island (cryo-oromediterranean, Chapter 3.8). This suggests a lowering of vegetation belts by approximately 500 m between the present and the Alleröd interval (Reille *et al.*, 1997).

A new expansion of *Artemisia* and Chenopodiceae coinciding with the decrease of all the mesophilous trees (*Quercus, Alnus and Tilia*) around 11 k radiocarbon years BP in Corsica is the best indication of the cooling and drying phase of the Younger Dryas (Reille *et al.*, 1997) (Figure 2.5). The vegetation response to this climate change was particularly abrupt at the start of the Younger Dryas and is marked by a sudden increase in steppe species in many of the records from mountain sites throughout the western Mediterranean between 11 and 10 k radiocarbon years BP (Beaulieu *et al.*, 1994). Insect evidence (e.g Ponel & Coope, 1990; Ponel & Lowe, 1992), and sea surface temperatures and salinity records (e.g. Paterne *et al.*, 1986; Kallel *et al.*, 1997; Combourieu-Nebout *et al.*, 1998; Cacho *et al.*,2001) also show the abrupt onset of the Younger Dryas and indicate that the shifts in the position of the North Atlantic Polar front were sudden (Peñalba *et al.*, 1997). The Younger Dryas was characterized by low annual temperatures and dry winters although precipitation was high in the summer months

compared to the end of the Last Glacial (Pons *et al.*, 1987; Guiot *et al.*, 1993; Beaulieu *et al.*, 1994; Peñalba *et al.*, 1997). Palaeoclimatic models have suggested that the mean July temperature during the Younger Dryas was up to 8°C below that of the present day in the western Mediterranean region (Beaulieu *et al.*, 1994; Peñalba *et al.*, 1997). Annual precipitation was likely to have been 400-500 mm less than present conditions (Pons *et al.*, 1987). Sea surface temperatures in the Alboran and Tyrrhenian Seas were 3-4°C cooler for throughout the duration of the Younger Dryas (Cacho *et al.*, 2001).

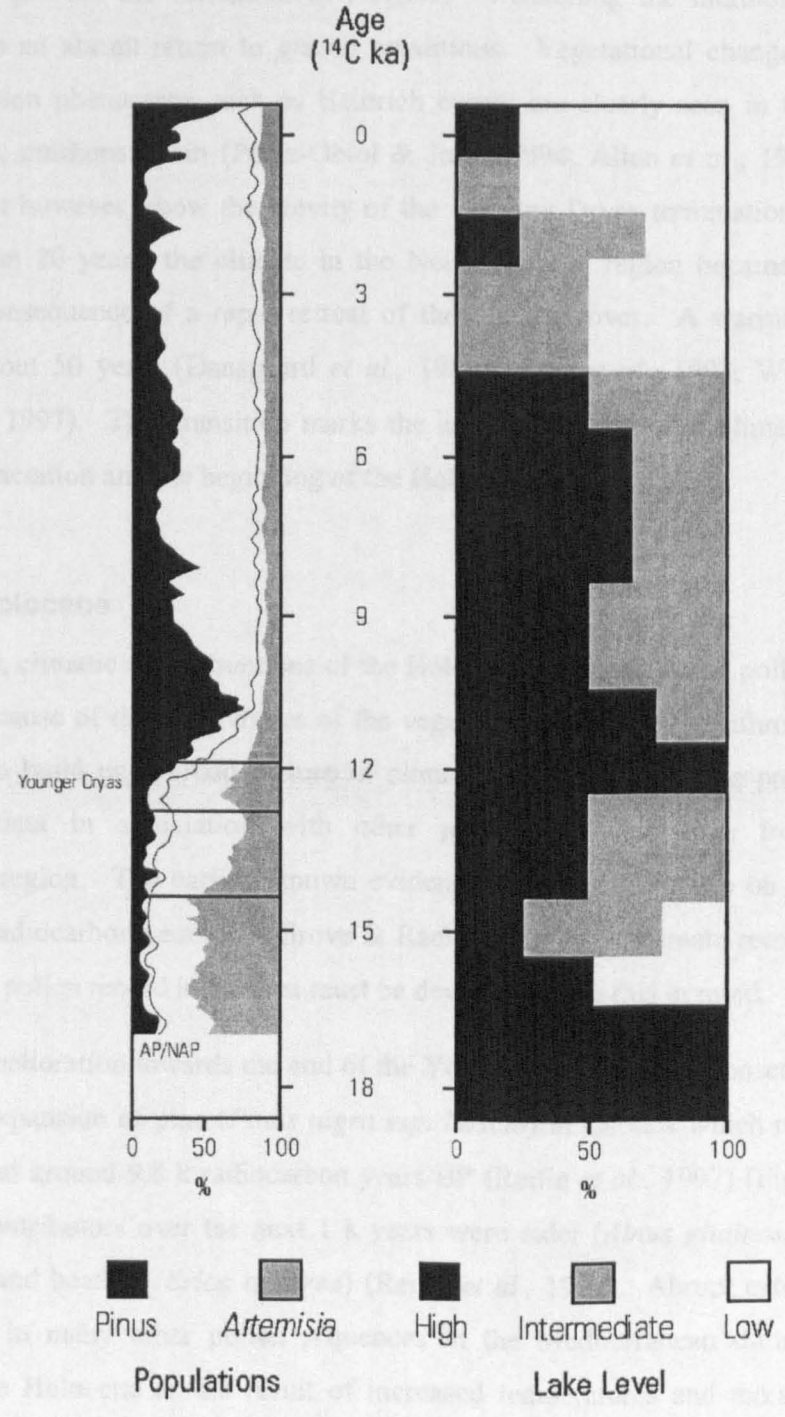

Figure 2.5 Pine (*Pinus*) and *Artemisia* populations from Lake Creno (Central Corsica) during the Last Glacial and Holocene periods (after Reille *et al.*, 1997, 1999) and lake levels from the western Mediterranean region from 18 ka (Harrison & Digerfeldt, 1993).

The Younger Dryas was the most significant rapid climate change event that occurred during the last deglaciation of the North Atlantic region and its origin is still strongly debated (Berger & Jansen, 1995; Alley & Clark, 1999 and references therein). However, general opinion rests with a mechanism disrupting the formation of NADW and ocean-atmosphere coupling. The abrupt cooling is regarded by some to be the result of the most recent Heinrich event, H0 (Bond *et al.*, 1993; Bond *et al.*, 1997). Others believe it is the consequence of a massive discharge of fresh water into the North Atlantic, notably Meltwater Pulse 1A (Bard *et al.*, 1996). Either event would cause a sudden influx of cold fresh water and lower the Atlantic surface salinity sufficiently to prevent the formation of NADW. Weakening the thermohaline circulation would provoke an abrupt return to glacial conditions. Vegetational changes in response to rapid deglaciation phenomena such as Heinrich events are clearly seen in the pollen record from Banyoles, northern Spain (Pérez-Obiol & Julià, 1994; Allen *et al.*, 1999). The pollen record does not however, show the brevity of the Younger Dryas termination. It is estimated that in less than 20 years, the climate in the North Atlantic region became milder and less stormy as a consequence of a rapid retreat of the sea ice cover. A warming of about 7°C occurred in about 50 years (Dansgaard *et al.*, 1989; Alley *et al.*, 1993; Watts *et al.*, 1996; Peñalba *et al.*, 1997). This transition marks the end of the last major climate reorganization during the deglaciation and the beginning of the Holocene.

2.4.3 The Holocene

In most regions, climatic reconstructions of the Holocene period based on pollen sequences are problematic because of the interference of the vegetation cover due to anthropogenic activity. It is possible to build up a broad picture of climate variation during the present interglacial using pollen data in association with other palaeoclimatic proxies from the western Mediterranean region. The earliest known evidence of human presence on Corsica is dated 8.56 ± 0.15 k radiocarbon years BP (Grove & Rackham, 2001). Climate reconstructions from the Lake Creno pollen record in Corsica must be developed with this in mind.

The climatic amelioration towards the end of the Younger Dryas and the onset of the Holocene promoted the expansion of pine (*Pinus nigra ssp. laricio*) in Corsica which rose to maximum values of 70% at around 9.8 k radiocarbon years BP (Reille *et al.*, 1997) (Figure 2.5). Other major pollen contributors over the next 1 k years were alder (*Alnus glutinosa*), yew (*Taxus*), beech (*Fagus*) and heather (*Erica arborea*) (Reille *et al.*, 1999). Abrupt extensions of forest are recognized in many other pollen sequences in the Mediterranean during the first few millennia of the Holocene as the result of increased temperatures and moisture. A second vegetation pulse is evident around 8.5 k radiocarbon years BP in the Mediterranean region when pistachio (*Pistacia*) and fir (*Abies*), spruce (*Picea*) and cedar (*Cedrus*) develop indicating

mild winters and humid spring and summer months (Combourieu-Nebout *et al.*, 1998). Lake levels in the western Mediterranean were high and indicate that conditions were wetter than at present during the early to middle Holocene (Figure 2.5) (Macklin *et al.*, 1995). The thermal optimum of the Holocene in Corsica is dated to around 7.7 k radiocarbon years BP (Reille *et al.*, 1999).

A major event approximately 7.6 k radiocarbon years BP in Corsica resulted in the drastic reduction of heather (*Erica arborea*) and alder (*Alnus glutinosa*). Reille *et al.* (1999) have argued that human activity is the cause of the change in vegetation cover rather than that of climatic change. Birch (*Betula*) and deciduous oak forests (*Quercus*) developed as a response to the disturbance from *ca.* 7.3 to 6.7 k radiocarbon years BP. Evergreen oak (*Quercus ilex)* forest is only well established in Corsica from this time, and expansion takes place over 2.5 k years later than in similar environments in France and Italy (Reille *et al.*, 1999). A time lag to allow soil development in the volcanic region in central Corsica is suggested as an explanation (Reille *et al.*, 1999). Moisture availability increased during the mid Holocene (*ca.* 6 ka BP) when fir (*Abies)*, yew *(Taxus)* and birch *(Betulus)* appeared and expanded in many regions of the western Mediterranean (Watts *et al.*, 1996).

Numerous records in the western Mediterranean basin show a distinct vegetation change around 4.5 to 4 k radiocarbon years BP. Deciduous forest was replaced in some regions by sclerophyll vegetation (Huntley & Birks, 1983; Huntley & Prentice, 1988). Low lake levels in the western Mediterranean indicate that arid conditions dominated (Harrison & Digerfeldt, 1993) suggesting reduced summer precipitation (Jalut *et al.*, 2000). This period is thought to be the beginning of the evolution of the Mediterranean climate exhibiting an increase in winter and summer temperatures and a decrease in precipitation during the growing season (Jalut *et al.*, 2000). However, there does not appear to be such a change in the pollen record from Lac de Creno in central Corsica. The pollen spectra for the period between *ca.* 6 and 3 k radiocarbon years BP corresponds to a period of stability dominated by oak forest, with a few openings and penetration of birch (*Betula*) and beech (*Fagus*) (Reille *et al.*, 1999). A mixed maquis of oak (*Quercus ilex*) and heather (*Erica arborea*) is also recorded in the pollen spectra which still exists today. Human induced fluctuations are clearly illustrated in the Corsican pollen record from *ca.* 2.1 k radiocarbon years BP (Figure 2.5).

More detailed palynological studies conducted in the western Mediterranean have identified periods of marked dryness during the Holocene between 8-7 ka, 3-4 ka and during 2 ka (Valero-Garcés *et al.*, 1998; Jalut *et al.*, 2000). Aridity in the western Mediterranean is related to the intensity and location of the winter rain belt which is strongly sensitive to atmospheric circulation patterns, especially the subtropical anticyclone belt (the Azores High) (Kutzbach *et al.*, 1993; Huntley & Prentice, 1993). Superimposed on the arid-humid phases of the Holocene

are shorter term oscillations from wet to dry or cold to warm, with a cyclicity of 260 years, or more infrequently 520 years (Roberts, 1998). It is not known whether this represents true regular cycles of natural variability or whether sunspot cycles or volcanic eruptions with large dust emissions may have had an influence.

It is difficult to be precise about the timing and magnitude of the climatic variations during the Holocene using pollen sequences due to the overprint of human activity on the climatic signature. Much of Corsica comprises primary forest so it is unlikely that the island experienced the mass deforestation recognized in other parts of the Mediterranean such as Spain and Italy during the early part of the Holocene. Anthropogenic activity is still evident in the Corsican pollen record however, especially from 2.1 k radiocarbon years BP (Reille *et al.*, 1999).

2.4.4 Historical climate change

Climate fluctuations which have occurred throughout Europe over the last few hundred years are relatively well documented (e.g. Pfister, 1995; Serre-Bachet *et al.*, 1995). Weather diaries, church records and instrumented data all enable accurate climatic reconstruction (see Lamb, 1977). The Medieval Warm Period (MWP) and the Little Ice Age (LIA) are the most recent analogues for conditions warmer and cooler than the twentieth century respectively. The LIA spans the time period between AD 1450 and 1850 (Grove, 1988) and is identified in many ice cores, marine and terrestrial climate proxy records in the northern hemisphere. The MWP includes a few centuries of milder climate prior to the LIA.

2.4.4.1 Little Ice Age

The LIA was in general a period of climatic deterioration when temperatures dropped 1°C from the norm and there were periods of enhanced precipitation (Grove, 1988). Conditions were sufficiently severe for glacial advance in the Alps and the prevention of new tree growth in marginal areas. The LIA was not consistently cold and wet, but comprised a series of cold and warm episodes (Bradley & Jones, 1995). Marked seasonality in temperature and precipitation generally characterized the period especially throughout the seventeenth to nineteenth centuries, although the magnitude and direction of climatic shifts varied between regions across Europe (Bradley & Jones, 1995).

There is a paucity of climate information in Corsica during the LIA, consequently, hydroclimatic reconstruction is based on datasets from instrumental records and documented evidence from sites within the wider western Mediterranean basin. A widespread cooling was experienced during the second half of the sixteenth century (Lamb, 1977; Pfister, 1988, 1995;

Camuffo & Enzi, 1995; Serre-Bachet *et al.*, 1995; Briffa *et al.*, 1999), especially during the 1560s and 1570s. Glacier advances in the Swiss and French Alps were also recorded throughout the last three decades of the sixteenth century (Pfister, 1988; 1995; Holzhauser & Zumbuhl, 1999). Increases in both flood magnitude and flood frequency were recorded in northern Italy during the 1500s (Pavese *et al.*, 1995; Brown 1998; Brázdil *et al.*, 1999). Sea flooding in Venice was also more prominent during the sixteenth century (Camuffo & Enzi, 1995) together with sea storms in the Adriatic Sea (Camuffo *et al.*, 2000). Weather diaries and dendrochronological evidence suggest that relatively mild conditions were experienced during the first half of the seventeenth century, with conditions becoming cooler and wetter towards 1690 (Pfister, 1995; Serre-Bachet *et al.*, 1995). Cold conditions prevailed during the second half of the eighteenth century and into the nineteenth century. Increased precipitation throughout Europe was documented in the 1760s and 1770s (Manley, 1969; Pfister, 1995; Jones & Bradley, 1995).

The first decade of the 1800s was cold and dry in central Europe (Pfister, 1995) and SW Europe (Serre-Bachet *et al.*, 1995). The climate warmed during the 1820s, but returned to cooler conditions in the 1840s (Serre-Bachet *et al.*, 1995). The cold-warm-cold oscillation during the 1800s is displayed in numerous instrumented and climate proxy records in Europe illustrating the high temperature and precipitation variability experienced towards the end of the LIA period. Mediterranean weather stations showed distinctly wetter conditions during the 1830s, 1850s and 1880s (Maheras, 1988; Jones & Bradley, 1995). Pfister (1995) comments that there were 2.5 times as many rainy days in the summer months during 1760-1860 than throughout the following century. Records from Marseille also show that the climate was much drier in the latter half of the nineteenth century, but also more stable. This climatic characteristic is more pronounced for the October to March period than April through to September (Serre-Bachet *et al.*, 1995).

As discussed above in Chapter 2.3, the driving mechanism of the LIA and other centennial-scale climate fluctuations observed throughout the Holocene could be the result of internal forcings such as the 1,500 year cycle and ocean-atmosphere interaction (Bond *et al.*, 1997). Other possible influences include volcanic eruptions (Robock, 2000) and solar activity (Eddy, 1977; Reid, 1997; Mauquoy *et al.*, 2002). However, year to year correlations between the isotopic record and sea surface and land temperatures over the North Atlantic during the period 1840-1970 (and perhaps the decades preceding) are related to changes in atmospheric circulation patterns such as the see-saw pattern of the North Atlantic Oscillation (NAO) (Barlow *et al.*, 1993) (Chapter 6.9).

2.5 RIVER BEHAVIOUR IN THE MEDITERRANEAN

Fluvial sedimentary sequences constitute one of the longest continental records of Quaternary environmental history (e.g. Macklin *et al.*, 2002). Although other climate proxy records such as ice cores, ocean core isotopic signals and lacustrine sequences are generally more continuous, fluvial sediments and landforms still provide valuable archives of palaeoclimatic data (Maddy *et al.*, 2001). However, it is important to appreciate that river channels are one of the most sensitive components of the physical landscape and respond to a number of external (allocyclic) and internal (autocyclic) controls (Chapters 1.6.1 & 1.6.2). In any particular sequence it is often unclear as to which of these allocyclic and autocyclic mechanisms are the primary controls on river behaviour and sedimentation style. Autocyclic mechanisms (e.g. channel avulsion and migration) may modify the short-term character of the fluvial system, leading to a change in the position of the channel. Only long-term allocyclic events (e.g. tectonics, base-level change, climate and anthropogenic activity) may alter channel width, channel depth, sediment caliber, sediment discharge, slope and planform causing major architectural changes (Miall, 1996).

It has been well documented that climate change may have a profound impact on fluvial systems and this can vary in both space and time (e.g. Blum & Törnqvist, 2000) (Figure 2.6). Over longer time scales, Milankovitch cycles of the Earth's orbit and tilt predominantly drive the glacial-interglacial cycles (Chapter 2.3). Climatic and sea-level changes over this timescale may have caused local transgressional or regressional sequences to form when fluvial systems aggrade or degrade (Leeder, 1993). In sediment-starved systems incision may occur, while in periods of increased sediment flux, aggradation may occur (Jones *et al.*, 1999). On a hemispheric spatial scale and shorter cyclic timescale, the ocean circulation and the strong coupling to the atmosphere control the El Niño Southern oscillation (ENSO) and the North Atlantic Oscillation (NAO) (Figure 2.6). The latter effects Europe and the Mediterranean region and influences the decadal climatic cycle (Chapter 6.9). Migration of jet streams in response to changing ocean circulation can affect the climate on a more frequent time scale, such as the Tropical Easterly Jetstream (TEJ) over North Africa or the westerly jet stream over Europe and the Mediterranean. Enhanced precipitation or aridity on a seasonal or monthly timescale has a more local effect on river basin sediment systems in which catchment characteristics play an important role in determining channel form.

There is often much controversy however, over the relative impact of climate change in the development of fluvial systems with respect to other possible forcing factors such as sea-level change, tectonics and anthropogenic activity. Changes in the long term record can often be attributed to numerous different mechanisms but which show very similar signatures, for example, climate and tectonics (Frostick & Reid, 1989; Amorosi *et al.*, 1996; Pedley &

Frostick, 1999 and references therein) and climate and sea level (Blum, 1990). Over shorter time scales, human intervention such as deforestation (Starkel, 1991) or initiation or intensification of agricultural practices (Knox, 1987) can have an indirect affect on fluvial activity. River response to these anthropogenically induced changes can often be difficult to distinguish from centennial and millennial scale climate change. The effects of human activity can often exacerbate the geomorphic response of river systems to natural variability as the removal of original vegetation increases catchment sensitivity to climatic events (Knighton, 1998). The relative importance of human and climate-related influences on river behaviour are relevant for the Holocene period and are addressed for the Mediterranean region in Chapter 2.5.2. The following section reviews the interpretation of Mediterranean fluvial landscapes throughout the Middle and Late Pleistocene when unravelling tectonic and climate signals in sedimentary successions has always been an important issue.

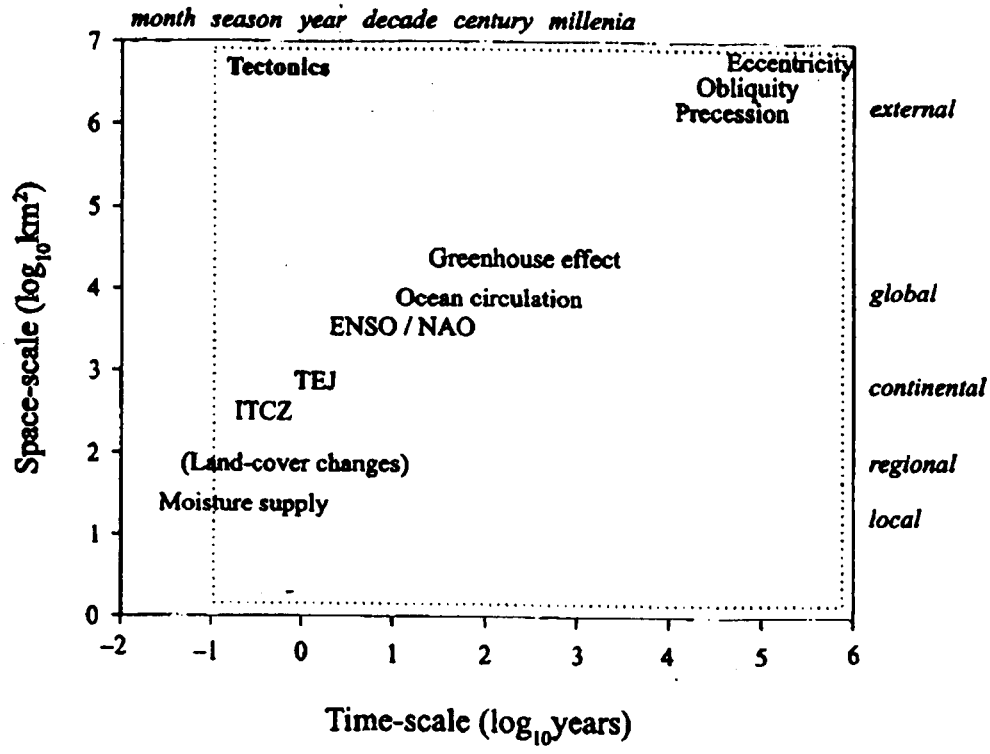

Figure 2.6 The space and timescales of various forcing mechanisms that can impact on river basin sediment systems (after Maddy *et al.*, 2001, modified from Hulme, 1994).

2.5.1 Middle and Late Pleistocene river behaviour: climate versus tectonic controls

Tectonics and structural controls have exerted a strong influence over fluvial systems in the Mediterranean basin by modifying both the size and shape of drainage basin morphologies (e.g. Collier *et al.*, 1995; Kuzucuoglu, 1995) and controlling river development in terms of changing their morphology (Macklin *et al.*, 1995). River systems are affected by tectonic processes operating both on long time scales, for example orogenic uplift or doming, and shorter time scales such as active faulting, folding and tilting processes. Quaternary tectonic activity has

been especially prevalent in the eastern Mediterranean basin affecting much of Greece and Turkey but is relatively quiescent in much the western Mediterranean, especially in the vicinity of Corsica (Chapters 3.4 & 3.5.3). A local change in valley slope or cross valley tilting induces a river response which involves the processes of aggradation and incision. It is not known however, to what extent river incision can be used to quantify both magnitude and rate of uplift (Kiden & Tornqvist, 1998; Maddy *et al.*, 2000). Where rivers flow across an area of rapid uplift or subsidence, drainage networks and long profiles can be disrupted leading to channel pattern changes and altered lateral and vertical tendencies. Earthquakes and faulting can also effect river stability and result in adjustments of channel morphology.

The influence of tectonics within each basin is very different. Within the Voidomatis region, northwest Greece, tectonic processes generally provide the underlying long term determinants on the pattern of river incision and aggradation, upon which the climatically-induced cycles of erosion and sedimentation are superimposed (Lewin *et al.*, 1991). In the Guadalope and Ebro river basins in northeast Spain, tectonic activity plays a minor role in the overall pattern of aggradation and incision cycles throughout the Late Pleistocene, although the well preserved terraces can perhaps be partly attributed to the slow uplift (~ 0.12 m/ky) in the region (Fuller *et al.*, 1998).

The evolution of dating controls over the past five decades has provided the opportunity to develop a chronology for climate change from palaeobiological indicators and independently for alluvial successions (Blum & Törnqvist, 2000). The effective limits of radiocarbon (*ca.* 40 ka) served to focus on the last glacial to interglacial transition in particular. Advances in other dating methods more recently have enabled more extensive chronological frameworks to be developed. Uranium series dating is used in environments where alluvial and colluvial sequences have been cemented by calcium carbonate (e.g. Pope & van Andel., 1984; Nemec & Postma, 1993; Maas *et al.*, 1998; Hamlin *et al.*, 2000). Infra-red stimulated luminescence (IRSL), thermo-luminescence (TL) and more recently optically stimulated luminescence (OSL) have also been widely employed in dating alluvial sequences and have a dating range in excess of 200 ka. The main advantage of luminescence methods is that the actual aggradation event can be dated rather than relying on ages that simply bracket the alluviation episode (Macklin & Passmore, 1995). TL dating was used in conjunction with electron spin resonance (ESR) and accelerator mass spectrometry (AMS) radiocarbon dating in the Voidomatis basin, northern Greece to establish the ages of alluvial sequences (Bailey *et al.*, 1990; Woodward, 1990; Lewin *et al.*, 1991). A series of sedimentary units were identified and correlated to Late Pleistocene cold stages. IRSL dating techniques have provided the basis for studies in northeastern Spain (Macklin & Passmore, 1995; Fuller *et al.*, 1996; 1998; Lopez-Aviles *et al.*, 1998). Studies conducted in the Mediterranean to evaluate the response of rivers to Mid-Late Pleistocene

environmental change with the application of reliable dating techniques are listed in Table 2.2. Other influential factors on river behaviour such as tectonics and base level change are also evaluated in several studies (e.g. Mather *et al.*, 1995; Roberts *et al.*, 1995; Mather, 2000) highlighting the complex interplay of controlling mechanisms acting on alluvial systems.

Fuller *et al.* (1998) present a 200 ka chronology of river response to climate-related environmental change in the Rio Guadalope basin, northeast Spain which constitutes one of the best documented records of Late Quaternary river behaviour for the North Atlantic region. Major aggradation phases correspond to periods of significant global cooling that are recorded in terrestrial records through analysis of pollen sequences (e.g. Burjachs & Julià, 1994; Pérez-Obiol & Julià, 1994; van Andel & Tzedakis, 1996) and revealed in ice core and marine oxygen isotope climate series (e.g. Keigwin *et al.*, 1994; McManus *et al.*, 1994; Thouveny *et al.*, 1994). Intervals of major valley infilling in the Guadalope are also coeval with Heinrich events and ice rafted debris pulses (e.g. McManus *et al.*, 1994; Stein *et al.*, 1996). The Younger Dryas, which is widely identified in northern hemisphere climate proxy records as a marked episode of climate cooling, is also linked with considerable tributary fan and trunk river sedimentation (Fuller *et al.*, 1998), as within the upper reaches of the Loire River in France (Colls *et al.*, 2001).

A detailed investigation of river activity has been conducted in northeast Mallorca, Spain (Rose *et al.*, 1999). OSL dating in conjunction with biostratigraphy was employed to build up a chronology of aggradation and incision episodes in small catchments over the last 140 ka. Alluviation was prominent during MIS 5d, 5b, 4 and 2, periods of climatic deterioration and cool temperate conditions (Rose *et al.*, 1999). The greatest thickness of fluvial sediments were formed during MIS 2. The extension and aggradation of large alluvial fans in addition to debris flow events during this period of glacial maximum are clearly evident. An extensive terrace attributed to a period spanning the LGM is also identified along the upper Loire which drains the Massif Central in France (Colls *et al.*, 2001).

It is well illustrated outside the Mediterranean region that glacial activity is a major agent of landscape modification with and influence extending well beyond the glacier margins affecting the river basin hydrology and sediment fluxes (Church & Ryder, 1972; Rose *et al.*, 1980; Macklin & Lewin, 1986; Church *et al.*, 1989). The downstream impact of glaciation upon Mediterranean river environments is poorly known however, despite the recognition of widespread occurrence of glacial features and sediments in many Mediterranean headwaters throughout the Pleistocene (Woodward *et al.*, 1995) (Chapter 4.3). One notable exception is provided by the Voidomatis River basin draining the Pindus mountains of northwest Greece where an appreciable body of geomorphological and sedimentological data has been assembled (Woodward 1990; Lewin *et al.*, 1991; Woodward *et al.*, 1992, 1994, 1995; Hamlin *et al.*, 2000).

It is believed that the Pindus Range was glaciated during the Pleistocene on at least three occasions. Glacial activity influenced the river regime by predominant spring and summer meltwater discharges accelerating sediment delivery from the headwaters to downstream reaches. The depositional environment was affected typically by large increases in both suspended and bed sediment loads dominated by glacially-derived material, a shift in channel planform and a substantial increase in the rate of valley floor accretion (Woodward *et al.*, 1995). During warmer interglacial periods, the extensive coarse grained, glacio-fluvial sediments were incised to form terraces which are now prominent landscape features.

Studies such as Fuller *et al.* (1998), Rose *et al.* (1999), and Hamlin (2000) provide an opportunity to compare river behaviour against the high resolution climate proxy records with the construction of detailed fluvial stratigraphies from accurate dating techniques such as IRSL and OSL. In broad terms, aggradation was coeval with climatic cooling during glacials or stadials when the Mediterranean forest vegetation was replaced by open scrub and frost action increased coarse sediment availability. An increase in storm frequency and enhanced seasonality of precipitation during cold periods caused by a southward shift in the jet stream (Prentice *et al.*, 1992) together with reduced tree cover is likely to have increased runoff and sediment transport. Major phases of channel incision were commonly a response to warmer conditions throughout interglacials or interstadials when i) less material was available for entrainment; ii) runoff was reduced due to more substantial vegetation cover and iii) channel flow was not so effective. This theory is reinforced by a recent review paper of Mediterranean alluviation during the last interglacial-glacial cycle by Macklin *et al.* (2002) which illustrates that river basins of varying sizes, lithologies and tectonic regimes are broadly coeval in their large scale aggradation phases during cooler intervals (Figure 2.7). Strong correlations are also identified between alluviation and Heinrich events (Macklin *et al.*, 2002) when sea surfaces temperatures were reduced and advection of low salinity Arctic water masses were weak (Bard *et al.*, 2000). This emphasizes the impact of rapid and high frequency climate variations identified in the North Atlantic region during the Last Glacial period on the Mediterranean region in terms of catchment-wide erosion and sedimentation as well as vegetation changes (Woodward *et al.*, 2001; Macklin *et al.*, 2002).

Table 2.2 Mediterranean studies which have assessed the timing and nature of fluvial activity during the Middle-Late Pleistocene (modified from Macklin *et al.*, 1995; Maas, 1998).

Reference	Region	River basin(s)	Fluvial setting	Present climate	Present tectonics	Dating control	Topic of investigation
Devereux, 1983; James & Chester, 1995	Algarve, southern Portugal	Arade, Enxerim, Lombos, Odelouca, Quarteira	Basin & range, coastal alluvial plain	Semi-arid to sub-humid	Moderate	^{14}C	River-sediment catchment source linkages, alluvial soil chronosequences
Alonso & Garzón, 1994	Central Spain	Jarama	Basin & range	Semi-arid	Moderate	^{14}C	Channel planform, sedimentation style and chronosequences
Fuller *et al.*, 1996, 1998	Northeastern Spain	Guadalope, Bergantes	Basin & range	Semi-arid	Low	IRSL	Climate and river behaviour correlation
López-Avilés *et al.*, 1998	Ebro basin, northeast Spain	Bergantes	Basin & range	Semi-arid	Low	IRSL	Floods and sedimentation in a bedrock-controlled reach
Mather *et al.*, 1995	Southeast Spain	Mula	Basin & range	Semi-arid	High	Relative dating	Impact of climate, tectonics and base-level change on river behaviour
Rose *et al.*, 1999	Northeastern Mallorca, Spain	Torrente d'es Coco, Torrente de sa Telaia Freda	Steepland, alluvial fan	Semi-arid	Low	OSL, biostratigraphy	River activity and environmental change
Barker & Hunt, 1995	Central Italy	Biferno	Basin & range	Sub-humid	High	^{14}C, archaeological	Influence of tectonics, climate and human activity on river erosion and sedimentation
Woodward *et al.*, 1992, 1994; Macklin *et al.*, 1997	Northwest Greece	Voidomatis	Basin & range, steepland	Humid	High to very high	ESR, ^{14}C AMS, U-Series	Mountain glaciation and fluvial sedimentation linkages, Upper Palaeoltihic settlement
Maas *et al.*, 1998	Southwest Crete	Aradena, Omalos, Rapanas, Samaria, Sfakia	Steepland, alluvial fan, basin & range	Semi-arid	High	^{14}C, U-Series	River response to environmental change
Rowan *et al.*, 2000	Northern Libya	Wadi Zewana	Alluvial fan	Semi-arid/arid	Low	U-Th, ESR, OSL	Reconstructing environmental change and river behaviour
Roberts *et al.*, 1995	Southern Turkey	Ibrala	Alluvial fan, basin & range	Semi-arid	High	^{14}C	Influence of vulcanicity, tectonics, climate and human activity on river development

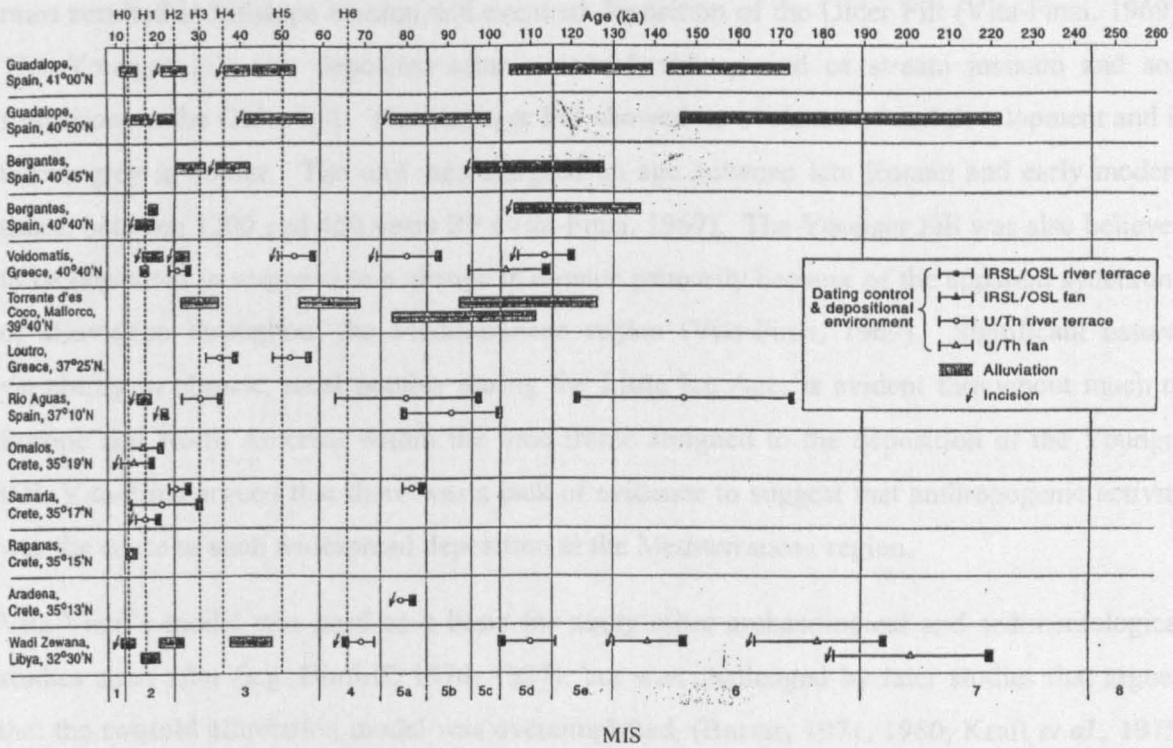

Figure 2.7 Latitudinal plot of dated Middle and Late Pleistocene alluvial units in Greek, Libyan and Spanish river basins (after Macklin *et al.*, 2002).

2.5.2 Holocene river behaviour: climatic versus anthropogenic controls

There has been much debate over the last four decades as to whether the phases of sedimentation observed in Mediterranean river basins are attributed to climate-induced factors or human intervention. Investigations identifying controls on erosion and sedimentation in the Mediterranean were initiated in the 1960s with numerous projects focusing on the relationships between Palaeolithic settlement and climatic change in Epirus, Greece (e.g. Higgs & Vita-Finzi, 1966; Higgs *et al.,* 1967). Geomorphological and archaeological surveys were conducted to assess landscape and settlement associations and climatic oscillations during the Late Pleistocene. Further work conducted by Claudio Vita-Finzi in various Mediterranean regions including Greece, Spain, Italy, Tunisia and Algeria, Morocco and Jordan culminated in the very influential and controversial volume *The Mediterranean Valleys: Geological Changes in Historical Time* published in 1969. A model of Late Quaternary alluviation history for the Mediterranean region was presented and describes a two stage depositional sequence. Two distinct valley floor sedimentary units were named the Older Fill and the Younger Fill and each phase of alluviation was followed by a period of stream incision (Vita-Finzi, 1969). The Older Fill, which was 20-40 m thick and deposited during the Late Pleistocene, between *ca.*50 and 10 ka BP, was identified by its red colouring and attributed as a response to climate change. Cold dwelling flora were identified in the Older Fill unit which reflected the severe climatic conditions experienced throughout the Last Glacial (Vita-Finzi, 1969). It was believed that an increase in frost weathering in Mediterranean uplands and the seasonal increase of more intense

rains resulted in hillslope erosion and eventual deposition of the Older Fill (Vita-Finzi, 1969). The Younger Fill was deposited after a considerable period of stream incision and soil formation on the Older Fill. The Younger Fill showed no evidence of soil development and is brown-grey in colour. The unit was assigned an age between late Roman and early modern times, between 1200 and 450 years BP (Vita-Finzi, 1969). The Younger Fill was also believed to be deposited in response to a change in climate primarily because of the apparent synchrony of alluviation throughout the Mediterranean region (Vita-Finzi, 1969). Significant natural variability in climate, most notably during the Little Ice Age, is evident throughout much of Europe and North America within the time frame assigned to the deposition of the Younger Fill. Vita-Finzi argued that there was a lack of evidence to suggest that anthropogenic activity was the cause of such widespread deposition in the Mediterranean region.

Vita-Vinzi's model was used as a basis for many other archaeological and sedimentological studies soon after (e.g. Bintliff, 1976, 1977), but was challenged by later studies that argued that the twofold alluviation model was oversimplified. (Butzer, 1971, 1980; Kraft *et al.*, 1975, 1977; Davidson, 1980; Wagstaff, 1981). Lithostratigraphical (e.g Bailey *et al.*, 1990; Woodward, 1990; Lewin *et al.*, 1991) and soil-stratigraphical approaches (e.g. Pope & van Andel, 1984; Demitrack, 1986; van Andel *et al.*, 1986, 1990) have been used to establish a more complex alluvial sequence originating from a number of extrinsic and intrinsic controls (Maas, 1998). A combination of geomorphological methods, dating techniques, archaeological finds and historical evidence led van Andel and others to identify seven periods of sedimentation in the southern Argolid, Greece (van Andel *et al.*, 1986; van Andel *et al.*, 1990). Three of these sedimentary units were found to date to the Late Pleistocene while another four marked sedimentation periods in approximately the last 5 ka of the Holocene (van Andel *et al.*, 1990). As with other parts of Greece such as the Larissa basin and the Argive plain, the Holocene sedimentation record appeared broadly coeval with human settlement and agricultural practices. Significantly, alluviation was not synchronous across the southeast regions which suggests that a 'universal agent' such as climate as suggested by Vita-Vinzi (1969), could not be responsible (van Andel *et al.*, 1986, 1990). This model was supported by other studies in other areas of the Mediterranean which demonstrated that both inadvertent and planned changes by humans have influenced and increased sediment delivery within river catchments and modified the channel form (e.g. Finke 1988; Barker & Hunt, 1995; Hunt & Gilbertson, 1995; Macklin *et al.*, 1995). The Mediterranean region is naturally vulnerable to the process of erosion, largely because of its high relief and steep slopes, thin soils and high intensity rainfall events (Woodward *et al.*, 1995). Changes in catchment vegetation cover such as excessive burning, overgrazing, agriculture expansion and intensification, all increase runoff and enhance erosion processes (Macklin *et al.*, 1995). However, short term climate variations or individual high magnitude storm events can not be excluded from causes of alluviation in the

Mediterranean (Alexander *et al*, 1994; Maas *et al.*, 1998; Grove, 2001). A full review of river response to recent decadal-centennial scale (Little Ice Age) climatic changes in Corsica is presented in Chapter 6.

2.6 SUMMARY

Major advances in our understanding of Late Quaternary palaeoclimatology have been derived from ice cores and marine sediments from which many sedimentary sequences have been closely correlated. These records illustrate the millennium scale linkage between the North Atlantic and the Mediterranean region, providing compelling evidence to discriminate between alternative mechanisms that may have generated climatic variability on such a timescale. Fluvial systems in the Mediterranean basin have responded in a similar and synchronous manner to ocean-atmosphere interactions initiated in the North Atlantic over the last interglacial-glacial cycle whereby during the cooler glacials and stadials, major aggradation predominated. More investigations are needed within the Mediterranean that provide well dated empirical records of fluvial systems in various settings and encompass the whole interglacial-glacial cycle. A robust age framework is vital for interpreting river responses to Late Pleistocene environmental change by unraveling the effects of tectonic activity, base level and climate change. The construction of a more detailed regional picture of river response to recent (e.g. LIA) short term climate variations is also important, although anthropogenic activities complicate the fluvial records by affecting flow and sediment supply. Again, good chronological controls are necessary in order to establish correlations between the alluvial archives and other palaeoenvironmental records.

3 REGIONAL SETTING AND BACKGROUND TO CORSICA

3.1 SYNOPSIS

This chapter draws upon a range of sources to outline the geographical and geological setting of Corsica. The chapter provides important context for later chapters by presenting information on the evolution of the Corsican landscape and its river systems. Many of the factors that strongly influence river regime and fluvial sedimentation style are described for the island. These include climate, tectonics, lithology, vegetation, land-use change and other features such as drainage basin sizes and drainage density.

3.2 INTRODUCTION

Corsica is centrally located in the western Mediterranean Sea between 8°E and 10°E and 41°N and 43°N and lies 170 km from southern France and 90 km from the northwest coast of Italy (Figure 3.1). The island is separated from Sardinia by the 11 km Strait of Bonifacio. Corsica is an island which rises steeply from the Mediterranean Sea and measures *ca.* 185 km by 84 km and which has a total area of 8,680 km^2. The landscape is dominated by the mountains (with 20 peaks > 2500 m) and the steep river systems draining from them. Corsica is the fourth largest Mediterranean island after Sicily, Sardinia and Cyprus.

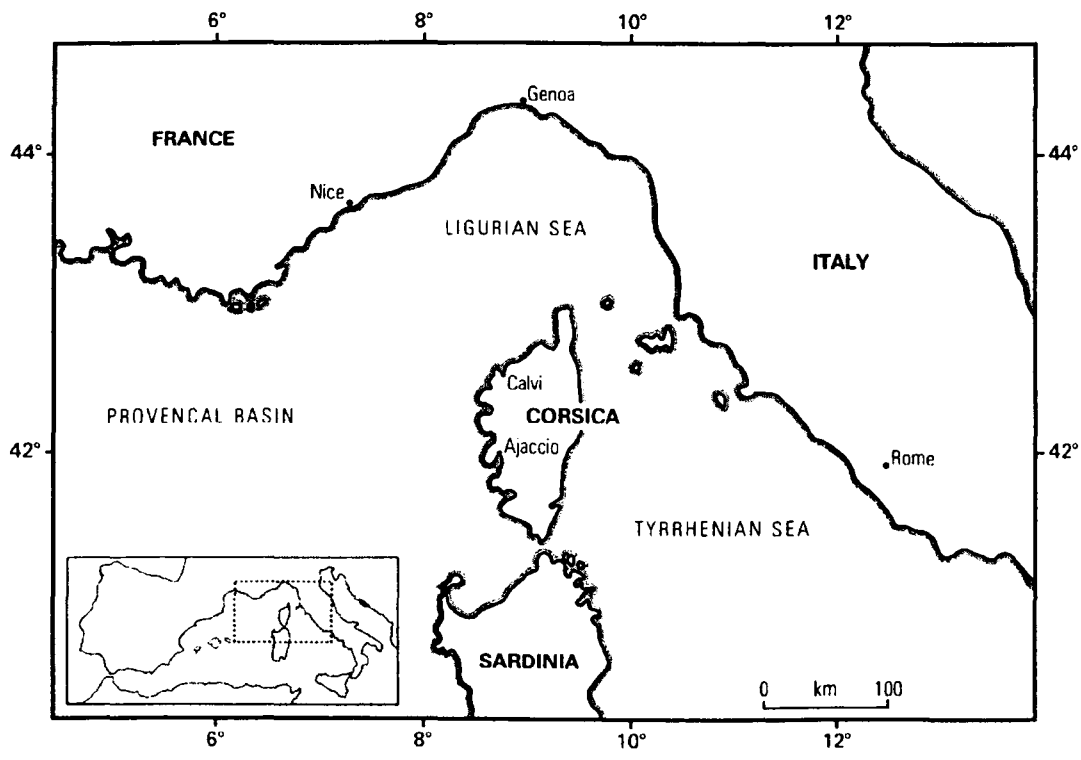

Figure 3.1 Location of Corsica in the western Mediterranean basin (modified from Conchon, 1975).

Fieldwork has been focused on four areas within Corsica. Two of them form the basis for work on the timing of glacial activity, one is associated with river response to Late Pleistocene environmental change and in the final area, river response to recent climate change is examined (Table 3.1, Figure 3.2). Each area will be described in more detail within the relevant chapters.

Table 3.1 Study areas in Corsica used in this investigation.

Location (Figure 3.2)	Study area	Focus of investigations	Chapter
1 2	Eastern flanks of Mt Giovanni Col de Vergio, Golo basin	Testing the use of cosmogenic dating to elucidate the timing of glacial activity	4
3	Tavignano River	Late Pleistocene river behaviour to environmental change	5
4	Figarella River reach	River response to recent (last 500 years) climate change	6

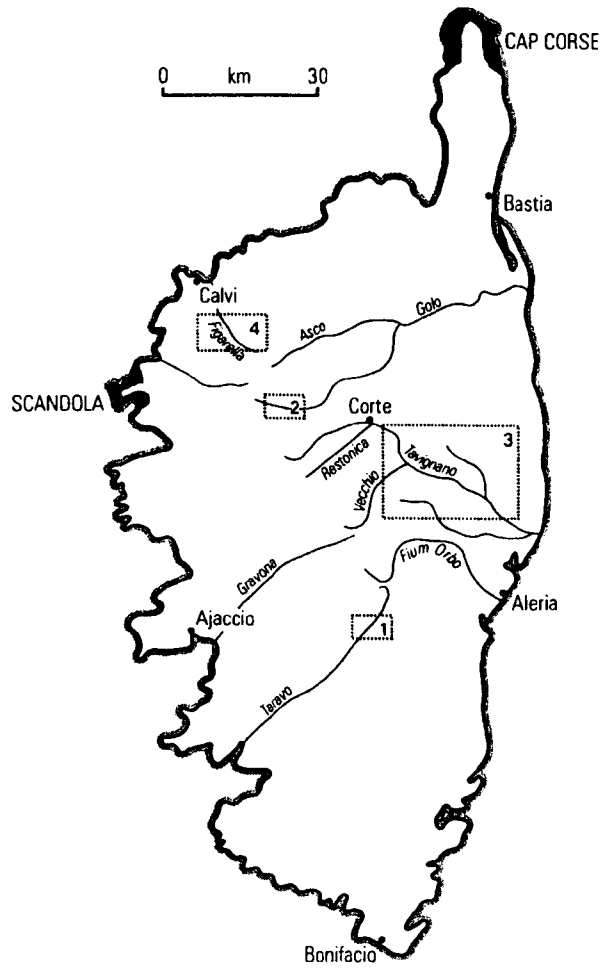

Figure 3.2 Location of study areas in Corsica (refer to Table 3.1).

The principal aim of this chapter is to describe the characteristics of the Corsican environment that play an important role in the development of river systems. For example, lithology and tectonic activity can be key factors for controlling rates of channel incision or aggradation (e.g. Jones *et al.*, 1999; Reneau, 2000). Climate change and human activity are two other factors which can have a strong influence on river behaviour through their secondary effects on

vegetation cover and runoff generation. The present climate of Corsica is also described in this chapter; a comprehensive review of climatic variability within the western Mediterranean throughout the Late Quaternary has been presented in Chapter 2. The objectives for this chapter are as follows:

i) To describe the pre-Quaternary geological history of Corsica and the main lithological units on the island of Corsica.

ii) To review Quaternary tectonic activity and sea-level changes.

iii) To describe the relief and drainage network of Corsica.

iv) To document the present climate of Corsica and vegetation cover.

v) To outline current understanding on the major changes in vegetation patterns in Corsica as a result of human occupation and land-use change during the Holocene.

3.3 PRE-QUATERNARY GEOLOGICAL SETTING

The evolution of the Corsican landscape is closely linked to the long-term tectonic history of the wider western Mediterranean basin. During the Palaeozoic (*ca.* 570-245 Ma) and Mesozoic (*ca.* 245-66 Ma) eras, Corsica was part of the southern mainland of France. A period of mountain building was initiated in Hercynian times (the last 100 m years of the Palaeozoic) and a unit of continental crust formed what is now the granitic backbone of the Corsican-Sardinia massif (Figure 3.3). Towards the end of the succeeding Mesozoic Era, compacted sedimentary material was thrust upwards as the African and Eurasian continental plates collided (Dewey *et al.*, 1973; Smith and Woodcock, 1982; Pasquale *et al.*, 1997; Bassi *et al.*, 1998). Compression continued throughout the first half of the Cenozoic (from 66 Ma) and formed the Alpine and Apennine mountain chains. Alpine Corsica, the northeastern part of the island is a southerly prolongation of the western Alps. This structurally complex unit consists of a stack of nappes derived from either oceanic protoliths (ophiolitic schistes lustrés) or continental basement which have been deformed and metamorphosed and thrust westward upon the continental unit of western Corsica (Jolivet *et al.*, 1991; Egal, 1992; Brunet *et al.*, 2000). Conglomerates of Middle Eocene age are exposed between the western granitic part and the eastern schistes lustrés (Carmignani *et al.*, 1995).

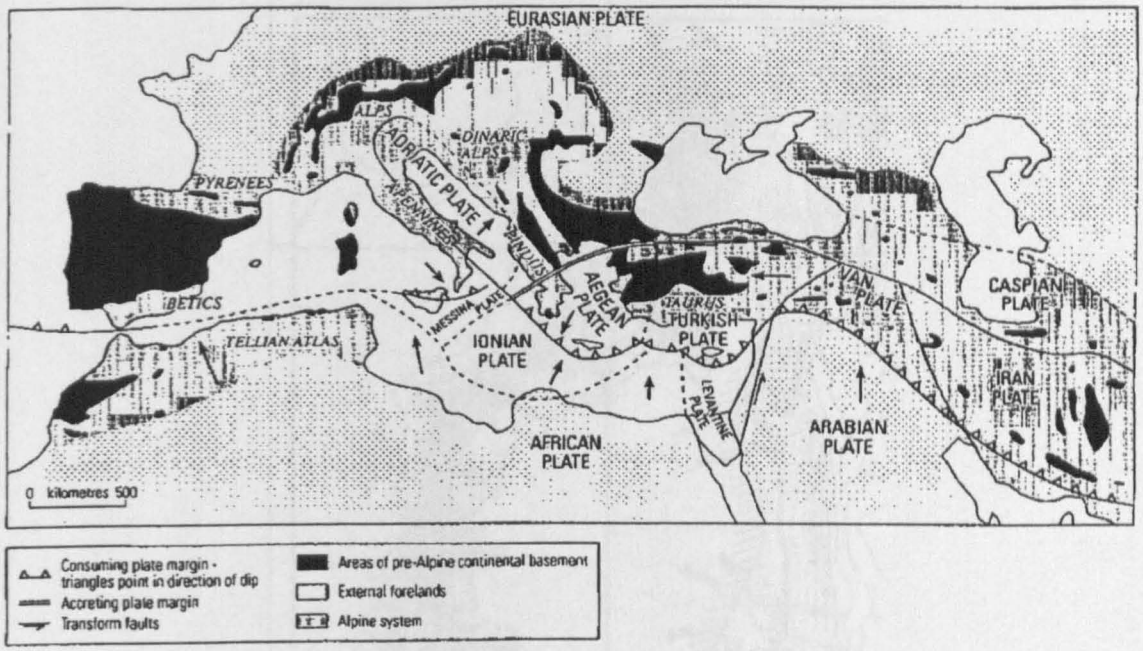

Figure 3.3 The present lithospheric plate configuration and types of plate boundary in the Mediterranean basin together with the distribution of pre-Alpine continental basement (after Dewey *et al.*, 1973 and Windley, 1984, from Macklin *et al.*, 1995).

During the late Oligocene (*ca.* 25-30 Ma) compression ceased in the Alps and the Corsican and Sardinian blocks rotated anticlockwise to their present positions (Jolivet *et al.*, 1991; Bassi *et al.*, 1998; Jolivet & Faccenna, 2000) due to regional extension and westward subduction of the Adriatic plate (Malinverno & Ryan, 1986; Egal, 1992; Pasquale *et al.*, 1997). This led to the opening of the Balearic and Liguro-Provencal oceanic basins and the Tyrrhenian Sea (Bassi *et al.*, 1997; Jolivet & Faccenna, 2000) and crustal doubling and overthrusting in the northern Apennines (Pasquale *et al.*, 1997). The Hercynian basement of the Corsica-Sardinia massif constitutes the hinterland of the Northern Apennines collision belt and is characterized by northeast trending transcurrent faults associated with the compressional margin (Carmignani *et al.*, 1995). These major faults are exploited by river systems such as the Tavignano. During the Miocene (*ca.* 24-5 Ma), shallow marine sediments were deposited in the south (Bonafacio), and the southwest of Cap Corse (Saint Florent) in northern Corsica (Figure 3.5) on the metamorphic rocks exhumed through extension (Carmignani *et al.*, 1995). The marine basin surrounding Corsica clearly shows that the western side of the island is steep and rocky and the eastern shelf is of a gentler gradient (Figure 3.4). Many of the main rivers draining into the Tyhrrenian Sea such as the Tavignano and the Golo once extended over 15 km beyond present day limits when the sea-level was lower.

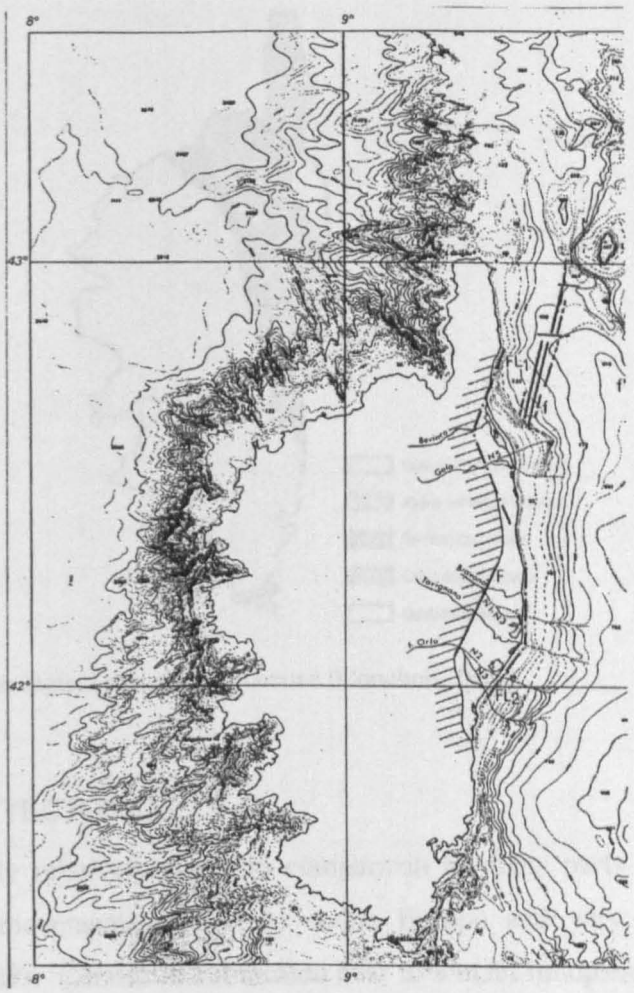

Figure 3.4 The marine basin of Corsica which characterizes the west as steep and rocky and the eastern side more gently sloping (Conchon, 1975).

3.3.1 Geological structure of Corsica

In summary, Corsica can be broadly divided into five geological units, although the island is essentially made up of two main parts; granite in the west and south, and schist in the north and east (Figure 3.5). The west is Hercynian in origin and formed of crystalline rocks (granite, gneiss and diorite) and is part of the Corsican-Sardinia massif, a Palaeozoic basement. The eastern part consists of younger sedimentary and metamorphic rocks (schist, slate and shale) and relates to the Alpine continental system. A central depression composed of Jurassic to Pliocene age sedimentary basins separates Hercynian Corsica from Alpine Corsica and extends from the northwest to the southeast. Outcrops of calcareous Miocene rocks are present only in the north and southernmost parts of the island. Quaternary alluvium lines the narrow eastern plain, the only significant expanse of flat, low lying land on the island. A range of Quaternary deposits is also present in all of the river valleys.

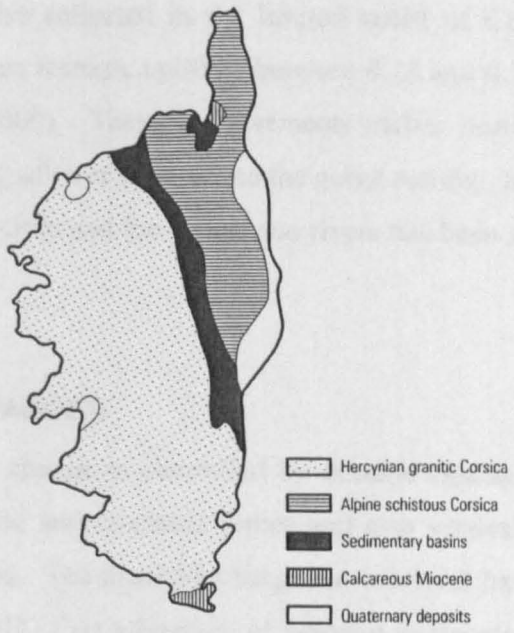

Figure 3.5 Simplified geological structure of Corsica (Conchon, 1975).

3.4 REGIONAL TECTONICS

Corsica is tectonically relatively stable in comparison to many parts of the Mediterranean, showing no lateral movements relative to stable Europe and very little seismic activity (Beccaluva *et al.*, 1989). Corsica is not located near to a main lithopsheric plate or microplate boundary (Figure 3.3) and only shallow microseismic events have been recorded on the eastern side of the island (Rebai *et al.*, 1992; Ferrandini *et al.*, 1994). The western margin of Corsica is aseismic. Sardinia and most of the northern Tyrrhenian region are also inactive (Flemming, 1969; Laborel *et al.*, 1994; Pasquale *et al.*, 1997) (Figure 3.6).

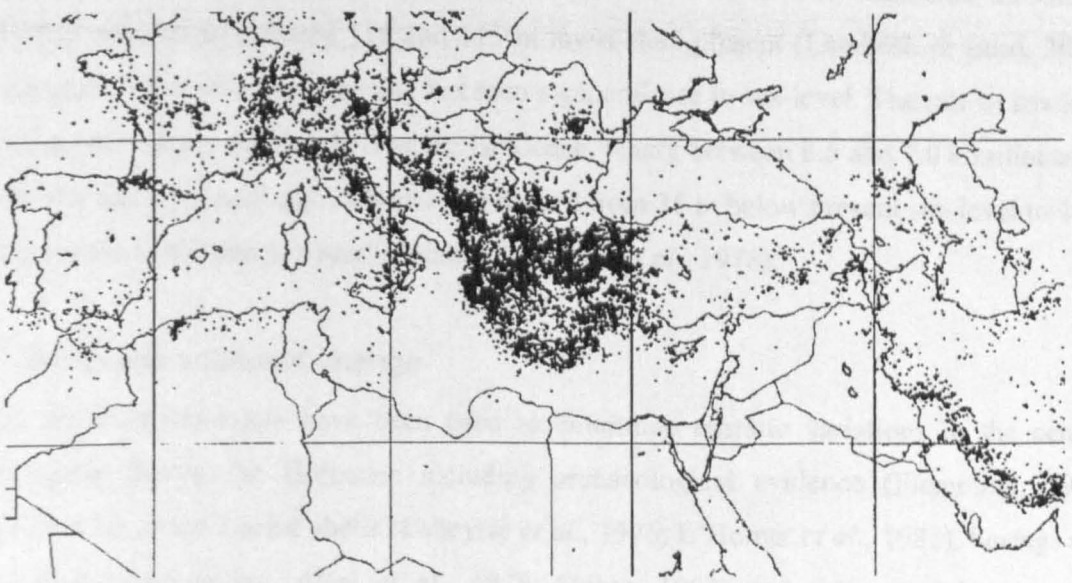

Figure 3.6 Seismicity map of the Mediterranean region plotted from data compiled by the National Earthquake Information Center of the US Geological Survey, showing all events above magnitude 4 between 1970 and 1989 (after King *et al.*, 1997).

The low seismicity is also reflected in the limited uplift of Corsica. Western Corsica is believed to have undergone tectonic uplift of between 0.15 and 0.3 mm per year for the last 3 ka (Lambeck & Bard, 2000). Tectonic movements earlier during the Quaternary are also inferred from the changing of river courses and the gorge cutting. In addition, upwarping of the fluvial terraces along the Golo and the Tavignano rivers has been reported by Conchon (1975, 1978) (Chapter 5.3.2).

3.5 SEA-LEVEL CHANGES

In broad terms, sea-level change is controlled by eustatic (glacial advance and retreat) and isostatic (glacial depression and rebound) forces and also vertical displacements originating from local tectonic stresses. The resultant changes in sea-level have widespread effects upon river behaviour (Bull, 1991). One advantage of working in steepland river systems is that the effect of sea-level change is regarded to be relatively insignificant in most of the catchment (Macklin *et al.*, 1995). Eustatic effects are more important in the lower reaches where the change in base level has a more direct impact on the rate of incision or aggradation to attain profile equilibrium (Kraft *et al.*, 1975, 1977; van Andel *et al.*,1990b).

3.5.1 Late Pleistocene sea-level change

In the last interglacial stage (5e) (*ca.* 120 ka) the sea-level in Corsica was higher than that of today (Figure 3.7). In the western Mediterranean this MIS 5e sea-level was a few meters above the present sea-level (Kindler *et al.*, 1997; Lambeck & Bard, 2000). During the Last Glacial Maximum (*ca.*18 k radiocarbon years BP) sea-level was at its lowest, estimated around the island of Corsica to be between 110 and 115 m lower than present (Lambeck & Bard, 2000). Over the past 15 kyr, climatic warming has seen a general rise in sea-level. The rate of sea-level rise was greater during the first half of the Holocene, where between 8.5 and 7.0 k radiocarbon years BP the sea-level rose approximately 22 meters from 36 m below present sea-level to 14 m yielding a rate of 14.7 mm per year (Figure 3.8) (Aloisi *et al.*, 1978).

3.5.2 Holocene sea-level change

Various sea-level indicators have been used to determine eustatic variations in the central Mediterranean during the Holocene including archaeological evidence (Flemming, 1969; Pirazzoli, 1976), dated marine shells (Labeyrie *et al.*, 1976; L'Homer *et al.*, 1981), borings and palynological observations (Alosi *et al.*, 1978; Dubar, 1987) and submerged beach rocks (Nesteroff, 1984). Many studies however have used biogenic littoral rims built up by coralline concretions (coralligène) to establish Holocene sea-level curves (Laborel *et al.*, 1994; Sartoretto *et al.*, 1996). Coralline algal buildups are abundant on the southern French coast and

on the rocky western coast of Corsica and are situated between 10 and 60 m below present sea-level. Laborel *et al.* (1994) employed this method to determine the rate of sea-level rise for two sites in Corsica, Cap Corse in the north and Scandola on the west coast (Figure 3.2). The northern and western coasts of Corsica experienced a rise of 1.6 m over the past 4.5 ka, and of a rate 0.4 mm per year between *ca.* 4.5 and 1.5 ka and 0.2 mm per year since 1.5 ka.

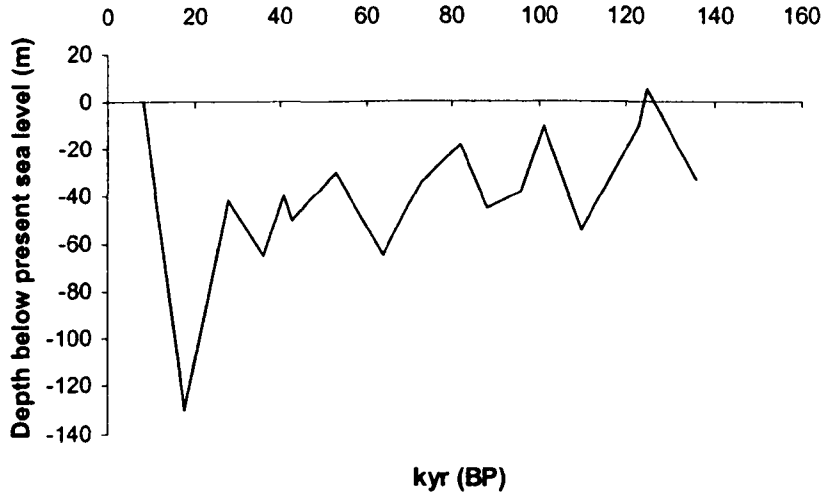

Figure 3.7 Late Pleistocene global eustatic curve indicating sea-level change (MIS 6-2) derived from δ^{18} variations (Chapell and Shackleton, 1996).

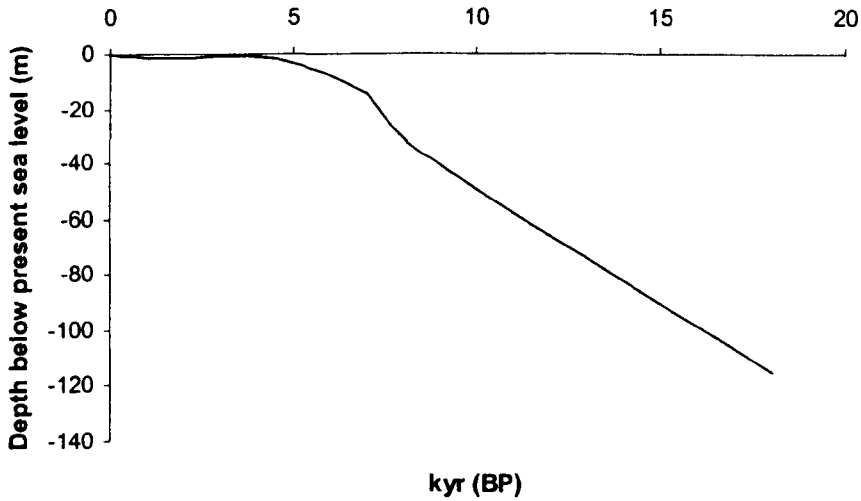

Figure 3.8 Sea-level rise around the coast of Corsica from the Last Glacial Maximum (drawn from data within Alosi *et al.*, 1978; Laborel *et al.*, 1994 and Lambeck and Bard, 2000).

3.5.3 Tectonic uplift derived from sea-level change

Lambeck & Bard (2000) compared the coralline data of Laborel *et al.* (1994) to their model of Holocene sea-level rise to establish possible vertical tectonic movements within Corsica. They suggested that western Corsica may have experienced slow tectonic uplift of between 0.15-0.3 mm per year for the past 3 kyr but northernmost Corsica is tectonically stable. The last interglacial shoreline is believed to be 20-40 m above present sea-level which is in agreement with Conchon (1988, 1989) who attributes marine sediments lying at an elevation of over 20m on the steep western coast of Corsica to MIS 5e.

3.6 TOPOGRAPHICAL FEATURES

The terrain of Corsica is largely mountainous, with 1,700 summits ranging in elevation from 300 to over 2,700 m. Two thirds of Corsica consists of an ancient crystalline massif that divides the island on a northwest to southeast axis and has a cluster of peaks exceeding 2,000 m. The highest peak is Mount Cinto which attains an elevation of 2,706 m and lies only 24 km from the western coast (Figure 3.9). Other massives include Monte Rotondo (2,622 m), Monte d'Oro (2,389 m), Monte Renoso (2,352) and Monte Incudine (2,128 m). The mountains descend steeply in parallel ranges to the west where the coast is cut into steep gulfs and is marked by high cliffs and headlands. To the east the mountain massif falls in broken escarpments to extensive alluvial plains. The schistous mountain range of Alpine Corsica in the northeast does not exceed a height of 1,765 m (Figure 3.9).

3.6.1 Glaciation in Corsica

Conchon (1975, 1982) has argued that the upper valleys in Corsica were glaciated at least four times (glacial or stadial stages) during the Quaternary. Glacial features show that all the high peaks (>2,000 m) were glaciated during the Quaternary (Conchon, 1975, 1985, 1988). Pleistocene glaciers of alpine type are inferred from erosional landforms and glacial sediments. Lateral moraines in the southern part of the mountain range (Monte Renoso massif) are better preserved than those further to the north (Monte Cinto, Monte Rotondo massives). Sediments from the oldest glaciation are inferred to be pre-Würmian in age (Chapter 4.3.3) (Conchon, 1975).

Two stages of valley glacier development have been proposed within the Würm period (Conchon, 1975, 1986). The glacier fronts have been reconstructed from lateral moraines, glacial deposits and glaciofluvial sediments and have been recorded at 700-1,100 m and 1,100-1,250 m elevation for the oldest and youngest glaciers respectively (Conchon, 1975). The glaciers were up to 7 km long. Subsequent glaciers had lengths between 3.5 and 5 km and a corresponding snowline of altitude 1,700-1,800 m. During the Lateglacial stage it is believed

that small glaciers occupied cirques at higher elevations between 1,600 m and 2,100 m in altitude. Reille *et al.* (1997) have argued from pollen data that Corsica has been ice free since the Alleröd (*ca.* 12.5 k radiocarbon years BP).

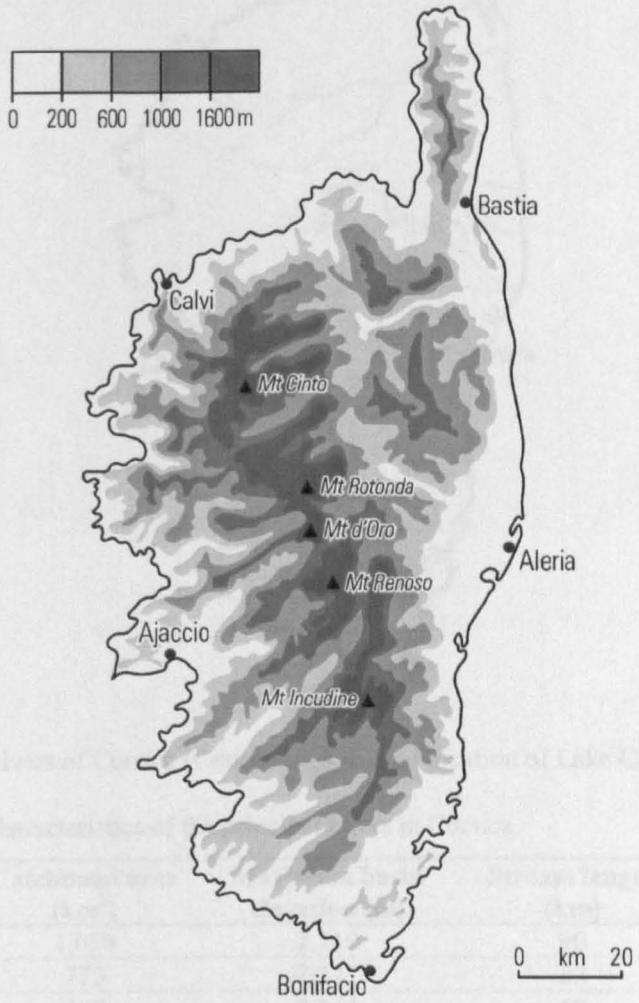

Figure 3.9 Relief and highest summits of Corsica.

3.6.2 Drainage network and hydrology

Both the eastern and western watersheds are drained by seasonally torrential rivers that rise in the mountainous centre and make their way through impressive gorges in the upper reaches to the coastline. These short steepland river systems are typical of the wider Mediterranean region (Macklin *et al.*, 1995). The principal rivers of the island are the Golo, Tavignano, Fium Orbo to the east and the Gravona and Taravo to the southwest (Figure 3.10) and their main characteristics are given in Table 3.2.

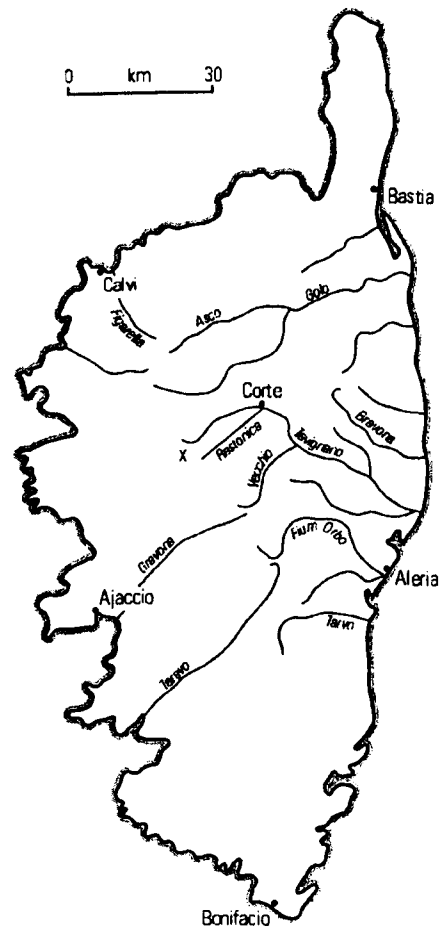

Figure 3.10 Principal rivers of Corsica (Conchon, 1975) and location of Lake Creno (x).

Table 3.2 Catchment characteristics of the principal rivers in Corsica.

River	Catchment area (km^2)	Maximum basin elevation (m)	Stream length (km)	Glaciated headwaters
Golo	1,050	2,710	90	√
Tavignano	775	2,327	82	√
Gravona	590	2,352	50	√
Taravo	480	1,950	64	√
Fium Orbu	255	2,352	44	√

In general, flow is low to moderate from June to September and often high from October through to May. A strong early spring peak flow is due to snowmelt. Flooding often occurs in summer as a result of thunderstorm activity, frequently enhanced by orographic rain, but its occurrence is often localized and the storms rarely last longer than two days. Flooding across the western Mediterranean is more common in the autumn, due to cyclonic disturbances that originate within the Mediterranean Basin (Chapter 3.7). Intense precipitation events in Corsica create high discharges and, together with the steep mountain environment provide the energy to transport a large quantity of sediment which can alter channel morphology. Material over 1 m in diameter was transported downstream by the Gravona River on 12 November 1980 when over 200 mm of rain fell in the headwaters over a 24 hour period (Conchon & Gauthier, 1985). Evidence of a large flood is also preserved within the channel of the Stanciacone river which

drains the Haut Asco region and flows into the L'Asco and Golo rivers downstream (Figure 3.10). The boulders deposited were in excess of 3 m diameter (Figure 3.11).

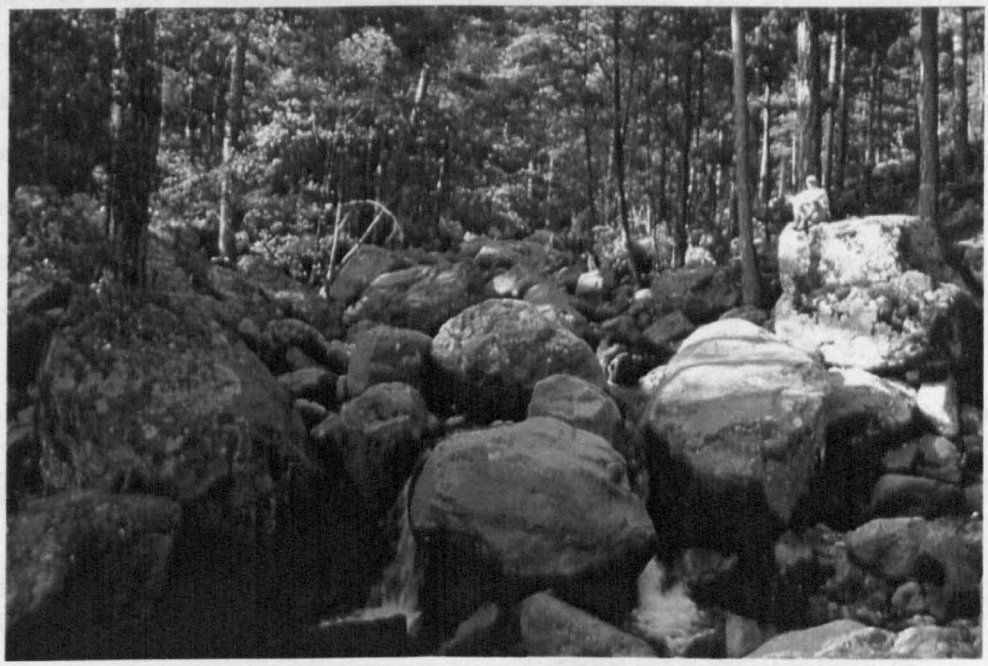

Figure 3.11 Large flood deposits within the Stranciacone river channel which leads into the Asco and Golo rivers. This photograph illustrates the competence of rivers in steep mountain catchments.

Recent discharge data for the rivers in Corsica could not be obtained. However it is documented that the larger rivers such as the Tavignano and the Golo have an average annual flow of 40-50 m^3s^{-1}, with regular high flows of up to 100 m^3s^{-1} (Conchon, 1975). The water levels are very irregular throughout the year, often rising abruptly in autumn and spring. For example, flow fluctuated from 0.42 m^3s^{-1} one day in September 1961 on the Golo river to 84.1 m^3s^{-1} in November (Conchon, 1975). Large floods on the Golo have been estimated in excess of 1,000 m^3s^{-1} in 1938 (Conchon, 1975). Similar discharges are believed to have occurred on the Tavignano (Conchon, 1975).

3.6.3 Flow regime during the Late Quaternary glacial and stadial periods

During the Quaternary cold stages, river regimes were probably more seasonal than at present and exhibited greater spatial and temporal variability (Macklin *et al.*, 1995). For the glaciated catchments in Corsica, low flow would have been during the winter months when precipitation fell as snow in the glaciated catchments. High flows would have occurred in spring and summer mainly due to snow and ice melt. Unlike present day conditions, a more continuous flow would have characterized the summer months, rising with increasing temperature. The high energy flow would also be efficient at transporting glacially-derived sediment and the principal rivers would likely have been braided in planform.

3.7 PRESENT CLIMATE

The geographical location and steep relief of Corsica are two factors which result in the island having a wide range of temperatures and precipitation totals. The wider Mediterranean basin lies between subtropical and mid-latitude atmospheric patterns and is sensitive to any shift in the boundary (Macklin *et al.*, 1995). The Mediterranean Sea and local orographic effects also strongly influence the climate of Corsica and the hydrology of the river basins. The steep relief of Corsica produces three main climatic types on the island (Table 3.3). Coastal and low altitudes experience a Mediterranean climate, whereas elevations between 600 and 1,200 m offer a continental variation and alpine features are characteristic of elevations above 1,200 m.

Table 3.3 Characteristics of the three climatic types identified within Corsica (after Simi, 1964; from Reille *et al.*, 1997).

Altitude (m)	Mean annual temperature (°C)	Annual precipitation (mm)	Climate characteristics
0-600	14-17	600-1100	Mild and humid. Long summer drought
600-1200	10-13	800-1500	High altitude Mediterranean climate. Shorter dry season than 0-600 m
>1200	<10	>1500	Very cold high altitude Mediterranean climate. Short, or non-existent summer drought

3.7.1 Temperature and precipitation

The temperature and precipitation regime of Ajaccio, the capital of Corsica situated at sea-level and on the west coast (Figure 3.1) is illustrated below in Figure 3.12. The maximal average of the temperature on the coast is 18°C and is between 23 and 36°C in the summer months. In winter, the monthly means generally exceed 6°C and the minima rarely drop below zero (Ballais, 1998). Precipitation is relatively abundant in Corsica, averaging about 655 mm a year and falling on about 115 days of the year. Higher elevations receive considerably more precipitation and it is clear that the rainfall distribution in Corsica strongly reflects relief (Figure 3.13). There is snow above *ca.* 1,500 m from September to May.

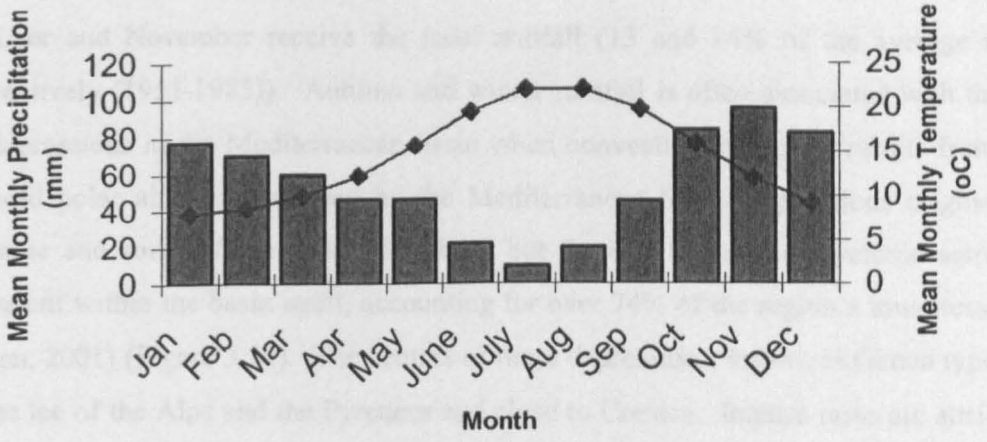

Figure 3.12 The average monthly temperature and precipitation in Ajaccio for the years 1951-1985 (WCD, Chadwyck and Healey, 1992).

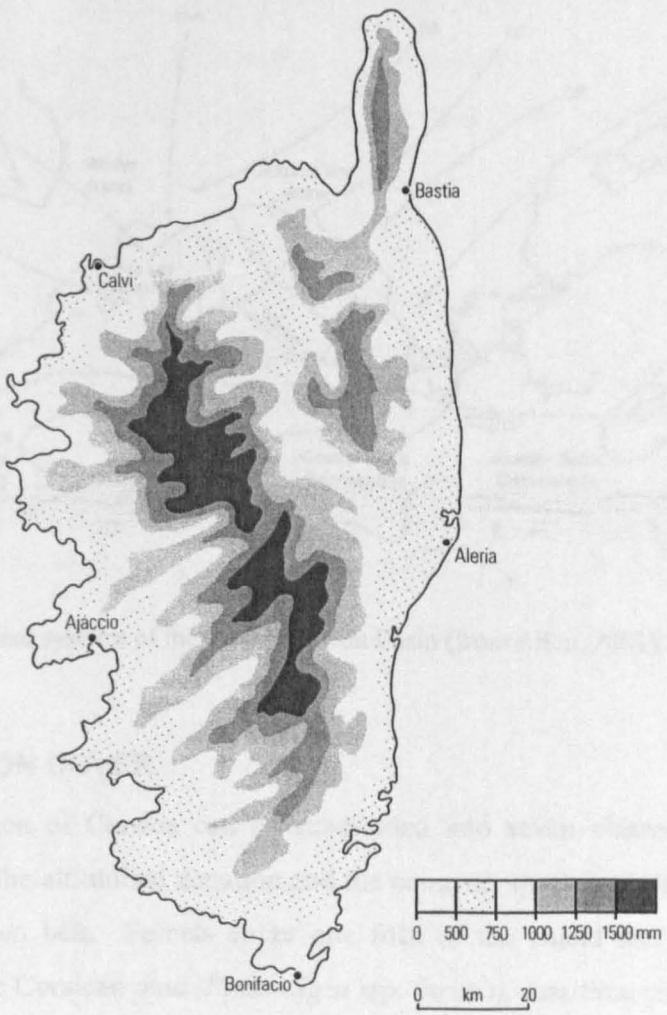

Figure 3.13 Mean annual precipitation across Corsica (after Simi, 1964; modified from Conchon, 1982).

3.7.2 Cyclonic activity

October and November receive the most rainfall (13 and 14% of the average annual total respectively (1951-1985)). Autumn and winter rainfall is often associated with the formation of depressions in the Mediterranean basin when convective instability results from incursions of cold polar air being warmed by the Mediterranean Sea. Depressions originate over the Atlantic and south of the Atlas Mountains but the development of cyclonic activity is most prevalent within the basin itself, accounting for over 74% of the region's low-pressure systems (Allen, 2001) (Figure 3.14). The centres of these depressions, known as Genoa types, originate in the lee of the Alps and the Pyrenees and close to Corsica. Intense rains are attributed to the warm front and heavy showers and thunderstorms follow behind the cold front. Cyclonic activity in the autumn is often the cause of major flooding in Corsica and much of the western Mediterranean. Recent flood events and the forcing factors for large floods are described in more detail in Chapters 6.4.2 and 6.4.3.

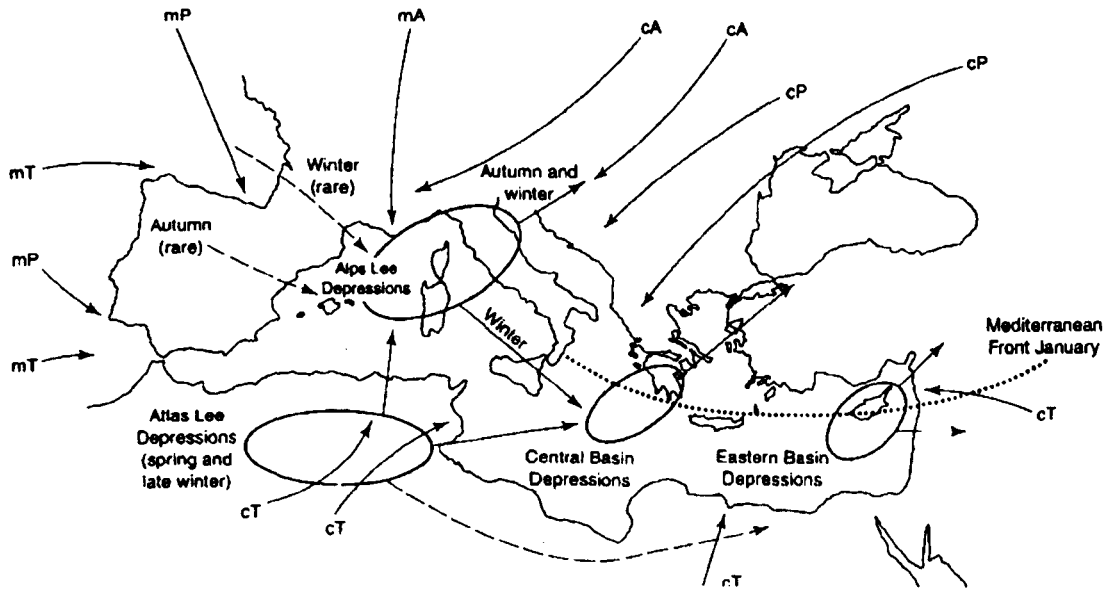

Figure 3.14 Depressional systems of the Mediterranean Basin (from Allen, 2001).

3.8 VEGETATION COVER

The present vegetation of Corsica can be subdivided into seven classes (Gamisans, 1991). Table 3.4 illustrates the altitudinal zonation and the common species of shrubs and trees found within each vegetation belt. Forests cover one fifth of the island and the main woodland species in Corsica are Corsican pine *(Pinus nigra ssp. laricio),* maritime pine *(Pinus maritima),* downy oak (*Quercus pubescens)* and beech *(Fagus sylvatica).* Chestnut forests occur at slightly lower elevations.

The Corsican pine is one of the most common and widespread trees in Corsica colonising the mountain and supramediterranean belts (Table 3.4). Corsican pine grows within a fairly large

climatic range where the annual precipitation is 800 to 1,800 mm and the temperature is between 12 and 7°C. The Corsican pine is characterized by a very straight trunk and can reach a height of 50 m and may live up to 1,000 years. The tree has a pioneer role in forest recolonisation. In forest where birches and firs have been felled, Corsican pine can establish and maintain itself easily and for a quite a long time until the natural regeneration of firs and beech trees. The Corsican pine generally occupies the southern slopes where it does not have to compete with these two species and on the poor and rocky substrata. The tree limit of *Pinus nigra laricio* is 1,800 m, a similar elevation to other species in Corsica but abnormally low in general for such southerly mountains (Reille *et al.*, 1997).

The typical vegetation growing above the treeline in Corsica in the high mountains include alder bushland (*Alnus virisis spp. Suaveolens*). The bush grows 1-3 m in height and consists of trunkless shrubs that form an impenetrable thicket. This vegetation is described as subalpine in Table 3.4. Silver birch (*Betula pendula*) is also evident in the lower part of the subalpine vegetation belt but predominates in the mountain belt and has a discontinuous distribution in the supramediterranean belt, *ca.* 500-1,300 m. Silver birch often forms open woodland with Corsican pine (*Pinus nigra laricio*), but is far less tolerant to drought than its counterpart (Reille *et al.*, 1999).

The unforested landscape of Corsica is characterized by vast pastures or abandoned areas without hedgerows (Said & Gegout, 2000). The pasture land is mainly covered with maquis, a scrubby underbush that is composed of aromatic, thorny or toxic shrubs of which many are fire resistant. The seedlings of non-resistant woody species are grazed by the livestock. The unpalatable evergreen shrubs usually present on the grassland include species such as gorse, barberry and juniper (Saïd & Gégout, 2000). Holm oak (*Quercus ilex*) and cork oak (*Quercus suber*) are also often found growing amongst the maquis on the lower ground.

Table 3.4 Altitudinal zonation of present vegetation in Corsica (modified from Reille *et al.*, 1997).

Vegetation belt	Altitude (m)	Vegetation type	Species present
Thermomediterranean	<150 in the south <100 in the north	Shrubs Maquis	Pistachio *(Pistacia lentiscus)* Evergreen oak *(Quercus ilex)* Olive *(Olea europaea)*
Mesomediterranean	0-700 (northern slopes) 0-900 (southern slopes)	Maquis	Heather *(Erica arborea)* Strawberry tree *(Arbutus unedo)* Cork oak *(Quercus suber)* Maritime pine *(Pinus pinaster)* Downy oak *(Quercus pubescens)* Sweet Chestnut *(Castanea sativa)*
Supramediterranean (Eurosiberian flora as abundant as the Mediterranean flora)	500-700 to 900-1,000 (northern slopes) 800-1,000 to 1,200-1,350 (southern slopes)	Maquis Varied forest Mixed woodstands	Heather *(Erica arborea)* Holm oak *(Quercus ilex)* Sessile oak *(Quercus petraea)* Downy oak *(Quercus pubescens)* Corsican pine *(Pinus nigra spp. laricio)* Silver birch (*Betula pendula*) Alder *(Alnus cordata)* Holly *(Ilex aquifolium)* English Yew *(Taxus baccata)* Hop-hornbeam *(Ostrya carpinifolia)*
Mountain (Eurosiberian flora up to 75%)	900-1,000 to 1,600 (northern slopes) 1,300 to 1,800 (southern slopes)	Forest	Corsican pine *(Pinus nigra spp. laricio)* Beech *(Fagus sylvatica)* Silver fir *(Abies alba)* Silver birch (*Betula pendula*)
Cryo-oromediterranean (Mediterranean flora > Eurosiberian flora because of the dry soils)	1,700-1,800 to 2,200 (southern slopes and crests only)	Dwarf bush (Grassland on windy crests)	Broom/gorse *(Genista lobelii)* *(Astragalus sirinicus ssp. Genargenteus)* *(Anthyllis hemanniae)* Thyme *(Thymus Herbabarona)* Barberry *(Berberis aetnensis)* Juniper *(Juniperus communis spp. alpina)*
Subalpine (61-82% Eurosiberian flora)	1,400-1,600 to 2,100 (northern slopes only)	Thick bushland (1-3 m in height)	Alder *(Alnus viridis spp. suaveolens)* Sycamore *(Acer pseudoplatanus)* Rowan *(Sorbus aucuparia)*
Alpine	> 2,100	Sparse vegetation, very arid conditions	62 endemic species, comprising 45% of flora available in this vegetation belt

3.8.1 Implications for runoff and slope stability

The summits of the highest mountains and the immediate flanks which surround them, often comprising scree, do not exhibit a vegetation cover. Factors such as the high altitude (>2,000 m) and low winter temperatures, the steep gradients and a lack of soil, prohibit vegetation growth but promote rapid runoff. However, the dense alder bushland characteristic of the mountain belt which varies between 900 and 1,800 m in elevation (Table 3.4) is a good interceptor of precipitation and a stabilizer of hillslopes. So too are the woodlands at lower altitude. Overall, Corsica's vegetation cover is relatively dense compared to other western Mediterranean countries, particularly Spain. Present day erosion rates are therefore likely to be considerably lower.

As well as climate and vegetation cover, the lithology has an important underlying influence on erosion. The marls and sandstones in areas like the Ebro basin in Spain are associated with rilling, gullying and badlands topography (Allen, 2001). Desertification is a great problem and projects such as MEDALUS have been attempting to quantify such factors since 1990 and develop solutions to moderate soil degradation in the Mediterranean since 1990. The granite lithology of Corsica, although impermeable and tending to enhance the flashy regime of steepland catchments, is not susceptible to such high sediment losses. In the Iberian Peninsula, erosion rates from marl are reported as 266 $tha^{-1}yr^{-1}$ whereas on granite surfaces the rate is 7.3 $tha^{-1}yr^{-1}$ (Conacher & Sala, 1998). Granite is susceptible to physical weathering processes such as freeze-thaw activity which is very effective at breaking the rock up into smaller fragments. During cooler times in Corsica, frost shattering would have been an important process. Sediment availability for fluvial transport would have been greater at these times, accentuated by the lack of vegetation due to the lower temperatures. Today, soil erosion is not a major problem in Corsica as the land is relatively well vegetated, due partly to the relatively high rainfall but also to the less intense anthropogenic activity and land-use (Chapter 3.9).

3.9 CULTURAL HISTORY AND LAND-USE CHANGE

The earliest known evidence of human presence on Corsica is Pre-Neolithic, 8.56 ± 0.15 kyr (Conchon, 1982; Grove & Rackham, 2001). Since then, deforestation resulting from felling or burning episodes over the last eight millennia has reduced the natural area of the deciduous oak (*Quercus*) forest and other wildwoods (Grove & Rackham, 2001). Maquis, steppe and savanna have since expanded, partly through burning, woodcutting and keeping livestock in the remaining natural vegetation (Grove & Rackham, 2001).

Prior to the nineteenth century, there is no great change visible in the lowland pollen record when the first settlements were established (Grove & Rackham, 2001). This may be because Corsica's population was spread out between thousands of hamlets a kilometer or so apart. In

contrast, Sardinia, also a mountainous island with a granite landscape, displayed scores of large villages and small towns separated by 20 km or more of empty countryside (Grove & Rackham, 2001). The demand on the land in Sardinia in the vicinity of the towns would have been far greater than Corsica and led to intensification of deforestation and agricultural practices.

There is evidence from maps and documents that between 1830 and 1840, when the local fisheries and marine transport fulfilled local needs, the slopes of Cap Corse in northern Corsica were not cultivated (de Raparaz, 1990). With the introduction of steam boats and big shipping companies and an increasing population between 1850 and 1880, people cleared the hillsides and organized a system of terraces which covered entire slopes. Having been in use for less than a lifetime, the terraces were then abandoned at the end of the nineteenth century when people migrated to the larger towns and the mainland for a more rewarding and less strenuous means of gaining a livelihood (de Raparaz, 1990) (Figure 3.15). Within fifty years from 1900, the population of Corsica dropped by a third from 300,000 to 200,000 (de Raparaz, 1990).

Figure 3.15 Abandoned terraces on the hillsides in the Figarella catchment, northwest Corsica.

Agricultural activities over the last century or so, notably grazing, caused slope erosion in some areas which resulted in thin soils and the lack of ability to retain water (Grove & Rackham, 2001). These conditions favoured the extension of evergreen (holm) oak (*Quercus ilex*) which has adapted to a wide ecological range and presently occupies the land up to 1,200 m, in the thermo- meso- and supramediterranean vegetation belts (Reille *et al.*, 1999; Grove & Rackham, 2001) (Table 3.4). The deciduous oak forest is recovering now that grazing is in decline. Presently in Corsica only 2% of the surface is cultivated (meadows, citrus fruits, vineyards) and according to Ballais (1998) erosion is no longer a major concern for farmers.

3.10 SUMMARY

Corsica is a large Mediterranean island with a dramatic granite landscape and steepland river catchments. During the Pleistocene cold stages many of the headwater valleys were glaciated. There are no glaciers at present, or even permanent snow, but the upland river environments are still sensitive to precipitation related changes in vegetation cover and sediment yield. The atmospheric circulations patterns, the regional orographics and the proximity of the Mediterranean Sea all play important parts in the rainfall regime of Corsica, and the western Mediterranean basin in general. Floods are particularly common in autumn and the competence of Corsican mountain river systems during intense precipitation events has been highlighted. Fine sediment loss is less severe in Corsica than many Mediterranean areas partly due to the relatively dense vegetation cover. Maquis and mixed woodstands occupy the lowland, forests comprising oak, pine, beech and birch are evident at mid elevation, and thick bushland of alder is common at higher altitudes. The following factors have all minimized erosion rates in Corsica:

i) A humid climate producing a well vegetated landscape.

ii) Resistant igneous bedrock in the main river catchments.

iii) Relatively low intensity human disturbance of the landscape.

Extrinsic factors which affect catchment hydrology and sedimentation style have also been examined and evaluated for Corsica. Sea-level has varied considerably during the Late Pleistocene, but it is recognized that changes in base level are not important upstream of the lower reaches of steepland rivers.

4 GLACIATION IN CORSICA AND THE MEDITERRANEAN

4.1 SYNOPSIS

This chapter describes present snowlines and the extent of Pleistocene glaciation within the Mediterranean basin. The timing of recent glacial activity is established in Corsica through the use of terrestrial *in-situ* cosmogenic nuclide dating of boulders on glacial moraines. The exposure ages obtained are placed into an environmental context using the data available for Corsica and the wider western Mediterranean region. A basic snowpack model is also presented to test the feasibility of glacier growth in Corsica during the periods of glacial activity indicated by cosmogenic nuclide dating.

4.2 INTRODUCTION

Recent work in other Mediterranean areas has shown that glacial activity had a major influence on river regimes and sedimentation styles during the Pleistocene (Chapter 2.5.1) (Woodward *et al.*, 1995; Macklin *et al.*, 1997). However, the precise timing of glacial activity in the Mediterranean mountain basins is not well known, principally due to the lack of dating control. This issue is addressed in Corsica by using terrestrial *in-situ* cosmogenic nuclide dating to establish exposure ages of boulders on the crests of moraines. Cosmogenic dating is one of the few tools which enables quantitative geomorphological studies to be conducted on timescales of 10^2-10^7 years (Lal, 1988). Developing a chronology for Mediterranean glacial and glacio-fluvial stratigraphies allows comparisons to be drawn with high resolution marine and oxygen isotope records and other palaeoenvironmental data (e.g. Macklin *et al.*, 2002).

This chapter has three main objectives:

i) To identify and map the main glacial features in the study regions.

ii) To assess the feasibility of using terrestrial *in-situ* cosmogenic nuclide dating techniques to establish the exposure ages of boulders on the crests of the moraines.

iii) To use the data from i) and ii) to construct a glacial chronology from the evidence preserved in Corsica and place these data in a broader context by reviewing the relevant terrestrial and marine palaeoenvironmental records.

4.3 GLACIATION IN THE MEDITERRANEAN

This section will first briefly describe the present day glaciation in the Mediterranean and surrounding mountain chains, and secondly, outline the available evidence for the timing and nature of glacial activity during the Pleistocene period.

4.3.1 Present glaciation and snowline altitudes

There is only limited glacial activity in and around the Mediterranean region today. There are glaciers present in parts of the Pyrenees, the mountains of Turkey and the south western part of the Alps (Messerli, 1967). The World Glacier Inventory compiled in conjunction with the World Glacier Monitoring Service (WGMS) and National Snow and Ice Data Center (NSIDC) (Hoelzle & Haeberli, 1999) provides data on the form and extent of glaciers in the World. Below displays information about glaciers in and around the Mediterranean region today (Table 4.1).

Table 4.1 Average[a] mountain and valley glacial extent in and around the Mediterranean region. Compiled from the World Glacier Inventory (Hoelzle & Haeberli, 1999).

	Pyrenees	SW Alps
Latitude	42.59 °N – 42.86 °N	44.12 °N – 45.0 °N
Longitude	0.29 °W – 0.90 °E	6.02 °W – 7.42 °W
No. of mountain & valley glaciers	67	219
Max. length of glacier (km)	0.48	0.88
Mean elevation of glacier (m asl)	2769	2969
Max elevation of glacier (m asl)	2883	3228
Min. elevation of glacier (m asl)	2663	2725
Snow line elevation (m asl)	2785	2817

[a] not always calculated from all of the glaciers in each region, only the data that are available.

There is one glacier in the Italian Apennines, Ghiacciaio del Calderone, which is the southernmost glacier in Europe (Messerli, 1980). Ghiacciaio del Calderone is a small glacier of about 5 hectares in area and located at 42°28'15"N, 12°27'08"E in the Gran Sasso, Abruzzo region in Italy between 2,650 and 2,850 m asl (D'Orefice *et al.*, 2000). Interestingly, the glacier is on a similar latitude to Mt Cinto in Corsica, the highest mountain in Corsica (2,706 m asl) (Figure 3.9).

The Apennines glacier is typical of the other Mediterranean glaciers in general, experiencing a constant rise in snowline altitude since the 1850s, as well as an almost continuous sequence of negative balances. The result has been the reduction of the surface area and thickness, illustrated in the case of the glaciers of the Southern Maritime Alps (Gellatly *et al.*, 1994; Pappalardo, 1999) and of the Pyrenees (Arenillas *et al.*, 1991). The Picado de Veleta glacier in the Sierra Nevada in southern Spain like many others soon became extinct prior to the 20th century (Messerli, 1980). At present, there is only a glacierized area of about 12 km^2 in the Mediterranean mountains and the Pyrenees (WGMS).

4.3.2 Pleistocene glaciation

During the Pleistocene Period, glaciation in the Mediterranean was much more extensive (Figure 4.1). The Sierra Nevada in southern Spain was glaciated and also the Picos de Europa region in northern Spain (Gale & Hoare, 1997). There is evidence of Pleistocene glaciation in the central Apennines (Giraudi & Frezzotti, 1997) and the southern Apennines (Boenzi & Palmentola, 1997) in Italy. The Albanian mountains (Boenzi & Palmentola, 1997), the Pindus mountain range in northwest Greece (Lewin *et al.*, 1991) and Mount Olympus in northeast Greece (Smith *et al.*, 1997) were all glaciated at one or more times during the Pleistocene. Glaciers have also been present on numerous occasions throughout the Pleistocene period in Corsica (Conchon, 1975, 1986) (Chapter 4.3.3).

Figure 4.1 Pleistocene glacial features and sediments in the Mediterranean basin and southern-central Europe (after Messerli, 1967, from Macklin *et al.*, 1995).

The timing and extent of glacial activity in the Mediterranean region during the Pleistocene has been evaluated in varying ways in different areas depending on the nature and quality of available evidence and applicable dating methods. As a result, straightforward interregional comparisons are difficult. In some cases, snow-line altitude calculations are shown to be the prime indicator of glacial extent (e.g. Boenzi & Palmentola, 1997) and in other studies, cirque floor elevation (e.g. Gale & Hoare, 1997; Giraudi & Frezzotti, 1997) and elevation of ice margin deposits (e.g. Birman, 1968) are the main parameters. Dating techniques such as luminescence (e.g. Lewin *et al.*, 1991), uranium-series (e.g. Hérail *et al.*, 1986; Woodward *et al.*, in press) and cosmogenic dating (this study) are not widely employed. Authors also employ the principal stage names of Günz, Mindle, Riss and Würm outside the Alps where the term has no stratigraphic meaning (Chapter 1.6.3).

4.3.3 Glaciation in Corsica

It is believed that the upper valleys in Corsica were occupied at least four times (glacial or stadial stages) during the Quaternary (Conchon, 1975, 1986). The oldest known glaciation is

presumed to be pre-Würm (Table 1.1) but no tills have been found. It has been proposed that Corsica experienced glacial advances in the early part of the Würm period but no glacial deposits are recognised from this episode. Conchon has attributed deposits of valley glaciers to two additional glacial stadials during the mid-Würmian. The oldest and youngest of these glacial events are believed to have had a lower elevation of between 700 and 1,100 m and 1,100-1,250 m elevation respectively (Table 4.2). Small cirque glaciers of elevations between 1,600 and 2,100 m are thought to have been present during the Lateglacial, perhaps during the cooling of the Oldest Dryas (Conchon, 1975, 1986) as evident in the Haut Asco region (Figure 4.2, Figure 4.3). Palynological records suggest that Corsica has been ice free since the Alleröd, from around 12.5 k radiocarbon years BP (Conchon, 1986) (Table 1.2). The stratigraphy becomes more tentative further back in time as evidence of the older glacial events is limited due to erosion by subsequent glaciers. Furthermore, the chronology is based upon weathering comparisons of glacio-fluvial and fluvial deposits from different regions such as the Alps and Pyrenees and must therefore be regarded as tentative.

Table 4.2 Tentative stratigraphy of glacial deposits in Corsica (after Conchon, 1986).

Time periods	Time divisions	Elevation of advancement (m)	Glacial and glacio-fluvial deposits	Non-glacial deposits in the valley (refer to Chapter 5)
Lateglacial	Younger Dryas Alleröd Older Dryas Bölling Oldest Dryas	1,600 – 2,100	Small glaciers/Cirque glaciers	Non-weathered fluvial (T7)
Würmian	Stadial	1,100 – 1,250	Non-weathered valley tills	Non-weathered grey fluvial (T6)
	Stadial	700 – 1,100	Light-weathered valley tills	Brown fluvial (T5)
	Stadial			Yellowish-red fluvial (T4)
Rissian	Stadial		Strong-weathered drift (valley glaciers)	Yellowish-red fluvial (T3)
?	Stadial			Yellowish-red fluvial (T2)
?	Stadial			Reddish-yellow fluvial (T1)

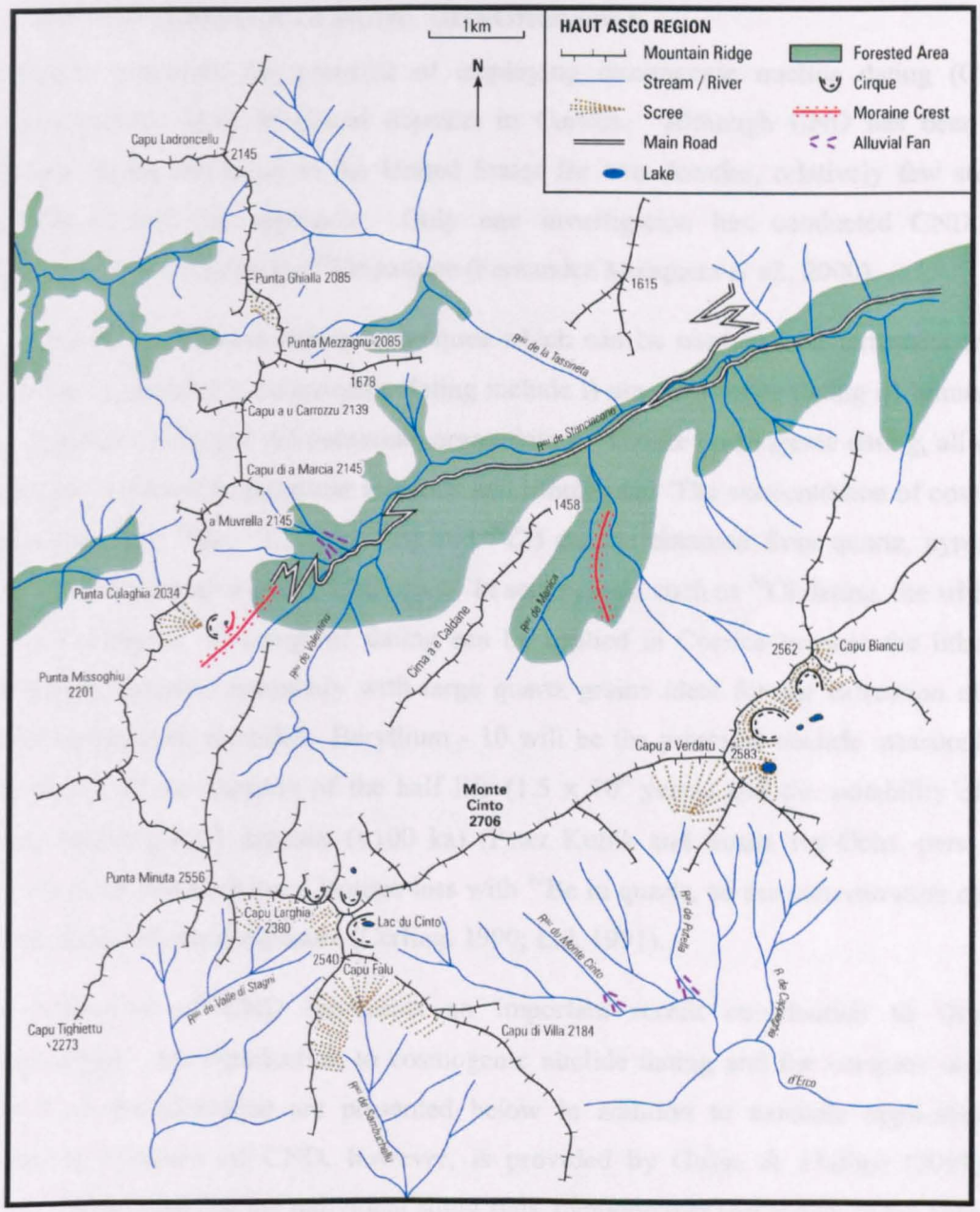

Figure 4.2 The main glacial features of the Haut Asco region (redrawn from Conchon, 1975 after modifications from aerial photographs).

Figure 4.3 Evidence of glaciation in the Haut Asco region.

4.4 ESTABLISHING A GLACIAL CHRONOLOGY

This chapter evaluates the potential of employing cosmogenic nuclide dating (CND) to elucidate exposure ages of glacial deposits in Corsica. Although CND has been a well established dating technique in the United States for two decades, relatively few studies in Europe have used the approach. Only one investigation has conducted CND in the Mediterranean region using the ^{21}Ne isotope (Fernandez Mosquera *et al.*, 2000).

Other common radiometric dating techniques which can be used to date terrestrial materials over similar timescales to cosmogenic dating include i) uranium series dating ii) luminescence dating (Chapter 5.6.1) and iii) potassium argon dating. Unlike cosmogenic dating, all of these methods are restricted to particular minerals and lithologies. The concentration of cosmogenic isotopes (e.g. ^{3}He, ^{10}Be, ^{14}C, ^{21}Ne, ^{26}Al and ^{36}Cl) can be obtained from quartz, pyroxene or olivine, minerals found in many lithologies. In some cases, such as ^{36}Cl dating, the whole rock is used for analysis. Cosmogenic dating can be applied in Corsica because the lithology is predominantly granite, commonly with large quartz grains ideal for the extraction of *in-situ* produced cosmogenic nuclides. Beryllium - 10 will be the principal nuclide measured in this study because of the duration of the half life (1.5 x 10^{6} years) and the suitability of dating relatively recent glacial deposits (<100 ka) (Peter Kubik and Susan Ivy-Ochs, pers. comm. 2000). There is also no natural isotope loss with ^{10}Be in quartz, so the concentration measured is that accumulated since exposure (Cerling, 1990; Lal, 1991).

The development of CND represents an important recent contribution to Quaternary geomorphology. An introduction to cosmogenic nuclide dating and the complex underlying principles of the technique are presented below in addition to example applications. A comprehensive review of CND, however, is provided by Gosse & Phillips (2001). The following sections outline the individual study sites, methodology and results of the cosmogenic dating technique.

4.4.1 Terrestrial production of *in-situ* cosmogenic isotopes

A variety of long-lived radioisotopes (e.g. ^{10}Be, ^{26}Al, ^{36}Cl) are produced *in-situ* as cosmic rays interact with minerals in rocks exposed at or near the Earth's surface (Table 4.3). These isotopes are produced in the upper surface of a rock by nuclear reactions induced by cosmic rays. The primary cosmic ray spectrum consists of galactic cosmic rays (energies 1-100 GeV) which originate outside the solar system, and of solar cosmic rays (energies 10-100 MeV) (Lal & Peters, 1967; Reedy 1987). The latter are insignificant for the production of cosmogenic isotopes in rocks. The galactic cosmic ray spectrum is made up of approximately 85% protons, 14% alpha particles and 1% heavier particles (Lal, 1988). A cascade of secondary particles consisting of protons, neutrons and muons is produced as the cosmic rays enter the earth's atmosphere. These particles, dominated by neutrons, produce cosmogenic isotopes in a rock

surface by spallation reactions, muon-induced reactions and neutron capture reactions and different production pathways dominate at different depths below the Earth's surface (Bierman, 1994; Reedy *et al.*, 1994). The primary mechanism of cosmogenic isotope production for ^{10}Be and ^{26}Al is spallation, a nuclear reaction whereby several lighter particles are emitted from a target nucleus hit by cosmic ray particles. For example, within a quartz grain located at the surface of an exposed rock, an oxygen atom hit by a cosmic ray particle will spall, losing several nucleons. One of the atoms that can be produced within the quartz lattice is a ^{10}Be atom (Ivy-Ochs, 1996).

With continued exposure, cosmogenic isotopes accumulate in the rock as a function of time and depth below the surface. Thus the time elapsed since initial exposure can be calculated from concentrations of cosmogenic isotopes in the rock (Equation 4.1).

$$N = \frac{P}{\lambda + \frac{\rho\epsilon}{\Lambda}}\left(1 - e^{-(\lambda + \rho\epsilon/\Lambda)T}\right) + N_0 e^{-\lambda T} \qquad \textbf{Equation 4.1}$$

Where N is the number if atoms/gram (of SiO_2 for ^{10}Be and ^{26}Al); N_0 is the number of atoms/gram of the cosmogenic isotope present at the beginning of exposure; P is the local production rate in atoms/gram•yr; T is the length of time the surface has been exposed in yrs; λ is the decay constant of the radionuclide in $1yr^{-1}$; ρ is the rock density in gcm^{-3}; ϵ is the erosion rate in $cmyr^{-1}$; Λ is the cosmic ray attenuation length in the rock surface in gcm^{-2}.

In order for the relationships of Equation 4.1 to have simple solutions, several assumptions must be satisfied. One assumption is that the concentration of the cosmogenic isotope at the beginning of exposure is zero or is known (N_0 in Equation 4.1). Likewise, the erosion of the rock surface from time of exposure is either known or assumed negligible. For cases where there is significant erosion, the time for which the radionuclide abundance is representative decreases. The concentration of the various radionuclides becomes constant after 3-4 half lives and is termed saturation or secular equilibrium, where the production and decay of nuclides are balanced. This steady state is reached earlier when there is a high rate of erosion (Lal, 1991). The half life of ^{10}Be is 1.5 Ma and the limit of applicability is ~ 5 Ma.

4.4.2 Applications of *in-situ* cosmogenic nuclide dating

For many studies, a thousand years of exposure history produces measurable amounts of *in-situ* cosmogenic isotopes (Cerling & Craig, 1994). The upper limit extends to millions of years (~5 Ma for ^{10}Be). This technique therefore helps to address the long standing problem of linking short term process studies to studies of long term landscape evolution. Terrestrial *in-situ* cosmogenic dating has the potential to reconstruct a geochronology of events (e.g. glacial activity) over the entire Quaternary which can be correlated on a regional and local scale.

Table 4.3 Commonly used terrestrial *in-situ* cosmogenic nuclide isotopes (modified from Bierman, 1994).

Isotope	Half-life (decay constant) (yrs)	Production rate atoms g^{-1} yr^{-1} sea level, > 60°	Production rate studies	Primary cosmogenic reactions (Lal, 1988)	Measurement technique (compound)	Common sample material
^{3}He	Stable	(olivine) 143 (olivine) 70-220 (olivine) 140 (olivine) 109 (silicate) 191	Kurz (1986) Kurz *et al.* (1990) Cerling (1990) Poreda & Cerling (1992) Brook & Kruz (1993)	Spallation of O, Mg, Si, Fe	MS	Olivine, pyroxene, quartz
^{10}Be	1.5×10^{6} (4.6×10^{-7} yr^{-1})	(olivine) 5.25 (quartz) 10 (quartz) 6.0 (quartz) 6.4 (quartz) 5.75	Nishiizumi (1991a) Middleton & Klein (1987) Nishiizumi *et al.* (1989) Brown *et al.* (1991) Kubik *et al.* (1998)	Spallation of O, Mg, Si, Fe	AMS (BeO)	Olivine, quartz
^{14}C	5730 (1.2×10^{-6} yr^{-1})	(quartz) 17.5 (silicate) 19	Lal (1991) Jull *et al.* (1992)	Spallation of O	AMS (C)	Quartz, whole rock
^{21}Ne	Stable	(olivine) 0.4 x ^{3}He (quartz) 0.4 x ^{26}Al	Poreda & Cerling (1992) Graf *et al.* (1991)	Spallation of Mg, Al, Si, Fe	MS	Olivine, plagioclase, quartz
^{26}Al	0.71×10^{6} (9.9×10^{-7} yr^{-1})	(olivine) 15.4 (quartz) 70 (quartz) 36.8 (quartz) 41.7 (quartz) 37.4	Nishiizumi (1991a) Midleton & Klein (1987) Nishizumi *et al.* (1989) Brown *et al.* (1991) Kubik *et al.* (1998)	Spallation of Si, Al, Fe	AMS (Al_2O_3)	Olivine, quartz
^{36}Cl	0.3×10^{6} (2.3×10^{-6} yr^{-1})	2600-3000 atom mol Ca^{-1} yr^{-1} 500-8500 atom mol K^{-1} yr^{-1} 1.2×10^{6} atom mol Cl^{-1} yr^{-1}	Yokoyama *et al.* (1977); Davis & Schaeffer (1995); Zreda *et al.* (1991); Swanson *et al.* (1993); Phillips *et al.* (1992)	Spallation of K, Ca, Fe and ^{35}Cl (n, γ) ^{36}Cl	AMS (AgCl)	Whole rock

The technique is also unique in that it provides information on the exposure history of rock surfaces over significant periods of time rather than by association with deposits or other chronological markers. By yielding information on spatial and temporal variations in rates of landscape change it greatly enhances our understanding of processes within geomorphic systems.

The number of studies employing cosmogenic isotopes in constraining rates of landscape evolution or landform age increased dramatically in the 1980s with the development of accelerator mass spectrometry (AMS). The sensitivity of the analytical technique has increased to permit measurement of small abundances of long-lived cosmic ray produced radioisotopes in terrestrial materials which allowed a large reduction in sample size from *ca.* 10-100 g to *ca.* 1-10 g (Lal, 1998). Improvements in the sensitivity of conventional mass spectrometers of ^{3}He and ^{21}Ne have also increased the potential of this technique. In 1986, successful exposure ages determinations using ^{3}He (Craig & Poreda, 1986; Kurz, 1986), ^{10}Be and ^{26}Al (Klein *et al.*, 1986; Nishiizumi *et al.*, 1989), ^{21}Ne (Marti & Craig, 1987) and ^{36}Cl (Phillips *et al.*, 1991) were reported.

This nuclear method applicable for the study of surface exposure ages, denudation and sedimentation rates is useful in a variety of geomorphic settings (Table 4.4). Studies ascertaining the precise date of a glaciers maximum stand by exposure dating boulders on the crest of moraines have measured concentrations of either ^{10}Be (e.g. Gosse *et al.*, 1995a, 1995b) or ^{36}Cl (e.g. Phillips *et al.*, 1990; Zreda & Phillips, 1995) or a combination of both (e.g.Ivy-Ochs *et al.*, 1996; Chadwick *et al.*, 1997, Phillips *et al.*, 1997). The ratio of the $^{26}Al/^{10}Be$ pair is also widely implemented to establish erosion rate, time of burial after cosmic ray exposure or exposure age (e.g. Evenson *et al.*, 1993; Nishiizumi *et al.*, 1991b; 1993; Brook *et al.*, 1995; Ivy-Ochs *et al.*, 1996; Bierman *et al.*, 1999). Shielding or burial allows the shorter-lived nuclide (^{26}Al) to decay relative to the longer lived nuclide (^{10}Be) (Bierman *et al.*, 1999). Many authors have emphasized the need to study multiple nuclides in order to provide an accurate estimate of the erosion rate and constrain the surface exposure age (e.g. Klein *et al.*, 1986; Nishiizumi *et al.*, 1991b; Lal, 1991). However, single cosmogenic nuclides have been used successfully to date young (<100 ka) glacial surfaces (Phillips *et al.*, 1990; Gosse *et al.*, 1995) following the constant exposure model of Lal (1991).

Cosmogenic dating has also been applied in a fluvial setting to estimate the rates of downcutting of the New River, Virginia (Granger *et al.* 1997) as well as to elucidate the ages of terraces in the Indus Valley (Burbank *et al.*, 1996; Sharma *et al.*, 1998). Catastrophic flooding events which were common towards the end of the last glaciation can also be dated (Cerling *et al.*, 1994). The age of meteor craters (Nishiizumi *et al.*, 1991c; Phillips *et al.*, 1991), volcanic events (Staudacher & Allégre, 1993; Shepard *et al.*, 1995), earthquake recurrence and debris flow fan deposits (Bierman *et al.*, 1995) have also been determined by CND (Table 4.4).

Table 4.4 Applications of terrestrial in-situ cosmogenic nuclide dating

Cosmogenic dating application	Radionuclides employed	Location	Geomorphic context	Age range (ka)	Reference
EARTHQUAKE RECURRENCE					
Holocene displacement	^{36}Cl	Nahel East, N. Israel	Bedrock fault scarp	3 – 14	Gran *et al.*, 1999
Prehistoric earthquakes	^{36}Cl	Hebgen Lake, Montana	Bedrock fault scarp	0.4 – 24	Zreda & .,Noller, 1998
Earthquake recurrence	^{10}Be & ^{26}Al	Sierra Nevada, California	Bedrock fault scarp	0.8 – 8.0	Bierman *et al.*, 1995
FLUVIAL					
Incision rates	^{10}Be & ^{26}Al	Green River, Kentucky	Cave sediments	700 - 2400	Granger *et al.*, 1997
Debris flow	^{10}Be & ^{26}Al	Owens Valley, California	Surface boulders	8 – 136	Zehfuss *et al.*, 2001
Debris flow	^{3}He	Grand Canyon, Arizona	Surface boulders	0.5 – 3.0	Cerling *et al.*, 1999
River behaviour	^{10}Be & ^{26}Al	Wind River, Wyoming	Strath terraces	118 - 510	Hancock *et al.*, 1999
Incision rates	^{10}Be & ^{26}Al	Indus River, Pakistan	Bedrock strath	7 – 65	Leland *et al.*, 1998
Alluviation	^{10}Be & ^{26}Al	Fremont River, Utah	Fluvial terraces	60 – 151	Repka *et al.*, 1997
Alluvial fan surfaces	^{10}Be	El Tigre fault, Argentina	Surface boulders	41 – 670	Siame *et al.*, 1997
GLACIAL					
Ice extent during LGM	^{36}Cl	Chukotka, E. Russia	Moraine/outwash deposits	10.1 – 25.8	Gualtieri *et al.*, 2000
Ice extent during Wisconsin	^{10}Be & ^{26}Al	Baffin Island, Arctic Canada	Boulders and bedrock	9 – 24	Marsella *et al.*, 2000
Pleistocene glaciations	^{36}Cl, ^{10}Be	Rocky Mountains, USA	Moraine/outwash deposits	16 – 130	Chadwick *et al.*, 1997
Timing of deglaciation	^{10}Be, ^{26}Al, ^{36}Cl	Julier Pass, Switzerland	Boulders on moraine crests	10.1 – 12.6	Ivy-Ochs *et al.*, 1996
Glaciation during Younger Dryas	^{10}Be	Wind River Mtns, Wyoming	Boulders and bedrock	11.4 – 13.8	Gosse *et al.*, 1995a
Glacial chronology	^{36}Cl	Sierra Nevada, California	Boulders on moraine crests	21 – 218	Phillips *et al,*. 1990
Glacial advance	^{10}Be & ^{26}Al	Sierra Nevada, California	Polished bedrock surface	<11	Nishiizumi *et al.*, 1989
METEORIC					
Crater	^{10}Be & ^{26}Al	Arizona	Meteor crater	<49	Nishiizumi *et al.* (1991c)
Crater	^{36}Cl	Arizona	Meteor crater	<49.7	Phillips *et al.* (1991)
VOLCANIC					
Eruption	^{36}Cl & ^{10}Be	Lunar Crater, Nevada	Basalt flow	38	Shepard *et al.* (1995)
Caldera collapse	^{21}Ne	Réunion, off Madagascar	Exposed rock from collapse	65 – 3.3	Staudacher & Allègre (1993)
Eruption	^{36}Cl	Lathrop Wells, Nevada	Basalt flow	81	Zreda *et al.* (1993)
Eruption	^{3}He & ^{21}Ne	Rio Grande Rift, New Mexico		17 – 80	Anthony & Poths (1992)

4.4.3 Factors affecting the isotope production rate

There are many known and unknown complicating factors that affect the production and buildup of the isotopes (Table 4.5). The known factors are those which are specific to the location of the sample and those which can be corrected for confidently. The unknown factors affecting the production rate are those which have varied through time or those which pertain to events in the past that cannot be known precisely. Such unknown factors can be divided into those relating to the cosmic ray flux and those which are site specific. The net effect of these influences is difficult to constrain, but all of these processes, with the exception of prior exposure, yield ages which are too young (Phillips *et al.*, 1996; Kurz & Brook, 1994).

Table 4.5 Known and unknown factors affecting isotopic buildup.

Known factors	Unknown factors
	Cosmic ray flux which is influenced by Time Solar Activity Earth's magnetic field
Site Specific factors	
Latitude Altitude Shielding from the surrounding hillsides Surface angle of sample Sample thickness	Burial by ice, snow, sediment Shielding by vegetation Erosion of the surface Shifting, rolling over or exhuming of boulders Mineral alteration due to rock weathering Prior exposure Tectonic activity

4.4.3.1 Known factors affecting isotopic buildup

The thickness of the atmosphere and the magnetic field affect the production rate of each isotope and correction factors can be applied for each exposed rock sample location. Latitude and altitude scaling factors that have been described by Lal & Peters (1967) and Yokoyama (1977) have been supplanted by Lal (1991). Lal (1991) represents the scaling factors in terms of a third degree polynomial and is based on the assumption of a dipole field. The experimental uncertainty in ^{10}Be production estimates is about 10% (Lal, 1991). Subsequent work, however, shows that the error on cosmogenic production rates is closer to 20% (Dunai, 2000, 2001; Desilets & Zreda, 2001).

The production rate of cosmogenic isotopes within the exposed rock is dependent on the cosmic rays that the rock surface is subjected to. Therefore, reduction of the cosmic rays by mountain peaks and ridges surrounding the sampling site reduces the production rate accordingly. The precise angle to the horizon and the number of degrees of the quadrant affecting the sample site can be used to calculate the reduction in production rate using Equation 4.2 (Nishiizumi *et al.*, 1989).

$$F(\theta) = \sin 2.3\,\theta \qquad \textbf{Equation 4.2}$$

Where $F(\theta)$ is the relative angular dependence of the cosmic ray nucleonic component and θ is the angle from vertical.

The slope of the rock surface and the surrounding skyline must both be accounted for. For example, a rock surface sloping at an angle of 25° results in a 2% reduction of the production rate (Ivy-Ochs, 1996). In certain circumstances cosmic rays are shielded by rocks or trees usually at relatively low angles above the horizon. The production correction is relatively small, however, if the shielding angles are low because attenuation of the cosmic rays by the atmosphere tends to be greater for low angle incident radiation where the atmosphere is thickest. In many cases shielding of incident cosmic radiation is minimal but for regions of high relief it may be more significant (Cerling & Craig, 1994).

A correction factor for the thickness of the sample is also needed. The production rate of cosmogenic nuclides decreases exponentially with depth as secondary particles from cosmic rays attenuate as they travel through the rock. The integrated production rate over a certain depth interval is obtained by Equation 4.3 (Ivy-Ochs, 1996):

$$P_{(o \text{ to } x)} = Po \frac{\Lambda}{\rho x}(1-e^{-\rho x/\Lambda}) \qquad \textbf{Equation 4.3}$$

Where $P_{(o \text{ to } x)}$ is the average production (atoms/g SiO_2•yr) for the interval from the surface to the given depth, x is the total rock thickness (cm). Po is the production rate at the surface (atoms/g SiO_2•yr), is the rock density and is taken as 2.7 gcm^{-3} (granite), is the cosmic ray attenuation length of 150 gcm^{-2} (Brown *et al.*, 1992).

Masarik and Reedy (1995) argue that near the rock surface, at depths less than ~5 cm, the cosmogenic production rate profile shows no or little difference. However, most authors (e.g. Gosse *et al.*, 1995; Ivy-Ochs *et al.*, 1996, 1999; Fabel & Harbor, 1999) do use the depth correction in final production rate calculations. The thickness correction has been applied in this study.

4.4.3.2 Unknown factors affecting isotope buildup

There is evidence to suggest that solar activity (Beer *et al.*, 1988, 2000; Bond *et al.*, 2001) and geomagnetic field intensity (Castagnoli & Lal, 1980; Lal, 1988; Frank, 1997; 2000), have fluctuated significantly and irregularly during the Pleistocene (Kurz *et al.*, 1990; Lal, 1991). Both factors greatly affect the cosmic ray flux and thus the isotope production rates. Higher production rates are associated with weaker winds and reduced irradiance (Masarik & Beer, 1999) and a weaker geomagnetic field (Lao *et al.*, 1992). The greatest change in production

rates will be at high altitudes and low latitudes (Kurz *et al.*, 1990; Cerling & Craig, 1994; Clark *et al.*, 1995).

Variations in the strength of the Earth's magnetic field is the most important factor controlling cosmogenic nuclide production (Frank, 2000). It is therefore crucial to establish the palaeointensity for the time period being investigated. Frank *et al.* (1997, 2000) analysed the relative variations in ^{10}Be production rates in marine and terrestrial sediments and ice cores and translated these into field intensity modulations. The record shows major periods during which the field intensity was between 10% and 40% of the present day value, resulting in an overall 30% reduced value for the past 200 ka. A low palaeomagnetic intensity at around 40 ka which is reflected in an increase of ^{10}Be is well documented in ice cores (Raisbeck *et al.*, 1987; Beer *et al.*, 1988) and deep sea sediment (Castagnoli *et al.*, 1995; Robinson *et al.*, 1995). During the LGM, the global average production rate of ^{10}Be was at least 25-30% (Frank, 2000). Translating these data into correction calculations for individual studies is difficult.

The site specific factors which cannot be easily constrained are numerous (Table 4.5). Intermittent shielding of the rock surface by snow, ice or sediment may have reduced the cosmogenic production rate since time of exposure. It is very difficult to quantify these effects as conditions and surroundings in the past are not the same as those at present and little evidence of that coverage remains. Few corrections have been made for snow cover, especially when the samples are collected from large boulders on the crests of moraines. In many cases, the substrate surface would have projected above the average snow depth and any snow falling on the rock surface would have been blown off (Clark *et al.*, 1995). It has also been shown that the isotopic abundances in near horizontal surface samples collected from the Sierra Nevada, California, which are prone to burial by snow, were no different to those samples collected in the same area but from slopes above a 45° angle (Nishiizumi *et al.*, 1989). This suggests that there has to be a considerable thickness of snow for the production rate to be significantly affected (Nishiizumi *et al.*, 1989). Sampling large boulders on the moraine crests also minimises the likelihood that the rock sample was covered in till matrix after moraine formation. Tall boulders are likely to have stood above the original level of the moraine crest (Phillips *et al.*, 1990).

The attenuating effects of tree cover on the amount of cosmic rays bombarding the sample is also a consideration for correction. Cerling & Craig (1994) calculate a 4% reduction in cosmogenic isotope production due to shielding of the samples in the forest of Puy de Dome, Massif-Central in France. The calculation is based on a method involving density and biomass of the forest. However, it is difficult to make corrections for past tree cover as present day vegetation may have very little in common with that since and during time of rock surface exposure. Most authors do not regard vegetation cover as a significant shielding factor and do not apply any correction factors to the production rates.

Erosion of the rock surface is an important factor affecting the isotope buildup particularly if the lithology of the rock is easily weathered (e.g. limestone boulders in northwest Greece (Woodward *et al.*, in press)) or if the exposure age is of considerable duration. Indication of no or negligible erosion since exposure such as glacial striae is useful but often rare, especially prior to the latest Pleistocene (Bierman & Gillespie, 1991). The multiple production mechanisms of ^{36}Cl make it possible to reveal erosion and erosion rates, similarly to the paring of ^{10}Be and ^{26}Al (Chapter 4.4.2). This has its most important application for surfaces with exposure ages in the range of several hundred thousand to several million years. Spalling of large flakes episodically from the rock surface can also lead to inaccuracies of exposure age where the assumption of steady state erosion is less valid.

Exposure ages which are too young can also occur due to post depositional movements or settling of the boulders on the moraine. Blocks may have rotated or rolled down the sides of the moraine due to processes such as frost heaving or as a result of the finer material on the moraine eroding away (Hallet & Putkonen, 1994; Zreda *et al.*, 1994). Sampling a large, stable boulder on the crest of a moraine minimises the uncertainty of the rock having overturned or having been exhumed after moraine formation. Ages which are overestimates may have been exposed to cosmic rays before the exposure age of interest. Prior exposure can occur from many scenarios such as exposure along a cliff surrounding a glacier, exposure in an older moraine and where sub-glacial erosion has been insufficient as to remove all of the previously exposed rock. For a boulder to have experienced several periods of exposure, the exact same rock face must always have been exposed upward to cosmic rays.

Weathering and alteration of individual mineral grains of the rock surface may lead to open system behaviour of the isotope and/or contamination with, for example meteoric ^{10}Be. This behaviour is not a problem in the case of quartz which is a very weathering resistant mineral, but is more significant in olivine or pyroxene (Ivy-Ochs, 1996). The substrate surface which is subjected to atmospherically derived ^{10}Be can fortunately be effectively cleaned by the hydrofluoric etching so that only the *in-situ* ^{10}Be concentration is measured (Nishiizumi *et al.*, 1989; Brown *et al.*, 1991; Kohl & Nishiizumi, 1992).

Lastly, tectonic activity is a factor that results in elevation change which subsequently leads to a change in cosmic ray flux and ultimately a variation in isotope production rates. Lal (1991) models elevation change with respect to erosion models and concludes that only when rock erosion rates are very low can elevation change be determined from *in-situ* nuclides. It is also stated that in regions with high uplift rates there tends to be high erosion rates too and so in many situations, the *in-situ* nuclide buildup would be primarily determined by erosion (Lal, 1991).

4.4.3.3 The production rate of Berrilyium-10

The most widely used production rate of ^{10}Be is that determined by Nishiizumi *et al.* (1989) of 6.0 atoms per gram SiO_2 per year at high latitude (>60°) and sea level, calibrated from exposure ages of glaciated rocks in the Sierra Nevada, USA, and most recently verified by Nishiizumi *et al.* (1996). Other production rate values include Brown *et al.* (1991) of 6.4, Nishiizumi *et al.* (1991) of 6.13 and Kubik *et al.* (1998) of 5.75 atoms per gram per year (Table 4.6). As an example of the differences between production rates, applying the rate of 5.75 compared to Nishiizumi *et al.* (1989) of 6.0 increases the age of a 12 ka event by about 0.6 ka.

Table 4.6 Published production rates of ^{10}Be (sea level and geomagnetic latitude $\geq 60°$).

Reference	Geomorphological context	Timescale	^{10}Be Production rate (atoms/yr g SiO_2)
Nishiizumi *et al.* (1989)	Sierra Nevada rocks	11 ka	6.03
Brown *et al.* (1991)	Antarctic rocks	$\leq$ 2.5 Ma	6.4
Nishiizumi *et al* (1991)	Antarctic rocks	$\geq$ 4 Ma	6.13
Masarik & Reedy (1995)	Theoretical	A few Ma	5.97
Nishiizumi *et al.* (1996)	Water Targets	~10 ka [a]	6.0 $\pm$ 0.3
Kubik *et al.* (1998)	Austrian rock slide	10 ka	5.75 $\pm$ 0.24

[a] Long term geomagnetic field correction is added

The production rates of Nishiizumi *et al.* (1989) however have been contested by Clark *et al.* (1995) who believe that the Late Pleistocene and Holocene production rates for ^{10}Be and ^{26}Al are probably at least 20% too young. New radiocarbon ages, stratigraphic evidence and palynological studies demonstrate that the Sierra Nevada was deglaciated at least several thousand years earlier than assumed when Nishiizumi *et al.* (1989) first calibrated the production rates on a time integrated average. Clark *et al.* (1995) show that uncertainties in ages of calibration surfaces and in geomagnetic field strength variations contribute substantially and are typically unstated errors to cosmogenic age estimates. These authors imply that many exposure ages calculated using previously accepted production rates are also too young. It is suggested that the field strength and the attendant production rate variations may generate age errors of over 20% over the past *ca.* 100 ka for all *in-situ* isotope systems if time averaged production rates are used to calculate exposure ages. However, this error is not believed to be significant for younger exposure ages.

4.4.4 Future developments and conclusions

Against the complex background it can be argued that the most important need to enhance the utility of this dating technique centres on the estimation of the isotopic production rate. More sites are needed where a wide variety of palaeoenvironmental evidence can be tested to accurately date the area in order to establish and verify production rates (Clark *et al.*, 1995). Improvements in models that predict how the flux of cosmic rays at the Earth's surface changes due to fluctuations in the Earth's and interplanetary magnetic fields will also be useful in

estimating cosmogenic nuclide production. Current research to evaluate the variability of the Earth's magnetic flux and the feasibility of using magnetostratigraphic records of palaeointensity to adjust cosmogenic nuclide production rates is being conducted. Further improvement of numerical simulations to corroborate empirically and theoretically determined production rate data can then follow with greater confidence.

It is becoming clear that the assumptions used in many studies to interpret experimental measurements of *in-situ* cosmogenic isotopes need to be reviewed. It is suggested that a 5% error or better is needed for each factor, such as elevation and shielding, in order to permit meaningful geomorphological conclusions (Reedy *et al.*, 1994). Paramount to the feasibility of cosmogenic dating is the knowledge of the geomorphological setting. An exposure history of a sample cannot be provided unless an appropriate exposure history model based on the geomorphological context can be utilised. The models and the simulations are also only as good as the data upon which they are derived.

Of equal importance to understanding the uncertainties and limitations of CND is recognition of the potential for quantitative geomorphologic studies. Cosmogenic nuclide dating is still in its infancy, but it has already proved to be an extremely valuable tool. The technique is superior to many surface exposure dating approaches such as relative methods involving soils and weathering and rock varnish for example, because it is based on a physical process and can be quantitatively related to time. Numerical ages, even minima, provide a great improvement in resolution over relative ages. The technique is useful over a full range of climatic settings and a wide range of lithologies and is also applicable over the whole Quaternary Era.

A dataset of terrestrial glacial chronologies is slowly developing which can be compared with marine and ice core records to establish the nature and impact of global climate change. Phillips *et al.* (1997) and others have already established links between glacial and fluvial deposits of the Wind River Range in Wyoming and the deep sea record, correlating cosmogenic chronologies to marine isotope stages. Other applications in a range of environments are expected to yield similar advances. With a gradual improvement in technology, methods, models and data quality, this field of geophysics will inevitably be refined and our knowledge of environmental change and landscape evolution will increase.

4.5 COSMOGENIC DATING OF MORAINES IN CORSICA

A total of ten rock samples (C1 to C10) were taken for surface exposure cosmogenic dating in Corsica in May 1999 and June 2000, however only two (and one blank) were fully prepared and processed. Five samples were intensively etched with hydrofluoric (HF) acid to isolate the quartz but only two (C1 and C2) yielded enough good quality quartz. Samples collected in the vicinity of Mt Cinto were rhyolitic and comprised of very small crystals. The potential of

obtaining a meaningful exposure age was very low so the preparation procedure was not continued. Four weeks intensive sample preparation was conducted during April 2000 at the Swiss Federal Institute of Technology (ETH) in Zürich under the guidance of Dr Susan Ivy-Ochs. The AMS analysis was conducted by Dr Peter Kubik of the Paul Scherrer Institut also based at ETH.

4.5.1 Study Sites

The two sites from which C1 and C2 rock samples were taken and *in-situ* cosmogenic nuclide surface exposure ages derived were the Taravo catchment in south-central Corsica and in the Golo catchment in northern Corsica respectively (Table 4.7). Both samples were taken from large boulders on the crest of lateral moraines.

Table 4.7 Sample site information for exposure age dating of glacial deposits in Corsica.

Field Ref.	Location	Grid Ref.	Altitude (m asl)	Lithology	Vegetation cover	Surface angle	Glacier front (m asl) Conchon,1975
C1	N 42° 00' 08 E 09° 10' 26	05667 41908	1,200	Granodiorite	Clearing in beech forest	Horizontal	700-1,000
C2	N 42° 18' 47 E 08° 55' 29	05405 42215	1,220	Granodiorite	Sparse pine forest	Horizontal	1,100-1,250

Sample C1 was collected from a large boulder from the southern lateral moraine of the northern pairing south east of Mt Renoso (2,352 m) in south-central Corsica (Figure 4.4, Figure 4.7). The moraine is parallel to a tributary of the Taravo river which drains a basin between Mt Grosso (1,985 m) and Mt Giovanni (1,950 m). Sample C1 is believed to be from a moraine derived from the glacial advance attributed to mid Würmian, sometime prior to the Last Glacial Maximum (Conchon, 1975; 1986). The altitude of the glacier front has been estimated to be between 700 and 1,100 m elevation and is associated with the T5 fluvial deposits (Table 4.2) (Conchon, 1975; 1986). The moraines further south are well preserved but less accessible (Figure 4.5). Sample C2 is taken from a moraine just north of the Catamalzi River, a tributary of the Golo in the Col de Vergio area in northern Corsica (Figure 4.6, Figure 4.7). It is taken from a similar altitude as C1 (Table 4.7) but from a lateral moraine which is thought to be of a later glacial phase in the Würmian with a glacier front of between 1,100 and 1,250 m elevation (Conchon, 1975, 1986).

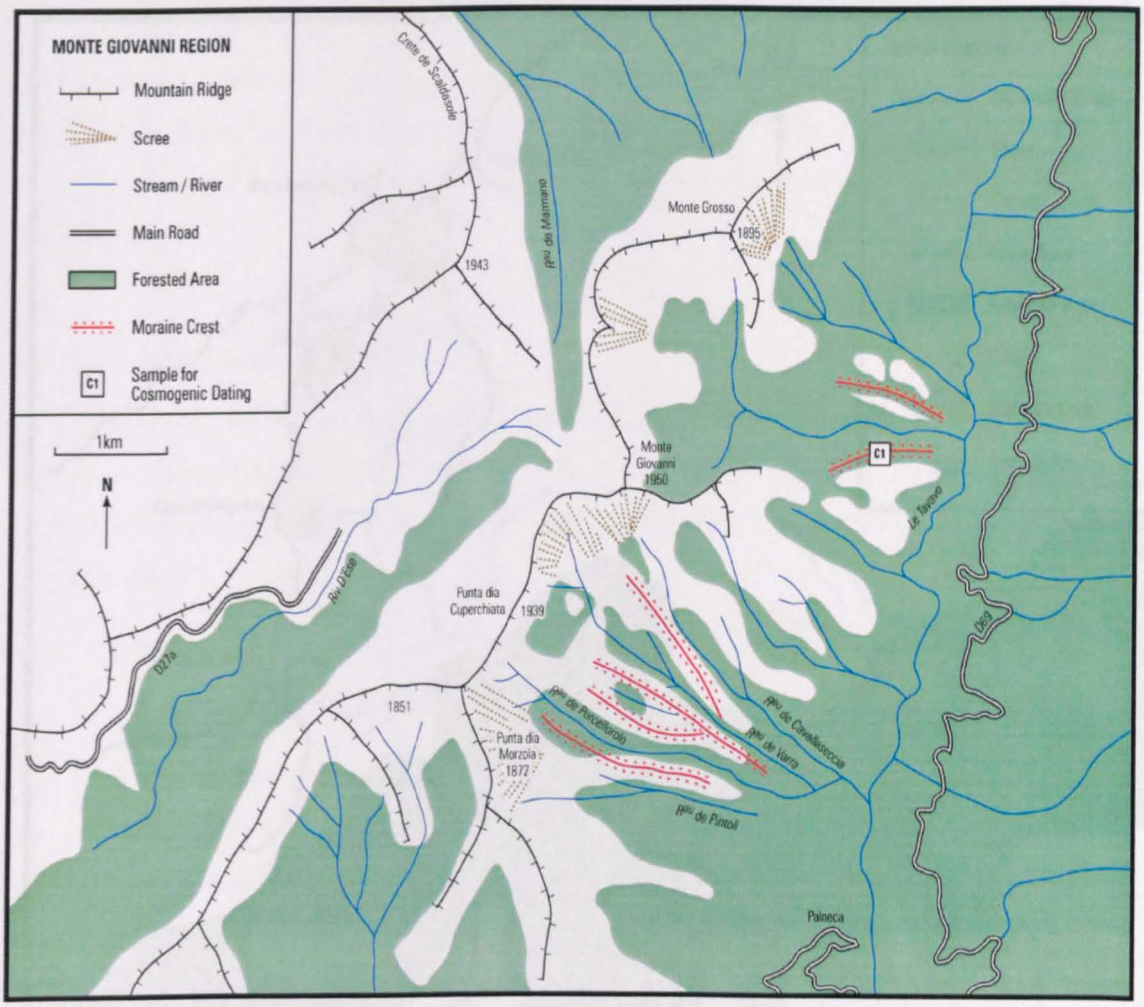

Figure 4.4 Location site of cosmogenic sample C1, collected from a boulder on the crest of a moraine in the Mount Giovanni region.

Figure 4.5 Series of lateral moraines flanking the southeast side of Mount Giovanni, alongside the rivers Cavallaseccia, Varra, Porcellorolo and Pintoli (Figure 4.4).

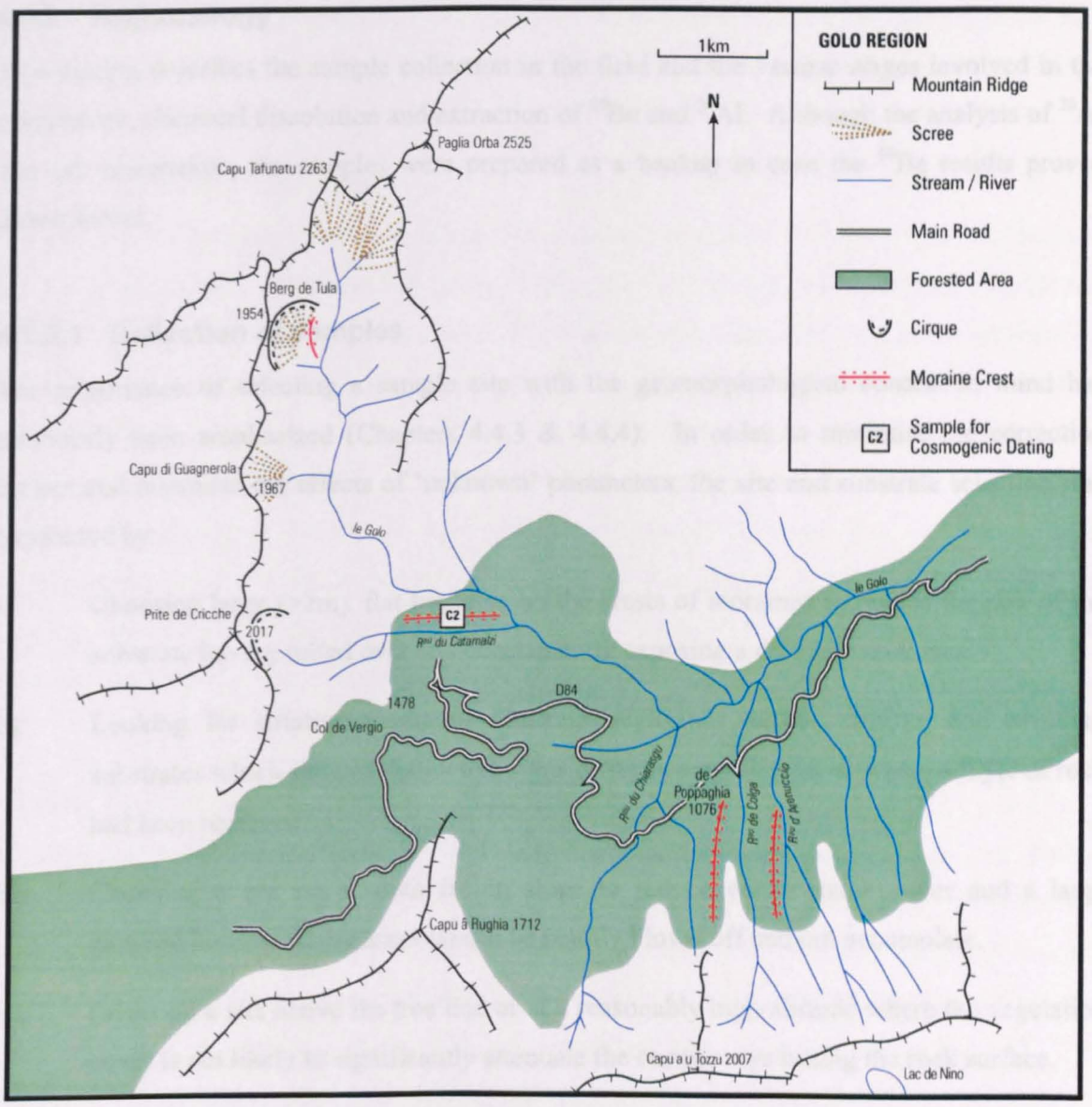

Figure 4.6 Location site of cosmogenic sample C2, collected from a boulder on a crest of a moraine in the Col de Vergio region, in the Golo basin.

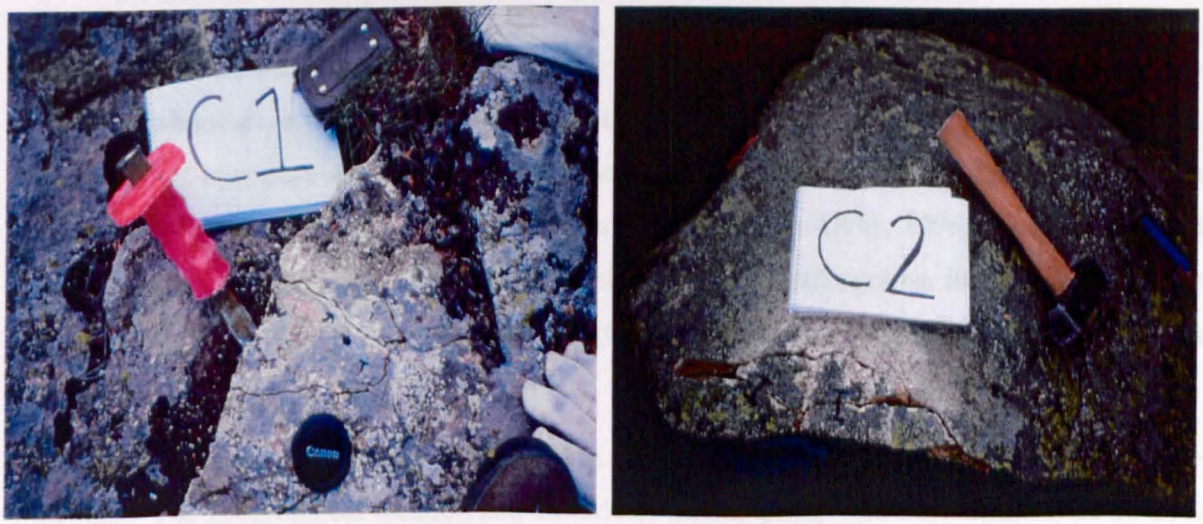

Figure 4.7 Samples collected from boulders on moraines in the Giovanni (C1) and Col de Vergio (C2) region for cosmogenic exposure dating.

4.5.2 Methodology

This section describes the sample collection in the field and the various stages involved in the preparation, chemical dissolution and extraction of ^{10}Be and ^{26}Al. Although the analysis of ^{26}Al was not undertaken, the samples were prepared as a backup in case the ^{10}Be results proved unsuccessful.

4.5.2.1 Collection of samples

The importance of selecting a sample site with the geomorphological context in mind has previously been emphasized (Chapters 4.4.3 & 4.4.4). In order to minimise the correction factors and minimise the effects of 'unknown' parameters, the site and substrate selection was conducted by:

i) Choosing large (>2m), flat boulders on the crests of moraines to reduce the risk of the substrate having rolled over and consequently exposing a different rock face.

ii) Looking for striation marks to illustrate negligible surface erosion, and avoiding substrates which showed distinctive signs of surface exfoliation or where a layer of rock had been removed.

iii) Choosing a site on a south facing slope to reduce winter snow cover and a large exposed boulder where snow would be readily blown off and not accumulate.

iv) Selecting a site above the tree line or at a reasonably high altitude where the vegetation cover is not likely to significantly attenuate the cosmic rays hitting the rock surface.

v) Choosing a site away from an adjacent valley sides and a sample from a horizontal or near horizontal surface to maximise the amount of cosmic ray bombardment at the rock surface and nuclide production, to yield more accurate measurements.

Once the boulders for sampling were selected, a hammer and chisel were used to exploit pre-existing weaknesses in the substrate. The sample size of the rock collected was between 1-2 kg. About 50 g of very pure quartz is needed for the making of BeO and Al_2O_3 AMS targets which is extracted from 0.5-1 kg of 0.5-2 mm sized crushed rock (Ivy-Ochs, 1996). Samples C1 and C2 were taken from grandiorite, a lithology exhibiting large quartz grains, ideal for cosmogenic nuclide extraction. The purer the quartz the greater the success of the Be and Al extraction procedure.

The rock thickness and lithology were noted in the field in addition to the strike and dip of the rock face. The geographical location and altitude of the sampling sites were determined by GPS and calibrated to reference points on the map. Topographic maps were also used to determine the cosmic ray shielding of the site by the surrounding hillsides and mountains. The precise

angle to the horizon and the number of degrees of the quadrant affecting the sampling site were established. Sketches and photographs were also taken of every site and sample.

4.5.2.2 Sample preparation

Where present, the rock surfaces were cleaned of lichens with a wire brush. A jaw crusher was then used to break the rock samples up into manageable sizes. The rock was then crushed and sieved to obtain the <2 mm size fraction. The material was then sieved again to separate the 0.5-1 mm and the 1-2 mm fraction. Ideally, the material should be as monominerallic as possible. The repeated sieving was adequate to reduce the bias (due to sample thickness and cosmogenic nuclide production) as not all the crushed material was used in the analysis. The steel jaw crusher and the sieves were cleaned thoroughly between the samples to avoid contamination. For the extraction procedures, general cleaning of all laboratory ware entailed rinsing with ultrapure (18Ω) water and dilute HCL. Teflon beakers were cooked for several hours in dilute HNO_3, then rinsed at least 10 times with ultrapure water.

4.5.2.3 Be and Al isolation and extraction from quartz

The two samples (C1 and C2) plus a blank were fully prepared and processed using the method of Ivy-Ochs (1996) modified from Kohl & Nishiizumi (1992) (Figure 4.8). Isolation and dissolution of the quartz was completed and repeated fuming of the samples were undertaken to remove all the fluoride. Iron extraction and cation exchange were conducted before the samples were precipitated. The samples were dried, baked and pressed onto a target for AMS ^{10}Be analysis. Each of these preparation stages is described in detail in Appendix I.

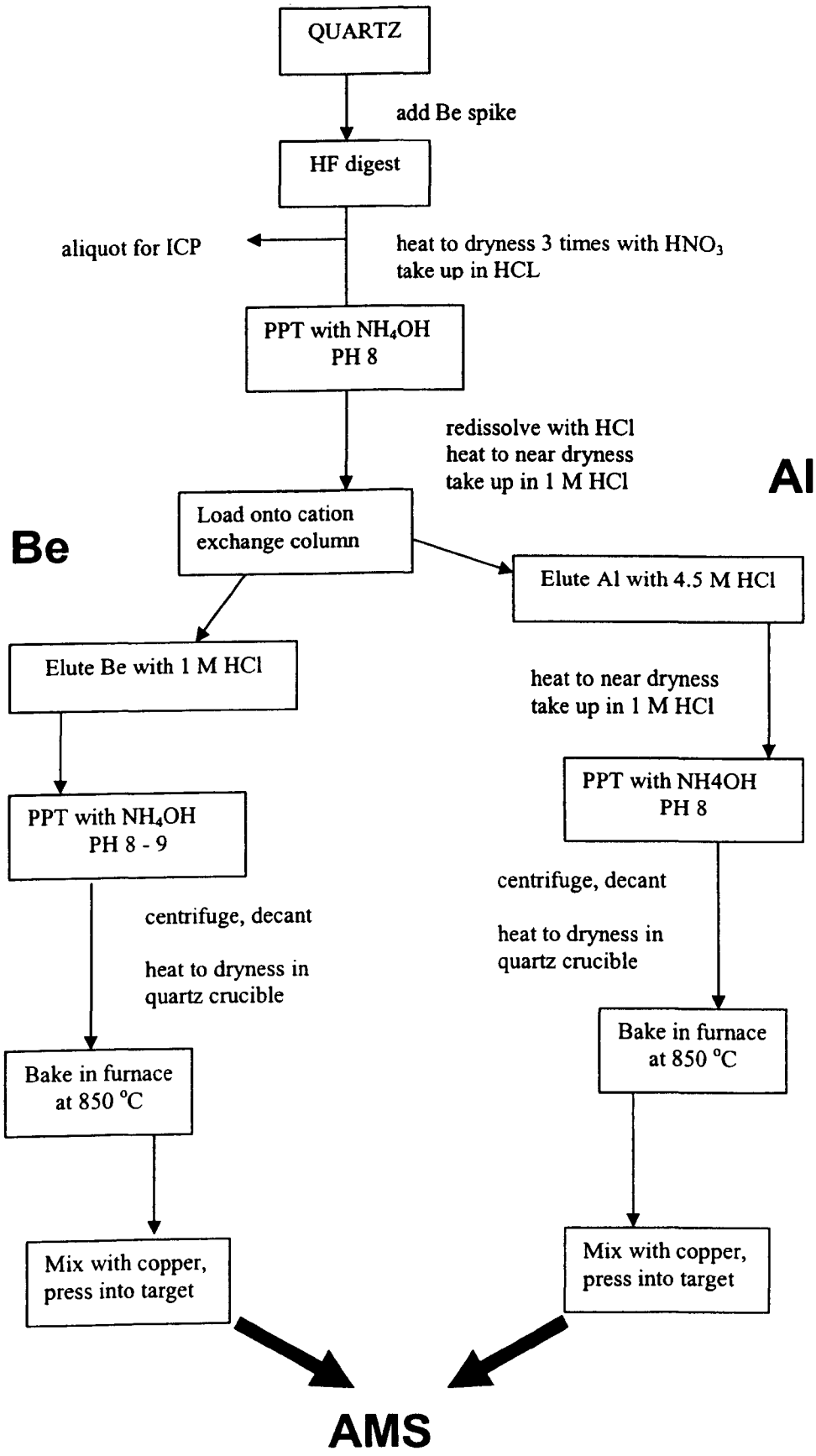

Figure 4.8 Flow chart showing the basic sample preparation steps for ^{10}Be and ^{26}Al extraction from quartz (PPT= precipitation) (after Ivy-Ochs, 1996).

4.5.3 Results

Using Equations 4.2 and 4.3, sample thickness and a shielding correction factor were calculated in addition to a geographical scaling factor for sample C1 and C2 (Table 4.8, Appendix II). The final ^{10}Be production rate is determined by the multiplication of all three factors.

The production rate (P) of 6.0 ^{10}Be atoms per gram SiO_2 per year at high latitude (>60°) and sea level is used for the age calculations (Nishiizumi *et al.*, 1989). This value is the most widely implemented and provides easy comparison with other data. The final number of Be atoms (N) has been calculated using Equation 4.1 and taking the blank sample into consideration (Table 4.9).

Table 4.8 Correction factors applied to the exposure age.

Field Ref.	Lab Code	Corrected ^{10}Be production rate for latitude/longitude/altitude (atoms/g SiO_2 • yr)	Thickness correction	Shielding correction	Final ^{10}Be production rate (atoms/g SiO_2 yr)
C1	ZB1047	14. 846	0.973	0.991	14.323
C2	ZB1048	15.109	0.965	0.991	14.447

Table 4.9 Number of ^{10}Be atoms per gram and final sample ratio error.

Field Ref.	Lab Code	$^{10}Be/^{9}Be$ ($1E^{-12}$)	Counting error (%)	Carrier (mg)	Weight (g)	Measured ^{10}Be (atoms/g)	Final number of ^{10}Be atoms (blank corrected) (atoms/g)	Final sample ratio error (%)
Blank	ZB1046	0.034	34.4					
C1	ZB1047	0.380	5.4	0.352	40.48	220900	201135	2.36
C2	ZB1048	0.318	4.9	0.349	36.13	205080	183153	2.58

4.5.3.1 Stated errors

Errors inherent in the dating technique which cannot be quantified have already been discussed (Chapter 4.4.3). However, analytical errors can be calculated precisely and included in the final error margin.

The uncertainty of an AMS measurement is caused mainly by the counting statistics (detection of the number of ^{10}Be counts from a sample). The counting error shown in Table 4.9 for the blank and for the samples is equivalent to (1/squareroot (number of counts)), approximated to the Poisson statistics error. The counting error for the blank is therefore high (34.4%) because there are fewer detected counts of ^{10}Be compared to within sample C1 and C2 (5.4% and 4.9% respectively) where the *in-situ* produced ^{10}Be has accumulated since exposure. The measured ratio of the chemistry blank is then subtracted from the measured ratios of the samples to correct for ^{10}Be in the carrier, any contamination during sample preparation and any cross contamination occurring in the AMS system (mainly from the ion source). Background due to

boron is also corrected (^{10}B is an interfering isotope as AMS recognises the atomic mass number for concentration measurement, so does not distinguish between ^{10}Be and ^{10}B). The potential of introducing boron into the sample during preparation is minimised by covering the samples at all times and by using deionised water. Dust and tap water are the two main sources of boron.

The final sample ratio errors for C1 and C2 are calculated to be 2.36 and 2.58 % respectively (Table 4.9). These are 1 σ measurement errors which includes the statistical (counting) error and the error due to normalisation to the standards and blanks. This is a fairly low error inferring the samples consisted of good quality quartz and the preparation was conducted with precision and thoroughness. A 5% sample reproducibility error has also been included in the error on each of the exposure ages. This is based on the reprocessing of several different rock samples by Ivy-Ochs (1996). Total sampling and analytical error is therefore calculated as 7.36% for sample C1 and 7.58% for C2. It is difficult to assign an error in relation to the correction factors and to incorporate the unknown parameters.

4.5.3.2 Exposure ages

The exposure age is calculated using Equation 4.4 below. The exposure ages are minima assuming known production rates, constant surface exposure and no erosion and assuming no isotopic inheritance.

$$T = \frac{\ln\left(1-\frac{N\lambda}{P}\right)}{-\lambda}$$ **Equation 4.4**

where T is the length of time the surface has been exposed in years, N is the number of atoms/gram, P is the local production rate in atoms/g $SiO_2 \cdot yr$, λ is the decay constant of the radionuclide in yr^{-1}.

This calculation gives exposure ages of 14.11 ka ± 1.04 for C1 and 12.71 ka ± 0.96 for C2 (Table 4.10). The data are calendar years and therefore do not require calibration. These exposure ages coincide with the Older Dryas and Younger Dryas events respectively. Both are episodes of cooling experienced in many parts of Europe (Chapter 2.4.2). The Younger Dryas is much more distinct in the palaeoenvironmental records than the Older Dryas and is widely recognised in the northern hemisphere. A climatic signature corresponding to the Younger Dryas has also been recognised recently in the southern hemisphere (e.g. Denton & Hendy, 1994; Ivy-Ochs *et al.*, 1996), although this is still controversial (e.g Singer *et al.*, 1998). The cosmogenic nuclide exposure age of C2 and the Younger Dryas corresponds very well with that from the Greenland ice cores: GISP2, 12.94 ± 0.55 to 11.64 ± 0.25 ka (Alley *et al.*, 1993) and GRIP, 12.7 ± 0.10 to 11.55 ± 0.07 ka (Johnsen *et al.*, 1992). The Older Dryas is also evident in the Greenland ice cores although it is less well illustrated in the Mediterranean palaeoenvironmental record. It is thought that the Older Dryas cooling may be associated with

a meltwater pulse occurring 14-14.5 ka and related to Antarctic melting. The significance of these ages is discussed in more detail below.

Table 4.10 Exposure ages calculated from concentrations of the cosmogenic nuclide ^{10}Be in sample C1 and C2.

Field Ref.	Lab Code	*In-situ* cosmogenic nuclide exposure age (ka)	Radiocarbon years (ka) [a]
C1	ZB1047	14.09 ± 1.04	13.07 ± 1.04
C2	ZB1048	12.70 ± 0.96	11.70 ± 0.96

[a] Converted by Oxcal. v. 3.5

4.6 THE LATEGLACIAL IN THE MEDITERRANEAN

The Lateglacial in Corsica and other parts of western and central Mediterranean has previously been described in some detail (Chapter 2.4.2). In this section, palaeoclimatic evidence for the Older Dryas and Younger Dryas cooling episodes is summarised. The timing and nature of glacial activity identified in the Mediterranean during the Lateglacial is also outlined. Finally, temperature and precipitation reconstructions are used to establish whether the conditions in Corsica were suitable for glacier growth during this period as the pollen data from Corsica suggests that the island was ice-free from the Older Dryas (Conchon, 1986). The cosmogenic ages yielded from this study suggest otherwise.

4.6.1 Older and Younger Dryas climatic signals identified in the Mediterranean

The cool event known as the Older Dryas which preceded the Alleröd interstadial is far less distinctive in the lacustrine sequence from Lake Creno in Corsica than the Younger Dryas interval (Figure 2.5). This lack of evidence suggests that the intensity and duration of the Older Dryas was far less than that of the Younger Dryas, and this difference is illustrated fro Europe as a whole in the schematic diagram Figure 4.9. The Older Dryas is dated to around 12 k radiocarbon years BP and lasted no longer than 500 years. The cooling signal is identified in many parts of central Europe by palynology and other climate proxy records (Table 4.11). The Older Dryas signal is marked by an increase in steppe-like vegetation and a reduction in tree pollen in the Cantabrian mountains, northern Spain (Watts, 1986), the Pyrenees (Andrieu *et al.*, 1993; Reille, 1993a, 1993b) and the Massif Central (Beaulieu *et al.*, 1985; Ponel & Coope, 1990). The Older Dryas is also identified by the reintroduction of certain beetle species in the Massif Central which are associated with cooler conditions (Beaulieu *et al.*, 1985; Ponel & Coope, 1990; Ponel & Lowe, 1992). The abrupt cooling of the Younger Dryas is clear in many of the pollen records from mountain sites throughout the western Mediterranean (Beaulieu *et al.*, 1994). An increase in *Artemisia* and a decline in tree pollen is clearly marked in many of the records from the Iberian Peninsula, the Pyrenees, the Massif Central and the northern Apennines (Table 4.11). Radiocarbon dating has constrained the timing of the Younger Dryas

event across these sites to between 11 and 10 k radiocarbon years BP. Sea surface temperatures and salinity records from the western Mediterranean also indicate cooling intervals during the Lateglacial synchronous with the Younger and Older (Oldest?) Dryas (Paterne *et al.*, 1986; Kallel *et al.*, 1997; Combourieu-Nebout *et al.*, 1998; Cacho *et al.*, 2001).

Glacial advances during the Lateglacial are also evident in southwest Europe. Glaciers in the central Pyrenees extended for the final time between 13.25 and 10.8 k radiocarbon years BP, perhaps corresponding to the Younger Dryas episode (Hérail *et al.*, 1986). Interestingly, periods of enhanced glaciation have been identified in the Gran Sasso region of the central Apennines not only during the Younger Dryas but the Older Dryas stadial (Giraudi & Frezzotti, 1997). Moraines of the two glacial advances recorded in the Campo Imperatore area have been dated to *ca.* 12.85 ± 0.2 k and 11.0 k radiocarbon years BP. It is estimated that the reduction in MAT during this time was 5.6 to 6.7 °C lower than present day, and that the discontinuous permafrost boundary was at an altitude of 1,900 m, with the equilibrium line altitude at 2,300 m. The glacial advances in the Apennines correlate well with the isotopic data of cores from the Tyrrhenian Sea (Paterne *et al.*, 1986). The onset of glacial retreat in the French and Italian Piedmonts of the Alps has been estimated to between 15 and 14 k radiocarbon years BP (Billard & Orombelli, 1986). At least two major advances are thought to have interrupted the Lateglacial deglaciation phase although the precise timing of these have not been established (Porter & Orombelli, 1982). The main valleys were free of ice from 10 k radiocarbon years BP which suggests that the cooling episodes responsible for the glacial advances between 14 and 10 ka may be that of the Older (or Oldest?) and Younger Dryas. It is postulated that the warmer, wetter phase separating the two glacial advances was the Alleröd-Bölling Interstadial (Billard & Orombelli, 1986).

The investigation conducted in Serra de Queixa, northwest Iberia using ^{21}Ne cosmogenic nuclide dating identified three different stages with the last terminating about 15 k calendar years BP (Fernandez Mosquera *et al.*, 2000). The error on this age is 7 ka BP so it is possible that the glacial phase could be attributed to the Older or Younger Dryas stadial. The calculated CND age of 15 ± 7 ka corresponds to the time of final glaciation and is supported by a radiocarbon date of 13.4 ± 0.4 ka for a lacustrine sediment from the same area (Fernandez Mosquera *et al.*, 2000).

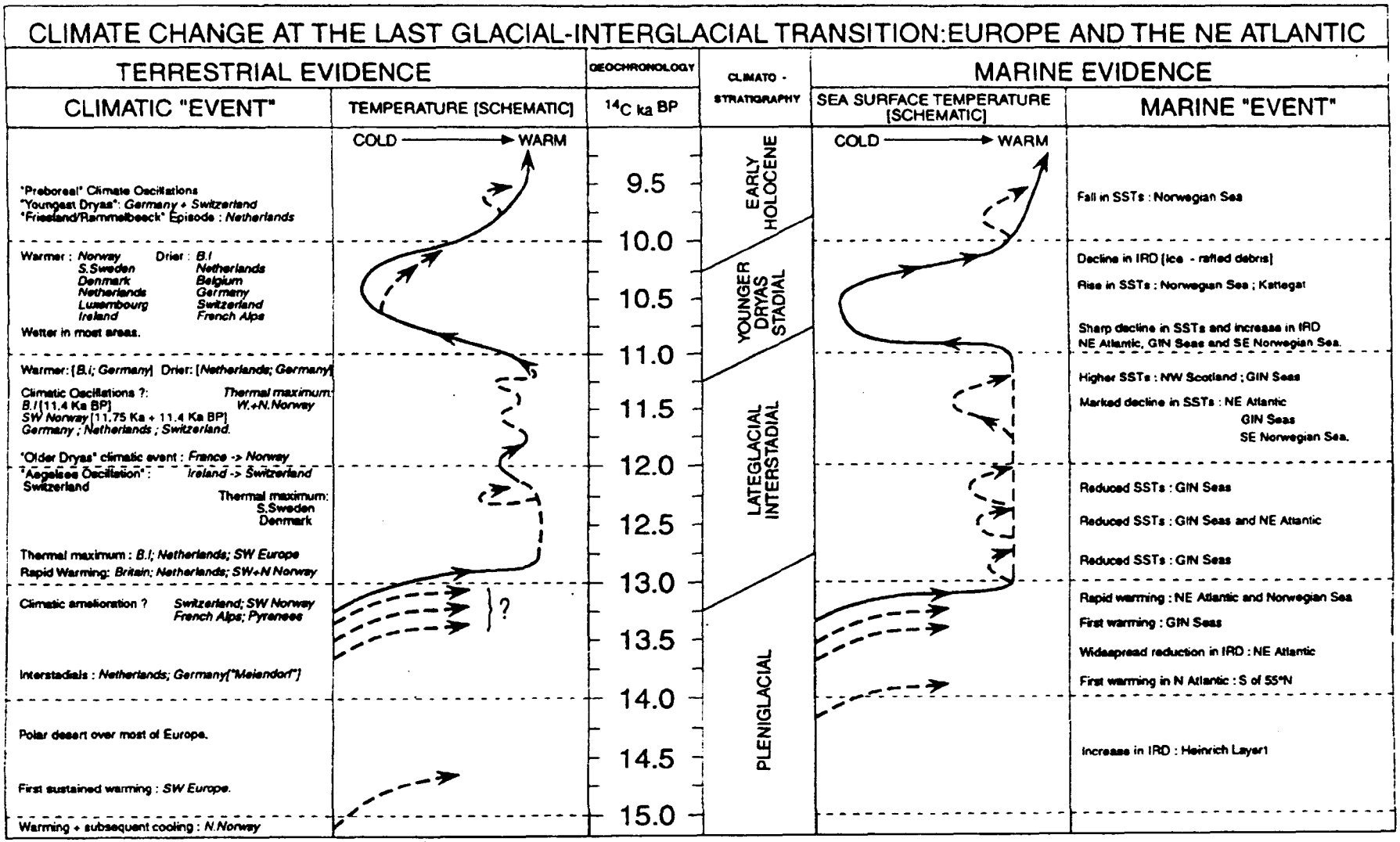

Figure 4.9 Summary of climatic changes in Europe at the last glacial transition reflected in terrestrial and marine records (after Walker, 1995).

Table 4.11 Terrestrial and marine palaeoenvironmental data illustrating signals attributed to the Older and Younger Dryas events.

Site	Younger-Dryas signal	^{14}C age (ka BP)	Older Dryas signal	^{14}C age (ka BP)	Reference
SPAIN					
Largo de Ajo NW Spain	Pollen change	11-10?	Pollen change	12.6	Allen *et al.*, 1996; Watts, 1986
Quintanar de la Sierra N Spain	Pollen change	10.65 - 10			Penalba *et al.*, 1997
La Paul De Bubal NE Spain	Pollen change	<10.785			Montserrat, 1992
Banyoles Lake NE Spain	Pollen change	12 ka (U/Th)			Pérez-Obiol and Julià, 1994
Padul S Spain	Pollen change	10 ± 2.1 to 9.93 ± 1.1			Pons and Reille, 1988
Alboran Sea	Sea surface temperatures	12-13 ka (cal. yr)			Cacho *et al.*, 2001
FRANCE					
Lourdes Region Pyrenees	Glacier advance	>10.8			Hérail *et al.*, 1986
Western/Central Pyrenees sites	Pollen change	11-10	Pollen change	>12.5	Andrieu *et al.*, 1993; Reille, 1993a
Eastern Pyrenees sites	Pollen change	11-10			Reille and Lowe, 1993; Reille, 1993b Turner and Hannon, 1988
Massif Central sites	Pollen change insect evidence	11-10.26	Pollen change, insect evidence	12	Beaulieu *et al.*, 1985; Ponel and Coope, 1990
French/Italian Piedmonts, Alps	Glacial advance	?	Glacial advance	?	Porter and Orombelli, 1982; Billlard and Orombelli, 1986
Lake Creno, Corsica	Pollen change	<11.44 ±0.15 to >10.04 ± 0.085			Reille *et al.*, 1997
ITALY					
Prato Spilla sites N Apennines	Pollen change Insect evidence	11-10.2	Insect evidence	<12.36	Lowe, 1992; Ponel and Lowe, 1992
Gran Sasso C Apennines	Glacial advance	11	Glacial advance	12.85 ± 0.2	Giraudi and Frezzotti, 1997
Laghi di Monticchio S Italy	Pollen change	10.5			Watts *et al.*, 1996
Tyrrhenian Sea KET80-19 KET80-03	Sea surface temperature and salinty changes	11-10	Sea surface temperature and salinity changes	Oldest Dryas 15 -13	Kallel *et al.*, 1997
Adriatic Sea MD 90-917	Pollen change and dinocyst abundance	11.1-9.7	Pollen change and dinocyst abundance	Oldest Dryas 14.4-12.7	Combourieu-Nebout *et al.*, 1998

4.7 RECONSTRUCTING YOUNGER DRYAS SNOWLINES IN CORSICA

In order to demonstrate whether the climatic conditions in Corsica during the Younger Dryas were suitable for glacier growth, a basic snowpack model has been developed. This section describes the inputs to the spreadsheet model, the temperature and precipitation scenarios that were tested and the assumptions and limitations attached to the model. The Older Dryas has not been included because very few climate reconstructions are available to parameterise the model.

4.7.1 Inputs and outputs of the snowpack model

There are two main inputs into the model (precipitation and temperature) and two associated parameters (rate of accumulation and rate of ablation). These, together with the temperature and precipitation offsets to reflect the Younger Dryas climate are used to obtain an output of net snow depth (Figure 4.10).

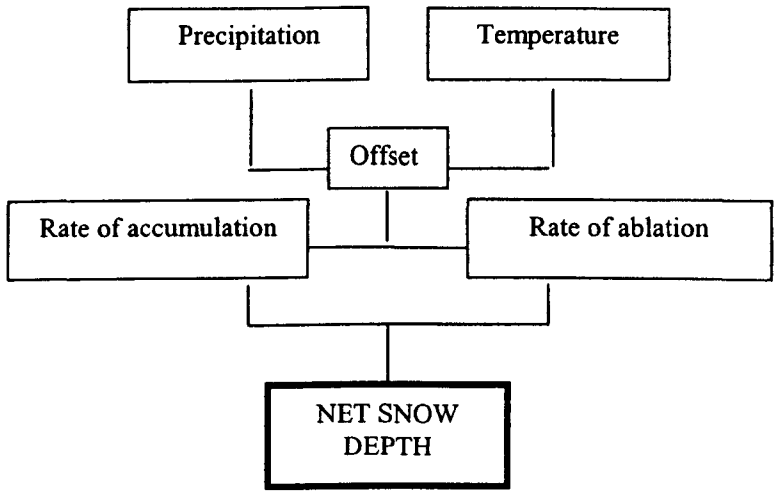

Figure 4.10 Inputs into the snowpack model.

4.7.1.1 Model parameters

The relationship between precipitation and elevation in Corsica was deduced by taking the mid point of the intervals for relief (Figure 3.8) and rainfall distribution (Figure 3.12). The change in rainfall with elevation was plotted on a graph and a linear trend line was applied to obtain an estimate of the average rainfall increase for every metre in elevation (Figure 4.11). The graph illustrates a relationship of 0.7724 mm rainfall increase per metre elevation. The r^2 value is 0.96, illustrating a good correlation and adequate for the use in this model.

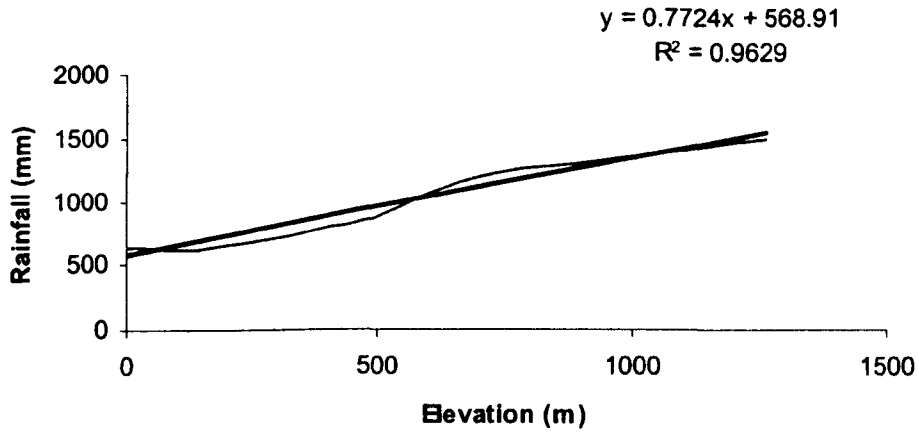

Figure 4.11 Rainfall change with elevation used as inputs to the snowpack model.

Precipitation is not distributed evenly throughout the year, so the percentage of precipitation presently received in Corsica for each month is applied to the model. For example, January receives 12% of the annual rainfall and July receives 2%. The relationship between temperature and elevation is determined by the Environmental Lapse Rate (ELR) of 6.5°C per kilometre which does not vary widely with respect to global position or altitude.

The rate of snow accumulation each month is described by the argument:

> 'if temperature < 0, accumulation of snow = total precipitation, otherwise it is zero'.

The rate of ablation each month is characterized by:

> 'if temperature > 0, ablation = snow melted per day degrees (5 - 6°C) multiplied by the temperature and multiplied by the number of days in the month, otherwise it is zero'.

4.7.1.2 Model offsets

The temperature offset is regarded as a sine function of the annual average temperature drop of the (winter + summer) – (summer - winter). The precipitation offset is more simply the reduction or increase in rainfall or snow during the Younger Dryas from present day levels.

4.7.1.3 Model output

The model output is the net snow depth and is equivalent to:

> 'the previous months total plus the accumulated snow minus the melt'.

The model shows the accumulated snow depth with respect to elevation over a five year period (Appendix III). The altitude at which a permanent snow line is obtained with set climatic conditions (Chapter 4.7.2) is compared.

4.7.2 Climate scenarios

The minimum and maximum values determined for temperature and precipitation during the Younger Dryas were based on published data available for southwest Europe during the Lateglacial (Table 4.12). The majority of the climatic reconstructions are based on pollen and coleoptera evidence (e.g. Ponel & Lowe, 1992; Guiot *et al.*, 1993; Peñalba *et al.*, 1997) which provide summer temperature estimates. Winter temperatures, however, are not so easily constrained. Lateglacial precipitation reconstructions are less well documented due to lack of climatic proxies enabling such inferences.

Climate models have been developed to simulate the climate during the Younger Dryas event in Europe, although many more have been constructed for northwest Europe than those that include the Mediterranean region (e.g. Rind *et al.*, 1986; Renssen & Isarin, 1998; Fawcett *et al.*, 1997). Recently, Renssen *et al.* (2001) has simulated the Younger Dryas climate for the whole of Europe using a Regional Climate Model (RCM). The RCM results show a winter (Dec., Jan. and Feb.) and summer (June, July and Aug.) temperature reduction of 5°C and 1°C respectively for Corsica during the Younger Dryas. A winter precipitation reduction of 1 mm per day is simulated but there appears to be no change in summer precipitation totals from present day conditions. Renssen *et al.*'s climate reconstructions for southern Europe during the Younger Dryas are significantly less severe than those inferred from pollen and coleoptera evidence (Table 4.12). It is highlighted in the RCM study that the simulated temperatures are minimum values which could have been higher in reality. The model results are also regarded as preliminary because the Younger Dryas climate simulation has a duration of only three years (Renssen *et al.*, 2001). Additional, and more advanced simulations are therefore needed to test the theory of a less extreme Younger Dryas climate than that implied by biogenic climate proxies. In this study, the RCM results are not seen to supersede the pollen and beetle data, however, the model results produced by Renssen *et al.* (2001) must not be overlooked. A 30, 40 and 55% reduction of present day precipitation were tested, in addition to a summer temperature drop of 4, 10 and 14°C and a winter temperature drop of 4, 6 and 8°C. Table 4.12 summarises the justifications for employing such a range of climate scenarios.

Table 4.12 Reasoning for chosen climate scenarios.

Climate parameter extremes	Reasoning
Summer temperature drop	
4°C	4°C below the current July temperature is 18°C. Using pollen as a climate proxy, a July estimate of 17°C was constructed from the site Quintanar de la Sierra, Northern Spain (Peñalba *et al.*, 1997). Investigations of glacial features in the Northern Apennines infer Younger Dryas temperatures to be between 5.6 and 6.7 °C below present (Giraudi & Frezzotti, 1997). Some studies suggest that the July temperature was 8°C below present day (e.g. de Beaulieu *et al.*, 1994). Coleoptera evidence in the central Apennines suggests that the summer temperature was between 9 and 13°C (Ponel & Lowe, 1992; Lowe & Watson, 1993).
14°C	Pollen and coleoptera evidence from the Massif Central imply that the July temperature during the height of the Younger Dryas was 8°C, 14°C below modern day temperatures (Figure 3.4).
Winter temperature drop	
4°C	In line with the summer temperature drop. Few studies constrain a winter temperature, but it is believed that the winter temperature was less extreme during the Younger Dryas compared to the summer temperature.
8°C	The annual temperature in Northern Spain is estimated at 7.5°C (Peñalba *et al.*, 1997), which is between 7 and 8°C below the present annual average of 14.6°C.
Precipitation reduction	
30%	Massif Central received ca. 400-500 mm less rainfall during the Younger Dryas (Pons *et al.*, 1987). Current annual total is approximately 1270 mm.
55%	A reduction of 400 mm amounts to 70% of the present day total. GCM simulates annual precipitation totals to be approximately 365 mm (~1 mm/day). This is a 55% reduction of the present precipitation total in Corsica (660 mm).

4.7.3 Other variables

Although the ELR of 6.5°C per kilometre is constant, and the rainfall with elevation is increasing linearly at 0.7724 mm per metre), the degree day factor which influences the rate of ablation varies (Figure 4.12). The melting of snow or ice during a particular time is assumed to be proportional to the sum of all the positive temperatures, i.e. the sum of positive degree-days (Singh & Singh, 2001). The degree day factor for snow is lower than that for ice (Braithwaite, 1995) and varies according to the albedo such that the dirtier the snow and ice the higher the value. Generally, the day degree factor is between 5 and 6 mm per °C per day (Table 4.13). Comparisons of model output were made between these two day degree factors.

4.7.4 Calibration

The climatic parameters were set to zero so that present day conditions could be simulated. The permanent snow line generated by the model was at an elevation of 2,716 m (Figure 4.13). This elevation is just above the summit of Mt Cinto (2,706 m), the highest mountain on the island. This is a reasonable output, as patches of snow are often seen on the summits in early summer. On a reconnaissance trip to Corsica in May 1999, there was snow at an elevation of 1,700 m in the Haut Asco region (Figure 4.2). In the June of 2000, all the snow had melted at this altitude

(Figure 4.14). The model corroborates well with the observations by simulating snow during May of the fifth year but showing no snow in June (Appendix III). This snowline is also comparable to others within the Pyrenees and southwest Alps (Table 4.1).

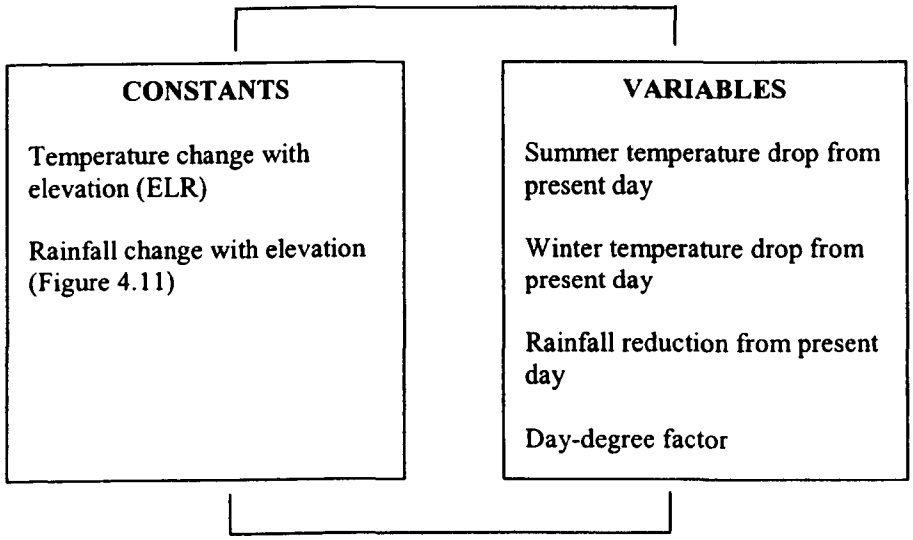

Figure 4.12 Constant and variable factors used in the snowpack model.

Table 4.13 Degree-day factor for snow and ice as reported by various authors (Table 6.7, after Singh & Singh, 2001).

Degree-day factor ($mm°C^{-1}day^{-1}$) Snow	Ice	Reference
-	5.0 – 7.0	Kasser (1959)
4.0 – 8.0	-	Yoshida (1962)
3.0 – 5.0	-	Borovikova *et al.* (1972)
5.4	-	Lang *et al.* (1977)
-	5.5 ± 2.3	Braithwaite (1977)
-	6.3 ± 1.0	Braithwaite (1981)
5.0	-	Abal'yan *et al.* (1980)
3.0	6.0	Woo & Fitzharris (1992)
4.4 – 5.7	6.4 – 7.7	Jóhannesson *et al.* (1993)
3.5 – 4.5	5.5 – 6.0	Laumann & Reeh (1993)
5.94	-	Singh & Kumar (1996)

4.7.5 Results

Twenty seven climate scenarios were run (Figure 4.13) and the snowline for each was recorded. Each run was initially conducted with a day-degree factor of 6 $mm°C^{-1}day^{-1}$. The snowline was taken as the elevation (1 m resolution) at which snow was present all year round in the fifth year. The basic model shows that the snowline altitude varies from 2,389 m to 974 m, according to the climate scenario set (Table 4.14, Figure 4.15). As expected, the highest elevation is generated when a 55% reduction in precipitation is applied together with the less extreme drops in temperature, (4°C in summer and winter). The lowest snowline corresponds to conditions with only 30% less precipitation than present day and the greatest drops in

temperature (14°C in summer and 8°C in winter). It is clearly seen that neither a winter temperature drop nor precipitation have as much impact on the accumulation of snow as the summer temperature drop. Even with a summer *and* winter temperature drop of 14°C and a 30% reduction in precipitation, the snow line elevation is only 889 m.

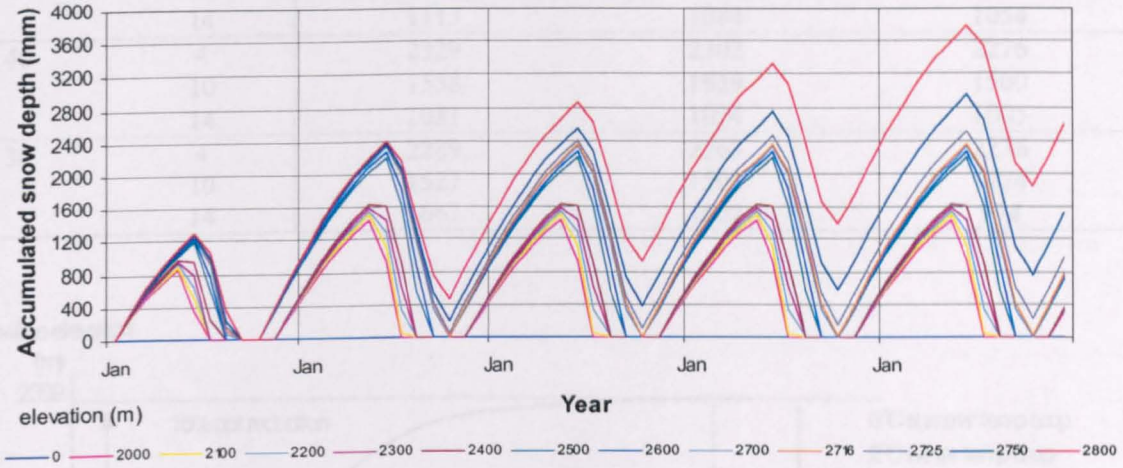

Figure 4.13 An example of the snowpack model output. Present day conditions are applied (Precipitation 0% reduction; summer and winter temperature drop, O°C; day-degree factor, 6 $mm^{\circ}C^{-1}day^{-1}$).

a)

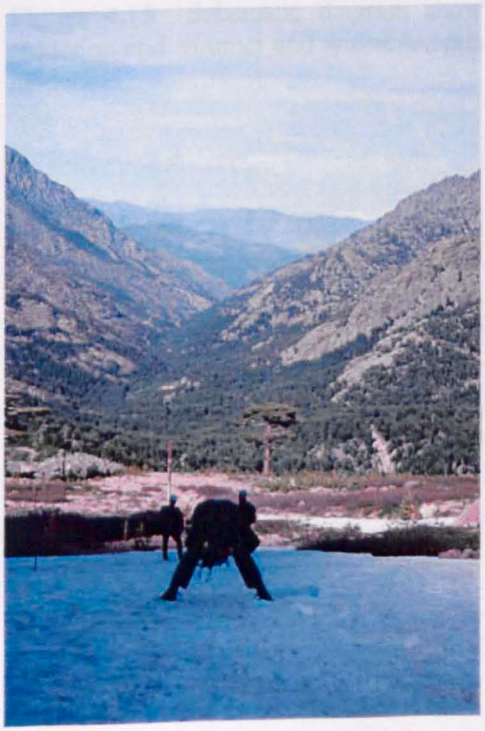

b)

Figure 4.14 a) Significant snow cover was evident above an altitude of 1,700 m in the Haut Asco region in May (1999), but b) only above an elevation of 2,000 m elevation in June (2000). Photograph b illustrates a small push moraine, perhaps from the cirque glacier headed by the peak Punta Culaghia (Figure 4.2). This region is rhyolitic so the lithology was not suitable for obtaining pure quartz for cosmogenic dating (Chapter 4.5).

Table 4.14 Snow line elevations generated with the different climatic scenarios and a day degree factor of 6mm°C^{-1}day^{-1}. The bold values correspond to the schematic diagram of Figure 4.15.

Precipitation reduction (%)	Summer temperature drop (°C)	Snowline elevation (m) with a 4 °C winter temperature drop	Snowline elevation (m) with a 6°C winter temperature drop	Snowline elevation (m) with a 8°C winter temperature drop
55	4	**2389**	2353	2335
	10	1621	1592	1562
	14	1113	1084	1054
40	4	2329	2302	2276
	10	1558	**1529**	1500
	14	1081	1034	1005
30	4	2289	2263	2236
	10	1527	1501	1474
	14	1067	1002	**974**

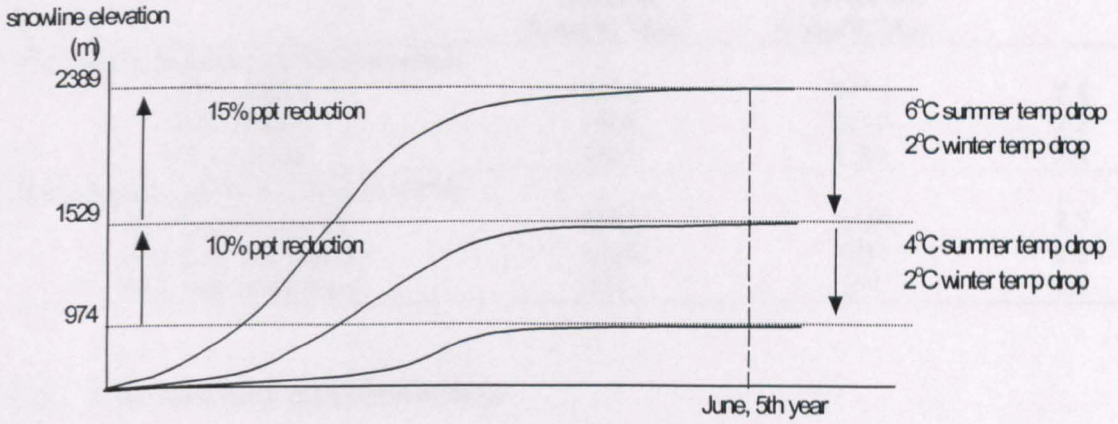

Figure 4.15 Schematic diagram showing the snowline elevation change with precipitation (ppt) reduction and summer and winter temperature (temp) drop after the fifth year of running the snowpack model.

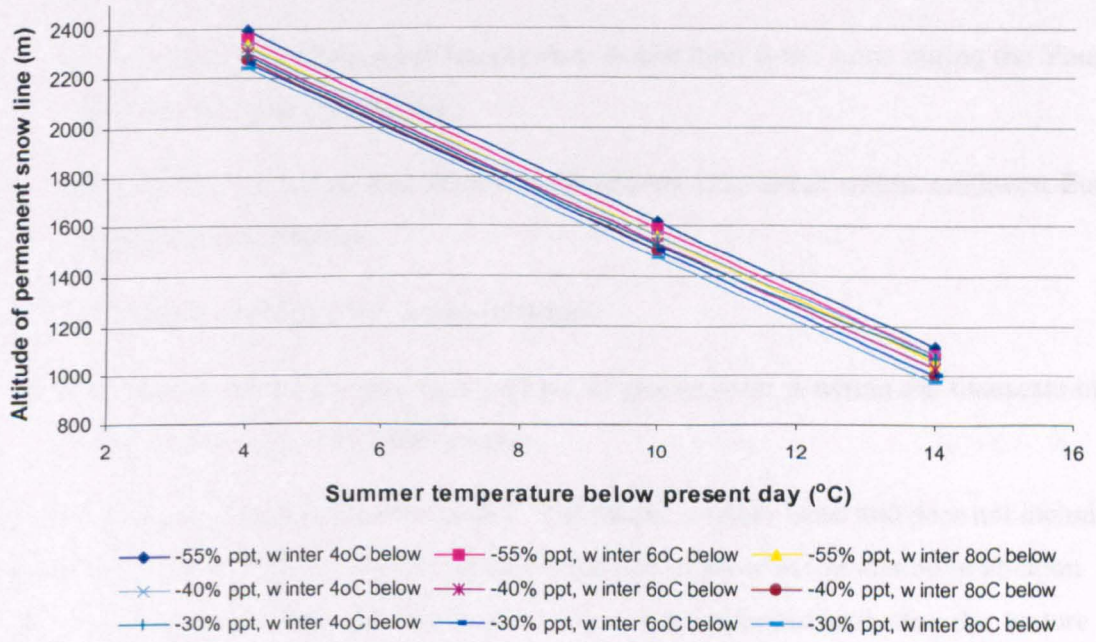

Figure 4.16 Permanent snow line altitudes for each of the climate scenarios described in Chapter 4.7.2, Table 4.1.

4.7.5.1 Day-degree factor

Several of the scenarios were repeated using a day-degree factor of 5 $mm°C^{-1}day^{-1}$ compared to 6 $mm°C^{-1}day^{-1}$ to assess the affect on net snow accumulation. Applying the lower day-degree factor results in a reduction of snowline elevation (Table 4.15). However, the percentage difference for all the given scenarios is less than 3%, with the exception of the setting 30% precipitation reduction, 8°C and 14°C temperature drop in winter and summer respectively, which is 4.5%.

Table 4.15 The difference in snowline elevation when using a day degree factor of 5 and 6 $mm°C^{-1}day^{-1}$ with different climate scenarios.

Climatic scenario	Snowline elevation (m) with a day-degree factor of 5 $mm°C^{-1}day^{-1}$	Snowline elevation (m) with a day-degree factor of 6 $mm°C^{-1}day^{-1}$	% difference
10°C drop in summer, 8°C drop in winter			
–30% rainfall	1434	1474	2.8
–40% rainfall	1468	1500	2.2
–55% rainfall	1525	1562	2.4
30% reduced rainfall, 8°C drop in winter			
4°C drop in summer	2182	2236	2.5
10°C drop in summer	1434	1474	2.8
14°C drop in summer	932	974	4.5

4.7.6 Assumptions and limitations

There are five assumptions attached to this model in addition to the arguments put forward in Chapters 4.7.1.1 - 4.7.1.3 which need to be highlighted. It is assumed that:

i) There is no inheritance of snow and ice from the Older Dryas period, the previous stadial within the Lateglacial.

ii) The monthly precipitation and temperature distribution is the same during the Younger Dryas period as the present day.

iii) The temperature and precipitation reconstructions from areas within southwest Europe are applicable to Corsica.

iv) The climate conditions set, remain constant.

v) the transformation between snow and ice to glacier form is within the timescale of the Younger Dryas (*ca.* 800-1,000 years).

There are numerous limitations to this model. The model is rather basic and does not include all the complex factors and processes that influence the rate of snow accumulation or ablation. For example, wind direction and the transport of snow are important and also the texture and structure of the snow with regards to compaction and ice formation. The accumulation of snow and the rate of development of a glacier are also dependent on the aspect and orientation, and

the catchment size and topography. The albedo of the snow and ice has an influence on the rate of ablation too which is not an integral part of the model. The albedo can vary from 84% for dry snow to 12% for debris covered ice (Paterson, 1994). The orography and the Mediterranean Sea also play an important part in influencing regional weather and snow accumulation, although these factors may already be incorporated to some extent within the present day precipitation and temperature regime on which the model is based.

Some of these limitations can be qualitatively evaluated in terms of encouraging glacier growth in Corsica. The two sites from which the cosmogenic samples were collected are east facing (Figure 4.4, Figure 4.6), which would not lead to maximum snow depletion, like a south facing slope. The valleys containing the glaciers in Corsica are also relatively small which would encourage early glacial development. Additionally, smaller glaciers tend to be more sensitive to climate change (Nesje & Dahl, 2000).

4.8 GLACIAL ACTIVITY IN CORSICA DURING THE YOUNGER DRYAS

There is an abundance of terrestrial and marine evidence to suggest that the Younger Dryas had a major impact on the Mediterranean landscape (Table 4.11). There is already some evidence of glacial advances within the Mediterranean area during the Lateglacial (e.g. Hérail *et al.*, 1986; Giraudi & Frezzotti, 1997), but due to the lack of dating techniques, very few glacial sediments and deposits have been dated by absolute techniques. The evidence presented in this chapter does suggest that glacial activity within Corsica may have taken place during the Lateglacial. Both the cosmogenic dates taken from boulders on two different moraines suggest a Lateglacial age. Although the errors associated with cosmogenic dating cannot be known precisely, the overall margin is estimated to be ± 10-20%. Even with this error included, the ages established for C1 and C2 are much younger than that of Conchon's proposed timing of two stadials within the middle Würm (Table 4.2). There are many factors which are likely to underestimate the exposure age (Chapter 4.4.3) but the sample sites and substrates were chosen with these parameters and the geomorphological context in mind. With regards to error margins it could be the case that sample C1 is associated with the Younger Dryas, rather than the Older Dryas. The brevity of the Older Dryas and the less extreme temperature drops may have prevented glacier growth, although it cannot be ruled out. Additionally, there is also the uncertainty as to the validity of the Older Dryas in Corsica. The few available palaeoenvironmental data for the island do not show a significant cooling during the Lateglacial at this time. Alternatively, C1 could be an underestimated exposure age of a moraine from the LGM stand (18-20 k radiocarbon years BP). This is a reasonable hypothesis, as no glacial deposits have been identified further down the valley that could be associated with a more extensive glacier and the LGM.

Reille *et al.* (1997) argue from a palynological perspective that Lake Creno (1,280 m) in central Corsica (Figure 3.10) has been ice free since the Older Dryas and when at 15 ka, sediment infilling occurred. However, it has been previously noted that Lake Creno may be a sheltered site (Chapter 2.4.2) and consequently may not have been glaciated during the Younger Dryas when other sites in Corsica may have been. The glacier front associated with the moraine from which sample C2 was taken and dated to 12.70 ± 0.96 ka is estimated to be between 1,100 and 1,250 m asl (Conchon, 1986), which means it is feasible that Lake Creno at an elevation of 1,280 m may have been ice free at this time.

It is reasonable to suggest that several more terrestrial *in-situ* cosmogenic nuclide exposure ages from boulders of the same moraines are necessary in order to be more confident that glacial activity was prevalent during the Lateglacial in Corsica. The basic snowpack model confirms, to a certain degree, that glacier growth is plausible in Corsica during the Younger Dryas, and not inhibited by the drier conditions (*cf.* Clapperton, 1995). The glacier fronts would be at a lower elevation than the permanent snowlines generated for each of the climatic scenarios. For example, Conchon (1975, 1986) proposes that the moraine from which sample C2 was taken (and dated to the Younger Dryas in this study) was associated with a glacier exhibiting a snowline of 1,700-1,800 m and a glacier front of 1,100-1,250 m elevation (Table 4.2). Using the results of the model (Figure 4.16), a snowline of between 1,700-1,800 m is obtained when a Younger Dryas summer temperature drop of between 8 and 9°C is set. This ties in very well with many of the Younger Dryas temperature reconstructions from southwest Europe (e.g. de Beaulieu *et al.* (1994) based on the method of Guiot (1990) and Guiot *et al.* (1993) for northern Spain; Ponel & Lowe (1992), Lowe & Watson (1993) for the northern Apennines; Ponel and Coope (1990) for the Massif Central). The July temperature estimation of 8°C for the Younger Dryas at La Taphanel, a site in the Massif Central (Figure 2.2) is also comparable if the elevation (975 m) is taken into consideration. A Younger Dryas snowline of 1,650 m has also been determined in the Prato Spilla valley in the northern Apennines (Lowe, 1992), comparing well with the snowline of 1,700-1,800 m determined by Conchon (1975, 1986) for a proposed Mid-Würmian glacier (Table 4.2), but dated to the Younger Dryas by cosmogenic nuclide techniques in this study. This value also seems reasonable given that the present day snowlines in the Mediterranean are between 2,700-2,900 m and glaciers are still evident in the northern Apennines today (Table 4.1) (Chapter 4.3.1).

The Lateglacial climate reconstruction based on pollen and coleoptera evidence is the most widely used in southwest Europe to date (Figure 2.4). However, recent RCM simulations (e.g. Renssen *et al.*, 2001) believe that the Younger Dryas climate in southern Europe was not so severe (Chapter 4.7.2). In fact, reconstructions of 40 to 50% reduction in precipitation and –7 to –10°C reduction in summer and winter temperatures may be more applicable to LGM conditions (Barron & Pollard, 2002). Therefore, the snowpack model may be simulating LGM

climate conditions, and the ages of the glacial deposits in Corsica dated to the Lateglacial in this study could just be underestimates. If however the proposed 'Mid-Würmian' glaciers are dated correctly to the Younger Dryas stadial, at what time were the cirque glaciers active? A discussion is presented in Chapter 7.

4.9 SUMMARY

Terrestrial *in-situ* cosmogenic nuclide dating has been successfully applied in Corsica to establish the exposure ages of glacial deposits from lateral moraines. More exposure ages are needed in order to be confident that glacial activity was prevalent during the Lateglacial, but the new ages conflict with the glacial chronology of Corsica proposed by Conchon (1975, 1986). The exposure ages suggest that the moraines sampled are of Older Dryas (14.1 ka) and Younger Dryas age (12.7 ka), although it is possible that both moraines are attributed to the latter stadial when the conditions were more suitable for glacier growth, or perhaps the LGM. A simple snow pack model developed for Corsica implies that snow accumulation and glacier advances were likely during the Younger Dryas. Snowline elevations generated for a 8-9°C summer temperature drop are in agreement with other climate proxy reconstructions and other equilibrium line altitudes estimated for the Younger Dryas in the western Mediterranean basin.

5 QUATERNARY RIVER BEHAVIOUR IN THE TAVIGNANO RIVER BASIN, CENTRAL CORSICA

5.1 SYNOPSIS

This chapter examines five Tavignano River terraces and develops an age model for major alluviation within the catchment during the Late Pleistocene and Holocene Periods. A number of pedogenic characteristics, including redness, clay content, organic carbon and calcium carbonate content are described for each of the terrace profiles. Mineral magnetic properties of the terrace soils are explored and optically stimulated luminescence dating of the alluvial units is employed. A profile development index is constructed and used in combination with the absolute dating to infer the timing of catchment-wide deposition within the Tavignano basin. This study illustrates the benefits for an integrated approach in developing an alluviation age model. Finally, comparisons with other Mediterranean river studies investigating large scale aggradation are made with the Tavignano example.

5.2 INTRODUCTION

Many mountainous parts of the Mediterranean were characterized by valley glaciers (Chapter 4.3.2) during the Pleistocene Period which waxed and waned with the alternation between stadials and interstadials respectively. It has been shown that glacial activity in parts of the Mediterranean had a strong influence on the storage and flux of sediment and water downstream (Woodward *et al.*, 1995). Many studies have illustrated the relationship between cold (glacial and stadial) intervals and phases of large scale alluviation (Chapter 2.5.1). Phases of incision are often associated with warmer periods. Terrace sequences which are formed by a phase of aggradation followed by a phase of erosional downcutting can therefore broadly reflect episodes of climatic change. Investigations of such fluvial features can provide insights into the nature and timing of river response to environmental change and the impact of Pleistocene glaciation on Mediterranean mountain river systems.

This chapter aims to establish the nature and chronology of an exposed terrace sequence along the Tavignano, a major eastward flowing river in central Corsica with glaciated headwaters (Figure 3.10). The objectives are three-fold:

i) To examine the stratigraphical and sedimentological features of the alluvial units and assess the river regime and nature of river development.

ii) To evaluate and compare the degree of soil development within and between each terrace, identify age-related indicators and develop a relative soil chronosequence.

iii) To obtain absolute ages for the terrace units using optically stimulated luminescence (OSL) dating.

5.3 STUDY BASIN

The Tavignano River is one of the four major river systems of Corsica, and six terraces can be identified altogether along its course (Conchon, 1975). This investigation concerns the pedostratigraphical and chronological analysis of the five youngest terraces. The oldest terrace is less well preserved, less accessible and exhibits fewer good exposures than the younger units.

5.3.1 Regional setting of the Tavignano River

The source of the Tavignano River is Lake Nino (1,743 m) located on the eastern flank of Capu a u Tozzo (2,007 m) in central Corsica. The headwaters are delimited by other high peaks such as Punta Artica (2,327 m), la Cimatella (2,101 m) and Punta a le Porte (2,317 m), many of which were glaciated during the Pleistocene Period (Conchon, 1975) (Figure 5.1). The Tavignano flows in an easterly direction towards the town of Corte where the Restonica River draining the Monte Rotondo massif (2,672 m) converges at 400 m asl. The Tavignano flows southwest from Corte, incorporating the discharge of three other major rivers before entering the Tyrrhenian Sea downstream of Aléria (Figure 5.1). Major tributaries include the Vecchio (24 km in length), the Corsigliese (22 km) and the Tagnone (31 km). The total length of the Tavignano River is 82 km with an average gradient of 21 m km^{-1} (1.22°). The Tavignano River has an initial slope of 60m km^{-1} (3.45°) from the source to Corte, where the Restonica River joins at 400 m asl (Figure 5.2).

5.3.2 Geology and tectonics

The upper course of the Tavignano flows through a granite terrain, much of which is deeply incised before arriving in a Jurassic to Pliocene aged sedimentary zone at Corte. From there, most of its course is in schistes lustrés before entering the Miocene plain, south of the Bravona River (Figure 5.2).

Conchon (1975, 1978) has argued that neotectonic activity is evident along the Tavignano by the upwarping of the fluvial terraces and the presence of gorges (Conchon 1975, 1978). The Aleria plain is downwarped in relation to the schistes lustrés zone and is uplifted in relation to the continental shelf on a north-south axis (Conchon, 1975). The Quaternary sediments on the Aleria plain are therefore terraced, the oldest being found at higher elevations near the present shoreline. However, the exact timing and rate of uplift of the eastern schistes lustrés zone is not known. Conchon (1975) has proposed that the tectonic activity occurred after deposition of the T4 unit but before the T5 unit (Table 5.2), and she dates this tentatively by weathering characteristics to between the lower and middle Würm, approximately 90-150 ka BP (Table

1.1). The upwarping is not thought to be solely attributed to hydroisostatic adjustment. Tectonic deformation is believed to be related to the evolution of the Tyrrhenian Sea, where sea-floor spreading may have extended to the Corsica Channel (Tuscany Trough) (Conchon, 1978). It is difficult to distinguish the relative influence of both mechanisms.

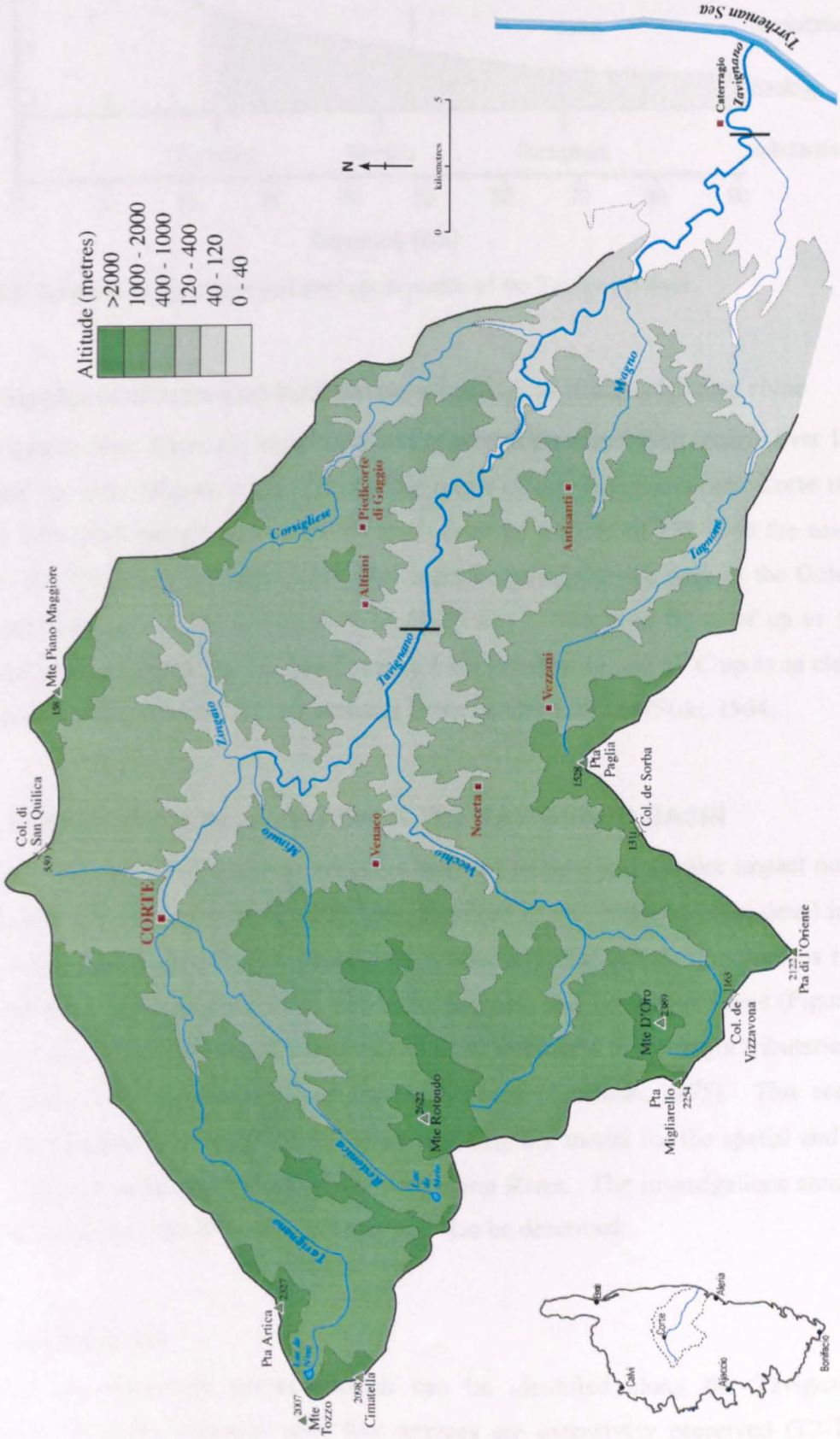

Figure 5.1 The Tavignano River catchment (redrawn from Conchon, 1975).

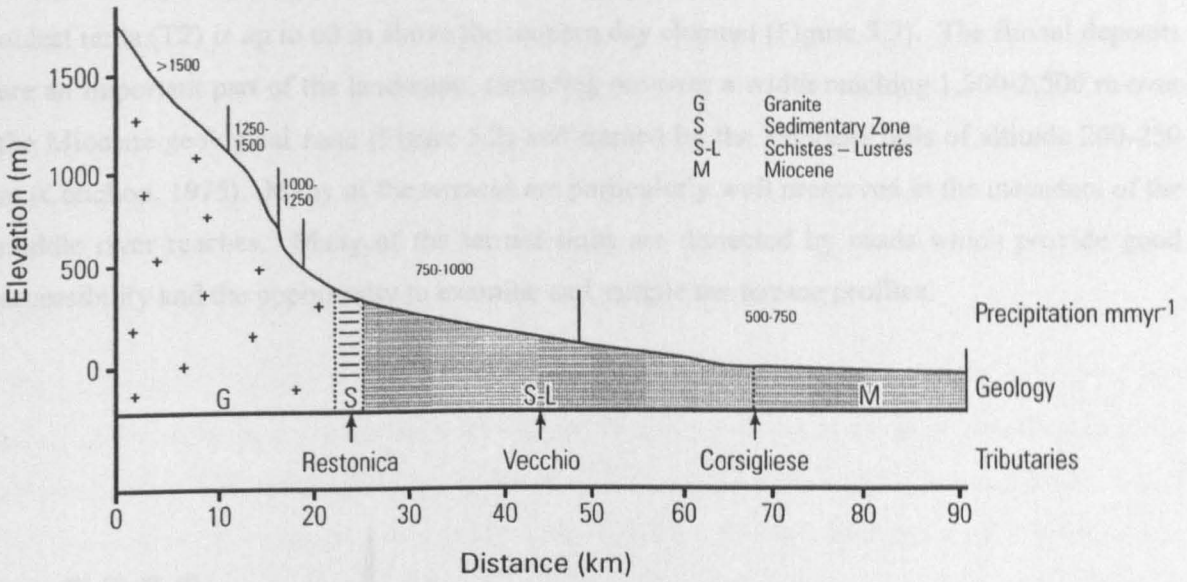

Figure 5.2 Schematic longitudinal and geological profile of the Tavignano river.

5.3.3 Regional climate and hydrological regime of the Tavignano river

The Tavignano river drains the high mountains of central Corsica which receive over 1,500 mm of rainfall per year (Figure 3.13). The middle reach of the Tavignano near Corte receives a MAP of 750-1,000 $mmyr^{-1}$ and the lower reach from an altitude of 150 m to the sea receives between 500-750 $mmyr^{-1}$ (Figure 5.2). The larger rivers of Corsica such as the Golo and the Tavignano have an average annual flow of 40-50 m^3s^{-1}, with high flows of up to 100 m^3s^{-1} (Conchon, 1975) (Chapter 3.6.2). MAT ranges from between 14 and 17°C up to an elevation of 600 m, and between 10 and 13°C for altitudes between 600-1,200 m (Simi, 1964).

5.4 PLEISTOCENE ALLUVIATION IN THE TAVIGNANO BASIN

The extent and timing of glaciation, which is believed to have had a major impact on the river regime and sedimentation style of many large Corsican rivers, is discussed in detail in Chapter 4. The associated fluvial deposits have been extensively mapped along numerous rivers and tentatively dated by Conchon (1975). The Golo, Bravona and Tavignano rivers (Figure 3.9) all illustrate a well preserved terrace sequence. Alluvial sediments in the major tributaries are also terraced and can be correlated to the main sequences (Conchon, 1975). This section will summarise Conchon's work (1975, 1978) by outlining her model for the spatial and temporal pattern of fluvial sedimentation along the Tavignano River. The investigations conducted by the author to advance the work by Conchon will also be described.

5.4.1 Spatial scale

There are six distinctive terraces which can be identified along the Tavignano River downstream of Corte, although only five terraces are extensively preserved (T2-T6). The

terraces are particularly well preserved on the southern side of the valley floor. One of the oldest units (T2) is up to 60 m above the modern day channel (Figure 5.3). The fluvial deposits are an important part of the landscape, spreading out over a width reaching 1,500-2,500 m over the Miocene geological zone (Figure 5.2) and framed by the Miocene hills of altitude 200-250 m (Conchon, 1975). Many of the terraces are particularly well preserved in the meanders of the middle river reaches. Many of the terrace units are dissected by roads which provide good accessibility and the opportunity to examine and sample the terrace profiles.

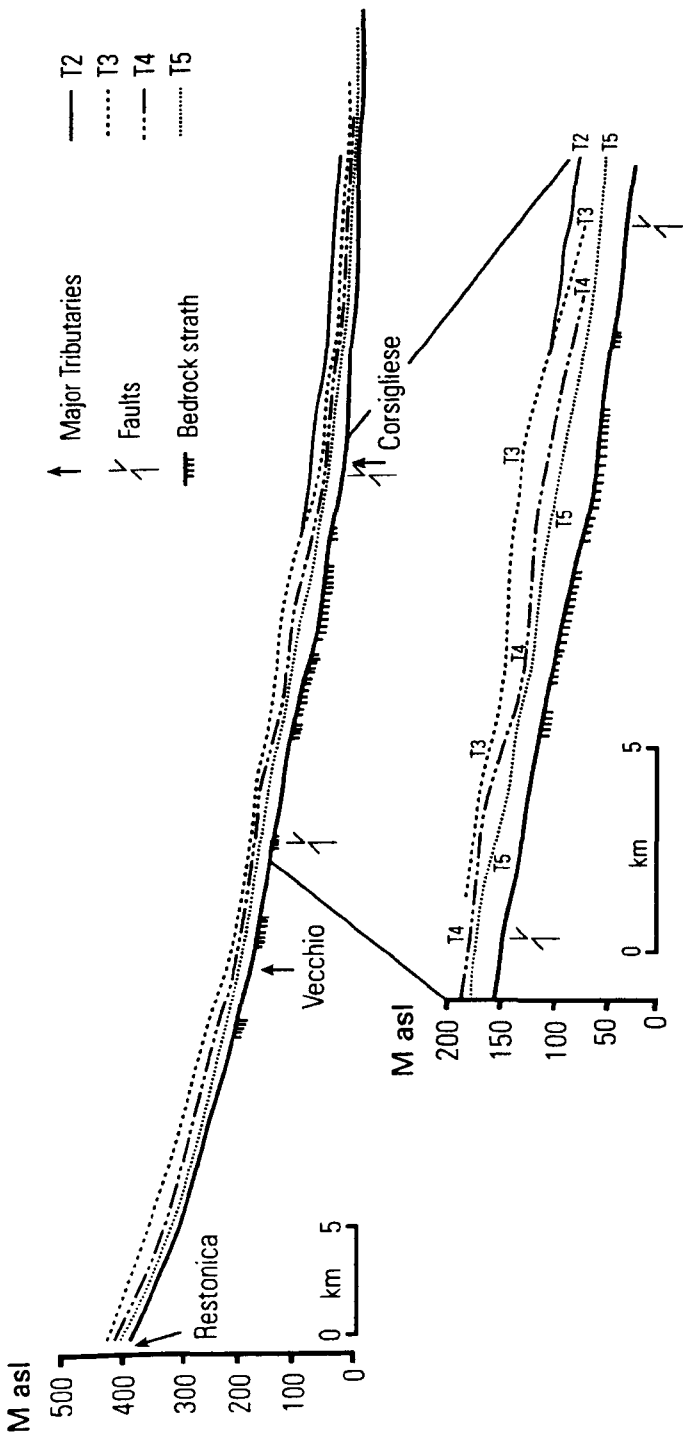

Figure 5.3 Longitudinal profile of the terraces (after Conchon, 1975).

5.4.2 Temporal scale

A maximum of six terraces are distinguished by Conchon (1975, 1978) by their elevation above the present channel and degree of weathering. The extent of rubification within the soil profiles, the thickness of the weathering rind and the abundance of grussified pebbles in each of the units were observed and linked to similar studies in the Alps and Pyrenees to determine the alluvial sequence and relative ages (Conchon, 1978). Table 5.1 summarises the pedostratigraphic information collated by Conchon (1975, 1978).

The sedimentological variations between T2, T3 and T4 are limited. Differences between the older units and the more recent units of T5 and T6 include the proportion of granitic and schist cobbles. The older units displayed approximately 55% granite and 23% schist cobbles within the terrace profiles, whereas the younger units showed a greater dominance of schist material (~46%), compared to granite (~27%) (Conchon, 1975). Relatively recent deposits comprise material from the Miocene slopes, schists and conglomerates transported by the Vecchio and Minuto rivers (Figure 5.1). Downstream, the more recent terraces contain schists from the Corgliese (Conchon, 1975).

Conchon (1978) argues that the scarcity of fossils of stratigraphic significance and the absence of prehistoric artefacts older than the Mesolithic period have meant that the Quaternary landforms and sediments themselves in Corsica are the only available evidence to establish chronological correlations. The tentative correlation of the Quaternary deposits in Corsica with glacial stages and substages in the Alps proposed by Conchon (1975, 1978) is given in Table 5.2.

Table 5.1 Weathering characteristics of units T1-T6 along the Tavignano River (Conchon, 1975, 1978).

Terrace	Colour	Maximum thickness (m)	Texture	Weathering
T1	Reddish-orange	20	26-40 % clay	Rotted ophiolites and schists
T2	Reddish-orange	12	24-48 % clay	Weathered, but not all are rotted. Ophiolite rinds 3-4 cm
T3	Reddish-orange	20	16-42 % clay	Ophiolite rinds 1cm , rotted schist pebbles, weathered granites
T4	Reddish-yellow	5-20	14-37 % clay	Grussified granite pebbles, Ophiolite rind 1-2 mm
T5	Brown	3-7	15-33 % clay	Powdery granite, most pebbles unweathered
T6	Grey, poorly developed soils.	<2	90% particles between 50-1600 μm	Coarse, well sorted grey sand. Grey fine silt covers alluvium T6, and is labelled T7

Table 5.2 Proposed chronology of the fluvial deposits in Corsica (Conchon, 1975, 1978).

Terrace	Corsica	Alps
T7	Fluvial deposits with poorly developed soil Cirque glacial deposits	Holocene Late Glacial
T6	Gray scree (in mountains only) Fluvial deposits with poorly developed soil Glacial deposits with brown cryptopodzolic soil	Upper Würm
T5	Brown scree Fluvial deposits Glacial deposits } all with brown soil	Middle Würm
T4	Red scree Fluvial deposits with red-yellow soil Traces of glacial erosion	Lower Würm
T3	Fluvial deposits with red-orange soil Glacio-fluvial deposits indicated by the shape of pebbles in the fluvial sediment	Riss
T2	Fluvial deposits with red-orange soil Glacial landscape?	Mindel
T1	Fluvial deposits with red-orange soil Glacial landscape?	Günz

5.4.3 Methods of investigation to advance previous work

Many studies use pedogenic parameters (e.g. McFadden & Weldon, 1987; Harden, 1988; Harvey *et al.*, 1995) and mineral magnetic properties (e.g. Maher, 1986; Dearing *et al.*, 1997; Pope, 2000) to establish relative chronologies of alluvial sequences. This study of the Tavignano River includes analysis of physical soil properties (redness, clay content) and chemical soil properties (iron oxide content) to determine a relative-age sequence of the terraces. An absolute chronology for the terrace units is obtained by OSL dating, a technique successfully applied in many fluvial settings (e.g. Fuller *et al.*, 1998; Rose *et al.*, 1999; Colls *et al.*, 2001). The development of robust chronologies are necessary to explore the role of forcing mechanisms acting on the system (e.g. climatic change, tectonics, anthropogenic activity) (Chapter 1.6.1).

An introduction to soil development and soil forming factors is presented in the following section in addition to river terrace chronosequence studies conducted in the western Mediterranean region. A background to OSL dating is outlined in Chapter 5.6. The relative and absolute dating of the Tavignano River terraces is described in the respective sections.

5.5 RELATIVE DATING OF THE TAVIGNANO ALLUVIAL TERRACES

A detailed understanding of pedogenic weathering and soil formation is of great significance to many geomorphological investigations. A knowledge of the processes and products of mineral weathering is vital for both contemporary studies of material transfer and for longer term investigations of sediment digenesis and landscape evolution (Woodward *et al.*, 1994). The study of pedogenic profiles is especially valuable for investigating landscape history and environmental change during the Quaternary Period (Birkeland, 1984; Catt, 1986; Bull, 1991)

and has proved to be especially useful in studies of long-term river behaviour (e.g. Alonso *et al.*, 1994; Harvey *et al.*, 1995).

5.5.1 Soil development

The nature and rate of pedogenic processes are regulated by the function of five factors of soil formation including parent material, climate, topography, organisms and time (Jenny, 1941; 1980) (Table 5.3), although additional factors such as airfall dust or salts may be regionally or locally important. The factors define the state of the soil system and if one factor changes, the soil adjusts accordingly. It has been argued that the parent material has the greatest influence on soil formation (e.g. Birkeland, 1999) although the relative importance of the factors varies from soil to soil, so it is difficult to evaluate each factor independently and obtain quantitative data. Moreover, many soils have formed under conditions in which several factors have varied. This is especially true with the many soils which have been impacted by the extremes of climate throughout the Quaternary. Cold and dry conditions concomitant with the glacial and stadial intervals often restricted weathering and soil development. These episodes alternated with periods of increased precipitation and temperature which accelerated pedogenesis (Morrison, 1978).

Table 5.3 The five main soil forming factors after Jenny (1941) and their impacts on soil profile development.

Soil forming factor	Impact
Parent material (lithology/geology)	Provides minerals which are susceptible to different rates and processes of weathering. Largely controls depth, texture, drainage (permeability) and quality (nutrient content) and influences soil colour.
Climate	Often the dominant influence upon pedogenic weathering regime. MAT and MAP effect the nature and rate of weathering and soil forming processes (e.g. leaching), the vegetation type and humus supply and content. The rate of chemical and biological processes in the soil are also influenced by climate.
Topography	Altitude and aspect affects MAP and MAT. Slope angle influences drainage and soil depth.
Organisms	Biota including plants, bacteria, fungi and animals all interact in the nutrient cycle and assist in the decomposition and decay of dead vegetation. Macro-organisms mix and aerate the soil.
Time	Time taken for a mature soil to develop depends primarily upon parent material and climate.

5.5.1.1 Soil forming processes

The relative importance of the processes responsible for the development of soil profiles also varies for any one soil. Soil formation has been described as the combined effect of i) additions to the ground surface, ii) transformations within the soil, iii) vertical transfers and iv) removals from the soil (Simonson, 1978). One of the most distinctive pedogenic trends developed in soil sequences under Mediterranean climates involves transformations of iron oxi-hydroxide (pedogenic Fe) and a subsequent increase in rubification (Torrent *et al.*, 1983).

5.5.1.2 Steady state condition

An important question is whether pedogenic parameters reach a threshold, beyond which there is no apparent change, even though there is energy in the system and reactions are taking place. Over the initial stages of soil development it is suggested that many properties have a fast rate of change which gradually slow down and level off over time. Each soil property will require a different amount of time to attain the steady state condition (e.g. Bockheim, 1980) and a steady state profile is reached when its diagnostic properties are each in a steady state (Figure 5.4). A steady state condition is recognised in soil profile development indices (Harden, 1982; Harden & Taylor, 1983). However, it is still debateable as to whether soils do ever reach this condition (e.g. Markewich *et al.*, 1987). It is important to be aware that morphological properties may have attained the steady state condition before that of various pedogenic parameters such as clay and Fe_d content (e.g. Simón *et al.*, 2000). Consequently, the appearance between older soils may be similar, but the chemical composition may be distinctly different. It is more likely that the rapidly forming processes such as organic carbon content reach a true steady state (Birkeland, 1990). However, for this reasoning to be valid, the climatic conditions must remain relatively stable over the entire period of soil development. In this study, the soils are likely to have evolved during different pedogenic episodes with changing climatic conditions. Bockheim (1980), Muhs (1982) and Busacca (1987) show that the rate of soil development slows down, but many properties continue to change over 10^6 yrs.

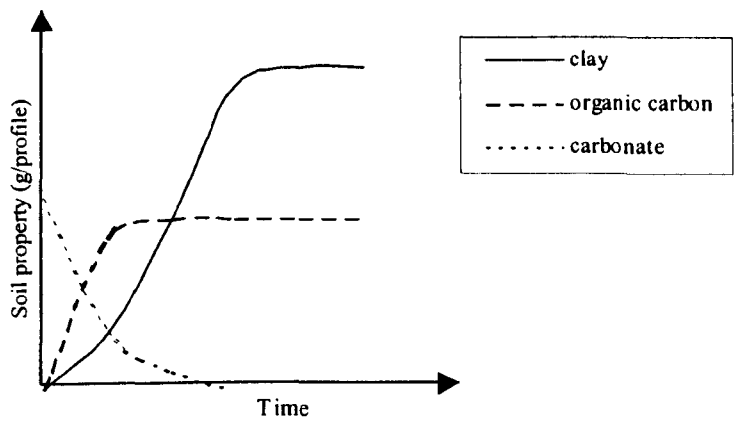

Figure 5.4 Hypothetical variation in several soil properties with time (based on Birkeland, 1999, figure 6.2).

5.5.1.3 Evolutionary pedogenesis

The soil formation theory has been challenged by an evolutionary view of pedogenesis. The model of Johnson & Stegner-Watson (1987) suggests the soil represents a function of both progressive pedogenesis and regressive pedogenesis. The progressive pathway includes factors and processes that promote horizonation, soil deepening with time, and the assimilation of any materials added to the ground surface. An example of this would be when the Bt horizon

becomes increasingly clay and Fe enriched and thicker. In contrast, the regressive pathway includes factors that help to simplify the profile with time. Examples include: i) erosion of a more developed profile to be replaced by a simpler pedon, ii) mixing of a strongly layered profile to produce one less layered, either through root growth or movement of organisms and iii) where pedogenic Fe buildup in the Bt horizon is depleted by ferrolysis (refer to Birkeland, 1999).

5.5.1.4 Age estimates

Absolute rates of soil development have not been determined in most soil chronosequence studies because few absolute ages of the soils are known. It is suggested that the error on age estimates from soil sequences is 50% (Kneupfer, 1988) or 70% using a profile development index (PDI) (Harden, 1987) if no other geochronometric ages can be ascertained. Temporal variations in rates of soil development due to climatic changes and related changes in dust and water, erosional histories and internally driven chemical and physical processes in addition to the complications of steady state and the evolutionary theory all contribute to this error. Very few chronofunctions characterize a linear model (see Woodward *et al.*, 1994), with most equations regarding soil property and geomorphic age of the soil surface to be best represented with logarithmic and power models (Bockheim, 1980; Harden 1982; Birkeland, 1984; Dorronsoro & Alonso, 1994). Soil chronosequences can therefore provide a broad age estimate, but are most useful for determining the relative ages of geomorphic surfaces, especially as pedogenic features can be related to profile maturity (e.g. Birkeland, 1982; McFadden & Hendricks, 1985; Dorronsoro & Alonso, 1994).

5.5.1.5 River terrace chronosequences

Post incisive chronosequences are the most common type of soil chronosequence investigations and are found in many landscapes such as glacial moraines, landslide scars, lava flows, alluvial fans and river and marine terraces. Deposition on the terrace surfaces ends at different ages and maximum time of pedogenesis is assumed to be the interval between the end of deposition and the present. River terraces have inarguably been the focus of most attention since they are good examples of natural soil sequences whose evolution has been essentially shaped by time. Once a floodplain has been formed into a terrace by river incision, they become isolated from additional fluvial deposition resulting in a simple age-related soil profile development. There are several advantages of using river terraces for relative age dating, i) the sediment sources are often similar over relatively large areas and ii) they are flat terrace surfaces where soil development usually starts at the time of deposition without much inheritance from the previous soils. Table 5.4 illustrates a number of soil chronosequence studies that have been conducted in the western Mediterranean from suites of river terraces. Redness ratings, clay content and the

concentration of iron oxides have all been shown to be good age related parameters. Morphological and physical properties such as structure, moisture, consistency, mottling colours and patterns, clay films and boundaries can also be used to determine the relative ages of soils (e.g. Bilzi & Ciolkosz, 1977; Harden, 1982; Ajmone Marsan *et. al.*, 1988b).

5.5.1.6 Sample sites and sampling strategy

Sample sites were chosen where i) flat terrace surfaces, ii) full exposure of soil profiles and iii) good access for sampling were evident. Sample sites were all located in deep road cuttings or natural river cut sections. To minimise any site dependent variations in soil profile character, the sampled sections were all situated in free draining portions of terraced alluvial sediments, exhibited similar surface vegetation, were not in the vicinity of steep sloping land or tributary junctions. Although it was difficult to collect pristine (unaltered) parent materials, sections for profile sampling were chosen where the least altered material could be obtained – this was often several metres below the bottom of the sampled profile.

Terraces T2, T3, T4, T5 and T6 were sampled in profile, their location along the Tavignano river is illustrated in Table 5.5 and on Figure 5.5. The vertical sections were cleaned by scraping away the surface soil and vegetation until an undisturbed profile was exposed. The sections were described in terms of sedimentology, sketched and photographed. Soil samples (*ca.* 200 g) were then collected at 20 cm intervals (unless distinct stratification dictated otherwise) from the terrace surface down to approximately 2 m depth or to the unweathered or least altered parent material (C horizon). The material was sieved on site to obtain the <2 mm fraction. A total of 55 soil samples were collected from the five terrace units, including 7 least altered parent material samples.

5.5.2 Sample collection and methodology

This section describes the sites which were selected for the soil profile sampling and outlines the sedimentological characteristics of the alluvial units along the Tavignano River. The soil properties and laboratory analyses to assess soil development are also described.

Table 5.4 River terrace chronosequence studies conducted in the western Mediterranean.

River	Region	Geology	MAT (°C) MAP (mm)	Number of terraces	Good parameters for relative age dating	Min and max age (ka)	Reference
Odelouca, Enxerim, Lombos, Arade and Quarteira	Algarve, S Portugal	Highland of metamorphosed flysch and thin-bedded shales, iron-rich phyllites and greywackes. Lowland of limestone and unconsolidated sands	15-17 363-1205	2 (plus catchment colluvium)	Redness rating, iron oxides	>7.5 <0.78	James & Chester, 1995
Almar	Central western Spain	Granite	11.0 412	7	Clay accumulation, water retention, extractable Fed, rubification	~ 0.5 ~ 600	Dorronsoro & Alonso, 1994 Alonso *et al.*, 1994
Aguas/Feos	SE Spain	Upper Miocene (Tortonian to Messinian) marine sediments including gypsum beds		5	Redness rating, horizon thickness, calcium carbonate, clay content, iron oxides	~2.3 700-1600	Harvey *et al.*, 1995
Aguas	SE Spain	Schist, quartzite, gneiss, limestone, marl, sandstone	18 250	15	Redness rating, Fe and Al content, clay illuviation	<10 >350	Schulte & Julià, 2001
Sesia and Elvo	NW Italy		As below	3	Iron oxides, organic carbon, silt/clay ratio, Ca/Mg ratio	10-13 >300	Arduino *et al.*, 1984 Scalenghe *et al.*, 2000
Agogna	NW Italy	Gneiss, quartzite, granite, rhyolite	10.1 1293	3 (of 6)	Redness rating, clay content, iron oxides, morphological characteristics	<10 500-750	Ajmone Marsan *et al.*, 1988b

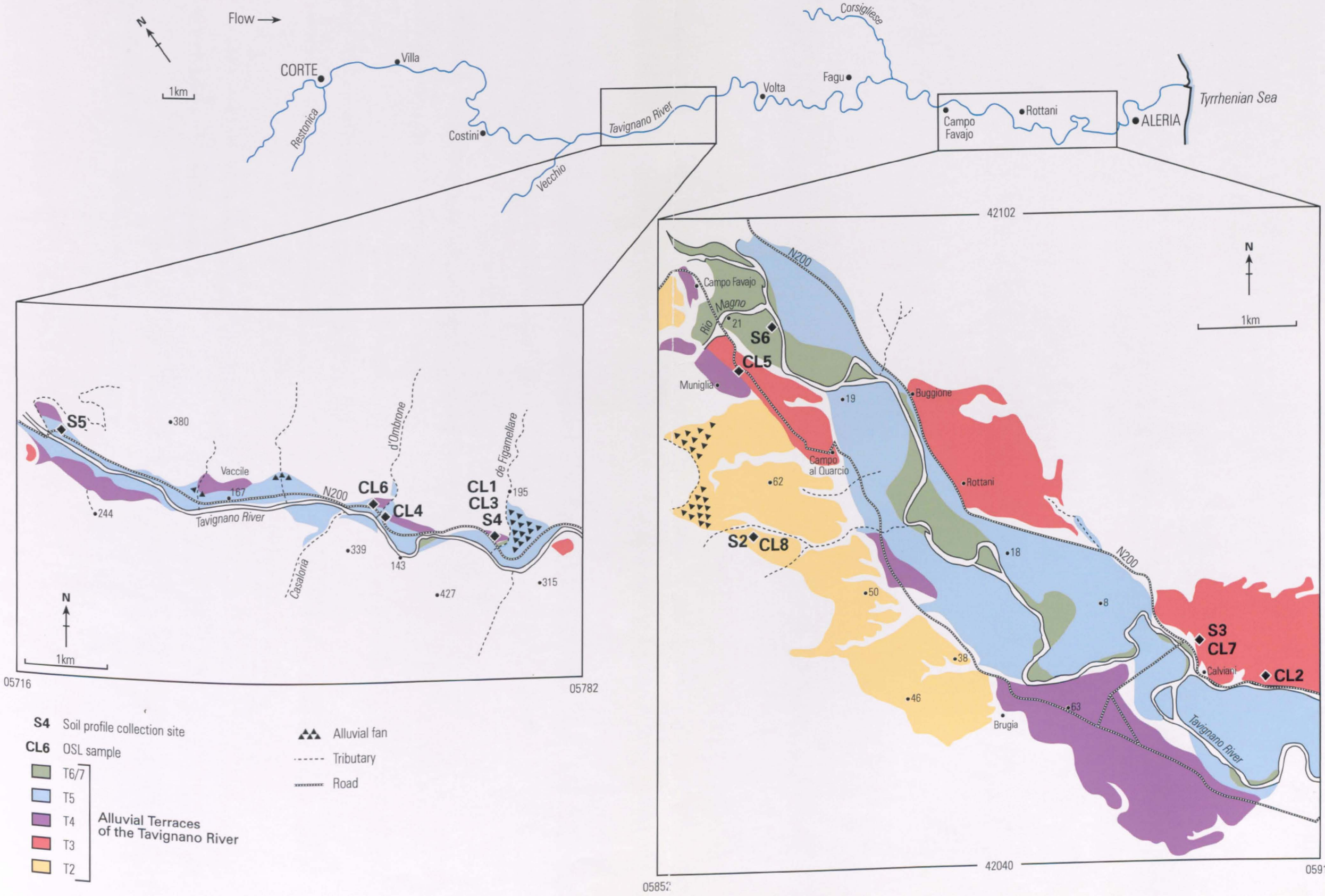

Figure 5.5 Soil profile and OSL sample sites along the Tavignano River

Table 5.5 Summary table of the soil profile samples taken from the Tavignano alluvial sequence.

Alluvial unit	Sample	Latitude/ longitude	Grid Reference IGN 1:25 000	Sampled profile depth (m)	Number of samples	Elevation above present channel (m)
T2	S2	N42°07'76 E09°26'15	05860 42072	4.1	8	40.0-45.0)*
T3	S3	N42°07'02 E09°29'31	05906 42058	2.0	10	25.0
T4	S4	N42°12'42 E09°19'41	05773 42139	1.8	9	12.0-15.0*
T5	S5	N42°13'17 E09°15'54	05720 42151	2.0	10	18.5
T6	S6	N42°09'03 E09°26'17	05861 46665	1.7	11	5.0

* estimated from IGN 1:10,000 map

5.5.2.1 Methods used to construct an alluvial chronosequence

Vegetation, topography and climate are similar for all the Tavignano terrace surfaces which may allow a comparison between sedimentary units and provide an opportunity to evaluate differences in soil property and soil development with time. It is important to appreciate that although all the sites are located along the trunk stream, parent materials may have varied slightly due to activation of sediment sources through time i.e. tributary fan material or headwater material. Numerous pedogenic parameters were evaluated on the five soil profiles to determine the most useful relative age indicators in this context (Table 5.6).

Mineral magnetic properties of the terrace profiles have also been investigated (Chapter 5.5.5). Parameters such as magnetic susceptibility (χ), anhysteretic remanent magnetisation (ARM) and isothermal remanent magnetisation (IRM) have been measured and interpreted (Table 5.9). These analyses were carried out by the author in Professor Barbara Maher's laboratory at the University of East Anglia in November 1999.

Table 5.6 Physical and chemical soil analysis (<2 mm fraction, unless stated in methodology). Full methodology in Appendix IV.

Property	Method
Redness rating	Based on Munsell colours of dry soil and using the Hurst index as modified by Torrent *et al.*, 1983
Particle size	Coulter®LS™ 230 analysed concentrations of clay (<2 μm), silt (<63 – 2 μm) and sand (<2000 – 63 μm) particles
% Organic matter, loss on ignition	Overnight at 110°C, 3 hours at 550oC (Gross, 1971)
% Calcium carbonate (Parry, 1999)	10-20 ml 5% HCL, stirred, rinsed, dried and reweighed (Gross, 1971)
Pedogenic oxyhydroxides	Fe_d, Fe_o determined by ICP spectrometry
Total pedogenic (Fe_d)	Dithionite-citrate method (Soil conservation service, U.S. department of agriculture, 1972, In: Ross & Wang, 1993))
Paracrystalline and organically complexed (Fe_o)	Acid ammonium oxalate method (McKeague & Day, 1966)

Table 5.7 Mineral magnetic parameters, instrumentation and interpretation used in this study (compiled from Maher, 1986; Higgit *et al.*, 1999; Walden *et al.*, 1999).

Parameter	Measurement and instrumentation	Interpretation
Susceptibility (χ) Ratio of magnetisation induced to intensity of the magnetising field. Measures the "magnetizability" of a material. No remanence is induced.	An in-field measurement and calculated on a mass specific basis (m^3kg^{-1}) on a single sample (dual frequency) susceptibility sensor (i.e. Bartington MS2 B).	Total concentrations of ferrimagnetic iron oxides (e.g. magnetite, maghemite, greigite) or of paramagnetic (e.g. from ferrihydrite) and canted antiferromagnetic minerals (e.g. hematite) if concentrations of ferrimagnetic minerals are low. Ferrimagnetic contribution depends on magnetic grain size also, with the finest (<0.02 μm) and coarsest (> 1μm) grains making the highest concentration per unit mass.
Low field susceptibility (χlf) Most widely applied measurement.	Single AC or DC low magnetic field (*ca.* 0.1 mT) at 0.46 kHz.	
High field susceptibility (χhf) Often only used to calculate χfd.	High DC field, typically 800 mT at 4.6 kHz.	Information about the paramagnetic and canted antiferromagnetic mineral component.
Frequency dependent susceptibility (χfd) The variation of susceptibility with frequency. Usually expressed as a percentage of χlf.	Calculated from the difference in χlf and χhf susceptibilities.	Dominated by the contribution from fine grains at the superparamagnetic (SP), stable single domain border (SSD). Maher's data (1988) suggest that only grains between c. 0015 μm and 0.025 μm make a significant contribution.
Anhysteretic remanent magnetization (ARM) Produced by a decaying alternating field with a small steady DC field superimposed. Often expressed as the susceptibility of ARM (χarm), the amount of ARM acquired per unit DC field.	Measured on a Molspin magnetometer with the use of an a.f. demagnetiser and ARM attachment. Maximum intensity of the alternating field used was 80 mT. The strength of the constant biasing field was DC 0.08 mT. Units of χarm are Am^2kg^{-1}.	Highly selective of the SSD ferrimagnetic grains in the 0.02 to 0.4 μm range. Similar values may be produced by high concentrations of relatively coarse (multidomain) magnetite grains as by much lower concentrations of finer (SSD) magnetites however. $IRM_{20mT}/\chi arm$ ratios may help to clarify the dominant control however (Yu & Oldfield, 1993).
Isothermal remanent magnetization (IRM) The remanence acquired in a sample after it has been induced at a particular magnetic (DC) field.	Field sizes applied to the samples include 10, 20, 50, 100 and 300 mT, induced by a Molspin pulse magnetiser. Samples demagnetised after ARM measurements. Units are Am^2kg^{-1}.	IRM up to 300 mT will be dominated by contributions from ferrimagnetic grains, especially those between *ca.* 0.03 and 0.1 μm. Paramagnetic and diamagnetic substances do not hold a remanence and do not therefore contribute to the signal obtained from any IRM measurement.
Saturated isothermal remanent magnetization (SIRM) Represents the largest magnetic field. A sample is magnetically saturated when progressively larger applied fields do not induce a greater remanence into the sample.	Measurement and units as IRM. Field size is typically 1T (1000 mT).	Ferrimagnetic minerals such as magnetite and maghaemite will be fully saturated in fields of 1T, although some canted (imperfect) antiferromagnetic minerals and most particularly goethite may not be. Failure of the samples to acquire significantly higher IRM between 300 and 1000 mT confirms that the magnetic properties of the samples are relatively little influenced by canted antiferromagnets.

5.5.2.2 Quality control of the sampling and laboratory methods

Although the investigation involves relative dating of the alluvial units, it is still important to appreciate the potential errors and limitations involved in the pedogenic and mineral magnetic analyses. Sampling bias was minimised by taking samples at regular intervals down the profile and sieving a bulk sample to collect a representative sample. Additionally, thorough mixing of the bulk samples was achieved by the paper corner folding method before sub sampling to test for the individual parameters. The tools used to collect and prepare the samples were thoroughly cleaned in-between the handling of different samples to avoid cross contamination. Laboratory ware during sample preparation was also soaked in 5% nitric acid for 24 hours. The methods employed to minimise errors for each of the properties measured are outlined below. Quantitative analytical and reproducibility errors are also provided where possible (Table 5.8).

Table 5.8 Methodology taken to minimise sampling and analytical error when conducting the pedogenic characteristics and the mineral magnetic properties of the soil.

Munsell soil colour test
This test is somewhat subjective, but not easily overcome without multiple testers. Bias was minimised by testing the soils blind, so there was no preconceived idea as to the likely colour (Appendix V).
Particle size
The clay proportion determined for the Tavignano terraces by Conchon (1975, 1978) is slightly higher than those obtained in this study (Table 5.1, Figure 5.7). It was thought that underestimates may have incurred due to the preparation of the samples by the lack of clay particle disaggregation. Therefore, analysis was repeated with several samples which were additionally sonicated for 3 hours. There was little variability between those prepared with calgon and shaken overnight and those sonicated (Appendix VI). As the reliability of the Coulter Counter has been tested against SEM (Pokar, 2001, pers. comm.), maybe the pipette method used by Conchon to determine particle size fractions overestimated the proportion of clay. The Coulter counter was calibrated at the start of every run with garnet as the reference material.
Organic carbon content
Reproducibility tests were less than 6% (Appendix VI).
Calcium carbonate
A large error is likely to have been introduced into the $CaCO_3$ testing as the method is fairly crude. However, as all but one of the samples contained a low concentration of $CaCO^3$ (<3%) (Appendix VI).it was not deemed necessary to conduct a more reliable method such as the displacement method.
Iron oxides
There was no reference material available for the Fe_2O_{3d} and Fe_2O_{3o} extraction procedures, but multi-element standards were used in conjunction with the sample analyses. In addition to numerous blank samples, three standards (Fe 2.5, 5.0 and 10.0 ppm,) were used for calibration. Repeat tests indicate that the variability is within 5% for Fe_2O_{3d} and 9% for the Fe_2O_{3o} extractions, which is reasonable (Appendix VII).
Mineral magnetic properties
Negligible error was evident regarding the magnetic susceptibility measurements. Less than 5% reproducibility error was measured for ARM and below 10% for the IRM (Appendix VIII). The Molspin magnetometer was calibrated every 10-15 samples to ensure accuracy.

5.5.3 Sedimentological analysis

Each of the five terrace profiles were photographed and logged (Figure 5.6) (Appendix IX, X). Terrace T2 exhibits a bleached layer of fines at the top of the profile, followed by a gravel/pebble bed which is separated in two by 15 cm of rubified fines. Clay aggregates are evident between 75-110 cm depth. At 110 cm, an indurated layer of coarse sand and fine gravel is evident, showing a high degree of rubification. Below is an 85 cm deposit of cobbles and boulders (60% 3-5 cm, 30% 5-10 cm, 10% 10-30 cm), overlaying 200 cm of granules and sand and fining upwards. At a profile depth of 415 cm, a layer of stratified cobbles of uniform size (6-8 cm) are evident. Below is another layer of fine-medium sand and a layer of matrix supported boulders.

Alluvial profile T3 shows a 20 cm thickness of sandy material which could be colluvial sediment. Below is approximately 600 cm of matrix supported cobbles and boulders associated with three deposition events. The upper layer consists of large (15-20 cm) angular cobbles. The middle layer comprises rounded and imbricated material, decreasing up profile in size to incorporate a higher proportion of pebbles and finer gravels. The lower bed exhibits well rounded cobbles and an increase of finer material up profile. A layer of granules is below which overlays a sandy lens and also a deposit of cobbles and boulders (average clast size 10-15 cm, largest < 30 cm).

Profile T4 comprises a 95 cm thick layer of coarse gravels, cobbles and boulders (average b axis, 5 cm), supported in a silty matrix. Below is a deposit of well rounded cobbles and boulders of various sizes (average clast size, 15 cm), with a gravel matrix, although in some places the deposition appears clast supported. At 175 cm depth, a silt/sand lens is apparent, varying laterally in thickness between 20 and 35 cm above the bedrock strath.

Terrace T5 is similar in composition to terrace T3, but not so red in appearance. The top 60 cm is a layer of coarse sand and fine gravel, with 10% volume of pebbles and cobbles. Below is a thick (90 cm) layer of matrix supported clasts (average size, 10 cm), overlying a deposit of angular granules in a sand/silt matrix. At a profile depth of 190 cm, coarser more angular clasts are evident, with the largest exhibiting a size of 30 cm. Between 225 and 275 cm in depth, clearly stratified layers of flat angular granules and pebbles are seen within a silty matrix. This deposit is a sharp contrast to the layer below which includes well rounded cobbles and boulders which are imbricated in the downstream direction.

Terrace T6 comprises distinctive layers of silt/sand. No weathering features or rubification are evident which suggests a relatively young profile. With the exception of T6, all the units comprise mainly well rounded coarse gravel within a sandy matrix with an abundance of

cobbles and boulders. There are also sandy layers and discontinuous lenses intermittent with the gravel dominated deposits. This random interbedding suggests pulses of aggradation, of high and low energy flow. The pebbles and cobbles are rarely stratified, and the roundness and imbrication of the material indicates that the rivers were characterized by a continuous and channelised flow with irregular floods (Conchon, 1978). A braided channel form is likely to have been adopted to transport the high sediment load.

Rotten pebbles and grussified cobbles were clearly evident within the terrace of T2. Unit T3 also displays rotten pebbles and cobbles with weathering rinds of 1-1.5 cm. This correlates well to the observations of Conchon (1975, 1978) (Chapter 5.4.2). Rates of rind thickness development is controlled by time exposed to weathering processes as well as by climate and specific rock type (Birkeland, 1999). The thickness of weathering rinds has not been used in this investigation for an indication of relative age as only a few examples were found.

5.5.4 Pedogenic characteristics

The results of the physical and chemical soil properties are presented and analysed for the Tavignano alluvial soil profiles. The data are recorded in detail in Appendices V-VII.

5.5.4.1 Degree of rubification and redness rating

There are numerous ratings which have been developed to evaluate soil redness. The hue, value and chroma (Appendix V) are used to calculate a score in order to quantify the degree of rubification. The rating of Hurst (1977) is widely used in soil chronosequence studies in addition to the calculation developed by (1983). The latter rating is used in this study as it is more widely applied across Europe. The rating is (10-H) x Chroma/Value, with H being the number that precedes the YR of the hue designation (Torrent *et al.*, 1983). Figure 5.7a illustrates the distinctly different degree of rubification between the profiles sampled along the Tavignano. The three oldest units (T2, T3, T4) all have a maximum redness rating of 8, although T2 and T3 have a high level of soil reddening to a greater depth (approximately 150 cm). Terrace T5 shows a more constant redness rating down profile, with perhaps a small enhancement at a depth of 60-100 cm, but not to the extent of T2, T3 and T4. The youngest unit, T6, clearly has a significantly lower rubification index, with a value of 3 and below throughout the profile and showing no red colouration below 105 cm.

The profiles appear to illustrate a good correlation between redness and surface age (on the basis of Conchon's (1975) stratigraphy). This finding is in agreement with many other studies of soil chronosequences in regions influenced by dry climates (Birkeland, 1974; McFadden & Hendricks, 1985; Ajmone-Marsan *et al.*, 1988). The reddening of subhorizons demonstrates that at least some authigenic ferric-iron oxides (pedogenic) have accumulated because rubified

soils require formation of minerals such as goethite and hematite (Torrent *et al.*, 1983). Goethite (FeOOH) is a common iron oxide and is characterized by hues of 7.5YR-2.5YR. Hematite (Fe_2O_3) is also widely found in highly weathered soils and typical hues are 7.5R – 5YR (Schwertmann, 1993). Another Fe oxide is ferrihydrite ($Fe_5HO_8{\cdot}4H_20$), generally formed in the argillic B horizon and which has a distinguishing colour of 5YR-7.5YR and a value ≤ 6 (Schwertmann, 1993). These are not dissimilar to those assigned to the units T2, T3 and T4 (Appendix V). Confirmation of the presence of such iron oxides can be found by measuring the concentration of ferric iron oxyhydroxides (Fe_2O_{3d}, Fe_2O_{3o}) (Chapter 5.4.4.5) and the mineral magnetic properties (Chapter 5.5.5).

The redness of the soil gives an indication of the amount of pigmenting material present, but soil texture is also an important factor. Less pigment would be needed to coat a coarse grained soil than a fine grained soil due to the lower surface area (Birkeland, 1999). This point is illustrated to a certain extent with T2 and T3, the latter terrace profile having a similar redness rating to the former even though the particles are coarser, especially below a depth of 80 cm (Figure 5.7b, Chapter 5.5.4.2).

5.5.4.2 Clay content

In a similar manner to redness rating, the oldest units T2, T3 and T4 units of the Tavignano have a significantly higher proportion of clay particles within the profile compared to the younger terraces T5 and T6 (Figure 5.7b, Appendix VI). Between depths of 50 and 100 cm, clay concentrations of T2, T3 and T4 exceed 30%, and characteristically, the older the soil, the greater the depth to which clay illuviation is evident. The thickness of the argillic B horizon is often determined in part by the clay distribution often indicating the degree to which the soil profile has weathered and broken particles into smaller fragments from its initial state (Woodward *et al.*, 1994). There is little variation in clay distribution for profiles T5 and T6 demonstrating no significant B horizon accumulation and a lesser degree of soil development in comparison to T2, T3 and T4. This process of mineral breakdown and clay translocation is relatively slow and largely time dependent (Birkeland, 1999). An increase in the pronounced accumulation of clay particles in the B horizon is often identified in older soils (Birkeland, 1974; McFadden & Weldon, 1987).

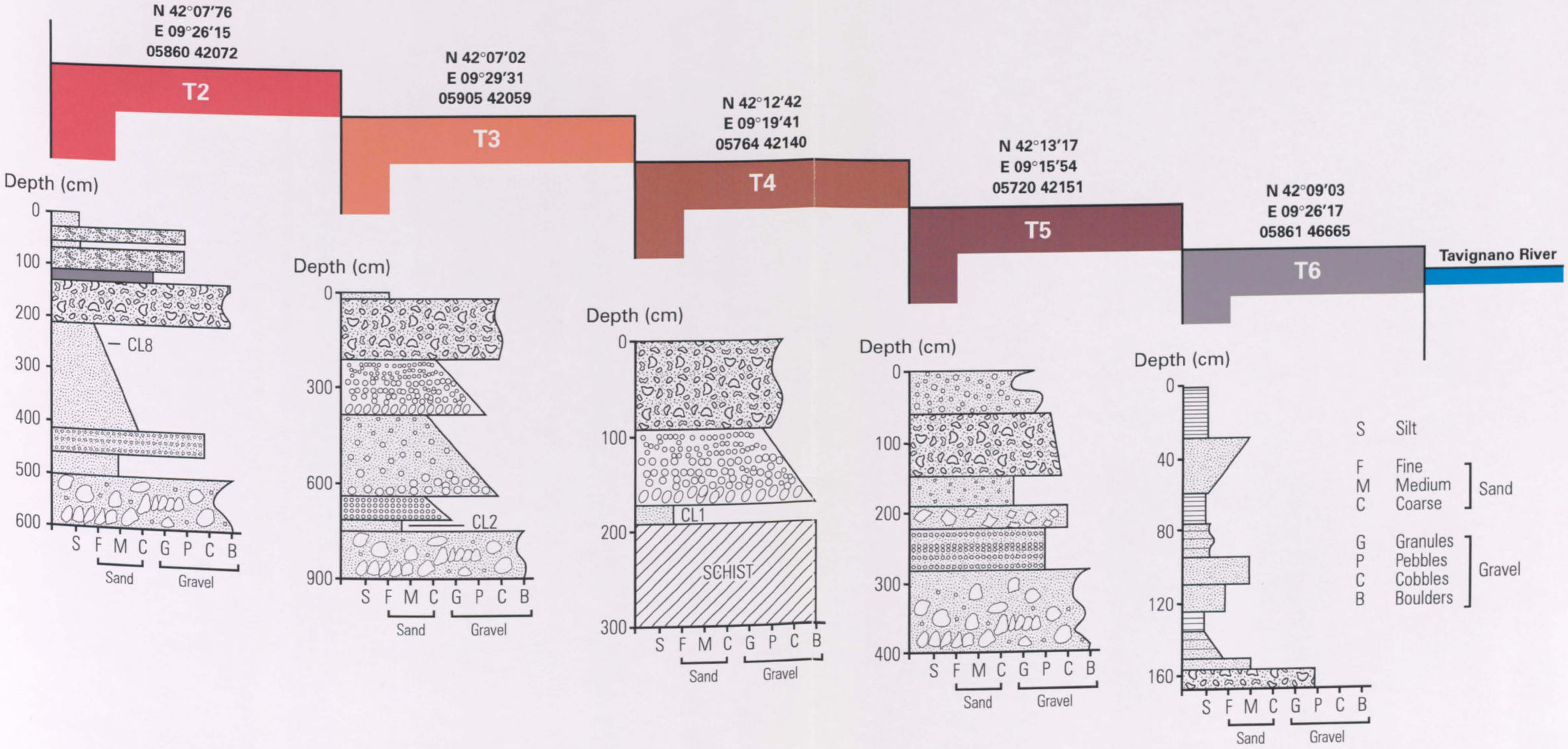

Figure 5.6 Sedimentology of the alluvial units sampled along the Tavignano River

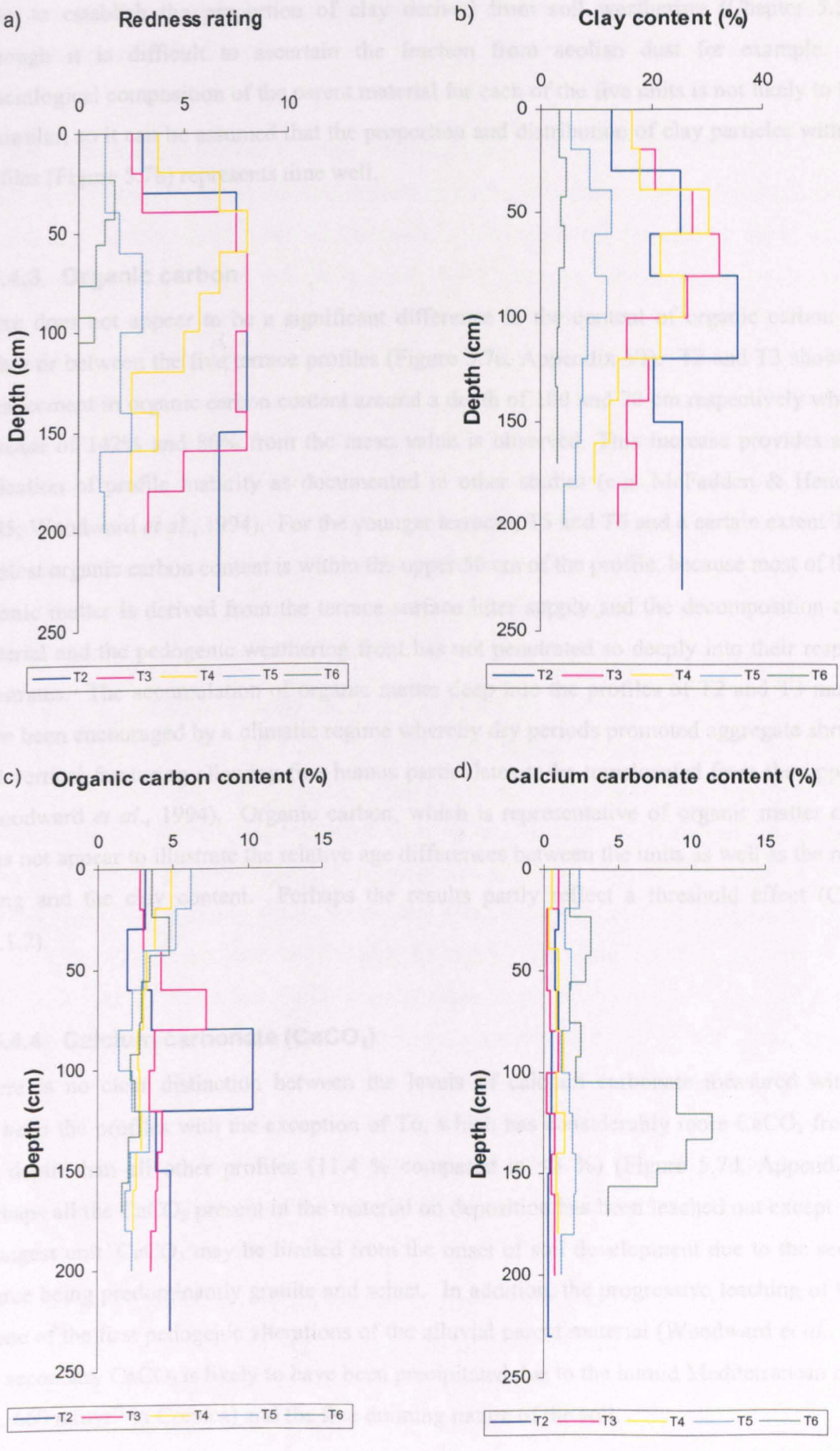

Figure 5.7 Variation of pedogenic parameters down profile, a) Redness rating (after Torrent *et al.*, 1983), b) Clay content (< 2 μm) (%), c) Organic carbon content (%), d) Calcium carbonate content (%).

It is crucial to determine the initial concentration of clay-grade material within the profile in order to establish the proportion of clay derived from soil weathering (Chapter 5.5.4.6), although it is difficult to ascertain the fraction from aeolian dust for example. The mineralogical composition of the parent material for each of the five units is not likely to be too dissimilar, so it can be assumed that the proportion and distribution of clay particles within the profiles (Figure 5.7b) represents time well.

5.5.4.3 Organic carbon

There does not appear to be a significant difference in the content of organic carbon either within or between the five terrace profiles (Figure 5.7c, Appendix VI). T2 and T3 show some enhancement in organic carbon content around a depth of 100 and 70 cm respectively where an increase of 142% and 80% from the mean value is observed. This increase provides a good indication of profile maturity as documented in other studies (e.g. McFadden & Hendricks, 1985; Woodward *et al.*, 1994). For the younger terraces, T5 and T6 and a certain extent T4, the greatest organic carbon content is within the upper 50 cm of the profile, because most of the soil organic matter is derived from the terrace surface litter supply and the decomposition of root material and the pedogenic weathering front has not penetrated so deeply into their respective substrates. The accumulation of organic matter deep into the profiles of T2 and T3 may also have been encouraged by a climatic regime whereby dry periods promoted aggregate shrinkage and vertical fracturing allowing fine humus particulates to be translocated from the upper soil (Woodward *et al.*, 1994). Organic carbon, which is representative of organic matter content does not appear to illustrate the relative age differences between the units as well as the redness rating and the clay content. Perhaps the results partly reflect a threshold effect (Chapter 5.5.1.2).

5.5.4.4 Calcium carbonate ($CaCO_3$)

There is no clear distinction between the levels of calcium carbonate measured within or between the profiles with the exception of T6, which has considerably more $CaCO_3$ from 100 cm depth than all other profiles (11.4 % compared to <3 %) (Figure 5.7d, Appendix VI). Perhaps all the $CaCO_3$ present in the material on deposition has been leached out except for the youngest unit. $CaCO_3$ may be limited from the onset of soil development due to the sediment source being predominantly granite and schist. In addition, the progressive leaching of $CaCO_3$ is one of the first pedogenic alterations of the alluvial parent material (Woodward *et al.*, 1994). No secondary $CaCO_3$ is likely to have been precipitated due to the humid Mediterranean climate (*ca.* 660 $mmyr^{-1}$ in Corsica) and the free draining nature of the soil.

The presence of $CaCO_3$ in the soil matrix retards chemical weathering processes and restricts the vertical movement of fine particles. This is illustrated in the T6 profile where at a depth of 100

cm, perhaps in association with a high concentration of $CaCO_3$, there is little clay, the redness rating lowers to zero and chemical processes such as iron oxide formation are significantly reduced (Chapters 5.5.4.1 -2 -5).

5.5.4.5 Iron oxhydroxides (Fe_2O_{3d} and Fe_2O_{3o})

Many studies have illustrated the time-dependent nature of pedogenic iron accumulation in soil profiles (e.g. Arduino *et al.*, 1985; McFadden & Hendricks, 1985; Ajmone Marsan *et al.*, 1988; Dorronsoro & Alonso, 1994; Schulte & Julià, 2001). Chemical weathering by oxidation takes place as ferrous iron-bearing minerals convert to insoluble ferric oxides or hydroxides (Woodward *et al.*, 1994), and the depth and thickness of the iron-enriched illuvial horizon appears to provide a useful measure of relative age. Total ferric iron (Fe_2O_{3d}) is determined by the dithionite-citrate method (Table 5.6, Appendix VII). The paracrystalline and organically complexed component (Fe_2O_3) is determined by the acid ammonium oxalate method and indicates the ferrihydrite concentration. The organically complexed proportion (Fe_2O_{3p}) established in many studies using the pyrophosphate extraction method has not been used in this study. Fe_2O_{3p} is a poor indicator of any iron mineral, although this was not thought to be always the case (e.g. Soil survey, 1977).

The change in iron oxide concentrations down profile are illustrated in Figure 5.8 (Appendix VII). The older soils (T2, T3, T4) have significantly higher concentrations of total ferric iron present in oxyhydroxide phases (Fe_2O_{3d}) than the youngest two terrace soils (Figure 5.8a). It can therefore be inferred that the older units have a greater proportion of pedogenic iron minerals within the profiles, especially hematite and goethite. Terrace T3 appears to have the greatest percentage of Fe_2O_{3d} within the profile, with a maximum of 2.5% at 60 cm depth. Unit T4 has a Fe_2O_{3d} concentration less variable throughout the profile, with an average of 2.0%. The oldest unit T2 has a low Fe_2O_3 concentration in the upper 80 cm but shows a greatly enhanced B horizon around 100 cm. Terrace T5 appears to have a greater total ferric iron content in the lower half of the profile; this does not demonstrate a B horizon enrichment, it is more likely to be a primary signal. The youngest terrace T6 soil has a variable Fe_2O_{3d} content in the upper section of the profile, fluctuating between 0.3% and 1.6%, illustrating no visible B horizon and a signal which has not been dampened over time. However, the concentration of Fe_2O_{3d} is consistently low below a depth of 100 cm.

The concentration of poorly crystalline ferric iron oxyhydroxides has also been determined within the profiles (Fe_2O_{3o}) giving an indication of the ferrihydrite content (Parfitt & Childs, 1988), an iron oxide recently formed within the soil (Figure 5.8b). The older terraces, T2, T3, T4 have the lowest proportion of ferrihydrite within the soil profile (<0.2%) and show little variation down profile. T6 has a low ferrihydrite content also, with a mean of 0.17%. Unit T5 has a significantly greater Fe_2O_{3o} content than the other units with an average of 0.4%, but

shows a very high Fe_2O_{3o} concentration between 160 and 180 cm of up to 0.7%. This pattern is similar to that observed in Figure 5.8a, and again could be explained by incorporation of aeolian material rather than chemical alteration. The weak relationship with age could be explained as follows:

i) The older units (T2, T3, T4) have the majority of iron oxyhydroxides in an advanced pedogenic form, such as hematite and goethite and produce less newly formed ferrihydrite as the chemical processes slow down (Chapter 5.5.1.2).

ii) Terrace T5 has relatively more iron oxyhydroxides in ferrihydrite state, that have yet to be converted into hematite for example, which often leads to the red colouration (Figure 5.7a).

iii) The youngest terrace T6 has a relatively low proportion of both Fe_2O_{3d} and Fe_2O_{3o} because the unit is not well developed and ferrous iron has not undergone the chemical process to convert to oxyhydroxides.

Figure 5.8c supports these points by showing the difference between Fe_2O_{3d} and Fe_2O_{3o} and is an estimation of the amount of iron sequestered in hematite and goethite. The younger units (T5 and T6) have a concentration of less than 1.4% and the older units of up to 2.2%.

The activity ratio of the iron oxides, which is described as the proportion of the Fe_2O_{3o} divided by the Fe_2O_{3d} content also provides evidence for formation of authigenic (pedogenic) ferric iron oxides in the soils (Blume & Schwertmann, 1969) (Figure 5.8d). As soils become older, progressively more iron oxides change into less active forms (e.g. hematite and goethite), creating a decreasing activity ratio with age (McFadden & Weldon, 1987; Harvey *et al.*, 1995). The lowest recorded activity ratio within the profiles T2, T3 and T4 can be seen to be the same ratio of around 0.05 at a depth of approximately 100 cm. Terrace T4 appears to have the most consistent proportion of low active iron oxides throughout the weathering profile, T2 and T3 have a similar distribution to each other showing an enhancement of hematite and goethite within the B horizon. Perhaps the sediment source was slightly different providing unit T4 with more ferrous iron-bearing minerals. Certainly the least altered material sampled had a greater proportion of ferric iron oxides compared to the other units (Table 5.9, Chapter 5.5.4.6). Goethite and hematite are the two most important iron minerals in well drained soils, each responsible for a distinct pigment of yellowish brown and red respectively (Schwertmann & Taylor, 1989, Schwertmann, 1993). Figure 5.8a-d clearly show some correspondence to the redness rating (Figure 5.7a, Chapter 5.5.4.1). As all three older terraces appear to have a high concentration of less active iron oxides (Figure 5.8d), perhaps as T4 is not as red as T2 and T3, the unit has a greater concentration of goethite minerals. One way to clarify this would be to use SEM analysis or X-ray diffraction. Torrent *et al.* (1980) also illustrates a good relationship between iron oxide concentration and redness rating.

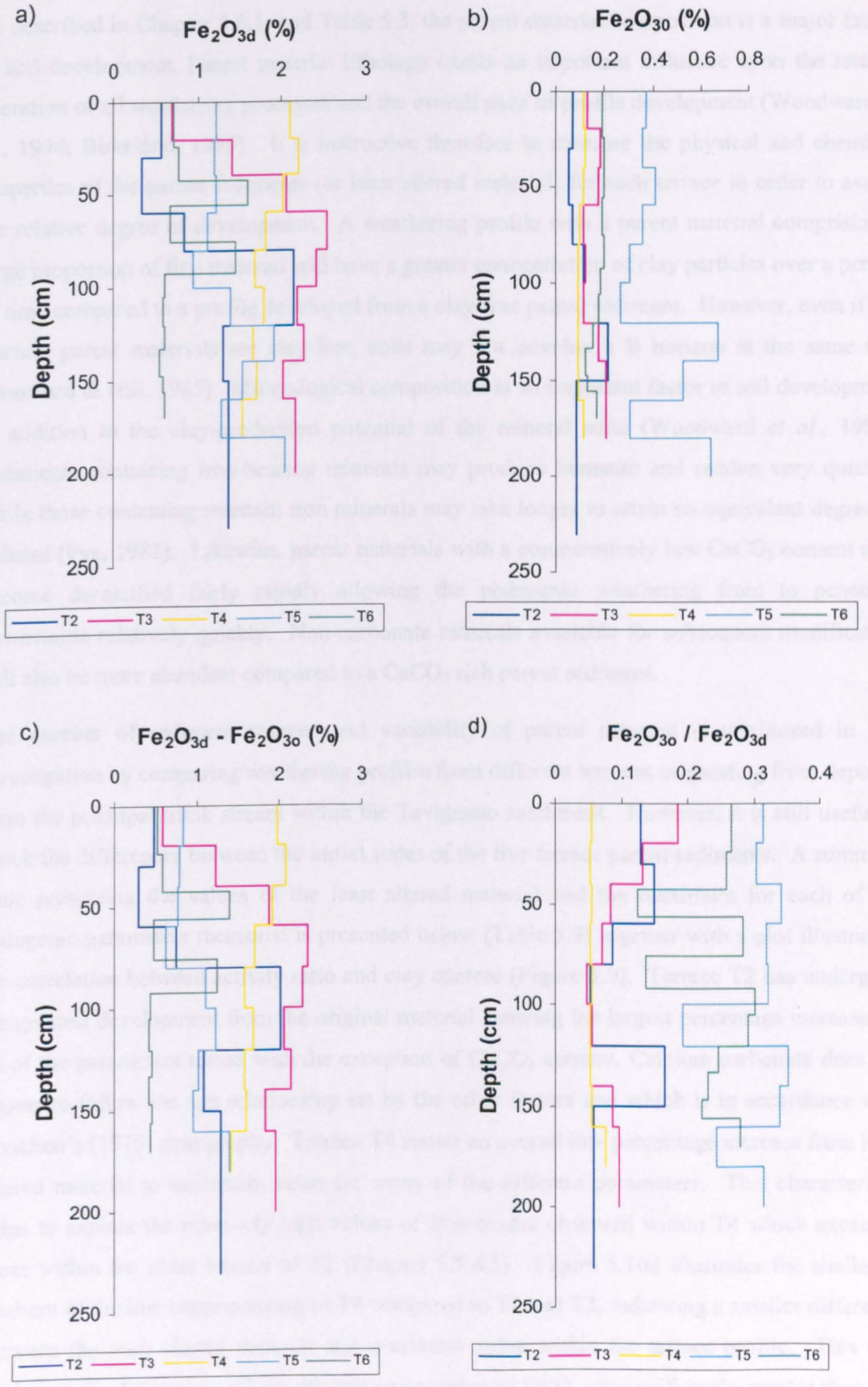

Figure 5.8 Concentrations of iron oxides within the profiles a) Fe_2O_{3d} (selective of pedogenic iron minerals), b) Fe_2O_{3o} (selective of mainly the ferrihydrite component), c) Fe_2O_{3d}-Fe_2O_{3o} (estimates of the Fe sequestered in goethite and hematite, d) Fe_2O_{3o}/Fe_2O_{3d} (activity ratio).

5.5.4.6 Influence of parent material

As described in Chapter 5.5.1, and Table 5.3, the parent material composition is a major factor in soil development. Parent material lithology exerts an important influence upon the rate of operation of all weathering processes and the overall pace of profile development (Woodward *et al.*, 1994; Birkeland, 1999). It is instructive therefore to measure the physical and chemical properties of the parent sediments (or least altered material) for each terrace in order to assess the relative degree of development. A weathering profile with a parent material comprising a large proportion of fine material will have a greater concentration of clay particles over a period of time compared to a profile developed from a clay-free parent sediment. However, even if the starting parent materials are clay-free, soils may not develop a B horizon at the same rate (Borchard & Hill, 1985). Mineralogical composition is an important factor in soil development in addition to the clay-production potential of the mineral suite (Woodward *et al.*, 1994). Sediments containing iron-bearing minerals may produce hematite and redden very quickly, while those containing resistant iron minerals may take longer to attain an equivalent degree of redness (Pye, 1983). Likewise, parent materials with a comparatively low $CaCO_3$ content may become decalcified fairly rapidly allowing the pedogenic weathering front to penetrate downwards relatively quickly. Non-carbonate minerals available for subsequent modification will also be more abundant compared to a $CaCO_3$ rich parent sediment.

The number of sediment sources and variability of parent material is minimised in this investigation by comparing weathering profiles from different terraces originating from deposits from the principal trunk stream within the Tavignano catchment. However, it is still useful to check the differences between the initial states of the five terrace parent sediments. A summary table presenting the values of the least altered material and the maximum for each of the pedogenic parameters measured is presented below (Table 5.9) together with a plot illustrating the correlation between activity ratio and clay content (Figure 5.9). Terrace T2 has undergone the greatest development from the original material showing the largest percentage increase for all of the parameters tested with the exception of $CaCO_3$ content. Calcium carbonate does not appear to follow the age relationship set by the other factors and which is in accordance with Conchon's (1975) stratigraphy. Terrace T4 shows an overall low percentage increase from least altered material to maximum value for many of the different parameters. This characteristic helps to explain the relatively high values of iron oxides observed within T4 which exceeded those within the older terrace of T2 (Chapter 5.5.4.5). Figure 5.10d illustrates the shallower gradient of the line corresponding to T4 compared to T2 and T3, indicating a smaller difference between the least altered material and maximum value within the terrace profile. This also applies to the T3 terrace, where the maximum value of Fe_2O_{3d} is significantly greater than that of T2, although the total pedogenic change is less; T2 has a greater difference between the least altered and maximum value as the gradient of the line is steeper. This feature is also reflected in the graphs displaying the other parameters (Figure 5.10a-c). It is clear from these graphs,

particularly from the redness rating values and the clay content that terraces T2, T3 and T4 are considerably more weathered than the T5 and T6 terraces, which suggests that they are significantly older. This is further exemplified by the bivariate plot showing the relationship between the clay content and the activity ratio (Fe_2O_{3o}/Fe_2O_{3d}) (Figure 5.9).

Table 5.9 Least altered material and maximum values for each weathering profiles from T2-T6.

	T2	T3	T4	T5	T6
Redness rating					
Least altered	2.5	2.5	2.5	1.0	0.0
Maximum value	8.0	8.0	8.0	3.0	1.67
% increase	220	220	220	200	0.0
Clay content (%)					
Least altered	10.6	13.8	9.6	4.2	3.0
Maximum value	35.6	32.2	30.4	12.7	4.5
% increase	235	133	217	202	50
Organic carbon (%)					
Least altered	3.3	3.6	2.4	2.3	1.6
Maximum value	10.4	7.2	4.9	6.2	4.8
% increase	215	100	104	170	200
Calcium carbonate (%)					
Least altered	0.4	0.8	1.0	1.2	4.4
Maximum value	1.0	1.0	1.4	2.4	11.4
% increase	150	25	40	100	159
Iron dithionite (%)					
Least altered	0.603	1.153	1.478	0.726	0.608
Maximum value	2.133	2.532	2.207	1.901	1.586
% increase	254	120	49	162	161
Iron oxalate (%)					
Least altered	0.047	0.115	0.081	0.156	0.169
Maximum value	0.212	0.207	0.120	0.669	0.199
% increase	351	80	48	329	18

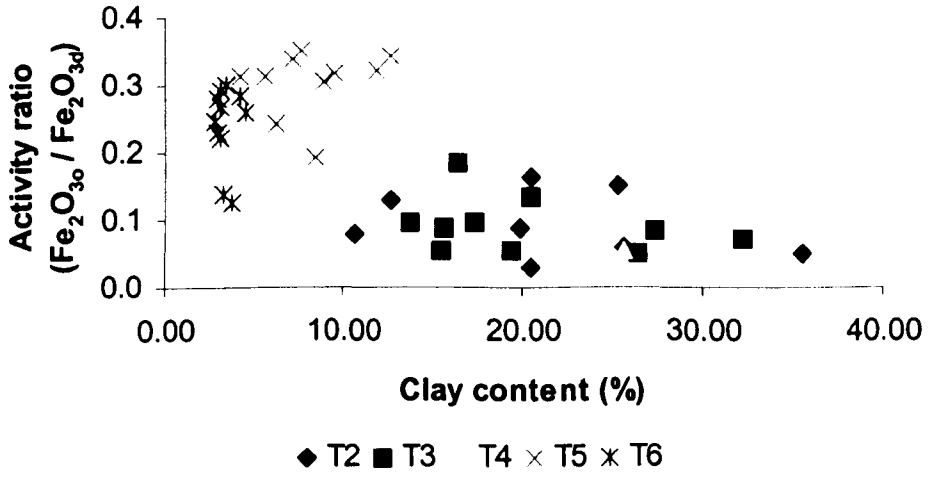

Figure 5.9 Bivariate plot showing the relationship between clay content (%) and the activity ratio for the five Tavignano alluvial terraces.

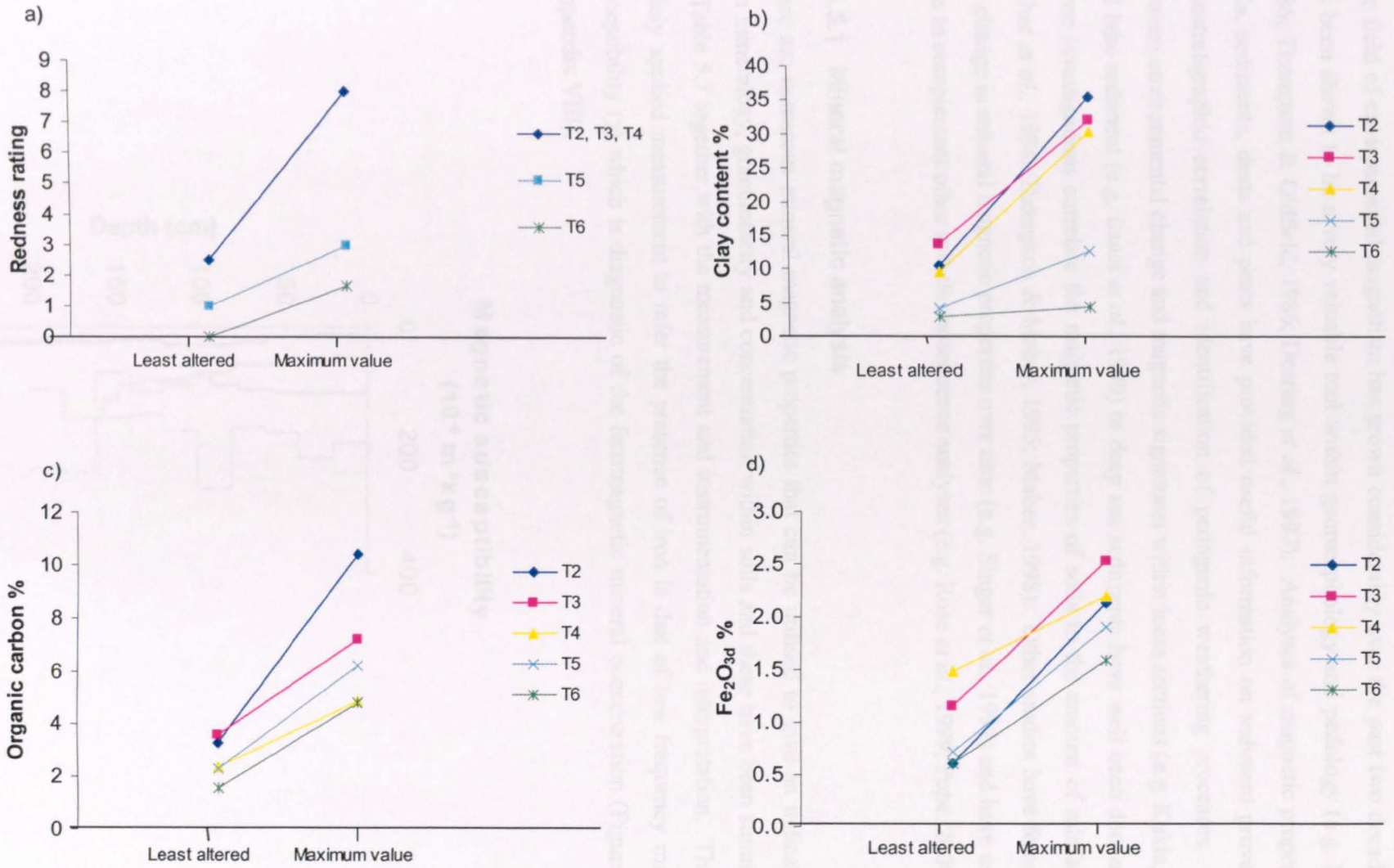

Figure 5.10 Values of the least altered material and the maximum within the profile for a) Redness rating (after Torrent *et al.*, 1983), b) Clay content, c) Organic carbon, d) Iron oxide (Fe_2O_{3d}) content.

5.5.5 Mineral magnetic properties

The field of environmental magnetism has grown considerably over the past two decades and has been shown to be a very valuable tool within geomorphology and pedology (e.g. Maher, 1986; Thompson & Oldfield, 1986; Dearing *et al.*, 1997). Analyses of magnetic properties in soils, sediments, dusts and peats have provided useful information on sediment provenance, lithostratigraphic correlation and identification of pedogenic weathering processes. Links between environmental change and magnetic signatures within loess sections (e.g. Kukla, 1988) and lake sediment (e.g. Lanci *et al.*, 1999) to deep sea sediments have well been documented. Some investigations correlate the magnetic properties of soils to the amount of rainfall (e.g. Maher *et al.*, 1994, Thompson & Maher, 1995; Maher, 1998). Other studies have focused on the change in mineral magnetic properties over time (e.g. Singer *et al.*, 1992) and have used the data to complement other soil chronosequence analyses (e.g. Rose *et al.*, 1999; Pope, 2000).

5.5.5.1 Mineral magnetic analysis

There are numerous mineral magnetic properties that can be utilised to give an indication of iron mineralogy, granulometry and concentration within soils and these have been summarised in Table 5.7 together with the measurement and instrumentation and interpretation. The most widely applied measurement to infer the presence of iron is that of low frequency magnetic susceptibility (χ) which is diagnostic of the ferrimagnetic mineral concentration (Figure 5.11) (Appendix VIII).

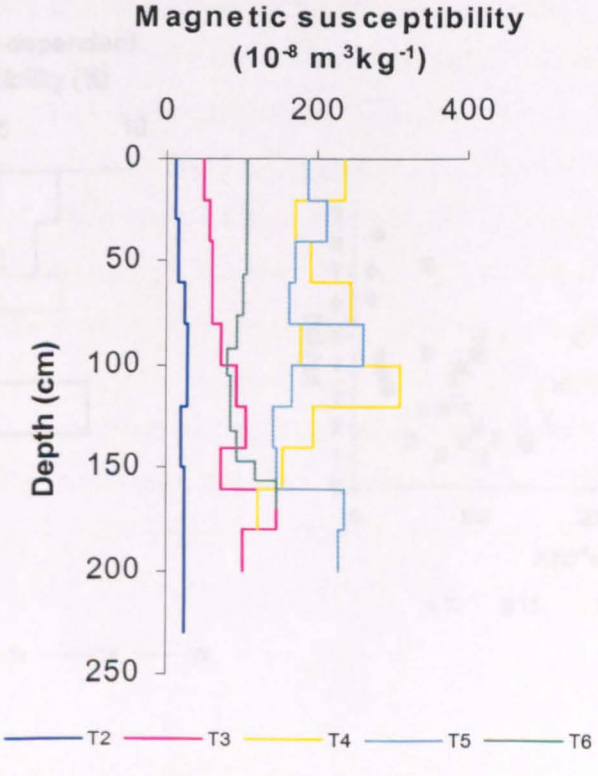

Figure 5.11 Low frequency magnetic susceptibility (χ) of the five Tavignano river profiles.

T2 and T3 appear to have the lowest magnetic susceptibility, averaging 22 and 83 x $10^{-8}m^3kg^{-1}$ respectively, whereas T4 and T5 have a significantly greater susceptibility with a mean of over 200 x $10^{-8}m^3kg^{-1}$. Ferrimagnetic minerals dominate the magnetic susceptibility measurement and little contribution is made by the canted antiferrromagnetics such as hematite and goethite (Walden, 1999). It has already been established that these two iron minerals may be relatively abundant in the older terraces (Chapter 5.5.4.1) so it is plausible to explain the relatively low χ by the presence of canted antiferromagnetics in T2 and T3. The high field susceptibility was also measured but little difference resulted between the high and low tests. The frequency dependent susceptibility (χfd%) is indicative of ferrimagnetic grain size which is an important influence on the susceptibility measurement (Table 5.7) and indeed many other mineral magnetic parameters. χfd% indicates the proportion of fine grains at the superparamagnetic (SP) and single domain border (SSD) between the range of 0.015 and 0.025 μm (Maher, 1988) and often reflects the presence of fine grained pedogenic magnetite (Dearing *et al.*, 1996b; Harvey *et al.*, 1999), showing an increase with increasing age. T2, T3 and T4 all have a generally greater concentration of fine grained magnetite (SP) grains than the younger units, T5 and T6 (Figure 5.12a). This is also illustrated in Figure 5.12b where samples with a χfd% of > 6% have a significant proportion of SP grains. In contrast, relatively coarse non SP minerals are dominant when a relatively high χ and low χfd% is displayed, such as T5. It is useful to establish grain size or domain size because of the influence over mineral magnetic parameters, but also because it provides insight into the formation of ferrimagnetic minerals (Table 5.10).

a) b)

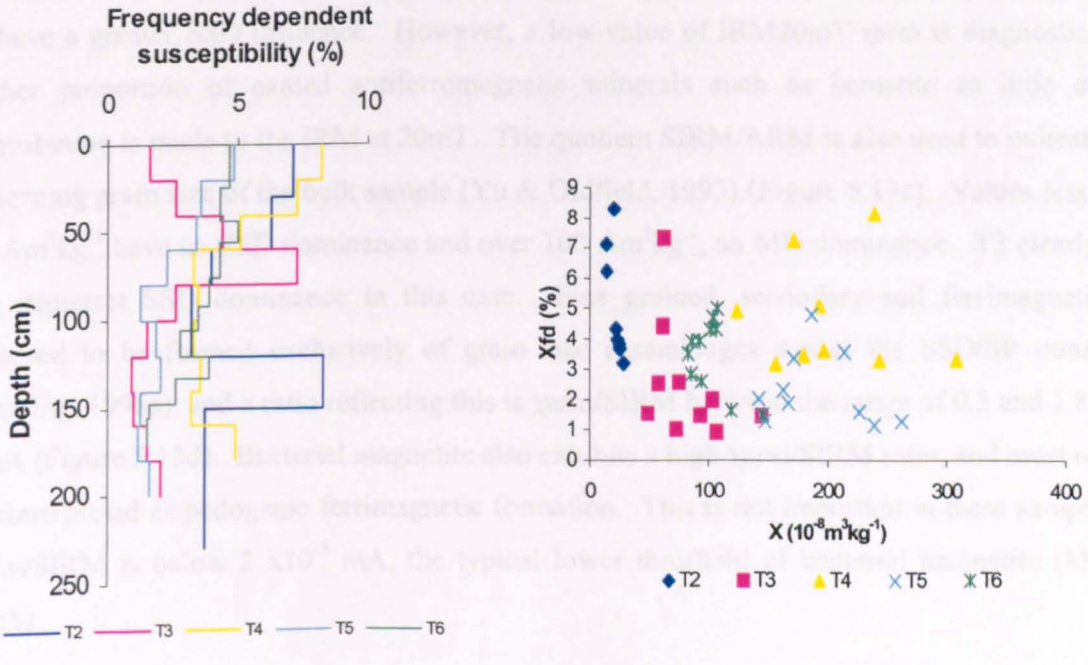

Figure 5.12 a) Frequency dependent susceptibility (% of the low frequency susceptibility) variation with depth for each terrace profile and b) Bi-variate plot of χ and χfd (%) to show the terraces with a significant proportion of SP grains (>6%).

Table 5.10 Origins of magnetite/maghaemite/greigite and domain size. MD, multidomain, PSD, pseudo-single domain, SSD, stable single domain, SP, superparamagnetic. (X), some evidence but not normally expected (from Dearing, 1999).

	MD	PSD	SSD	SP
Primary				
Magnetite, titanomagnetite	X	X	(X)	(X)
Secondary				
Fuel combustion	X	X	(X)	(X)
Pedogenesis		(X)	X	X
Bacterial magnetosomes		(X)	X	X
Dissimilatory bacterial magnetite			X	X
Burning			(X)	X
Authigenic/biogenic greigite			X	X

Further mineral magnetic parameters and quotients can be measured and calculated to determine the dominant grain size more fully. The χarm (Table 5.7) is highly selective of the SSD ferrimagnetic grains (in the 0.02 to 0.4 μm range, Maher, 1988) which in addition to the superparamagnetic grains are common in pedogenic development (Table 5.10). It appears that terrace T4 has considerably more SSD grains than the other units with a susceptibility of anhysteretic remanent magnetisation (χarm) average of 576 $x10^{-8}Am^2kg^{-1}$ with the surface sample exceeding 1000 $x10^{-8}Am^2kg^{-1}$ (Figure 5.13a) (Appendix VIII). T2 for example has only an average of 62 $x10^{-8}Am^2kg^{-1}$. This parameter, however, is concentration dependent and similar values might be produced by high concentrations of relatively coarse (MD) magnetite grains as by much lower concentrations of finer (SSD) magnetites (Walden, 1999). Yu and Oldfield (1993) suggest that IRM20mT/χarm ratios discriminate between ferrimagnetic mineral assemblage dominated by SSD (0.02 to 0.4 μm) or MD (>1 μm) grain sizes (Figure 5.13b). Terraces T2, T3, T4 have similar dominant SSD controls upon χarm, although T5 and T6 appear to have a greater SSD influence. However, a low value of IRM20mT/χarm is diagnostic of a higher proportion of canted antiferromagnetic minerals such as hematite as little or no contribution is made to the IRM at 20mT. The quotient SIRM/ARM is also used to indicate the governing grain size of the bulk sample (Yu & Oldfield, 1993) (Figure 5.13c). Values less than 30 Am^2kg^{-1} have an SSD dominance and over 100 Am^2kg^{-1}, an MD dominance. T2 clearly has the strongest SSD dominance in this case. Fine grained, secondary soil ferrimagnets are believed to be formed exclusively of grain size assemblages across the SSD/SP transition (Dearing, 1996a), and a ratio reflecting this is χarm/SIRM between the range of 0.5 and 1.8 $x10^{-3}$ mA (Figure 5.13d). Bacterial magnetite also exhibits a high χarm/SIRM ratio, and must not be misinterpreted as pedogenic ferrimagnetic formation. This is not important in these samples as χarm/SIRM is below 2 $x10^{-3}$ mA, the typical lower threshold of bacterial magnetite (Maher, 1988).

The differences in the isothermal remanent magnetization (IRM) acquired in various magnetic fields (Table 5.7) allows further interpretation of the dominant magnetic mineral types and concentration. Only certain mineral types are capable of carrying a permanent remanence acquired in a field. Paramagnetic and diamagnetic substances do not hold a remanence and will therefore not contribute to the signal obtained from an IRM measurement. Ferrimagnetic material such as magnetite and maghaemite acquire a strong remanence in relatively low field strengths and all but the finest grains will have reached saturation by 200 mT, labelling them as magnetically soft. In contrast, canted antiferromagnetic minerals such as hematite acquire the majority of their remanence at larger field sizes and are referred to as magnetically hard. The IRM/SIRM ratios show the relative proportion of acquisition from the field size measurements of 10 to 1000 mT (Figure 5.14). The five soils do not appear to have very different average ratios. Unit T2 soil appears to have the proportionally greatest low (< 100 mT) acquisition which suggests a relatively high concentration of ferrimagnets. However, the IRM20mT values representing the concentration of the majority of the magnetically soft minerals shows T2 to have the lowest amount, with an average of 24 $x10^{-5}Am^2kg^{-1}$ (Figure 5.15a). The T3 unit also has a significantly low IRM20mT (average 83 $x10^{-5}Am^2kg^{-1}$) compared to T4 and T5 units of 330 and 299 $x10^{-5}Am^2kg^{-1}$ respectively. This may imply that the older units T2 and T3 comprise hematite, or goethite or some other antiferromagnetic minerals which do not contribute to the IRM at low fields. The proportion of magnetically hard minerals can be represented by the difference between the SIRM and IRM at 300 mT (Figure 5.15b), although full saturation may not be fully achieved in a field of 1T. This is most likely to explain the lower values than expected with units T2 and T3. Furthermore, the contribution towards total SIRM of even relatively large quantities of antiferromagnetic minerals such as hematite may well be masked by the presence of much lower concentrations of fine grained SSD ferrimagnets, as illustrated in the plot χarm/SIRM (Figure 5.13d) (Thompson & Oldfield, 1986) (Figure 5.16). The amount of remanence acquired by a given quantity of hematite is clearly 2 to 3 orders of magnitude less than the remanence acquired by an identical quantity of magnetite (Thompson & Oldfield, 1986). The pedogenic parameters (Chapters 5.4.4.1 & 5.4.4.5) also reinforce the presence of hematite in the soils, especially within the older profiles of T2, T3 and T4.

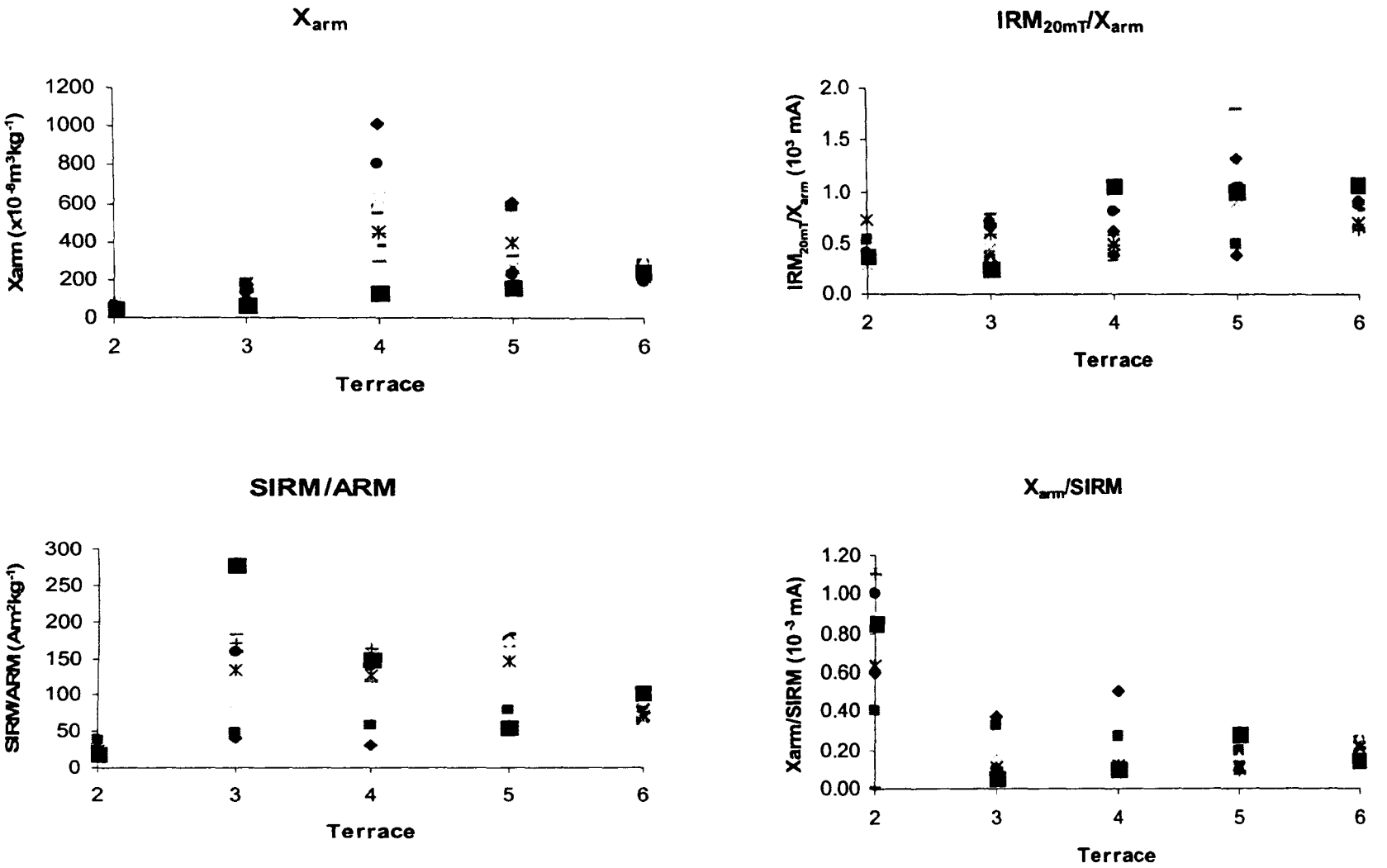

Figure 5.13 Mineral magnetic parameters and quotients of the Tavignano alluvial samples. ■ refers to the least altered material for each terrace.

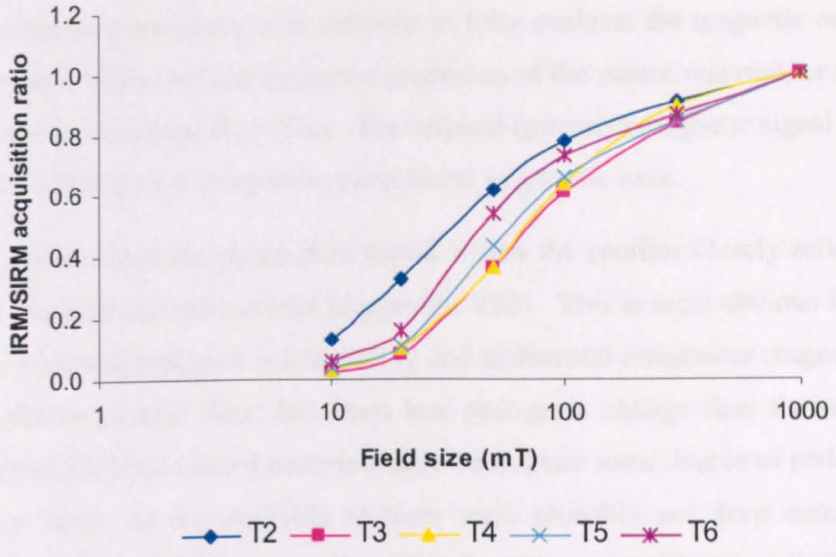

Figure 5.14 Average IRM/SIRM values for each unit, showing the relative proportion of acquisition from fieldsize 10 to 1000 mT. Low acquisition (< 100 mT) reflects the concentration of ferrimagnets. Higher acquisition is associated with the proportion of antiferromagnetic minerals.

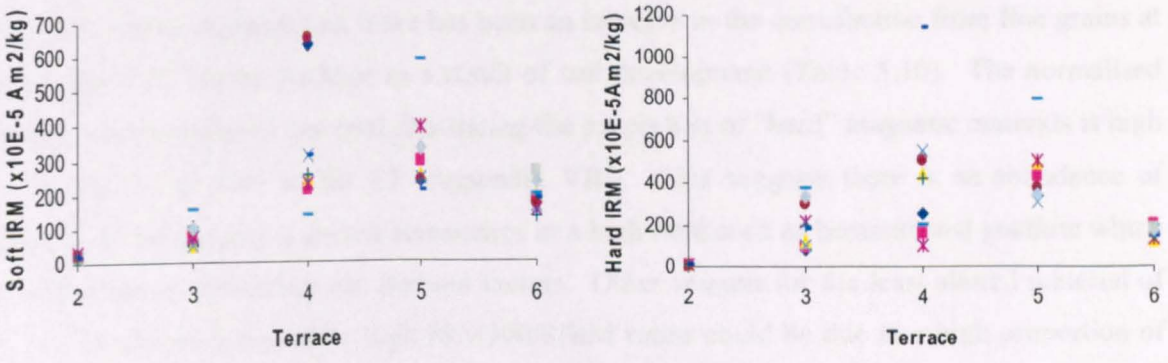

Figure 5.15 a) Soft IRM (IRM 20 mT) and b) Hard IRM (IRM I000 mT – 300 mT) (mass specific).

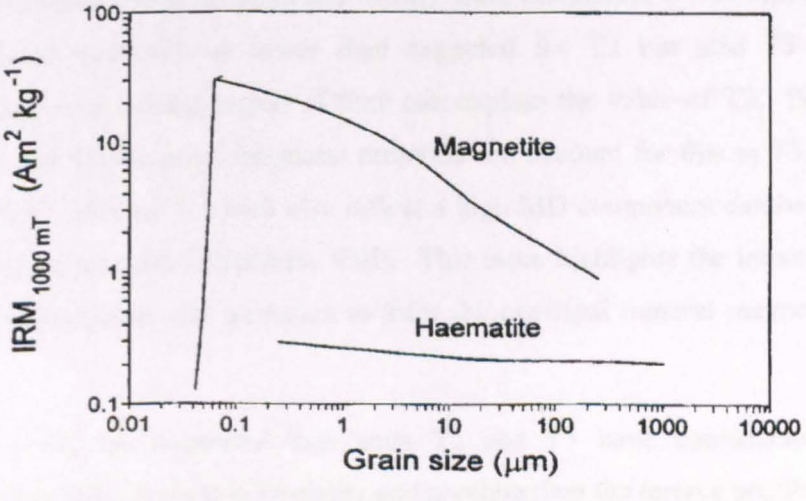

Figure 5.16 Variation of mass specific SIRM (1000 mT) with grain size for pure magnetite and hematite (after Thompson & Oldfield, 1986).

5.5.5.2 Mineral magnetic analysis of the parent material

As with the pedogenic parameters, it is valuable to fully evaluate the magnetic modification of the units by comparing the mineral magnetic properties of the parent material, or a least altered sample with those in the sampled profiles. The original (primary) magnetic signal is likely to be strong due to the abundance of magnetite often found in granitic rock.

Many of the mineral magnetic parameters tested within the profiles closely reflect the values determined for the least altered material (Appendix VIII). This is most obvious for the T2 unit which shows a very low magnetic susceptibility and isothermal remanence magnetisation. It is difficult to establish whether there has been less pedogenic change than the terrace profiles suggest or whether the least altered materials have undergone some degree of pedogenesis. It is likely to be the latter, as the available sections were probably not deep enough to expose unaltered material (if this exists), especially within the older units. This is well illustrated in the χarm/SIRM quotient where the T2 value is significantly greater than the other terrace profiles (Figure 5.13d) and reflects the proportion of fine grained secondary soil derived ferrimagnets. The magnetic susceptibility (χ) is relatively high for all the least altered parent material samples with the exception of T2 (Appendix VIII). All the frequency dependent susceptibilities are below 5% which suggests that there has been an increase in the contribution from fine grains at the SP and SSD border perhaps as a result of soil development (Table 5.10). The normalised IRM for the least altered material illustrating the proportion of "hard" magnetic minerals is high for T5 and T6 as well as for T2 (Appendix VIII). This suggests there is an abundance of materials which acquire a greater remanence in a high field such as hematite and goethite which are indicative of secondary soil derived factors. Other reasons for the least altered material of T5 and T6 showing unusually high IRM300/SIRM ratios could be due to a high proportion of very coarse magnetite grains (Figure 5.16). Fine grained ferrimagnetic material is often concomitant with secondary soil derived material. It is likely that the younger units have yet to develop fully.

The SIRM/ARM value which is diagnostic of MD grain dominance (>100 Am^2kg^{-1}), a common property in parent materials, is lower than expected for T2 but also T5 (Figure 5.13c). Pedogenic change over a long period of time can explain the value of T2. Perhaps a diverse mixture of fine and coarse grain magnetic minerals can account for this in T5. However, low ratios of SIRM/χ (<10 kAm^{-1}) which also reflect a high MD component can be seen in both T2 and T5 least altered samples (Appendix VIII). This issue highlights the importance of using a combination of parameters and quotients to infer the principal mineral magnetic properties of the soils.

In summary, it can be suggested that units T2 and T3 have considerably more canted antiferromagnetic minerals such as hematite and goethite than the terrace profiles of T4, T5, and T6 (low χ, low IRM20mT). T4 has a greater relative proportion of ferrimagnetic material (high

χ, ARM, SIRM). T5 and T6 have relatively less ferrimagnetic minerals, or perhaps have a greater abundance of coarser magnetite grains (lower χ, ARM, SIRM). T2 has the relatively high dominance of SSD fine grained minerals (high χarm/SIRM, low SIRM/χ), which is likely to be the result of secondary formation through soil-derived ferrimagnets (Table 5.10).

It is worth noting that there appears to be no distinct enhancement of secondary derived magnetic minerals within the B horizon of any units except for T2, but it is only illustrated in this profile by the χarm/SIRM ratio of terrace T2 (Figure 5.13d, Appendix VIII). However, numerous decreasing down profile trends can be seen in the frequency dependent susceptibility and the ARM/χ showing the concentration of fine SSD grains (Figure 5.12) (Appendix VIII). Increasing down profile trends include the SIRM/ARM quotient diagnostic of the MD dominance. These trends demonstrate the decreasing influence of pedogenesis down the profiles in all the units and it can be seen that T2 quite often has the smallest variation from the surface to the base of the profile.

5.6 ABSOLUTE DATING OF THE TAVIGNANO ALLUVIAL TERRACES

A brief outline of luminescence dating is given below with the field and laboratory techniques selected for dating terraces along the Tavignano River in central Corsica.

5.6.1 Theoretical background to luminescence dating

There are relatively few techniques that allow direct dating of the time of clastic sediment deposition (Chapter 2.5.1). Luminescence dating is one of the principal methods for dating over the latter half of the Quaternary timescale which has become firmly established over the last 20 years or so (Aitken, 1992; Duller, 1996). Recent reviews of luminescence dating techniques (Duller, 1996; Wintle, 1998; Botter-Jensen, 1998) in addition to reviews of their application (Berger, 1996; Roberts, 1997) have highlighted the developments in this field.

Optically stimulated luminescence (OSL) and thermoluminescence (TL) dating are based on the theory that radioactive isotopes such as ^{238}U, ^{230}Th and ^{40}K occur naturally in rocks and sediment and emit continuous alpha (α), beta (β) and gamma (γ) rays to the surrounding material (Lowe and Walker, 1997). Minerals such as quartz and feldspars within buried sediments will gradually acquire this energy through time and this provides the basis for an age estimate for the time of sediment deposition. The ionising α, β and γ radiation interact with the crystalline structure of these minerals freeing electrons which are then trapped and which accumulate through time (Huntley *et al.*, 1985; Bailiff, 1992). The electrons only become liberated when heated or exposed to sunlight and return to a vacant position left by the absence of a previously displaced electron. This "recombination" process releases energy and is termed luminescence. The removal of the charge is often referred to as zeroing or bleaching and is one of the fundamental requirements of the method. It is crucial that the mineral grains are exposed

to adequate daylight in order to reset the luminescence signal prior to subsequent deposition. Once buried, the quartz and feldspars are once again returned to darkness and accumulation of the trapped charge proceeds as before. This luminescence signal which increases with time is termed the equivalent dose (ED) or palaeodose. The ED increases at a greater rate with higher concentrations of U, Th and K in the surrounding sediment. This background radiation or annual dose (Grays) must therefore be measured, either in the field with a gamma spectrometer or through analysis of U, Th and K in the sediment sample. The age of the sample from the time of deposition can then be determined by Equation 5.1:

$$\text{Luminescence Age (ka)} = \frac{\text{Equivalent Dose (ED) (Gy)}}{\text{Annual Dose (Gy/ka)}} \qquad \textbf{Equation 5.1}$$

It is in the determination of ED that different techniques have been developed to stimulate the luminescence signal (Aitken, 1998). Thermoluminescence (TL) dating was the first widely applied luminescence method for sediments which was developed to trap the electrons by continual heating in the laboratory. Further reviews can be found in Aitken (1985, 1998) and Wintle (1991, 1998). The drawback of the technique is that zeroing of the TL signal requires a relatively long duration of light exposure and may not always be complete (Bailiff, 1992). Optically stimulated luminescence dating was developed to overcome this problem by using laser illumination which only measures electrons from the most light sensitive traps within the mineral crystal lattice (Huntley *et al.*, 1985). OSL is therefore particularly useful for dating fluvial sediments (Fuller *et al.*, 1994; 1996) where rapid erosion, transportation and deposition by water is likely to lead to inadequate exposure for TL (Aitken, 1998). OSL has been successfully applied to many fluvial studies to date Late Pleistocene and Holocene alluvium (e.g. Macklin *et al.*, 1997; Fuller *et al.*, 1998; Rose & Meng, 1999; Colls *et al.*, 2001; Woodward *et al.*, 2001) showing good agreement with ^{14}C results and other dating techniques such as U-Th (e.g. Hamlin, 2000). One of the main advantages of luminescence dating is that the sediment itself is dated and not a potentially erroneous stratigraphic marker representing a minimum or maximum age such as organic material as in the use of radiocarbon dating.

5.6.2 OSL technique selection

A number of different wavelengths of light can be used for OSL, including monochromatic green light (GSL), blue plus green light (BGSL) and also infra-red wavelengths (IRSL). IRSL signals from feldspars have been measured from a range of depositional environments (Clarke, 1996) but has been especially effective in the dating of fluvial deposits (e.g. Fuller *et al.*, 1994; Lang, 1994). Although optical dating has been successfully applied to feldspars (e.g. Duller, 1991; Duller, 1995; Galloway, 1996), quartz does not exhibit the anomalous fading of the accrued dose sometimes evident in the former mineral (Wintle, 1977, Aitken, 1998) which results in an underestimation of age.

5.6.3 Evaluation of palaeodose

There are two basic approaches that are used to determine the palaeodose, the additive method and the regeneration method (see Aitken, 1998). Each compares the natural signal acquired during burial with the artificial signals acquired from laboratory doses of radiation. The regeneration method has an advantage over the additive method by not relying on extrapolation to determine the palaeodose. The regeneration method involves interpolation and therefore reduces, if not totally eliminates, the uncertainty of nonlinearity.

Multiple- or single-aliquot methods are used in conjunction with either the additive or regeneration approaches. A single aliquot method is the preferred optical dating procedure as it has advantages over the conventional multiple aliquot methods by avoiding normalisation problems (one, not numerous aliquots being stimulated by the same dose) and reducing the effort involved in preparing many aliquots of the same sample. The single-aliquot additive dose method has been conducted using sedimentary quartz by many workers (e.g. Murray *et al.*, 1997; Hong *et al.*, 2000). The single aliquot regeneration (SAR) method was less successful initially because of changes in sensitivity of the sample with re-use (Wintle & Murray, 1999). This problem has been overcome by correcting for such sensitivity variations (e.g. Murray & Wintle, 2000) and by the development of the single aliquot regeneration method (Mejdahl & Bøtter-Jensen, 1994, 1997).

5.6.4 Time range and error

The upper limit for OSL dating is controlled by the length of time taken to saturate the sediments with radiation dose (Lowe and Walker, 1997) and the stability of the luminescence sample (Duller, 1996). The upper limit is therefore variable but is generally in excess of 100 ka (Huntley *et al.*, 1985). This range gives a distinct advantage over radiocarbon dating as ages beyond 40 ka are commonly unreliable. The lower limit has been progressively lowered to approximately 100 years by recent developments (e.g. Stokes, 1992; Murray, 1996). This lower limit is dictated by the need for a sufficient OSL signal to have accumulated and a low residual luminescence to have been present (Duller, 1996).

The error associated with OSL dating incorporates systematic uncertainties with the determination of the annual dose and errors associated with the ED determination, such as calibration of laboratory radiation (Lowe & Walker, 1997). There are also inaccuracies regarding the determination of the palaeomoisture content, which has a strong influence on the annual dose received from the surrounding medium (Wintle, 1991). The largest uncertainty lies with the assumption of complete sample bleaching, although semi-quantitative tests can be carried out to assess the extent of bleaching (Chapter 5.6.8).

5.6.5 Sample collection in the Tavignano basin

The location and sedimentary unit from which samples were taken for OSL dating in the Tavignano basin are illustrated in Figure 5.5. Samples were taken from sandy lenses in the vicinity of the section profiles which were sampled and logged (Figure 5.6, Table 5.11). Samples were collected by hammering aluminium tubes (approximately 6 cm diameter by 25 cm in length) horizontally into freshly cleaned vertical exposures of sediment (Figure 5.17). The tube was carefully excavated and both ends were immediately sealed with opaque tape. The depth of the sample from the terrace surface was noted and a sediment sample was taken nearby for the assessment of moisture content and U, Th and K analysis (if the background radiation could not be taken in the field).

Table 5.11 Summary table of the OSL samples taken along the Tavignano (location map, Figure 5.6).

Sample	Latitude/ longitude	Grid reference (IGN 1:25,000)	Unit (Conchon, 1975)	Bedrock lithology	Altitude (m asl)	Elevation above present channel (m)	Depth below surface (m)
CL1	N42°12'37 E09°19'47	05773 42139	T4	Schist	170	12.0-15.0 *	2.0
CL2	N42°06'81 E09°30'30	05910 42055	T3	Miocene Sandstone	10	15.0*	7.5
CL3	N42°12'30 E09°19'38	05772 42138	T4	Schist	180	12.0-15.0*	1.3
CL4	N42°12'72 E09°18'89	05760 42140	T5 (fan material)	Schist	170	17-0-18-0	4.0
CL5	N42°08'47 E09°26'03	05860 42088	T3	Miocene Sandstone	50	15.0 – 20.0	0.55
CL6	N42°12'87 E09°18'77	05758 42142	T4 (fan material)	Schist	170	17.0 – 18.0	5.0
CL7	N42°07'05 E09°29'53	05906 42058	T3	Miocene Sandstone	150	25.0	7.4
CL8	N42°07'76 E09°26'15	05860 42072	T2	Miocene Sandstone	50	40.0 - 45.0*	2.5

* estimated from IGN 1:10,000 map

Figure 5.17 Collection of CL6, a sample for OSL dating from the alluvial unit T4.

5.6.6 Experimental procedures

The preparation and palaeodose determination methods used in this investigation are briefly described below. The OSL preparation was conducted by the author at the Sheffield Centre for International Drylands Research (SCIDR) at the University of Sheffield under the supervision of Dr Mark Bateman during February 2001. The OSL measurements were also conducted at the SCIDR.

5.6.6.1 Preparation

Five of the samples were initially selected for final preparation and analysis, CL1, CL2, CL4, CL6 and CL8 (Table 5.11). All preparation was conducted in a dark room, with the aid of a red filter lamp. The first two inches of sediment at each end of the tube was discarded and the bulk sample was left overnight in HCl to remove the carbonates and to assist in the disaggregation of clay. The samples were then individually wet sieved to various fractions (e.g. CL1, 4, 6, 8 to 90-125 μm; CL2, to 90-180 μm). Quartz and other light mineral grains were then separated from denser materials using sodium polytungstate (ρ = 2.7 g cm^{-3}). The samples were finally etched in hydrofluoric acid (HF) for 1 hour in order to remove all the remaining non-quartz material, in particular the feldspars. The refined quartz was rinsed thoroughly and stored in sealed containers. Sample aliquots were made up by mounting the refined quartz grains onto aluminium discs. The preparation procedure was based on Bateman & Catt (1996) and more detail is given in Appendix XII.

The percentage moisture was determined and an uncertainty range of ±5% was used in the annual dose calculations (Appendix XIII). The concentrations of U, Th and K were determined by ICP spectrometry after HF digestion using facilities at the University of Wales, Aberystwyth. The U, Th and K results from the γ- ray spectrometer were cross checked with those measured by ICP-MS. Conversions from elemental concentrations to the effective dose rate were made using the coefficients given by Aitken (1998), incorporating attenuation factors relating to sediment grain size, density and a palaeomoisture value based on the present day value (M. Bateman, pers. comm.). The contribution to the dose rate from cosmic sources was calculated using the expression published in Prescott & Hutton (1994). The dose rate calculated is therefore based on analyses of the sediments at the present day and is only valid if no significant change has taken place since sediment burial.

5.6.6.2 Palaeodose determination

Equivalent dose (ED) measurements were made on an upgraded DA-12 RISØ luminescence reader fitted with a 150 W filtered (GG-420) halogen lamp. Samples were dosed using a calibrated ^{90}Sr beta source and preheated to remove the unstable signal generated by laboratory irradiations (Bateman, 2000). Analysis was conducted using the single-aliquot regenerative

(SAR) approach (Murray & Wintle, 2000), in which an interpolative growth curve is constructed using data derived from repeated measurements of a single aliquot which had been given various laboratory irradiations. Five regeneration points were used with points 1 and 5 being a repeat to check that any sensitivity changes caused during the course of the measurement had been corrected for. Replicates with a recycling ratio exceeding ±10% of parity were excluded from the dataset. The total number of aliquots used for each sample analysis given in Table 5.11.

5.6.7 OSL ages

The summary table below (Table 5.12) details the results of the OSL dating for the units of the Tavignano River. With the exception of CL1, the absolute ages obtained for the units adhere to the relative chronology proposed by Conchon (1975) and the soil profile maturity data discussed earlier. However, the ages are much younger than those proposed by Conchon and those suggested by the pedogenic parameters of the soil profiles. CL8 and CL2 which correspond to units T2 and T3 respectively appear to have been deposited during the period of the LGM (Chapter 2.4.1). The OSL dates obtained for units T4 and T5 suggest that the fan deposits from which the samples were collected from accumulated during the middle-late Holocene. The stratigraphy clearly shows that this is not the case, as the bed of the Tavignano is presently over 15 m below the fan deposits. No major incision phase appears to have occurred within the fan deposits. Although CL1, collected from the terrace of T4 suggests a much older age of 30 ka, the error margin associated with this date is substantial (nearly ±40%). The reliability of the OSL dates can be partly related to the degree of bleaching. This can be assessed by various methods.

Table 5.12 Summary of OSL results.

Lab code	Field reference (unit, Conchon, 1975)	Total number of aliquots used (rejected)	Dose rate (μG ya^{-1})	Palaeodose (Gy)	Age (ka)
Shfd01004	CL8 (T2)	26 (7)	4020 ± 173	80 ± 9	19.9± 2.5
Shfd01001	CL2 (T3)	9 (5)	3681 ±229	68 ± 13	18.4 ± 3.7
Shfd00006	CL1 (T4)	15 (7)	4431 ± 342	136 ± 51	30.7 ± 11.8
Shfd01003	CL6 (T4)	10 (0)	4277 ± 236	15 ± 2	3.4 ± 0.6[a]
Shfd01002	CL4 (T5)	17 (0)	5892 ± .007	19 ± 1	3.2 ± 0.3[a]

[a] samples taken from fan material.

N.B. Sensitivity of the ages with moisture content: CL8 dry (0%) 18.3 ka, saturated (25%) 25.4 ka: CL4 with the ICP measurements compared to the gamma ray spectrometer measurements; 3.9 ± 0.3 (+0.7 ka).

5.6.8 Sedimentary bleaching behaviour

As described in Chapter 5.5.4, incomplete bleaching of the sediment during the last period of transport or exposure leads to inherent inaccuracies in the calculation of a palaeodose. Clarke (1996) devised a method for estimating the degree of sedimentary bleaching at the time of burial. The standard deviation (SD) for each sample is divided by the mean palaeodose (ED) where the SD > 5 Gy to determine the Sn value (Table 5.13). Moderately bleached samples typically obtain Sn values between 0.05 and 0.1, whilst well bleached samples derive a value of <0.05. All samples with a SD < 5 Gy are considered to be sufficiently bleached.

Duller (1995) also explored this relationship by plotting a simple linear regression between the palaeodose and the natural luminescence signal. Whereas the Clarke test investigates the degree of scatter, the regression displays the gradient of any trend. Duller (1995) argues that the samples which display consistent ED values despite independently variable luminescence intensities (horizontal regression) may be considered well bleached. Conversely, steep positive regression gradients effectively display an increasing signal with increasing ED, indicating a variety of bleaching histories or depositional events.

Although these two tests may seem somewhat subjective, they provide an indication as to the relative performance of the sample against theoretical models. Both tests were conducted on the samples CL2, 4, 6, 8 (Table 5.13,

Figure 5.18). In addition to these two tests, Colls (1999) technique was also used, which gives a standardised value of ED and natural OSL.

Table 5.13 Data required for the bleaching tests of Duller (1995), Clarke (1996) and Colls (1999).

Lab code	Field reference (Unit, Conchon, 1975)	Mean ED (Gy)	SD (Gy)	Sn (Gy)	Sn <0.1 (mod. well bleached)	Sn <0.05 (well bleached)	r^2
Shfd01004	CL8 (T2)	85.3	12.5	0.15	No	No	0.05
Shfd01001	CL2 (T3)	67.7	12.9	0.19	No	No	0.27
Shfd00006	CL1 (T4)	136	51	0.37	No	No	0.31
Shfd01003	CL6 (T4)	13.5	2.6	(0.19)	Sufficient	No	0.00
Shfd01002	CL4 (T5)	18.9	1.2	(0.06)	Sufficient	No	0.14

The sample of CL1 shows the greatest inter-aliquot variability, with a high Sn value (0.37) and r^2 value (0.31) indicating poor bleaching. This variability is reflected in the large errors assigned to the OSL age. Although CL2 and CL8 do not suggest the sedimentary material is even moderately well bleached, only a weak correlation is displayed between luminescence intensities and ED (0.27 and 0.05 respectively). Most of the sample points are within 2 SD (Colls, 1999) (

Figure **5.18**), with a large majority within 1 SD. Clarke's (1996) test suggests that the samples CL4 and CL6 are sufficiently bleached as the S.D.<5 Gy. The error associated with each aliquot is less than ± 2 Gy (Table.5.13), which confirms very little inter-aliquot variation.

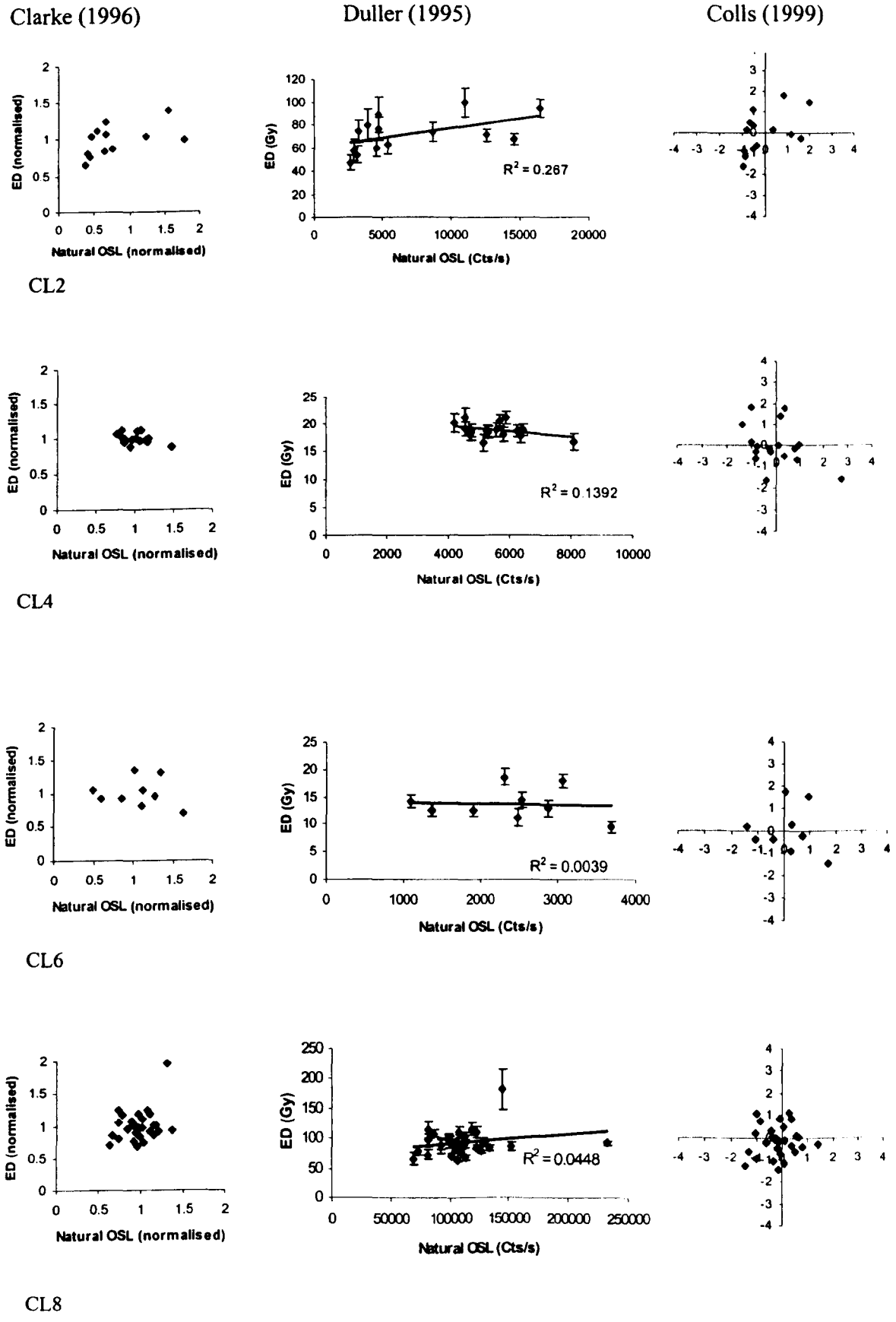

Figure 5.18 Bleaching tests for Clarke (1996), Duller (1995) and Colls (1999) for samples CL2, CL4, CL6 and CL8.

5.7 CONSTRUCTING AN ALLUVIAL CHRONOLOGY

This section attempts to construct an age model for the Tavignano alluvial terraces on the basis of the pedogenic characteristics and the OSL data. Several studies have evaluated the degree of soil development by using quantitative indices for each horizon within the profile by determining the intensity of change from the original parent material (e.g. Harden, 1982; Birkeland, 1984). Parameters such as clay content, redness, iron oxide concentration, as well as morphological properties have all been used to construct a profile development index (PDI) or profile weathering index (e.g. Woodward *et al.*, 1994; Alonso *et al.*, 1994; Scalenghe *et al.*, 2000).

With regards to developing a PDI for the alluvial soils of the Tavignano, the main sources of error may include:

i) The inherent difficulty in obtaining original material and the use of the least altered, which are in different stages of development for each of the profiles.

ii) The variability of the B horizon thickness for each of the tested parameters.

A combination of all the parameters could be used to develop a weathering index but the data suggest that some properties are more strongly related to age than others. The clay content and the redness rating both show distinct B horizon enhancements (Figure 5.7a,b) and, to a certain extent, so do the Fe_2O_3 concentrations (Figure 5.8). It is difficult to incorporate the mineral magnetic properties into a weathering index because no individual parameter showed a distinct B horizon enhancement (Chapter 5.5.5.1). The thickness of the B horizon, together with the least altered composition and the maximum value are tabulated below individually for redness rating, clay content and Fe_2O_3 (Table 5.14). The index is based on Woodward *et al* (1994) whose PDI worked well in the Voidomatis region. The index is the product of the total thickness of the strongly weathered horizon and the difference between the maximum value and the least altered sample.

From the combined PDI it appears that terrace T2 is considerably older than T3, with a total PDI of 4,590 compared to 2,748. The weathering index totals suggest that T3 and T4, and also T5 and T6 are closer in age, the latter pair of terraces having been formed significantly later than T4 however. The index of 2,287 for T4 and 771 for T5 clearly indicates this. It must be emphasized however, that the PDI is only a relative indicator of age in the absence of reliable OSL ages and the interpretations made so far are with the assumption of a linear relationship between profile development and age. This is not always the case, as discussed in Chapter 5.5.1.2. However, a similar index has been shown to be strongly linear with age up to at least 30 ka in the Voidomatis basin in northwest Greece (Woodward *et al.*, 1994).

Table 5.14 Calculating a profile development index for the Tavignano terrace profiles T2-T6. This is a unique index but is partly based on Woodward *et al.*, 1994.

Parameter	Unit	B horizon development (cm)	Total thickness (cm)	Difference between maximum value and least altered (Table 5.9)	PDI
Redness	T2	30-230	200	5.5	1100
	T3	40-160	120	5.5	660
	T4	20-120	100	5.5	550
	T5	40-100	60	2.0	120
	T6	24-56	52	1.7	88.4
Clay content	T2	30-150	120	25.0	3000
	T3	40-140	100	18.4	1840
	T4	40-120	80	20.8	1664
	T5	40-100	60	8.5	510
	T6	24-76	52	1.5	78
Iron oxide	T2	60-380	320	1.530	489.6
	T3	20-200	180	1.379	248.2
	T4	0-180	100	0.729	72.9
	T5	80-200	120	1.175	141
	T6	43-92	49	0.978	47.9

N.B. Combined total of all three indices T2, 4,590; T3, 2,748; T4, 2,287; T5, 771; T6, 214
These indices can be plotted separately or all three can be added together to give a combined weathering profile index total (Figure 5.19).

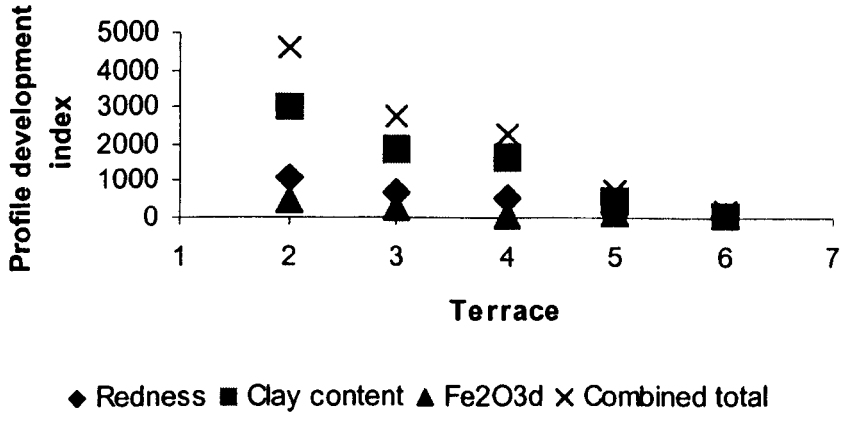

Figure 5.19 Profile development indices of redness rating, clay content and iron oxide (Fe_d) concentration, and the combined total of all three. The index is calculated by the B horizon thickness multiplied by the difference between the maximum parameter value and that of the least altered material (after Woodward *et al.*, 1994).

Luminescence dating was conducted on samples from four of the terraces to provide more detailed information on the timing of major aggradation events in the Tavignano valley. The ages obtained (Table 5.12) can be used in conjunction with the PDI to construct an alluvial history. A plot of PDI and OSL ages can be constructed (Figure 5.20). Plotting the CL2, CL4, CL6 and CL8 ages (with the oldest age of 19.9 ka) against the weathering index gives an r^2 relationship of 0.67. The one sample which was collected in addition to another from terrace T4 displays a much greater age (30.7 ka ± 11.8, compared to 3.4 ka ± 0.6 of CL4). CL1 was taken from the trunk stream deposits rather than from fan material as CL4. Although there is little

confidence in the fact that CL1 has been adequately zeroed (Chapter 5.6.8), the age seems more appropriate than 3.4 ka with regards to the geomorphological and pedogenic evidence presented in Chapters 5.5.3 & 5.5.4. The relatively high rubification, clay content and total ferric iron concentrations in T4 suggest that the terrace has experienced more than 3.4 ka of development. Grussified granite pebbles and weathering rinds of 1-2cm provide further evidence that weathering processes have been in effect for a significantly longer period that 3.4 ka. Conchon (1975) suggests an age relating to the Lower Würm for terrace T4, perhaps *ca.* 60 ka. It is likely that the samples with underestimated ages have been subjected to light since the deposition event of interest, resetting the luminescence signal. Perhaps the samples taken from the alluvial fans may have undergone some reworking. This argument can be extended to units T2 and T3, for which OSL ages of 19.9 ka ± 2.5 and 18.4 ka ± 3.7 were obtained from the main channel deposits respectively. Although these ages coincide with the LGM, a period which favoured major aggradation within the Mediterranean region (Chapter 2.5.1), the degree of profile development within both of these terraces suggests that deposition was far earlier than 18-20 ka. Conchon (1975, 1978) also tentatively assigns these deposits to the Mindel and Riss stages of the Alpine stratigraphy, which date back to approximately 420-240 ka and 220-180 ka respectively (Table 1.1).

Assuming that the OSL ages of CL2, CL4, CL6 and CL8 are underestimates, and that the age of CL1 is more representative of the Tavignano T4 terrace, ages could be suggested for the other units by extrapolating the trend line through CL1 and interpolating the graph (Figure 5.20). These estimated ages would also depend on the assumption that the PDI closely characterizes the ages of the units and that the development is linearly proportional with time. Taking the error margin of CL1 into consideration, the estimated age model results are as follows (Table 5.15).

These ages must of course be regarded with extreme caution due to the number of assumptions inherent in their determination. It is important to appreciate that the climatic conditions have changed considerably throughout the Late Pleistocene (Chapter 2.4.1) and may have strongly influenced soil development. Warmer, wetter conditions are more favourable for weathering processes than cold and dry conditions (e.g. Schulte & Julia, 2001). Therefore, development rates are likely to have been variable over time. More importantly, the age model is based on only one absolute date, so the terrace ages are extremely tentative. However, the following section will discuss the controlling mechanisms of such river behaviour in Corsica and will compare the ages estimated here with other studies in the Mediterranean. Patterns of alluviation across the Mediterranean region have already been briefly described (Chapter 2.5).

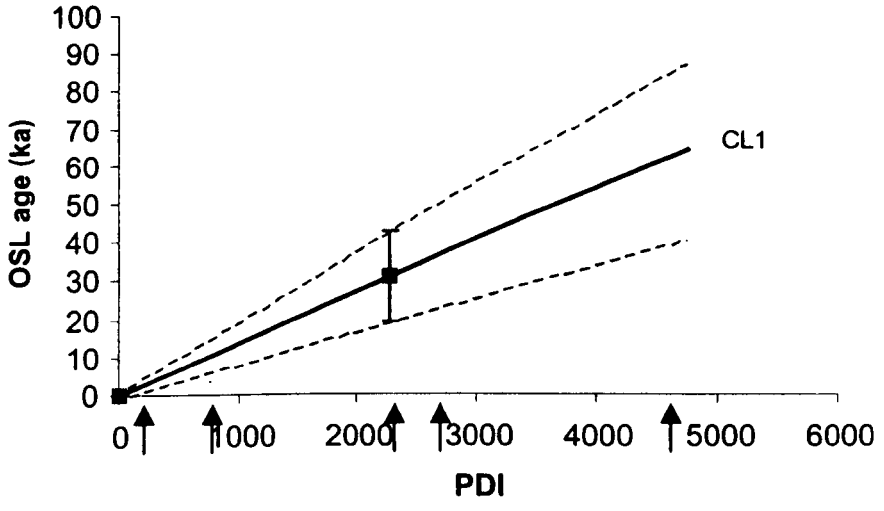

Figure 5.20 The relationship between soil profile age, determined by OSL dating for CL1 (Table 5.11) and the profile development index (PDI) (▲) derived from the redness rating, clay content and iron oxide concentration (Fe_2O_{3d}) (Table 5.14).

Table 5.15 Extrapolated ages and error margins of units T2-T6 from CL1 and Figure 5.20.

Terrace	Maximum age (ka)	Minimum age (ka)	Estimated age (ka)
T2	85	39	62 ± 23
T3	50	22	36 ± 14
T4	43	19	31 ± 12[a]
T5	15	5	10 ± 5
T6	3	1	2 ± 1

[a] OSL age from sample CL1

5.8 ENVIRONMENTAL CONTROLS ON LATE QUATERNARY RIVER ACTIVITY

Elucidating the controls on Late Pleistocene and Holocene river development in the Mediterranean has become a major topic in Quaternary geomorphology (Chapter 2.5). Distinguishing between the effects of tectonic, climatic or human activity within a catchment has often been a contentious issue. In the case of the Tavignano valley, the absence of significant anthropogenic influence over the Late Pleistocene suggests that climate and tectonics are the two dominant extrinsic controls on river development. Evidence of tectonic activity influencing the Tavignano river has already been presented in Chapter 5.3.2. Uplifting occurred sometime between T4 and T5 (Conchon, 1975, 1978) which may have resulted in aggradation downstream, but the extent of upwarping is not known exactly. Over longer timescales, such as 10^5-10^7 years, tectonics have inarguably been important in controlling the drainage pattern and fluvial sedimentation (Collier *et al.*, 1995; Lewin, 1995). The deep gorges of the Tavignano river are evidence of tectonic movements.

Climatic change has also been a prime factor in Quaternary river development (Macklin *et al.*, 2002) (Chapter 2.5.1). The improved geochronological controls used to date alluvial deposits and the higher resolution records of climatic change now available for the North Atlantic region enable comparisons between river activity and climate to be made. The Holocene record is complicated by human occupation and activities such as deforestation to which increased sediment supply and alluviation have often been attributed (Chapter 2.5.2). The behaviour of the Tavignano river during the Holocene will be discussed in Chapter 5.8.2.

5.8.1 Late Pleistocene river response to climatic change in the Mediterranean

There are several recent studies that have illustrated the association between large scale (catchment wide) sedimentation and climatic changes in the Mediterranean over the past 200 ka (Macklin *et al.*, 1997; Fuller *et al.*, 1998; Maas, 1998; Rose & Meng, 1999; Hamlin *et al.*, 2000). The timing of such river behaviour has been summarised in Macklin *et al.*, (2002) which documents at least 13 major alluviation episodes in the Mediterranean over the last interglacial-glacial cycle. Although the amplitude, frequency and possibly duration of these events may have varied across the region, there appears to be some broad synchrony of the major phases (Figure 2.7). Many of these alluviation phases coincide with cold climatic conditions. Widespread sedimentation occurred during MIS 5d (~109-111 ka), most notably at the 5a/5b boundary (~88 ka) and frequently throughout MIS 2 and 3 when highly fluctuating unstable climatic conditions were characteristic (Chapter 2.4.1). Climate-related changes in catchment hydrology and vegetation cover are thought to favour such river activity (Bull 1979, 1988). Hamlin (2000) also documents the synchronicity between Mediterranean-wide aggradation events, and notes the dominance of cold climates (Figure 5.21).

Sedimentation around 60 ka, in MIS 4 seems prominent across the Mediterranean (Figure 2.7, Figure 5.21), with alluviation in the northwest Greece (Hamlin, 2001), Mallorca (Rose & Meng, 1999; Rose *et al.*, 1999), and northeast Spain (Fuller *et al.*, 1996; 1998). This is suggested to equate with the stadial identified in the records at Lago Grande di Monticchio in Italy (Figure 2.2) around 60.5-63.5 ka (Allen, *et al.*, 1999). This depositional phase may also be related to Heinrich event 6 at ~66 ka (Macklin *et al.*, 2002). If the extrapolated age around 62 ka for the Tavignano is correct, unit T2 could also be in response to this climatic deterioration. Heinrich events are thought to bring sudden cooling and large floods across the Mediterranean and northern Europe because of the southward migration of the jet stream (Chapter 2.3). Intense winter precipitation in addition to the glacial meltwater discharges in spring would enable large sediment loads to be transported down. Sediment supply would be high due to the increased mechanical rock breakdown by frost shattering processes and glacial erosion. Stadials during the Late Pleistocene were dominated by *Artemisia* steppe-like environments (Figure 2.3). Low vegetation cover would prohibit soil development and promote slope instability, increasing the

supply of sediment available for entrainment. Rapid runoff from the bare headwaters would also exacerbate alluviation. The thickness of the Tavignano deposits is evidence of a high sediment supply. Parts of the units are dominated by matrix-supported large cobbles and boulders seen in vertical section (Figure 5.6) and display the efficiency of glacial and bedrock erosion and the high competency of the river. The fine grained layers illustrate low energy deposition and are perhaps the result of the waning peak discharges.

Table 5.16 Selected studies used in Figure 5.21 (from Hamlin, 2000).

No.	Reference(s)	Study site	Dating technique
1	Hamlin (2000), Hamlin *et al.*, (2000)	Voidomatis River, NW Greece	$^{230}Th/^{234}U$
2	Rose & Meng (1999), Rose *et al.*, (1999);	Torrente d'es Coco & Torrente de sa Telaia Freda, NE Mallorca, Spain	OSL
3	Fuller *et al.*, (1996, 1998)	Mas de Las Matas, Guadalope River, NE Spain	IRSL
4	Fuller *et al.*, (1996, 1998)	Castelseras, Guadalope River, NE Spain	IRSL
5	Maas (1998)	Samaria Gorge, SW Crete, Greece	$^{230}Th/^{234}U$
6	Maas (1998); Maas *et al.* (1998)	Rapanas & Omalos Rivers & Aradena Gorge, SW Crete, Greece	$^{230}Th/^{234}U$

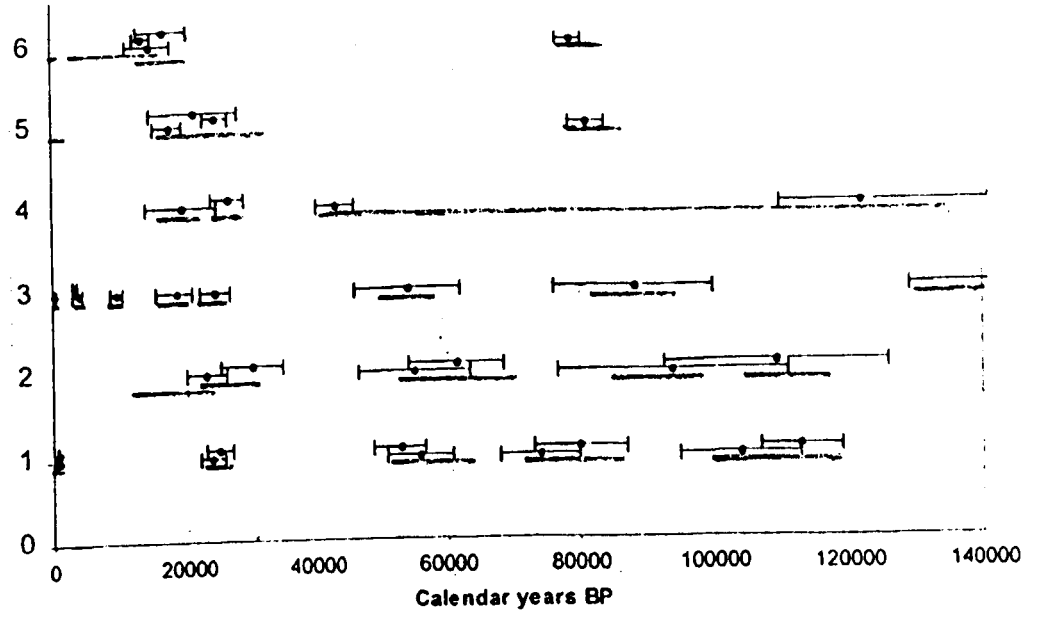

Figure 5.21 Comparison of selected chronologies of Late Quaternary sedimentation in the Mediterranean region. Details of the studies are provided in Table 5.16 (Hamlin, 2000).

Enhanced fluvial activity is also noted during MIS 3 which is a period punctuated by sharp climatic oscillations (Figure 2.3). Alluviation events are dated to around 48 ka and 38 ka (Macklin *et al.*, 2002) which correspond to stadial events identified in palaeoenvironmental records (Allen, *et al.*, 1999), and which coincide with Heinrich events 5 and 4 respectively.

Although the error margins on the extrapolated PDI- based model ages are large, the deposition age of T3 based on the PDI is around 36 ka. T4 is also assigned an age of 31 ka ± 12, which may correlate to these alluviation events, or perhaps be a result of cooling initiated by Heinrich Event 3. Indeed, these links are tenuous and the error margin of this assigned date could feasibly allow for deposition during the LGM, a period of heightened alluviation occurring 18-20 ka. Figure 2.7 and Figure 5.21 display Mediterranean wide sedimentation between 10 and 30 ka. Multiple alluviation events centre between ~28 ± 4 and 30 ± 4.7, 21 ± 0.8 and 26 ± 2, 16 ±3 and 19 ± 1, 12.5 ±1.5 and 13 ±2 ka (Macklin *et al.*, 2002). The former is thought to correspond to H3, and the others correlate well with abrupt decreases in sea surface temperature in the North Atlantic (Bard *et al.*, 2000; Macklin *et al.*, 2002). HO, which is labelled the Younger Dryas, correlates to the last of the age ranges. The Younger Dryas is known to have been a particularly abrupt cool period resulting in major glacier advances and downstream sedimentation (Chapters 2.4 & 4.6). Although the error margins on the age model for the Tavignano terraces do not allow for such precise dating, it could be suggested that the large scale aggradation events evident in Corsica may have been in response to these rapid climatic changes.

5.8.2 River behaviour during the Holocene

The influence of climatic change on river behaviour is complicated throughout the Holocene due to landscape disturbances caused by human action. The timing and impact of anthropogenic activity within the catchments of Corsica is not known (Chapter 3.9). In many areas of the Mediterranean, deforestation of the land led to significant changes in the hydrological and sedimentological regime of the river, often resulting in alluviation (e.g. van Andel *et al.*, 1986, 1990) (Chapter 2.5.2). Corsica is unlikely to have undergone such major deforestation. Much of the land is still wooded today. It is difficult however, to be certain of the factors controlling sedimentation during the Holocene. It is unclear whether the deposition ages of 10 ± 5 and 2 ± 1 ka for the T5 and T6 terraces relate to climatically or anthropogenically induced changes. Deposition of T5 may have been climatically derived due to the high variability during the Glacial-Interglacial transition. T6 could be the result of a combination of both climate and anthropogenic activity but is ambiguous. Mediterranean river behaviour during the Holocene has been one predominantly of incision, and this is observed today in the present Tavignano channel. The warmer interglacial conditions and the reduced sediment supply has led to an entrenching nature during most of the Holocene period.

Fuller *et al.* (1996, 1998) document sedimentation in Mas de Las Matas in northeast Spain around 3.4 and 3 ka which is attributed to a neoglacial event recorded in the palaeoenvironmental records of Meese *et al.* (1994). It is worthy to note that the OSL ages of CL4 and CL6 for alluvial fan material of T4 and T5 are similar to this (3.4, 3.2 ka). Perhaps

these samples are representative of a period of cooling which promoted a flux of sediment that now overlays the main T4 and T5 deposits. However, no geomorphological or stratigraphical evidence of such an episode is observed in the fan sections.

5.8.3 Evaluation of Conchon's chronology

The high resolution climate proxy records and the increasing number of well dated fluvial deposits in the Mediterranean provides compelling evidence that high frequency climatic change in the North Atlantic during the Last Glacial period had a strong influence on river alluviation through changes in vegetation cover, catchment erosion and flow regime. The fact that these rapid fluctuations have been observed only relatively recently in the palaeoenvironmental records might explain the conventional stratigraphy proposed by Conchon in the 1970's (Table 5.2). Large scale, catchment wide scale aggradation in Corsica has been assigned to the glacial periods when the climatic conditions, as discussed above, enhanced flood frequency and magnitude, and indirectly increased the sediment calibre and load available for transport downstream. It may have been thought that the warmer interglacial periods could not have provided such major sedimentation due to the lack of glacial erosion and the stable, forested slopes. Our present knowledge of Late Pleistocene climatic change allows the correlation between major Mediterranean river aggradation and stadial episodes, a cold phase much more frequent than the "glacial" episodes. The magnitude and abruptness of stadial events in terms of climatic conditions and their effects on the landscape has only recently been recognised.

More absolute dating needs to be applied to this investigation to be sure of the relationship between climatic change and alluviation in the Tavignano catchment. It must be stressed that the depositional ages for the Tavignano terraces provided in this chapter cannot be relied upon. The profile development index, the numerous assumptions made about the linearity of the weathering-time relationship and the use of one OSL age does not provide the confidence in the dating of the units.

5.9 SUMMARY

It is likely that the Tavignano terraces were deposited during cold stages, as illustrated for many other fluvial system in the Mediterranean, however the timing is still uncertain. Although the terraces may be older than the ages obtained using the PDI and CL1 extrapolation due to non linearity, they may not have originated during the Alpine glacial stages proposed by Conchon. The high resolution climate proxy records display highly fluctuating conditions during the Late Pleistocene, and the high frequency, high magnitude cold stadial episodes could be as effective as the full glacial periods in promoting large scale aggradation.

This chapter has illustrated that relative ages can be constructed for the alluvial units from pedogenic parameters. This study shows that the redness rating, clay content and the iron oxide concentrations provide a good relationship with time. However, other than the χfd%, the mineral magnetic parameters were not as successful in obtaining a relative age sequence. A full characterisation of the mineral and grain size assemblages is a complex task even in purely qualitative terms. The results depend on mineral type, mineral concentration and grain size, and it is often difficult to distinguish between the dominant factors and controls. This study also illustrates the need for more absolute ages for each of the alluvial units to be confident in the timing of the deposition phases. The study highlights the importance of using sedimentological and relative weathering features in addition to absolute data to construct an alluvial history.

6 RIVER RESPONSE TO RECENT ENVIRONMENTAL CHANGE IN NORTHWEST CORSICA

6.1 SYNOPSIS

Firstly this chapter outlines the variations in climate over the past 50 years in Corsica and describes recent flood events experienced on the island and in the wider western Mediterranean region. The forcing factors of heavy precipitation events and flooding are also described for the western Mediterranean basin. Secondly, a 450 year flood history is established for the Figarella, a small steepland river system in northwest Corsica by lichenometric dating. The identified periods of enhanced flooding are compared to other empirical studies conducted in the Mediterranean and secondary data to determine the degree of synchrony and possible controls on flooding. Daily rainfall records are also analysed for Corsica and other parts of the western Mediterranean to explore the influences of the North Atlantic Oscillation on flood frequency in the area.

6.2 INTRODUCTION

Steepland river systems can be sensitive to environmental change whether this is driven by climatic or anthropogenic influences (Macklin *et al.*, 1995) (Chapter 2.5.2). These influences are well illustrated in the Mediterranean region for the Holocene period as there is widespread evidence for marked changes in river behaviour (e.g. Vita-Finzi, 1969; van Andel *et al.*, 1990; Lewin *et al.*, 1995a; Poesen and Hooke, 1997). Mountain catchments in seasonally-dry regions are particularly susceptible to both land-use and climatic change. The steep relief, thin soils and high intensity rainfall in Mediterranean regions often results in flashy stream regimes capable of transferring large quantities of coarse sediment (Macklin *et al.*, 1995; Maas *et al.*, 1998).

More generally, over the past few decades there has been an increasing interest in the varying morphogenetic impacts of floods. Human activity was once thought to have been the dominant influence on flooding and associated river behaviour during the Holocene. Many studies evaluated river response with regards to land use change (e.g. Wagstaff, 1981). With the exception of Vita-Finzi (1969), who stressed that the role of climate was important within the fluvial system (Chapter 2.5.2), climatic change was considered to be relatively insignificant because of the traditional assumption of stationarity in flood series on a timescale of 10^0- 10^2 years (Knox, 1984). More recent investigations have shown that small scale, high frequency climatic variations have had significant impacts on river regime and catchment geomorphology (e.g. Macklin *et al.*, 1992; Brown; 1998; Maas *et al.*, 1998; Merrett and Macklin, 1999; Hamlin, 2000; Maas & Macklin, in press).

Fluvial response to rapid, short term climate fluctuations is a major current focus, reflecting the need to understand the implications of recent and potential climatic change for earth surface systems (e.g. Maddy *et al.*, 2001). Investigations of past fluvial activity offer analogues to future channel and floodplain responses. There is an increasing importance to investigate the natural variability of the climate system on a decadal-centennial timescale in order to better understand the significance of climatic fluctuations in the future and isolate anthropogenically forced trends such as greenhouse global warming.

The principal aim of this chapter is to assess the timing and nature of river response to environmental change over the last *ca.* 450 years in northwest Corsica. The objectives of this study are as follows:

i) To establish the synoptic conditions responsible for the generation of large floods in Corsica.

ii) To reconstruct the flood history of the Figarella River, northwest Corsica by lichenometric dating.

iii) To evaluate the relationship between decadal and century scale climatic change, flooding and river development in Corsica.

iv) To compare the identified periods of enhanced flooding and fluvial activity in Corsica with other parts of the western Mediterranean basin and to ascertain potential forcing mechanisms.

6.3 STUDY SITE

The Figarella River (N 42° 26', E 8° 50') drains the northwestern flanks of the rhyolitic massif of Mount Cinto (2,706 m) in northern Corsica, and enters the Mediterranean Sea approximately 4 km to the east of Calvi (Figure 6.1). The study catchment and reach (Figure 6.2) were chosen for several reasons:

i) The Figarella river is a small (132 km^2), steepland mountain river system with cobble and boulder (< 3 m) bed channels (Figure 6.3).

ii) Coarse deposits attributable to large magnitude flood events are evident on a series of terrace surfaces and mid-channel bars.

iii) There is abundant lichen colonisation on the coarse flood deposit surfaces. In some cases there is more than one species present. Numerous graveyards in the vicinity provide a good number of dated substrates in order to construct a lichen size-age calibration curve.

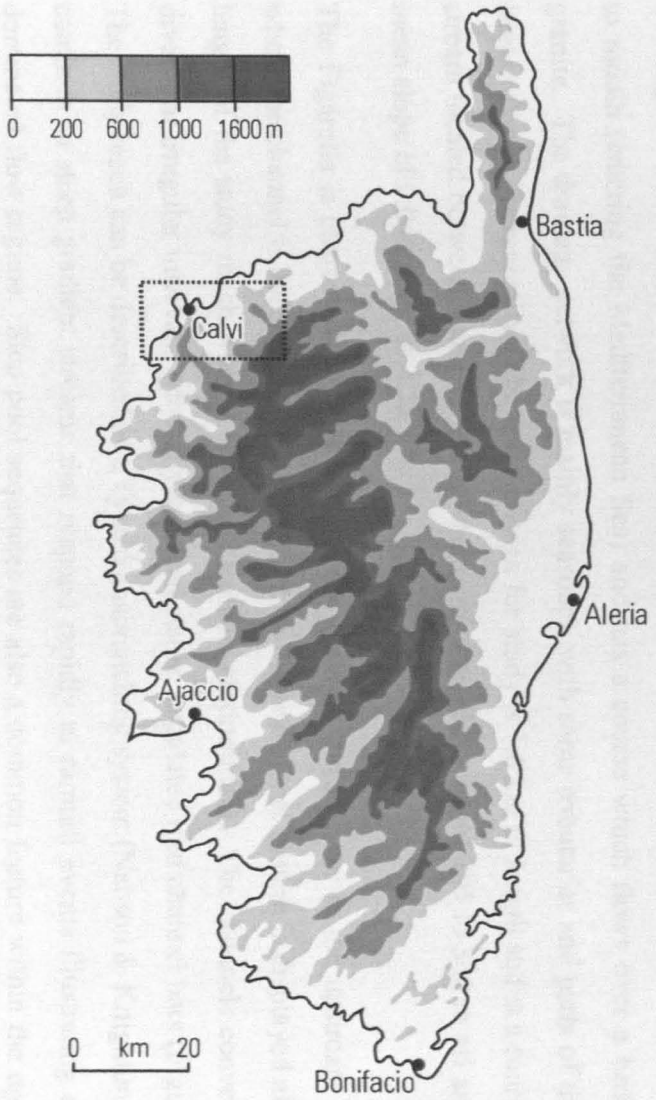

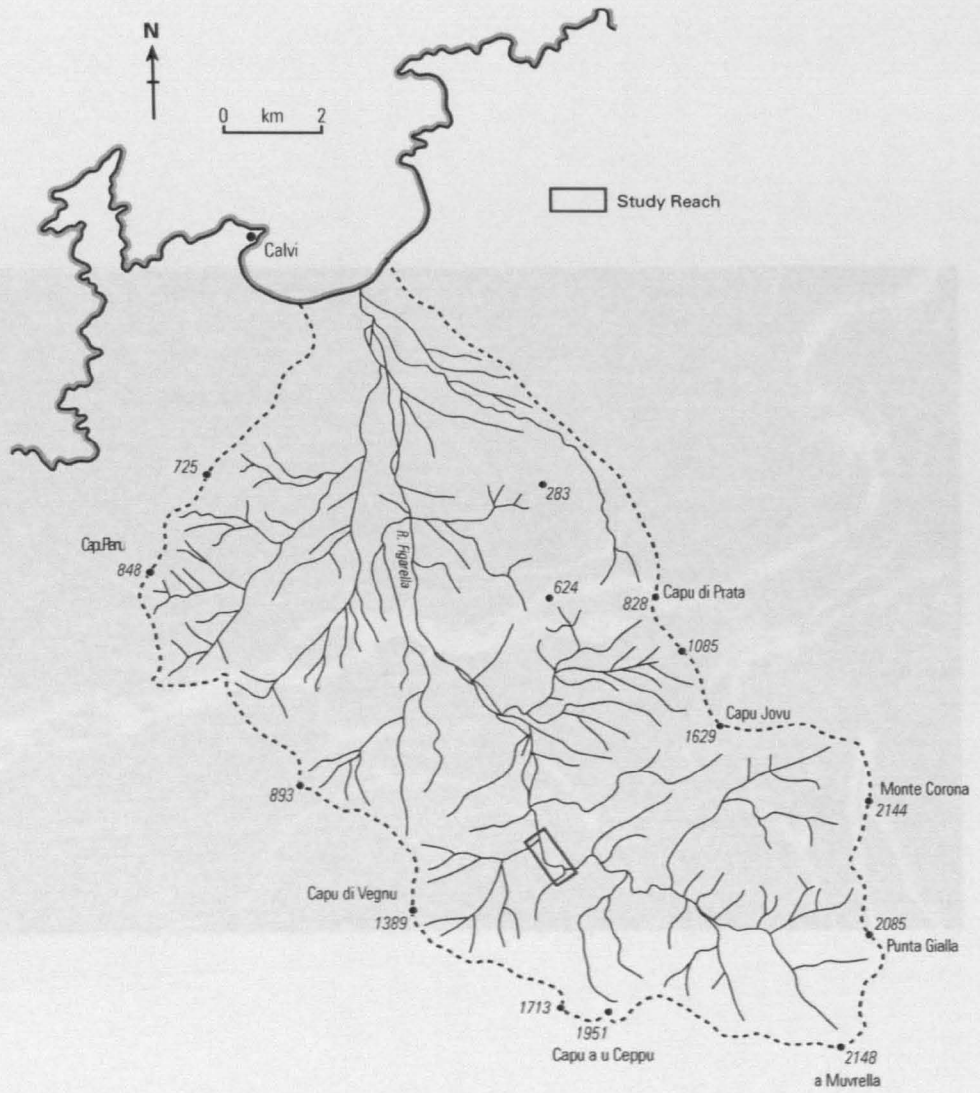

Figure 6.1 The drainage of the Figarella River, northwest Corsica

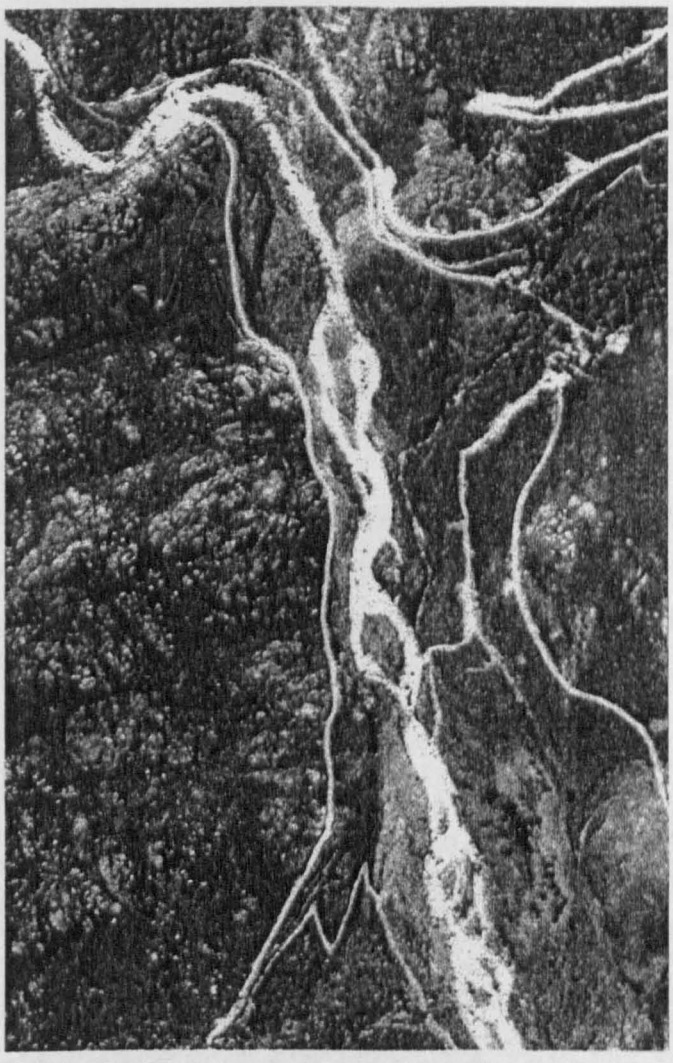

Figure 6.2 Aerial photograph (1996) of the Figarella River study reach (refer to Figure 6.1). Flow is down the page. Scale is approximately 1: 10,000 (1 cm = 100 m).

The Figarella river is approximately 25 km in length from source (Lac de la Muvrella, 1,910 m) to mouth (entering the Mediterranean Sea) and has a course which flows over a bedrock of granite. The drainage network is mainly seasonal, with some tributaries and parts of the trunk stream flowing perennially. The reach chosen for study is 1.6 km in length and is a fourth order stream located between 9 and 11 km downstream at an elevation of 295 to 360 m asl and has a mean slope of 0.041 mm^{-1} or 2.33°.

The Figarella is characterized by a low sinuosity, single thread river in the upstream reaches where the channel is constrained by bedrock. A multiple channel system is displayed along the length of the study reach where two main channels predominate. The channels converge and diverge at irregular intervals, generally between stable, vegetated mid channel bars (Figure 6.3). The study reach can be described as a Type 6 anabranching system (Nanson & Knighton, 1996), common in steep gradient streams that respond rapidly to rainfall events illustrating a flood-dominated flow regime. Step pool sequences are also a common feature within the upper and middle reaches of the Figarella. The valley floor in the upper section of the study reach is approximately 100 m wide, with a single channel width of 30 m. Downstream, the floodplain

widens to approximately 300 m. The two main channels are approximately 20-25 meters across, joining in places to form a channel greater than 60 m in width. The stream has a wandering planform 20 km downstream where the gradient is much lower and the valley floor much wider. The valley floor is predominantly covered with scrub vegetation, comprising maquis and low lying shrubs and trees (cork oak (*Quercus suber*), holm oak (*Quercus ilex*) and corsican pine (*Pinus nigra, spp. laricio*)). The hillslopes are stable and exhibit beech *(Fagus sylvatica*), alder *(Alnus cordata*) and pine *(Pinus nigra*) trees. Several areas immediately downstream of the study reach have been cleared of trees, terraced and cultivated but are now abandoned (Figure 3.15).

The modern Figarella River is undergoing a period of incision. The present supply of sediment to the trunk stream appears limited. Scree slopes in the headwater region are inactive with over two thirds stabilised by vegetation. No debris cones or gullies contribute sediment to the Figarella and several tributaries in the vicinity appear to be sediment-starved.

a)

b)

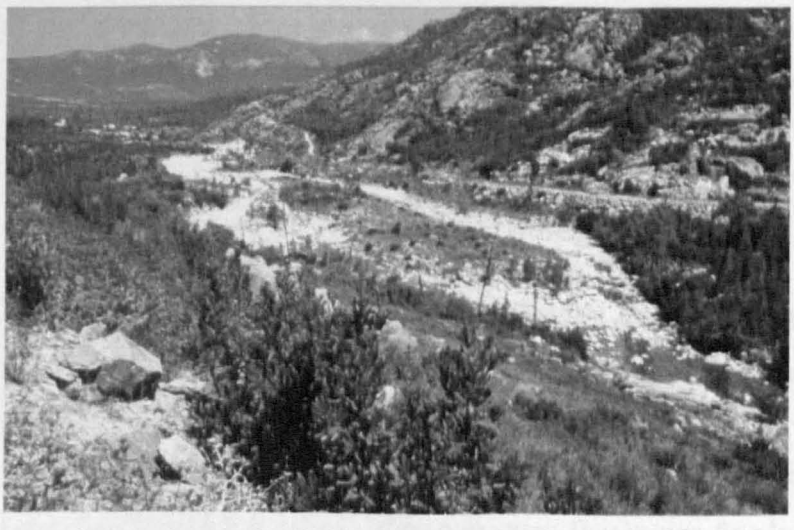

Figure 6.3 The Figarella River is a cobble and boulder bed channel in which vegetated mid channel bars are prominent. a) Looking upstream, the height of the terrace on the right is approximately 4.6 m and the channel width is 25 m. b) Looking downstream, the mid channel bar is approximately 45 m in length.

6.4 RECENT CLIMATE CHANGE IN CORSICA AND THE ASSOCIATED CONTROLS

Corsica, like all Mediterranean environments, is characterized by strong seasonal climatic contrasts with hot dry summers and mild, wet winters. Corsica is also sensitive to both short and long term climatic variability. The climate of the Mediterranean basin as a whole is a product of both subtropical and mid latitude weather systems and is susceptible to any shift in the boundaries of the two (Wigley & Farmer, 1992; Reddaway and Bigg, 1996; Romero *et al.*, 1998).

In addition to the climate data given in Chapter 3.7, it is necessary within this chapter to provide details on the recent precipitation trends since instrumentation began in Corsica (Chapter 6.4.1) and report on the timing and magnitude of large floods known to have recently occurred in the region. Possible forcing mechanisms of intense or prolonged rainfall will also be described (Chapter 6.4.3).

6.4.1 Recent precipitation trends

Precipitation within Corsica averages about 900 mm per year and falls on about 115 days of the year, although higher elevations receive considerably more (Figure 3.13). The annual precipitation totals for Ajaccio from 1856 to 1987 do not appear to illustrate any distinct linear trends, although some prolonged periods throughout the interval are wetter or drier than the long term average. Figure 6.4 shows the departure from the 1951-1980 mean (the common reference period for World Climate Disk data, Chadwyck & Healey, 1992). Sustained periods of above average precipitation include 1898-1908 and 1923-1929. Periods with below average precipitation include 1865-1870 and 1889-1896. The last 50 years or so of the Ajaccio record show that the annual precipitation totals have been more variable and the annual totals overall are significantly less than the first half of the century (Figure 6.4). Maheras (1988) illustrates a significant decrease in western Mediterranean precipitation from 1980. Another recent Mediterranean climate trend that numerous authors have documented is increased seasonality, with regards to frequency and intensity of cyclones (Maheras *et al.*, 2001) and rainfall (Sumner *et al.*, 2001).

6.4.2 Recent flood events in Corsica and the western Mediterranean

Historical records from central Europe and parts of the Mediterranean provide evidence of increased precipitation and flooding over the past 500 years. Flooding was particularly prevalent in Europe during the Little Ice Age (LIA) 1450-1850 (Grove, 1988), a period of hydroclimatic instability (Chapter 2.4.4.1). However, very few major floods prior to the last century appear to have been documented for Corsica.

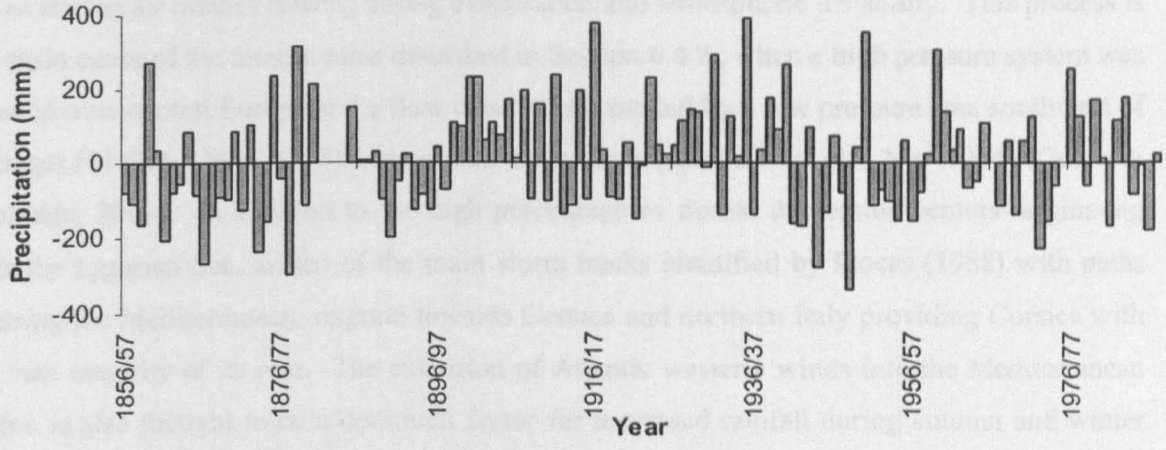

Figure 6.4 Annual (September to September) precipitation totals as the departure from the mean for 1951-1980 for the period 1856 to 1987(Ajaccio WCD, Chadwyck & Healey, 1992).

Instrumentation and the recording of intense rainfall resulting in catastrophic flooding or "deluges" is much more recent. In Corsica, intense rainfall often falls on the eastern side of the central mountains (Grove & Rackham, 2001). During the last 36 years, the largest event was on 31 October-1 November 1993 and yielded 1 km^3 of rainfall on the island alone, with 3,000 km^2 receiving between 300 and 900 mm. At Col de Bavella, where the annual rainfall is approximately 1,400 mm, 906 mm of rain fell in two days. Corsica also received a vast amount of rainfall on 4-5 November 1994 when a deluge on the Upper Po produced more than 2 km^3 of water (Grove & Rackham, 2001). About 12,000 km^2 received over 200 mm of rain, 1,300 km^2 received 300 mm and 600 km^2 over 400 mm. Intense rainfall events often occur in autumn (Figure 6.5), typically a little before the peak rainy season in October e.g. at Barcelona, Ajaccio and Rome (Llasat & Rodriguez, 1997).

6.4.3 Forcing factors of heavy precipitation events and flooding in the western Mediterranean

In Corsica, convective storms are common during May to September and these can result in localised flooding. However, the mountain storms rarely last longer than 48 hours. Snow melt also has an important impact on the hydrological regime of small, mountainous catchments in spring and early summer but this is rarely the cause of catastrophic flooding in the Mediterranean region. Over 60% of the precipitation in the western and central Mediterranean region results from cyclonic disturbances generated within the Mediterranean Sea, especially over the Ligurian Sea and Bay of Genoa, north of Corsica (Flocas, 1988; Wigley, 1992; Grove 2001; Sumner *et al.*, 2001) (Figure 3.14). The most frequent seasons in which Corsica experiences these frontal depressions are autumn and winter. Thus, 70% of the precipitation falls between September and February. In common with much of the Mediterranean region, and as displayed in Figure 6.5, the relative maximum precipitation occurs in October and November

when torrential rains occur due to the strong contrast between the sea surface temperatures and the overlying air masses causing strong evaporation and atmospheric instability. This process is the main cause of the intense rains described in Section 6.4.2., when a high pressure system was situated over central Europe and a flow of air was provided by a low pressure area southwest of Portugal (31 Oct-1 Nov, 1993) and cold air from the north and west (4-5 Nov 1994) (Grove & Rackham, 2001). In addition to the high percentage of frontal depression centers originating over the Ligurian Sea, all ten of the main storm tracks identified by Flocas (1988) with paths crossing the Mediterranean, migrate towards Corsica and northern Italy providing Corsica with the vast majority of its rain. The extension of Atlantic westerly winds into the Mediterranean region is also thought to be a dominant factor for increased rainfall during autumn and winter (Sumner *et al.*, 2001).

Location & record length	S	O	N	D	J	F	M	A	M	J	J	A	Total
Med. France (36 yrs)	24	**35**	18	5	8	6	2	2	2	5	4	8	119
NE Pyrenees (120 yrs)	0	6	**1**	1	0	0	1	0	0	1	0	0	11
SE Spain (83 yrs)	9	19	**12**	8	11	8	10	2	1	3	0	2	85
Corsica (36 yrs)	3	11	**6**	0	0	3	0	2	0	0	0	0	25

Bold numbering is the month with the highest total mean rainfall

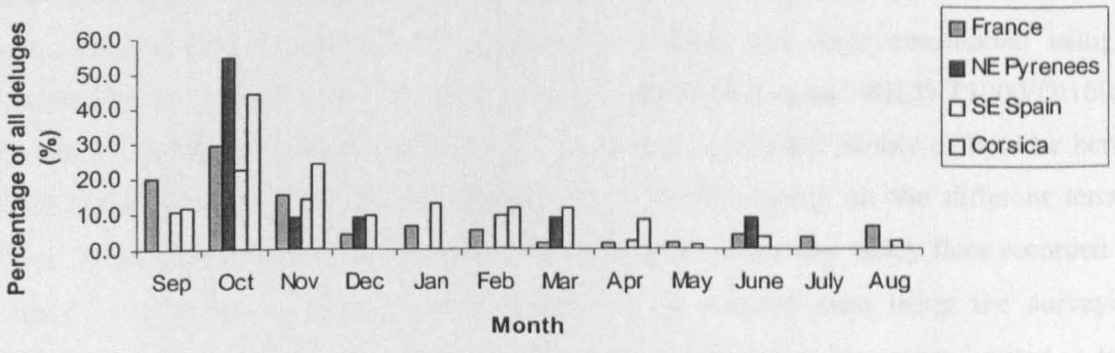

Mediterranean France and Corsica: number of situations (apparently > 190 mm) 1958-94, from Météo-France (1995)

SE Spain: inundaciónes 1900-83 mentioned by Font Tullot (1988)
NE Pyrenees: deluges 1820-1940 mentioned by Pardé

Figure 6.5 Monthly frequency of floods or "deluges" in the Mediterranean (after Grove & Rackham, 2001).

Rainfall patterns are also thought to be closely linked to the North Atlantic Oscillation (NAO), defined as the normalised sea level pressure difference between Stykkisholmer (Iceland) and Ponta Delgadas (Azores) (Rogers, 1984). Periods of low precipitation across the Mediterranean basin can be attributed partly to high NAO index values when strong westerly winds take

storms across central and northern Europe. The winter NAO (December to March) exerts the strongest influence on surface climate in Europe and the Mediterranean region (Hurrell, 1995; Osborn *et al.*, 1999; Jones *et al.*, 2001) and is often used to evaluate the strength of the teleconnection to non-seasonal and inter- and multi-annual precipitation variability (e.g. Hurrell, 1995; Piervitali *et al.*, 1997; Qian *et al.*, 2000; Quadrelli *et al.*, 2001). Orographic factors, prevailing winds, land-sea controls and other local effects also exert a significant influence on precipitation patterns and intensity of the western Mediterranean basin (Wigley & Farmer, 1982; Macklin *et al.*, 1995).

6.5 FIELD METHODS AND AVAILABLE DATA SETS

The fieldwork in the Figarella catchment was conducted in August 2000 after reconnaissance visits in May 1999 and June 2000. This section describes the methodology and the climate datasets used to establish river response to environmental change in northwest Corsica.

6.5.1 Geomorphological mapping

Geomorphological maps depicting the main valley floor features were constructed by field survey with the aid of 1:25,000 aerial photographs taken in 1996 (Figure 6.2). The sequence of alluvial terraces and coarse flood units were identified and recorded on the base map together with areas of recent sedimentation, palaeochannels and the course of the active channel. The terrace surfaces were determined by longitudinal profiles that were constructed using a theodolite and an electromagnetic distance measurer (EDM) (Theomat WILD T1000/DI1000). The coarse flood deposits within the Figarella study reach consisted mainly of boulder berms and boulder bars and gravel splays (Macklin *et al.*, 1992) resting on the different terrace surfaces. Each boulder berm was identified and its location within the valley floor recorded on the map. Cross-section surveys were carried out at selected sites using the surveying equipment described above. At some locations where accessibility was more limited, a tape measure and a clinometer were used.

6.5.2 Lichenometric dating

Lichenometry is an established method for dating rock surfaces and is widely used in geomorphological studies of recent environmental change. Various workers have used lichenometry in the fluvial environment to establish flood histories in northern Britain (e.g. Harvey *et al.*, 1984; Macklin 1986; Macklin *et al.*, 1992; Merrett and Macklin, 1999) and the method has also been recently applied to steepland catchments in the Mediterranean (e.g. Maas *et al.*, 1998, Hamlin, 2000; Maas & Macklin, in press). Lichenometry is a geochronological method that spans the time range between historically recorded events (decades or centuries) and radiocarbon dating (>1000 years). Lichenometric dating is the principal technique

employed in this study to provide a chronological framework for the deposition of the coarse flood sediments. Therefore, it is important to understand the theory which underpins lichenometric dating to minimise any sampling errors and to be aware of the limitations of the technique.

6.5.2.1 Sampling approach

Lichenometric dating is based on the principle that the size of the individual lichen thalli is directly related to the age of the colonised substrate. The longest thalli diameter of the lichens colonising the coarse flood deposits (e.g. individual boulder bar or berm) along the valley floor were measured to the nearest 0.1 cm. The most abundant lichen colonising the granite boulders in the Figarella system are the single crustose species *Rhizocarpon geographicum agg.* (RZ). RZ was the principal species measured and the one used to construct the flood history. For cross-checking purposes a second lichen *Lecanora rupicola* spp. (LR) was measured wherever both species colonised the same flood deposit site (Figure 6.6). Five of the largest thalli were measured, and the average size was used to represent the exposure age. By measuring a small population of largest lichens, discrepancies in the single largest lichen are minimised (Mottershead, 1990). This sampling approach of taking several of the largest lichens to characterize the minimum age of a surface by lichenometry is the consensus view (Goudie *et al.*, 1990) although a number of other sampling methods have been employed by different workers (Table 6.1). Anomalously large lichens evident on a restricted number of clasts, possibly due to the result of reworking, were excluded from measurement. Care was also taken to exclude those lichens which had coalesced, those of an irregular shape or those which had become fragmented.

Table 6.1 Preferred lichenometric dating sampling methods.

Preferred lichenometry sampling strategy	Example author	Comment
Single lichen measurement	Miller,1973	
	Webber and Andrews,1973	Smaller thalli are late colonisers or slow growers.
	Harvey *et al.*,1984	
	Innes, 1985	Used if rock type differs.
Mean diameter of the three largest lichens	Macklin *et al.*, 1992	
Mean diameter of the five largest lichens	Matthews, 1974, 1975 Innes, 1984, 1985	
Area of lichen	Armstrong, 1974	Less easily assessed in the field.

6.5.2.2 Size-Age calibration

The relationship between lichen size and age was established empirically by measuring the largest thalli on dated susbstrates such as gravestones and bridges and applied to the deposits of interest to give a minimum age estimate. A growth curve for both RZ and LR species was

constructed using 15 and 26 measurements respectively (Figure 6.7, Appendix XIV). These were collected from locations within a radius of 25 km from the study site to minimize climatic variability. Each point on the size-age plot represents the mean of up to the five largest lichens on the dated substrate surfaces. The oldest calibrated surfaces measured for RZ and LR were 100 and 110 years respectively. A linear trend line was fitted to the size-age plot to give a growth rate of 0.27 $mmyr^{-1}$ for RZ and 0.93 $mmyr^{-1}$ for LR. The size-age relationship is strong for both lichen species. There is limited scatter and both calibration curves yield r^2 values > 0.83. This gives confidence in assigning minimum age estimates to the Figarella coarse flood deposits.

Figure 6.6 *Rhizocarpon geographicum agg.* (green lichen) and *Lecanora rupicola spp.* (white lichen) colonising coarse flood deposits within the Figarella catchment. A5 book for scale.

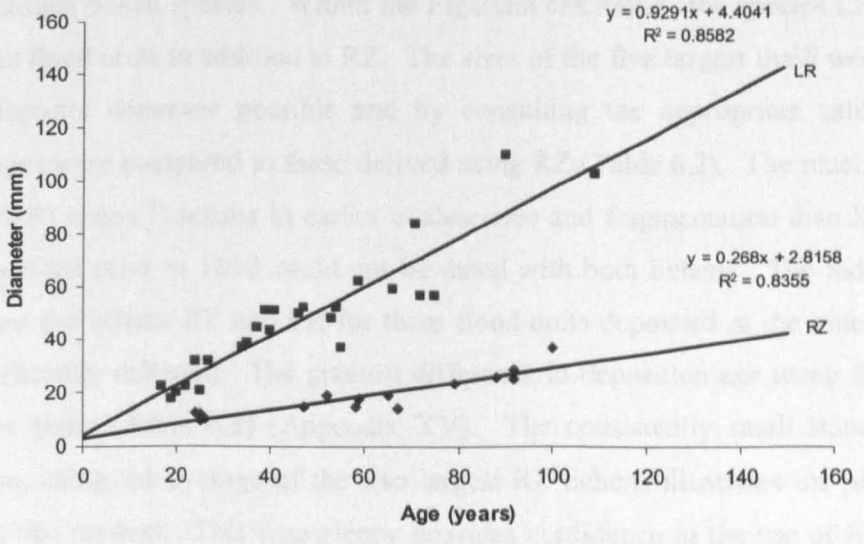

Figure 6.7 Growth curves for the lichen species *Rhizocarpon geographicum agg.* (*RZ*) and *Lecanora rupicola spp. (LR)*. Each point represents the average of up to the five largest lichens colonising a dated substrate in Northwest Corsica.

The growth rate for RZ in northwest Corsica is relatively slow compared to the range 0.36-0.39 $mmyr^{-1}$ reported by Macklin *et al.* (1992) for northeast England. Easton (1994) comments that crustose lichens such as RZ have a growth rate between 0.25 $mmyr^{-1}$ and 1 $mmyr^{-1}$ which varies from year to year and between habitats. Saxicolous (rock inhabiting) species generally have a high tolerance of environmental factors, the most important being light intensity, water content, substrate stability and texture and pH (Armstrong, 1974). The slower growth rate in Corsica compared to that observed in northeast England may be due to a moisture deficiency of a drier and warmer climate. It has been recognised that lichen thalli on substrate surfaces near streams may be larger as moisture is the major controlling influence on lichen metabolism (Beschel, 1961; Benedict, 1967, Innes, 1985). This microenvironmental factor is regarded insignificant in the Figarella system as precipitation is relatively abundant; the headwaters receive over 1,500 mm a year on average (Chapter 3.7). The lichens would not have to rely on obtaining the essential moisture from the stream. Lithology may also be a significant factor for growth rate. The Carboniferous sandstones, limestones and shales within the region of northeast England studied by Macklin *et al.* (1992) may have been a more conducive substrate for lichen growth than the granite lithology of northwest Corsica.

Another important factor to be aware of is the possible time lag between substrate exposure and lichen colonisation. This lag is generally thought to be less than five years, although it has been reported that the RZ species is an early coloniser (Harvey *et al.*, 1984). It follows that the older the lichen the less significant this time lag will be to the final age.

6.5.2.3 Cross checking

To examine the reliability of using lichen size as a chronological tool, the age of the coarse flood deposits predicted from the lichen thalli size and growth curve of RZ were cross checked with an additional lichen species. Within the Figarella catchment, the species LR is present on several of the flood units in addition to RZ. The sizes of the five largest thalli were recorded on the flood deposits wherever possible and by consulting the appropriate calibration curve, deposition ages were compared to those derived using RZ (Table 6.2). The much faster growth rate of LR (0.93 $mmyr^{-1}$) results in earlier coalescence and fragmentation than RZ. The flood material deposited prior to 1800 could not be dated with both lichens. The independent ages obtained from the lichens RZ and LR for three flood units deposited in the nineteenth century are not significantly different. The greatest difference in deposition age using the two lichens was only six years (Table 6.2) (Appendix XV). The consistently small standard deviation acquired from using the average of the five largest RZ lichens illustrates the precision of the technique in this context. This consistency provides confidence in the use of lichenometry to date the coarse flood deposits. Using techniques such as dendrochrology in conjunction with lichenometry can also serve to corroborate age estimates (Chapter 6.7.2).

Table 6.2 Cross-check of three flood unit ages where both *Rhizocarpon geographicum* agg. and *Lecanora rupicola* lichen species were present. The five largest lichens were measured to obtain an average (Appendix XV).

Flood unit (Figure 6.9.)	Lichen species	Mean thalli size and standard deviation (mm)		Predicted age
g	*R. geographicum* agg.	47.8	3.27	1832
	L. rupicola	161.6	8.17	1831
i	*R. geographicum* agg.	34.6	2.88	1881
	L. rupicola	111.4	6.36	1885
l	*R. geographicum* agg.	45.6	6.02	1840
	L. rupicola	154.0	7.21	1834

6.5.2.4 Extrapolation and limitations

To enable alluvial deposits older than 100 years to be dated and a chronology of flood events in the study region to be established, the linear size-age relationship has been extended. It is assumed that the growth rate of both species has remained constant over the last 400 years. Calibration curves for *Rhizocarpon geographicum* agg. collected in the Yorkshire Dales, northeast England display a linear growth rate for over 200 years (Merrett and Macklin, 1999), whereas in the Colorado Front Range, USA, only a 100 year linear relationship is recorded. Several other documented calibration curves for RZ illustrate a 'flattened S-shape' (e.g. Innes, 1983; Harvey *et al.*, 1984; Macklin *et al.*, 1992). Consequently, it must therefore be recognised that the assumption of linear growth throughout the life of a lichen may not be strictly valid for the whole timescale involved. Age estimates for deposition of the coarse flood material, especially at sites exceeding 200 years will most likely be underestimates rather than overestimates (relative to flood deposits < 200 years in age).

In conclusion, lichenometric dating is a valid technique which allows the construction of a temporal framework where few other geochronological controls are available. The reliability and precision of lichenometric dating varies according to the field data available (substrates of interest and calibration record), the sampling strategy and the assumptions made (e.g. reworking, coalescing). The sampling approach used in this investigation was designed to maximise reliability and precision. However, like all dating techniques, lichenometry has a margin of error. Innes (1988) remarks that lichenometry can be used to date a surface to within 10% of the actual age. It has also been argued that the dating tool is accurate to ± 5 years over the last 200 years (Porter, 1981).

6.5.3 Dendrochronology

The majority of the valley floor in the Figarella catchment is stable and covered by maquis, a scrub type vegetation consisting of cistes, calycotomes, junipers, thistles and blackberries. Some of the landforms are colonised by large shrubs and bushes (mainly beech (*Fagus sylvatica*) and alder (*Alnus cordata*)) and several pine (*Pinus*) species. Vegetation type and

density can be used to assess the stability of the unit surface upon which it is growing and can be used as an indicator of relative age. The vegetation cover on the terrace surfaces in the Figarella catchment was therefore recorded.

Tree ring dating can be employed to estimate the minimum age of the unit surface. Cores were taken from trees on the terrace surfaces in the vicinity of the lichenometric-dated coarse flood deposits. The age of the tree provides a minimum age estimate for the terrace surface, an indication of the age of the flood event which deposited the coarse material. Not all the identified boulder berms had trees growing nearby. There were many small shrubs and bushes colonising the terrace surfaces which were unsuitable for coring. The application of dendrochronology was restricted to Corsican pine trees (*Pinus nigra laricio*). Cores were taken from those trees with the largest circumference growing on the surface in the vicinity of the coarse flood deposits. The corer was screwed horizontally into the middle of the tree trunk, approximately 1.5 m from the base until the centre of the trunk was reached. The core was carefully extracted to reveal the total number of tree rings. Each tree ring increment is indicative of one year's growth. In gymnosperms, such as pine trees, tree rings are particularly distinctive as there is a pronounced colour difference between the dark, late wood and the following season's light early wood. The growth cycles are normally seasonal and are determined by the regular alternation of winter and summer climatic conditions. Detailed climatic interpretation of the cores has not been conducted in this study.

It is assumed that any vegetation that may have colonised the unit prior to the flood was destroyed, and the trees now present grew soon after the overbank event. The lag time between flood and tree colonisation is longer than that for lichen growth. There needs to be an adequate quantity of fines on the unit surface before a sapling can grow. This may require time for slope wash to reach the surface or several overbank flood events to deposit fine grained alluvium. In addition, trees in most environments do not live for more than several centuries, and so their use as an age indicator is therefore restricted to such a timescale (Goudie *et al.*, 1990).

Dendrochronology can be valuable dating tool when used in conjunction with other chronological controls such as lichenometry. The technique can be especially useful in establishing minimal ages where there is dense vegetation and where lichen growth may not be optimal. The dendrochronology data are presented in Chapter 6.7.2.

6.5.4 Climate datasets

Investigating the changing climate over the last 400 years involves the analysis of available secular series of quantitative data which can be extended by using proxy data and historical documents (see Lamb, 1977). Europe has the most abundant and extensive instrumented hydroclimatic records. For this study, monthly precipitation data for Ajaccio (1856-1990),

located on the west coast of Corsica have been accessed from the World Climate Disk (WCD) (Chadwyck & Healey, 1992). Daily precipitation records for Ajaccio from 1990-1996 from the British Atmospheric Data Centre (BADC) archives have also been utilised in this study. An extended daily precipitation series from Barcelona (1900-1985) was also obtained (Burgueño, 1980) as daily precipitation and discharge data were not available for Corsica. Over 100 years of daily precipitation data from Barcelona are valuable in order to compare the timing of the flood periods identified in the Figarella catchment with any prolonged or intense precipitation events in the northeast of the Iberian Peninsula. The raw data for catastrophic flooding of rivers on the Spanish Mediterranean coast over the past 500 years has also been made available (Barriendos-Vallve & Martín Vide, 1998). The significance of large scale atmospheric patterns such as the North Atlantic Oscillation (NAO) (which have been shown to affect Mediterranean precipitation) have also been evaluated against the occurrence and frequency of storm events in Barcelona. Thus, the normalised NAO index values (1824-1999) were accessed from data compiled by the Climatic Research Unit at the University of East Anglia.

Historical sources and proxy data for climate reconstruction over the past five centuries or so are also widely available for many parts of Europe. There is abundant evidence dating back to the sixteenth century in the form of weather diaries and illustrations which have been used to construct a chronology of enhanced precipitation and flood frequency (e.g. Camuffo & Enzi, 1995; Barriendos-Vallve & Martin-Vide, 1998). Ecclesiastical documents have also been exploited to investigate decadal and centennial changes in climate in southern Europe (e.g. Martin-Vide & Barriendos, 1995; Pfister, 1999; Piervitali & Colacino, 2001). Phenological (e.g. Pfister, 1995) and dendrochronological data (e.g. Serre-Bachet *et al.*, 1995; Briffa *et al.*, 1999) are also good climatic proxies that have been employed to deduce the climatic conditions over the past few centuries.

In addition to historical documentation and instrumental observations, the fluvial geomorphological record of flood events can provide a high resolution geochronology of environmental change in the region. Lichenometry, dendrochronology and radiocarbon are all dating methods that can be used over this timescale in a fluvial setting. This study is based primarily on the first of these techniques in conjunction with instrumental and secondary sources to determine river response to climate change in northwest Corsica.

6.6 RECENT RIVER BEHAVIOUR OF THE FIGARELLA RIVER

Four distinct terrace surfaces have been identified within the study reach of the Figarella catchment (Figure 6.8, Table 6.3). The oldest terrace (T4) is not spatially extensive and preservation is evident only for several hundred metres in the upper section of the reach (Figure 6.9). The height above the modern channel is over 10 m at location S, where the oldest coarse flood deposits were identified (Cross section A, Figure 6.10). The second oldest unit (T3) is

also evident upstream of the bridge, but is also preserved on the left hand side 400 m downstream (location K) and stands 7 m above the channel (Figure 6.9). Both T3 and T4 surfaces show degradation in the downstream direction. Some soil development is also evident on these two terraces. The most extensive terrace surface is T2 which can be seen along the whole length of the study reach downstream of the bridge on both sides of the valley floor. The unit surface is no higher than 5 m above the channel bed. The lowest and youngest terrace (T1) is composed of mainly mid channel islands, with several localised areas of aggradation on both the right (e.g. P,Q) and left (e.g. J) banks (Figure 6.9). The elevation of this surface is 1-3 metres above the present river bed. Table 6.3 summarizes the four units in terms of minimum and maximum terrace heights, sedimentation style and the vegetation cover, in addition to the characteristics of the coarse flood deposits on the unit surfaces.

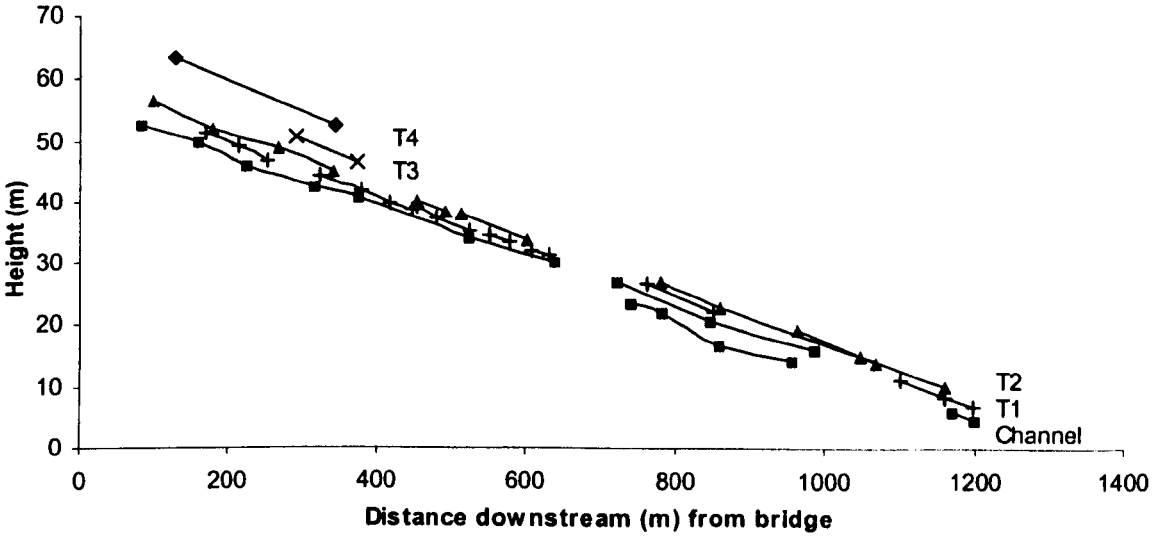

Figure 6.8 Longitudinal profiles of the four terraces along the Figarella river, downstream of the bridge marked on Figure 6.9.

Table 6.3 Characteristics of the alluvial terraces and the overlying coarse flood deposits within the Figarella study reach.

Terrace surface	Min./max. elevations (m) above modern channel bed	Sedimentological features of unit (exposed sections) and interpretation	Vegetation cover	Coarse flood deposit features [a]
T1	1.55 - 3.56	Clast supported, weak imbrication. Boulders irregular in size (>20<100 cm). Fines washed in.	Maquis Scattered bushes/trees.	Boulder splays and bars (broad features and low surface relief) and weakly imbricated.
T2	2.42 - 6.13	Unsorted, unstratified, clusters of clast supported and matrix supported (sandy gravel) sediment. Large clast size range (pebbles, cobbles and boulders up to 200 cm). Hyperconcentrated flow deposition alluvium?	Dense maquis Shrubs (0.5-1 m height) such as alder (*Alnus cordata*) and scattered Corsican pine (*Pinus nigra larcio*).	Essentially boulder bars. Material fining downstream, sandy matrix.
T3	4.86 – 10.7	Clast supported, weak imbrication. Boulder size <1.2 m and sandy matrix.	Shrubs (>2 m) dominate, densley packed, no undergrowth. Tall pine trees.	Boulder bars and boulder berms, aligned parallel to flow direction, over 1m thick, moderately well imbricated.
T4	7.88 – 9.66	Clast supported material, less size variation than T2 and T3 (~ 70% 40-90 cm) and comprises of less sand and gravel.	Dense vegetation consisting of deciduous and evergreen bushes and trees. Impassable.	Boulder berms evident on very degraded terrace surfaces and well developed soil.

[a] after Macklin *et al.*, 1992

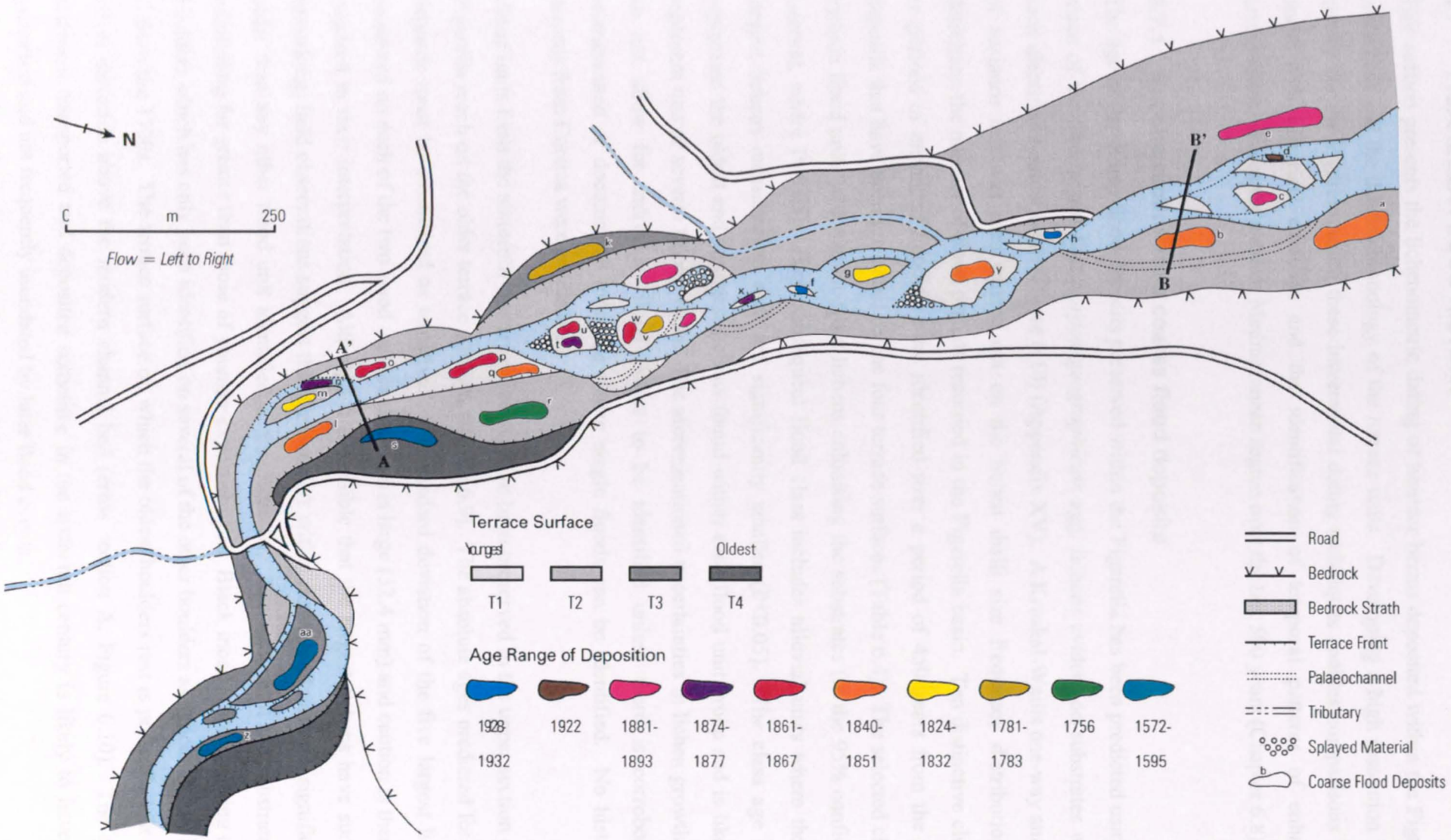

Figure 6.9 Geomorphological map of the Figarella study reach illustrating the terrace surfaces and the location and age of the coarse flood deposits.

6.7 FIGARELLA FLOOD HISTORY

This section presents the lichenometric dating of boulder berms deposited within the Figarella catchment and the dendrochronology of the terrace units. Developing a high resolution flood history for the Figarella using these incremental dating techniques enables comparisons to be made with historical evidence and the identification of temporal patterns of enhanced precipitation across the western Mediterranean region over the last 500 years (Chapter 6.8).

6.7.1 Reconstruction from coarse flood deposits

The age of the coarse flood deposits preserved within the Figarella has been predicted using the mean of the five largest *Rhizocarpon geographicum* agg. lichens evident on substrates within each identified boulder berm (Figure 6.10) (Appendix XV). A Kruskal-Wallis one-way analysis of variance test was then carried out on the lichen thalli size frequency distributions to determine the number of flood periods recorded in the Figarella basin. Ten distinctive clusters or periods of enhanced flooding were identified over a period of 450 years from the flood deposits that have been preserved on the four terrace surfaces (Table 6.4). The selected classes include flood units with similar-sized lichens colonising the substrates (to the 95% confidence interval, where $P>0.05$). Each subsequent flood class includes alluvial units where the five largest lichens measured on each are significantly smaller ($P<0.05$). The class age range represents the oldest and youngest lichens found within each flood unit group and is likely to represent one or several flood events. The aforementioned uncertainties in lichen growth rates do not allow for individual flood events to be identified unless there is corroborative instrumented or documented evidence where single floods can be identified. No historical records from Corsica were accessible.

Flood units from the sixteenth century (class A) have been preserved in the upper section of the Figarella reach on the older terrace surfaces (Figure 6.9). The absolute ages predicted for these deposits must be considered as tentative. The standard deviation of the five largest lichens measured on each of the two flood units in this class is large (32.4 mm) and caution is therefore required in their interpretation. Although it is possible that the largest lichens have survived reworking, field observations suggest that the boulders within these flood units are significantly older than any other flood unit identified in the Figarella. The surface of the substrates are exfoliating far greater than those of younger exposure ages. Black moss is also growing on the boulders which has only been identified on several of the other boulders assigned to class B and C from the 1700s. The terrace surface on which the oldest boulders rest is presently just under 10 m elevation above the modern channel bed (cross section A, Figure 6.10). The coarse sediment transported and deposited sometime in the sixteenth century is likely to have been preserved and not frequently inundated by later flood events.

Table 6.4 Flood unit age classes based upon lichen thalli size and determined to the 95% confidence interval ($P \leq 0.05$) by the Kruskal-Wallis test.

Age class	Number of flood units per class	Mean thalli size and standard deviation (mm)	Class age range	Class P value (P>0.05)	Comparison with subsequent class (P<0.05)
A	2	114.5 32.4	1572-1595	0.209	(A-B) 0.002
B	1	66.8 4.76	1756	-	(B-C) 0.019
C	2	61.3 2.50	1781-1783	0.672	(C-D) 0.000
D	2	48.9 4.23	1824-1832	0.525	(D-E) 0.020
E	5	44.4 4.31	1840-1851	0.865	(E-F) 0.000
F	4	39.1 3.26	1861-1867	0.620	(F-G) 0.002
G	3	36.2 1.66	1874-1877	0.120	(G-H) 0.005
H	4	33.5 4.27	1881-1893	0.282	(H-I) 0.001
I	1	23.8 0.84	1922	-	(I-J) 0.009
J	2	21.6 1.26	1928-1932	0.107	-

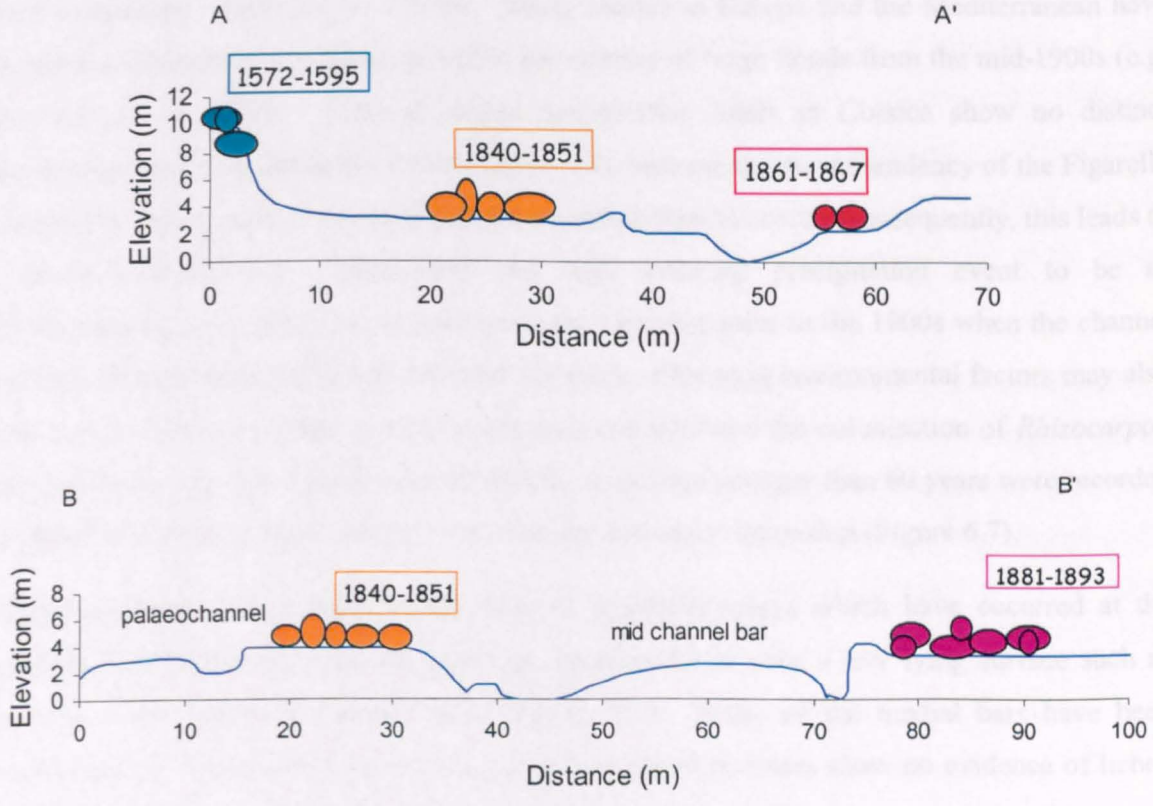

Figure 6.10 Cross sections A and B (refer to Figure 6.9) showing age of coarse flood deposits and height above the modern channel.

There are no flood units preserved in the Figarella dating from the seventeenth century, and only three identified from the mid to late eighteenth century. The majority of the flood units (18 in total) recognised in the Figarella system were deposited during the nineteenth century and occupy much of the middle to lower sections of the study reach (Figure 6.9) as shown in cross section B (Figure 6.10). The age of these flood deposits reflects either a reduction in sediment supply during the 1600s and early 1700s and an increase towards the end of the century and into

the 1800s, or a change in precipitation regime and flood magnitude. Alternatively, field evidence for flood events prior to the 1800s may have been destroyed by subsequent floods. The oldest floods (Classes A-C) may have only been preserved due to significant subsequent incision in the upper sections. The surface of terrace T4 lies up to 10 m above the modern Figarella channel.

Interestingly, within the Figarella there are also only three flood units identified from the twentieth century (Table 6.4). This most recent flood class in which lichens colonise the boulder surfaces is dated between 1928-1932. No other coarse alluvial material where lichens showed the exposure age to be less than 60 years was found in the study reach, which could be the result of a reduction in sediment supply. Although there appears to be abundant material within the channel and banks for reworking in the study reach, this is less likely to be the case further upstream where the channel is narrower and constrained by bedrock. A decrease in flood magnitude could also be a factor. Many studies in Europe and the Mediterranean have recorded a decrease in precipitation and in the number of large floods from the mid-1900s (e.g. Piervitali *et al.*, 1999). Even if annual precipitation totals in Corsica show no distinct decreasing trend throughout the 1900s (Figure 6.4), because the recent tendency of the Figarella has been to incise, there is less potential for overbank flow to occur. Consequently, this leads to a lower potential for a prolonged and high intensity precipitation event to be as 'geomorphologically effective' as perhaps in the centuries prior to the 1900s when the channel was less entrenched and allowed overbank flooding. Changing environmental factors may also have had an effect on lichen growth in the area and inhibited the colonisation of *Rhizocarpon geographicum agg.* but this considered unlikely as lichens younger than 60 years were recorded on dated substrates in the vicinity to construct the size-age relationship (Figure 6.7).

Recent aggradation is evident in the form of overbank splays which have occurred at the upstream end of the mid channel bars (e.g. location Y) or over a low lying surface such as location J mid reach on the left bank (Figure 6.9). Many of the medial bars have been overtopped by floods relatively recently as the deposited boulders show no evidence of lichen colonisation. It is not apparent whether the splays are the result of normal seasonal flow or a large flood event. The boulders are less than 0.4 m in diameter, considerably smaller than the boulders which were deposited in the eighteenth and nineteenth centuries (*ca.* 1-2 m).

6.7.2 Establishing minimum age estimates of the flood units using dendrochronology

There were few suitable trees to core on the identified terrace surfaces in the vicinity of the coarse flood deposits. Table 6.5 shows the age of the largest tree presently colonising the same surface near to the coarse flood deposits located in the study reach.

Table 6.5 Minimum age estimates for each of the identified units established from cores of the largest trees. The number of tree rings correspond to the age of the tree; this minimum age is compared to those determined by lichenometry for the boulder berm.

Flood group (Table 6.4)	Terrace Surface (Figure 6.8)	Location (Figure 6.9)	Age (RZ lichenometry)	Tree Core No.	Minimum Age (years)
		Splay	-	TC10	10
A	T1	f	56	TC6	12
A	T1	h	72	TC7	27
C	T2	e	107	TC5	84
E	T1	p	133	TC2	48
F	T1	q	149	TC3	96
F	T2	b	157	TC8	100
J	T3	aa	227	TC12	121
J	T3	z	405	TC11	174

The age estimates established by counting the tree rings provide a minimum age for the surface and in all cases provide a significantly younger age than those determined using lichenometric dating. This difference is likely to be the lag time associated with the deposition of fines within the coarse sediment in order for the trees to colonise (Chapter 6.5.3). Regeneration of trees from the intermittent bush fires in the area could also partly explain the very young minimum age compared to the lichenometric date. Corsica is prone to fires, especially in late summer when the maquis is very dry. There is significant evidence of fire damage along the Figarella valley floor. There is also evidence of tree felling which may account for some of the young ages.

Nonetheless, the relative ages of the units can be broadly distinguished using dendrochronology. The pine trees growing on the youngest identified unit (T1) may be much younger than the actual age unit due to the greater potential of flood waters to uproot the trees due to their small size and low elevation above the present channel. There were many log jams evident in the Figarella. The cored trees on the higher surfaces (T2-T4) are established on more stable surfaces because they are older and have had a greater time to develop.

6.8 CLIMATIC OSCILLATIONS AND FLOOD EVENTS EXPERIENCED IN THE MEDITERRANEAN OVER THE LAST 500 YEARS

The paucity of climate data for Corsica (Chapters 6.4.2 & 6.5.4) does not allow for the direct assessment of the Figarella river response to climatic change. It is valuable, however, to establish whether there are common flood periods identified in other parts of the western Mediterranean region with those deduced by lichenometry in the Figarella (Table 6.4). Other Mediterranean flood records, whether empirically-based (e.g. Maas, 1998; Hamlin, 2000), constructed using historical sources (e.g. Barriendos-Vallve & Martin-Vide, 1998) or instrumental (e.g. Benito *et al.*, 1996) can also be used to appraise the synchrony of such fluvial activity across the Mediterranean region.

Benito *et al.* (1996) have ascertained from secondary sources and continuous precipitation records that flooding was prevalent throughout the Iberian Peninsula during the second half of the nineteenth century. These authors report that there was persistent precipitation over most of the peninsula during the late nineteenth century. The River Ebro experienced severe flooding between 1850 and 1910 (Benito *et al.*, 1996), with five cases between 1888 and 1895 (Gellatly *et al.*, 1995). This flooding interval is broadly in line with the climatic oscillation identified between 1830 and 1870 through the reconstruction of catastrophic floods on the Spanish Mediterranean coastal area by Barriendos-Vallve and Martin-Vide (1998) (Figure 6.11). This period was one of three climatic oscillations recognised during the LIA 1450-1850 (Chapter 2.4.4.1). Other distinctive hydroclimatic fluctuations were established during the periods 1760-1800 and 1570-1630. These periods closely correspond to the age ranges established using lichenometry for the deposition of the coarse flood material in the Figarella system over the past 500 years (Table 6.6).

Similar intervals of enhanced flood magnitude across the Mediterranean region are displayed in Figure 6.12. There appears to be synchrony in the timing of flood events during the late eighteenth century, particularly in the western Mediterranean region. Benito *et al.*, (1996) comment on the occurrence of large floods on rivers within the Iberian Peninsula during 1770-1790. This phase correlates well with the climatic oscillation maxima 1772-1797 identified by Barriendos-Vallve & Martin-Vide (1998) in the same region. Arnaud-Fassetta & Provansal (1999) report on the high discharges recorded on the River Rhone, southern France during the seventeenth and eighteenth century and discuss the rapid and constant adjustment of the fluvial system. It is likely that the unstable climate during the LIA may have had a strong influence on the hydrological and geomorphological river activity. Palaeoenvironmental data and historical documents from Europe and the Mediterranean confirm that the climate was variable during the LIA and that conditions were especially cold and wet during the second half of the 1700s (Manley 1974; Pfister, 1988, 1995; Jones & Bradley, 1995). Sea storms in the Adriatic were also prominent during the late 1700s (Camuffo *et al.*, 2000) and increased flood frequency in Venice (Camuffo & Enzi, 1995). Extreme floods were also identified by lichenometric dating of coarse flood deposits in the Voidomatis and Aoos basin in Northwest Greece between 1780-1800 (Hamlin, 2000). Rumsby and Macklin (1996) comment on enhanced flooding and fluvial activity throughout Europe during the second half of the eighteenth century and the nineteenth century.

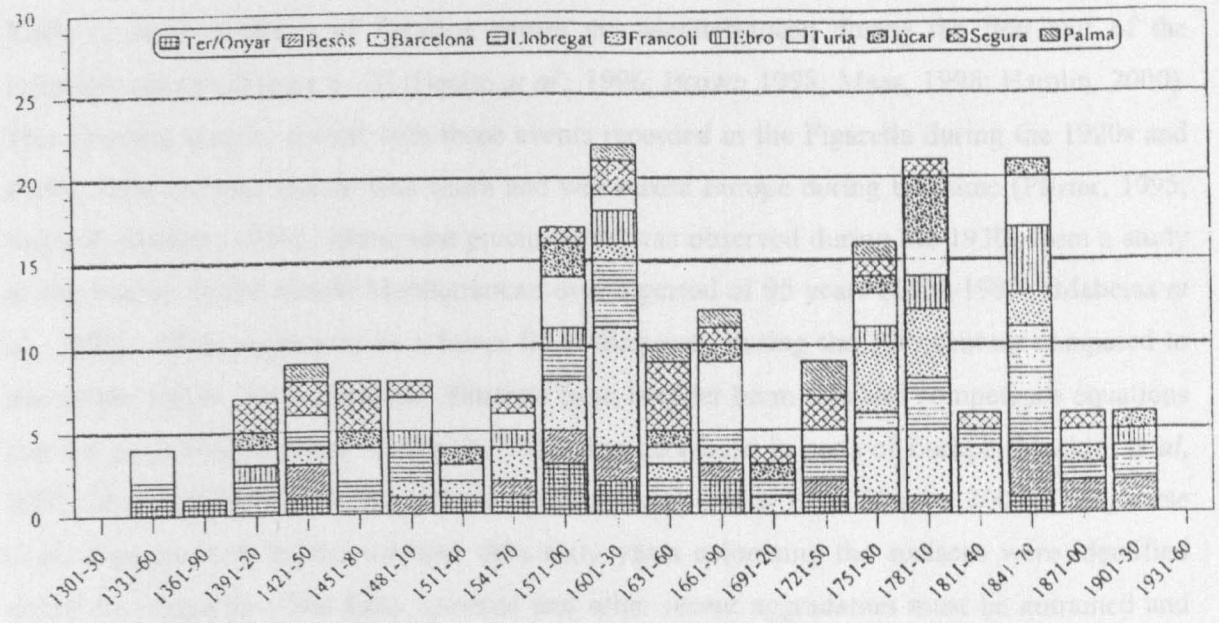

Figure 6.11 The number of catastrophic floods identified along ten rivers on the Spanish Mediterranean coast in 30 year periods (Barriendos-Vallve & Martin-Vide, 1998).

Table 6.6 Climatic oscillation intervals identified in Spain during the Little Ice Age compared to the age range of the lichenometric dated coarse flood deposits in the Figarella, northwest Corsica.

Northwest Corsica Figarella system age classes	Northwest Corsica Figarella system age ranges of coarse flood deposits	Iberian Peninsula Climatic oscillation intervals Barriendos-Vallve and Martin-Vide (1998)
A	1572-1595	1570-1630 (maxima 1588-1596)
B,C	1756-1783	1760-1800 (maxima 1772-1797)
D-H	1824-1893	1830-1870 (maxima 1848-1868)
I,J	1922-1932	

Nineteenth century climate was characterized by a cold-warm-cold oscillation and annual precipitation totals were high, especially in the Mediterranean during the 1830s, and between 1850-1880 (Jones & Bradley, 1995; Serre-Bachet, 1995) (Table 6.7). It is evident from Figure 6.12 that there was widespread flooding during the 1800s. Barriendos-Vallve and Martin-Vide (1998) comment on the catastrophic flooding experienced along nine rivers along the east coast of Spain during 1830 and 1870. The timing of flood events along the Figarella also correspond to those noted in Spain (Benito *et al.*, 1996; Barriendos-Vallve and Martin-Vide, 1998) and the climatic interpretations noted across Europe (Table 6.7). Coarse flood deposit age classes of 1824-1843 and 1846-1893 were identified along the Figarella study reach. These dates are inline with the nineteenth century flood events identified in northern Greece in the 1830s, 1850s and 1880s (Hamlin, 2000) and in Crete between 1847-1857 and 1877-87 (Maas, 1998). With regards to the western Mediterranean, Figure 6.13 displays clearly the increased precipitation received during the last two decades of the 1800s.

There is some evidence of flooding across the Mediterranean during the first half of the twentieth century (Figure 6.12) (Benito *et al.*, 1996; Brown 1998; Maas, 1998; Hamlin, 2000). This flooding may be coeval with those events recorded in the Figarella during the 1920s and 1930s. The climatic regime was warm and wet across Europe during this time (Pfister, 1995; Jones & Bradley, 1995). Maximum precipitation was observed during the 1930s from a study of ten stations in the central Mediterranean over a period of 95 years (1894-1988) (Maheras *et al.*, 1992). There appears to be a lower flood frequency during the 20th century compared to that of the 1800s. Several authors illustrate from boulder berm size and competence equations that the magnitude of floods during the 1900s has decreased in parts of Europe (Macklin *et al*, 1992; Merret & Macklin 1998) and the Mediterranean (Maas 1998, Hamlin 2000). No coarse flood deposits with lichens younger than sixty years colonising the surfaces were identified within the Figarella. The splay material and other recent aggradation must be entrained and transported downstream too frequently for lichens to colonise the surfaces.

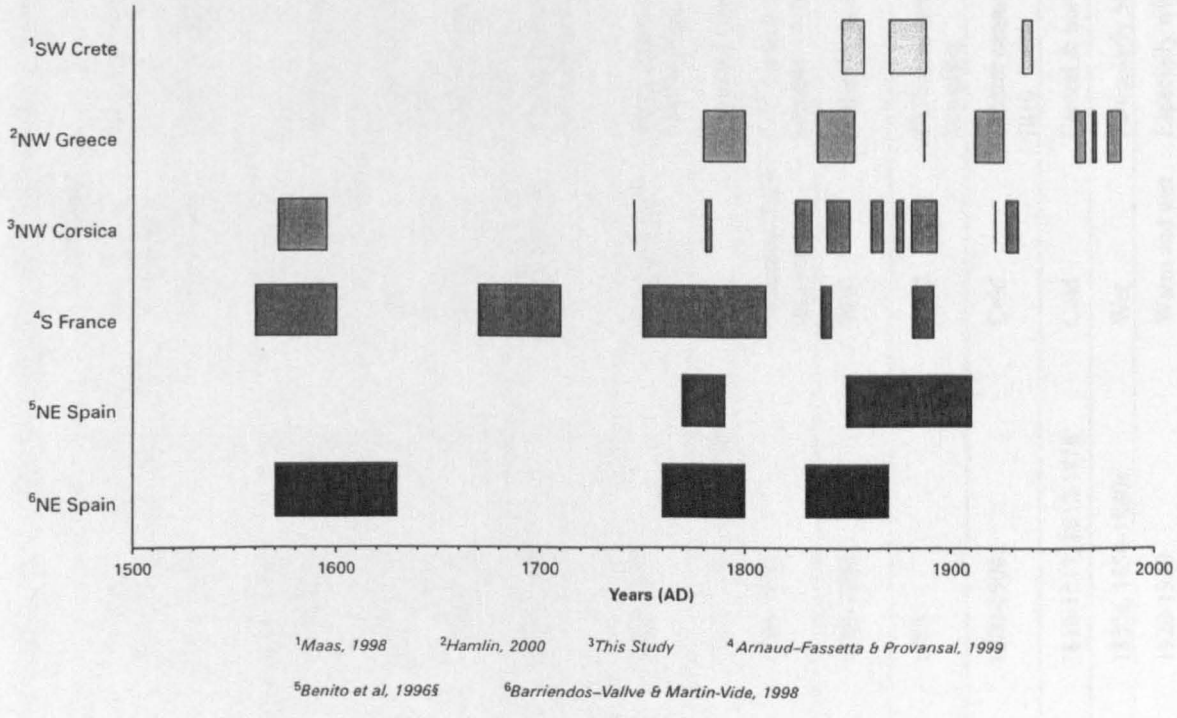

Figure 6.12 Periods of enhanced flooding identified across the Mediterranean basin.

Table 6.7 Palaeoenvironmental data from various parts of the Mediterranean and Europe for the last 500 years

Location	Climate Source/Proxy	Date	Conditions	Comment	Reference
C Europe	Phenological data	1555, 1573, 1627, 1628, 1642, 1675, 1698, 1740, 1816, 1879	Cold summer temperatures	Extreme delays in vine flowering & wine harvest	Pfister (1995)
C Europe	Historical documents	1570-1600	Cold and wet	Summer temperatures decreased 0.8°C, 20% wetter	Pfister (1995) Pfister (1988)
C Europe	Dendrochronology	1570-1600	Cold and wet		Briffa *et al.*, (1999)
N Italy SW Europe	Historical documents Dendrochronology	1570-1614	Cold	Increased frequency of severe winters	Camuffo & Enzi (1995); Serre-Bachet *et al.*, (1995)
C Europe	Historical documents	1565-1600	Wet	Fourfold increase in flooding compared to *ca.* 1530-1565	Pfister (1995)
Alps	Glacier fluctuations	1570-1600	Cold	Glaciers advanced several hundred meters. Cold summers	Pfister (1988, 1995); Holzhauser & Zumbühl (1999)
C Europe N Italy SW Europe	Historical documents	1600-1690	Warm and dry	Wetter summers 1600-1630, 1670s, 1685-1699, although temperatures similar to 20°C	Pfister (1995); Camuffo & Enzi (1995); Serre-Bachet *et al.*, (1995)
C Europe	Historical documents	1690-1699	Cold and wet	Mean annual temperatures 1°C lower than 1901-1960 average.	Pfister (1988, 1995)
C England	Historical documents	1690-1705, 1745-1790		Increased snowfall	Manley (1974)
Italy	Sea flooding	1740-1800	Increased flood frequency	0.35 per year respectively compared to <0.1 per year between 1540-1740	Camuffo & Enzi (1995)
C Europe	Historical documents Instrumented data	1760-1790	Wet	Persisting warmth from 1700	Pfister (1995); Jones & Bradley (1995)
C Europe	Phenological data	1785	Cold	8°C below average. Extreme delays in cherry flowering	Pfister (1995)
C Europe	Instrumented data	1800-1900	Cold	Coldest century since 1500, all seasons, esp. 1800-1810	Pfister (1988, 1995)
SW Europe	Instrumented data	1810-1817, 1832-1838	Cold	Central & northern Europe	Serre-Bachet *et al.*,(1995)
Europe	Instrumented data	1830s, 1850-1880s	Wet	Particularly Mediterranean regions	Jones & Bradley, 1995
Europe	Instrumented data	1920-1930	Warm and wet	Especially winter	Pfister (1995); Jones & Bradley (1995)

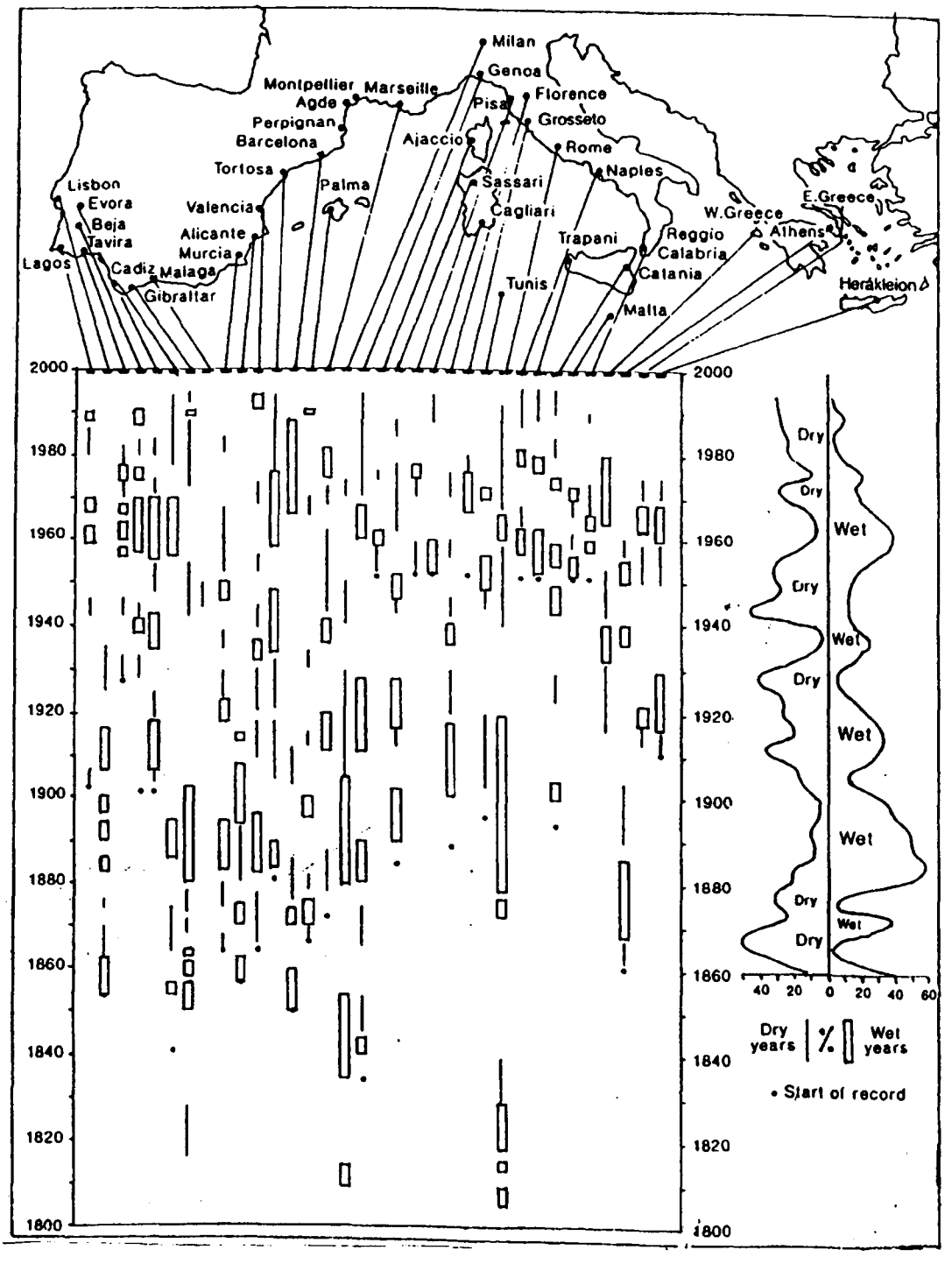

Figure 6.13 Runs of wetter-than-average and drier-than-average years at individual stations. The graph at the right gives a general percentage of the number of stations experiencing wet and dry periods over southern Europe as a whole (from Grove & Rackham, 2001).

6.9 THE INFLUENCE OF THE NORTH ATLANTIC OSCILLATION ON MEDITERRANEAN FLOOD FREQUENCY

It has been argued that the LIA is the latest expression of a millennial-scale climate cycle lasting approximately 1,500 years based on studies of ice-rafted debris in northern Atlantic sediments (Bond *et al.*, 1997) (Chapter 2.3). Changes in the North Atlantic thermohaline circulation are thought to have been the driving mechanism of the LIA and other climatic phases of similar amplitude (1,500 years), such as the cold period experienced in the thirteenth century and the Medieval Warm Period. Various proxy data time series (e.g. Stuiver, 1980; Briffa *et al.*, 1990) and numerical simulation models (e.g. Manabe & Stouffer, 1988; Stocker & Mysak, 1992) have led to the belief that decadal- and century-scale climate variations may well also be the manifestation of natural variability within the coupled-atmosphere-ocean system. Again, the North Atlantic ocean plays an extremely important role by instigating the NAO atmospheric circulation pattern which is believed to have a very strong influence on European and Mediterranean climate (Hurrell 1995, 1996, 2001; Hurrell & van Loon, 1997) (Chapter 6.4.3).

This section investigates the relationship between flood frequency in Corsica and other parts of the western Mediterranean with the NAO index (Section 6.4.3). The resolution of the NAO and available climate records (Chapter 6.5.4) together with the Figarella flood history allows such climate and river behaviour associations to be examined in detail. The extent to which the NAO may be a forcing mechanism of heavy precipitation events and flooding episodes in Corsica and other western Mediterranean regions is explored (Chapter 6.9.1) in addition to the longer term (>150 year) NAO influence on Mediterranean climate. Extended NAO reconstructions back to the sixteenth century can be broadly compared to Figarella flood history (Chapter 6.9.2).

6.9.1 Decadal scale NAO and precipitation in Corsica

Periods of low precipitation across the Mediterranean basin can be attributed partly to high NAO index values when strong westerly winds take storms across central and northern Europe. Conversely, intervals of high precipitation can be partly attributed to negative NAO index values. The winter NAO (December to March) exerts the strongest influence on surface climate in Europe and the Mediterranean region (Hurrell, 1995; Osborn *et al.*, 1999; Jones *et al.*, 2001) and is often used to evaluate the strength of the teleconnection to non-seasonal and inter- and multi-annual precipitation variability (Hurrell, 1995; Piervitali *et al.*, 1997; Qian *et al.*, 2000; Quadrelli *et al.*, 2001) (Figure 6.14).

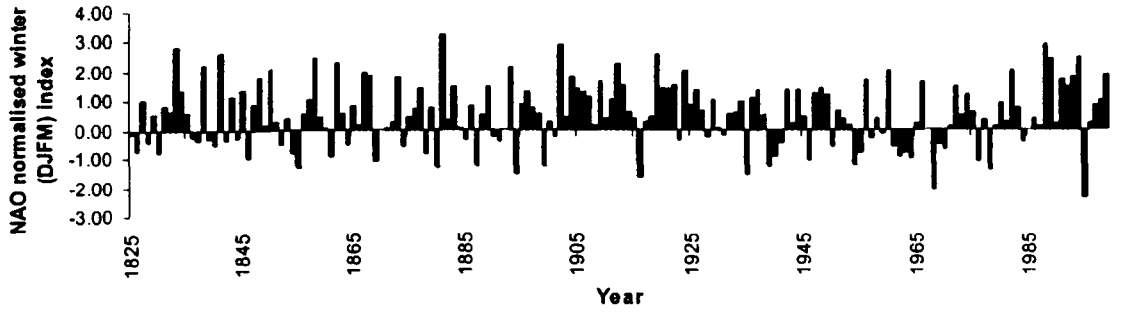

Figure 6.14 North Atlantic Oscillation normalised winter index (1824-1999) (Data from Climatic Research Unit, University of East Anglia).

Ajaccio is the capital of Corsica and is located on the west coast of the island (Figure 6.1). Winter rainfall may be influenced in part by the NAO. There is a weak, but significant relationship between winter rainfall and the corresponding NAO value ($r^2$of 0.23) over a period of 132 years from 1856 to 1988 (Figure 6.15). This illustrates that the NAO has an influence on precipitation totals, but it may not be the only forcing factor responsible for non-seasonal rainfall variation. Hurrell (1995) reports a -0.48 correlation coefficient (to the 99 % confidence level) between total winter precipitation and the NAO index over 42 years in Ajaccio.

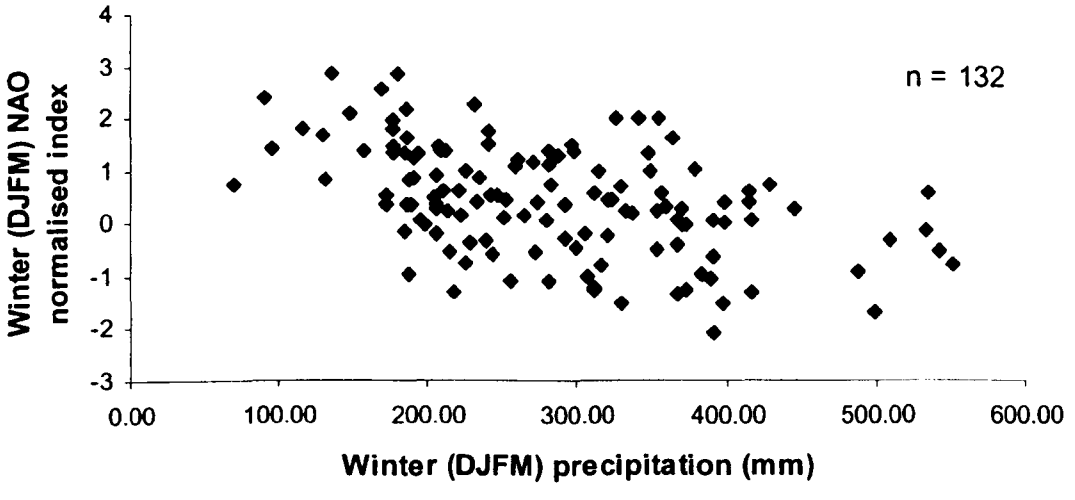

Figure 6.15 The relationship between mean winter (December to March) precipitation in Ajaccio and mean winter NAO index values 1956-1988.

Increased precipitation in winter (December to March) during strong (>2) negative NAO indices in comparison to strong positive NAO index values is clearly evident in Ajaccio (Table 6.8, Figure 6.16). Mean winter precipitation totals between 1860 and 1980 during strong negative winter NAO show on average a 278% increase in precipitation compared to winters characterized by a strong positive NAO.

There are three decades (1900s-1920s) which show a greater percentage of winter rainfall during strong positive NAO events compared to negative events (Figure 6.16). The winter and annual precipitation totals for these three decades were above average but it can be seen from Figure 6.14 that the thirty years from 1900 were dominated by positive NAO index values, with only four years having negative NAO index values in total and 3 winters from 1900-1929 having an average NAO of less than –0.4. The persistence of a high NAO over winters during the first three decades of the twentieth century was caused by anomalously low seasonal pressures in the region of the Icelandic low and higher than normal pressures at lower latitudes. This high NAO resulted in warmer than average winter conditions over much of Europe (Hurrell, 1995), although the winter precipitation totals in Ajaccio between 1900 and 1930 were not below the mean (Table 6.8).

The last 25 years has also been dominated by a strongly positive NAO, and it is well documented that the western-central Mediterranean region has experienced warmer conditions and has received less winter rain (Palutikof *et al.*, 1996; Piervitali *et al.*, 1998; Buffoni *et al.*, 1999; Brunetti *et al.*, 2000; 2001; Quadrelli *et al.*, 2001). However, precipitation intensity in the Mediterranean region has been shown to have increased over the last few decades (Brunetti *et al.*, 2001), although an observed decline in the intensity of Mediterranean cyclones is thought to be slowing down (Trigo *et al.*, 2000). This trend is consistent with the atmospheric circulation where an increase in the westerlies has resulted in the addiction of warm and moist air over large areas of central and northern Europe (Hurrell, 1995, 1996; Jones *et al.*, 1997) and more frequent and persistent subtropical anticyclones over the Mediterranean during the cold season (Piervitali *et al.*, 1997; Schönwiese & Rapp, 1997; Rodwell *et al.*, 1999).

Table 6.8 Differences in mean precipitation totals between winter months (D,J,F,M) characterised by a strong positive (>2.0) and a strong negative (>-2) North Atlantic Oscillation. Values in bold indicate that greater amounts of precipitation than on average fell during months with a strong negative NAO.

Decade	Number of winters with a strong positive NAO	Mean winter precipitation (mm)	Percentage of total winter precipitation (%) (A)	Number of winters with a strong negative NAO	Mean winter precipitation (mm)	Percentage of total winter precipitation (%) (B)	Percentage differences in mean precipitation (%) (A-B)
1860	13	25.8	14.1	4	110.5	18.6	**4.5**
1870	3	45.3	5.2	5	101.2	19.2	**14.0**
1880	5	47.4	15.2	3	123.6	23.8	**8.6**
1890	9	30.7	10.1	6	88.8	19.5	**9.4**
1900	6	73.7	14.6	4	97.7	12.9	1.7
1910	12	46.9	19.7	3	98.0	10.3	9.4
1920	13	67.4	26.3	2	127.5	7.6	18.6
1930	8	39.0	10.5	4	90.0	12.1	**1.6**
1940	6	16.5	3.6	5	114.6	21.1	**17.4**
1950	4	46.7	6.2	4	82.0	10.9	**4.7**
1960	5	18.3	3.2	5	76.8	13.3	**10.2**
1970	6	43.6	8.8	4	86.8	11.7	**2.9**
1980	9	60.0	21.0	6	94.6	22.1	**1.1**

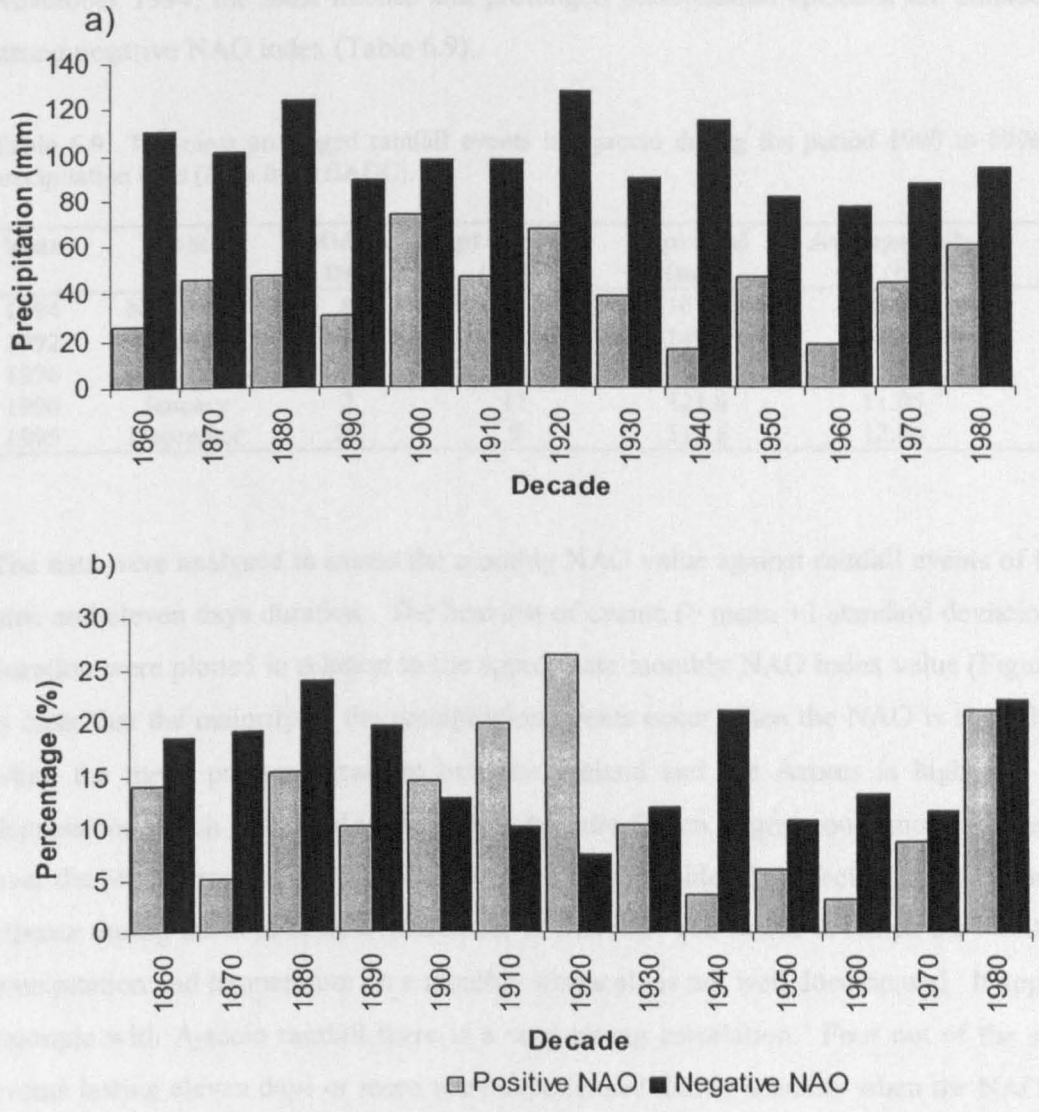

Figure 6.16 Mean (a) and percentage (b) of winter precipitation during strong (+/- 2) NAO positive and negative NAO indices.

6.9.2 Annual scale NAO and precipitation in Corsica

Corsica and many other parts of the Mediterranean experienced prolonged and intense precipitation leading to catastrophic flooding during the early 1990s. Daily precipitation in Ajaccio between 1990 and 1996 (BADC) was analysed to establish the top five storms in order of precipitation totals (Table 6.9). The rainfall event which occurred in early November 1994 has already been briefly described (Chapter 6.4.2 and 6.4.3), when a total of 161 mm of rain fell within 7 days. Heavy precipitation events in the western Mediterranean such as this event have been used in many numerical simulation models to help understand the causes and dynamics of such precipitation events. Such studies have also attempted to evaluate the influence exerted on flooding by the orography, the Mediterranean Sea and atmospheric circulation patterns such as the North Atlantic Oscillation (Ramis *et al,* 1994; Jansa *et al.*, 1995; Doswell *et al.*, 1998). The complexity of the Mediterranean basin in terms of topography and ocean-atmospheric interactions is strongly emphasized. It is interesting to note however that with the exception of

November 1994, the most intense and prolonged precipitation episodes are connected with a strong negative NAO index (Table 6.9).

Table 6.9 The most prolonged rainfall events in Ajaccio during the period 1990 to 1996 in term of precipitation total (Data from BADC).

Year	Month	Middle Day	Ppt duration (days)	Ppt total (mm)	Average daily ppt (mm)	Monthly NAO value
1994	November	8	7	161.2	23.03	1.68
1992	October	8	11	149.6	13.60	-3.33
1996	November	22	9	123.8	13.76	-0.05
1996	January	2	11	121.6	11.05	-3.27
1995	December	29	9	116.6	12.96	-3.33

The data were analysed to assess the monthly NAO value against rainfall events of five, seven, nine and eleven days duration. The heaviest of events (> mean +1 standard deviation) for each duration were plotted in relation to the appropriate monthly NAO index value (Figure 6.17). It is clear that the majority of the precipitation events occur when the NAO is strongly negative, when the mean pressure gradient between Iceland and the Azores is high and the frontal depressions which generated in the North Atlantic Ocean migrate on a more southerly latitude over the Mediterranean region. Many studies only consider the effect of the NAO on European climate during the cold season (December to March). The extent to which the NAO influences precipitation and temperature on a monthly timescale is not well documented. It appears in this example with Ajaccio rainfall there is a very strong correlation. Four out of the seven storm events lasting eleven days or more were experienced during a month when the NAO index was –3 or lower. One event was recorded in December 1996 when the monthly NAO was –4.7. Out of the seven storm events, two occurred in October, two in December, and one each in November, January and April.

Flooding is also likely to be the result of intense and short duration precipitation events. There were 43 days during the years 1990 to 1996 in Ajaccio when the precipitation total exceeded 30 mm. For example, on 6 November 1993, 71 mm of rain fell during the day. Such intense rainfall events can be just as catastrophic (or more so) than those prolonged rainfall events. Steepland mountain systems are especially sensitive to intense rainfall, and local flash flooding is common (Kochel, 1988). Rainfall is also likely to be considerably greater in the Figarella catchment than that recorded in Ajaccio which is only 2 m above sea level. The headwater zones in Corsica receive as much as three times the rainfall as the coast regions (Figure 3.13). It is likely that these intense rainfall events encourage entrainment and deposition of sediment such as the splay material presently evident up stream of many of the mid channel bars in the Figarella study reach. This material is not colonised by lichens which suggests that it has been deposited within the last several years.

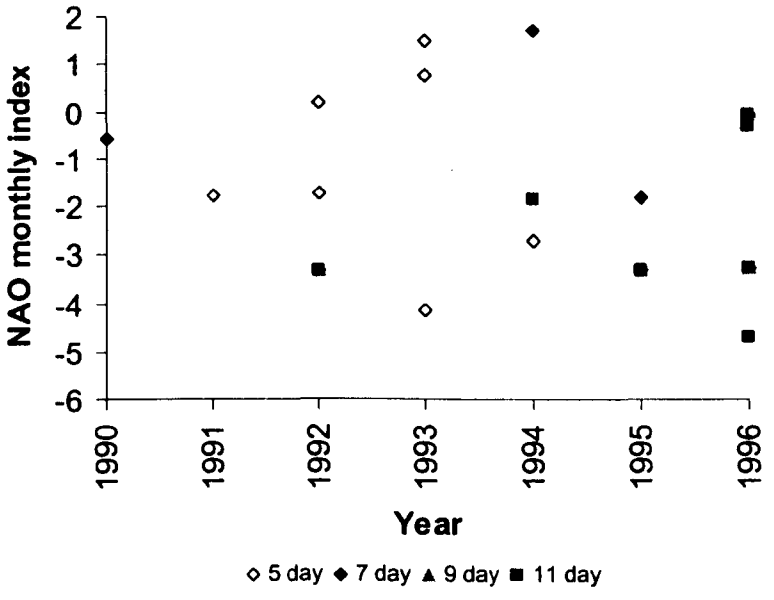

Figure 6.17 Monthly NAO indices and the heaviest rainfall events in Ajaccio (1990-1996).

6.9.3 Long term NAO and rainfall events in the western Mediterranean

From the preceding discussion it is clear that the NAO has an influence on Mediterranean precipitation. To ascertain whether there is a longer term relationship between the NAO and seasonal rainfall patterns, daily rainfall data for Barcelona between 1990 and 1985 have been analysed. A long series of daily precipitation values for Corsica is not available. On the assumption that the western Mediterranean basin is affected by the same heavy precipitation events (Figure 6.12, Figure 6.13, Appendix XVI), it is likely that the timing of many storm events in Barcelona may be similar to those experienced in Corsica and other parts of the basin. Five, seven and nine day duration rainfall events were identified in the record and were ranked in order of precipitation totals. Those events with totals above the mean plus one standard deviation were graphed on a temporal scale with the corresponding normalised winter NAO index. The timing of the rainfall events correlate well with negative phases of the winter NAO. Figure 6.18 shows the largest five day storm events during the period 1900 and 1985 and illustrates semi-quantitatively the influence the negative winter NAO may have on initiating and sustaining heavy and prolonged rainfall events (Appendix XVII).

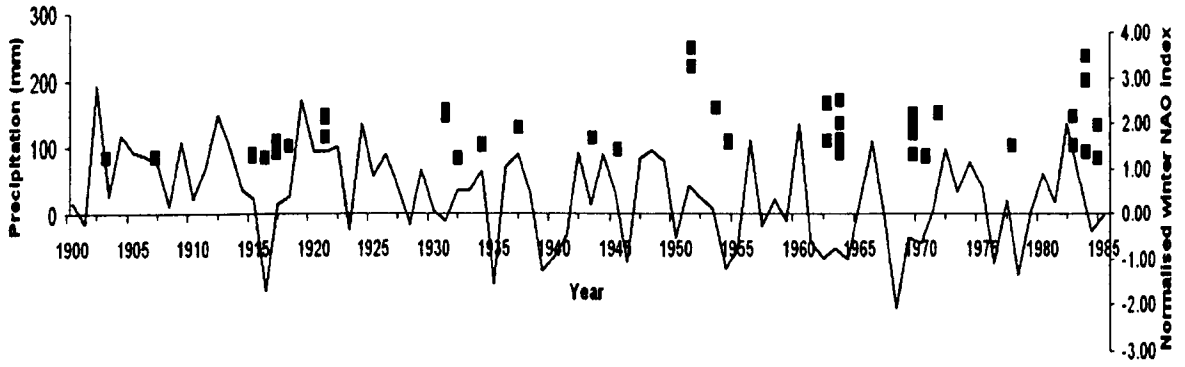

Figure 6.18 The largest (> mean + 1 standard deviation) five day storm events in Barcelona (1900-1985) (Appendix XVII) and the NAO winter index. Data provided by Burgueño (1980).

6.9.4 Extended NAO reconstructions from documentary and proxy records

The North Atlantic Oscillation is one of the major multiannual climate fluctuations in the Northern Hemisphere and clearly plays an important role in European and Mediterranean climate. As well as influencing seasonal and annual temperature and precipitation fluctuations (Chapter 6.8.2 and 6.8.3), the NAO is also believed to be an important source of decadal-scale climate fluctuations (Rogers, 1984, 1990; Moses *et al.*, 1987; Hurrell, 1995, 1996; Hurrell and van Loon, 1997). In order to provide more reliable information about the NAO variability and identify the dominant time scales associated with this climatic oscillation, a longer time series is necessary. Extended NAO reconstructions are also important for quantifying natural and anthropogenic changes in NAO behaviour. This change has been especially significant in the last 25 years when the strongly positive NAO - bringing warmer and drier conditions to the Mediterranean - is thought to be partly the result of human activity. By extending the series it is possible to determine past prolonged positive or negative NAO periods and evaluate the variability with respect to anthropogenically driven processes such as possible increasing greenhouse gas emissions and global warming. In this section, the extended NAO record will be used to examine the flood frequency record over the last 400 years.

Extended NAO reconstructions have been conducted using a variety of documentary and natural proxy records. Historical sources (e.g. Jones *et al.*, 1997; Luterbacher *et al.*, 1999), tree ring data (e.g. D'Arrigo *et al.*, 1993; Cook *et al.*, 1998) and ice core data (e.g. Barlow *et al.*, 1993; Meese *et al.*, 1994; White *et al.*, 1997; Appenzeller *et al.*, 1998) have all been employed to estimate the long term NAO. Some proxy reconstructions have proved to be more accurate than others and many of the early records are not in agreement with one another and the instrumentally-based indices (Schmutz *et al.*, 2000). One explanation for this inconsistency may be that the variance in common between the northern hemisphere temperature and the NAO is not always of the same magnitude (Osborn *et al.*, 1999). The natural climate proxies also record different parameters in association with the NAO. For example, ice accumulation rates reflect the variability in precipitation while tree ring widths largely represent changes in

temperature and the instrumented records document the pressure difference between the Azores high and the Icelandic low. The strength of the NAO signal received by different proxies in different locations may also vary. Calibration to the instrumented index over the last one hundred or so years and the use of multiproxy composite reconstructions of the NAO indices helps to minimise these differences (e.g. Cullen *et al.*, 2001)

The normalised proxy NAO index based on western Greenland ice accumulation rates (Appenzeller *et al.*, 1998) closely reflects the variability of the NAO established from instrumented measurements and this adds weight to the reliability of the extended series. Like many reconstructions, this proxy index is also dependent on precipitation rather than temperature and is therefore more suited to this investigation. The proxy index shows particularly low values around 1880, whereas the highest indices are recorded at 1695 (Figure 6.19). Persistently low values occur during the second half of the nineteenth century, in agreement with Cook *et al.* (1998) and Luterbacher *et al.* (1999). A prolonged phase of negative values was also identified during the last quarter of the seventeenth century which coincides with the Late Maunder Minimum (Lamb, 1977). Intervals of persistent positive NAO values include the early eighteenth and early twentieth centuries.

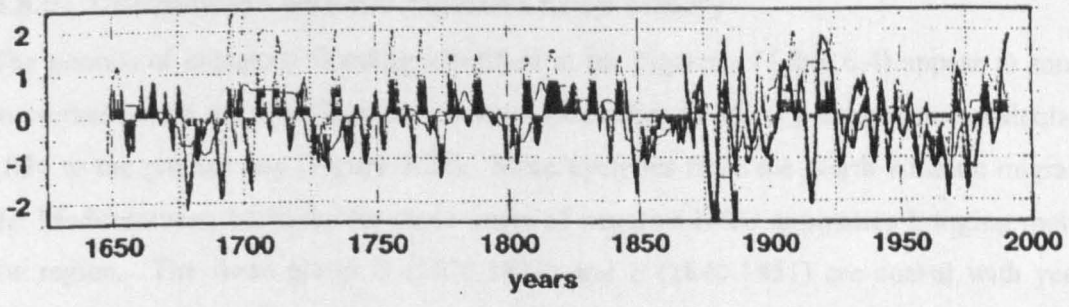

Figure 6.19 Extended reconstruction of the normalised North Atlantic Oscillation based on western Greenland ice accumulation rates (shaded) and normalised instrumental NAO index (Hurrell, 1995) (thick line) (after Appenzeller *et al.*, 1998).

The dynamics of the NAO are explored in many studies to evaluate the multiannual and century scale oscillations. Periodicities of 24, 8 and 2.1 years have been identified as long term features in the North Atlantic climate system (Cook *et al.* 1998). These oscillations are in agreement with many other studies (e.g. Folland, 1983; Ghil & Vautard, 1991; Plaut *et al.*, 1995) which have found spectral peaks of similar periodicities in temperature series, with the 8 year oscillation being the most prominent (Felis *et al.*, 2000). An oscillation of approximately 70 years is also strongly evident in the NAO record from 1850 (Appenzeller *et al.* 1998; Cook *et al.*, 1998). This oscillation corresponds to a number of independent temperature proxy analyses from the North Atlantic sector (e.g. Schlesinger & Ramankutty, 1994; Stocker & Wright, 1996; Shabalova & Weber, 1999; Felis *et al.*, 2000) and agrees well with ocean-atmospheric models (e.g. Delworth *et al.*, 1993, 1997). New multiproxy reconstructions of the NAO also indicate a prominent 70 year oscillation throughout the last three centuries (Cullen *et al.*, 2001).

Interestingly, the frequency of 5 day storm events in Barcelona, which has been shown to be in accordance with negative winter NAO phases (Figure 6.18) is approximately 8 years. This is concomitant with the oscillation periodicity identified in the proxy records described above. There are roughly ten clusters of high magnitude storm events over a period of 85 years. The storm event record is not long enough to show the 24 year cycle clearly, and is not of a sufficiently high resolution to portray the 2.1 year oscillation. There is a greater frequency of 3 day storm events which may be more likely to depict the shorter oscillation, although this cannot be as easily tested.

The NAO is also characterized by having a number of active intervals which are interspersed with passive phases (Appenzeller *et al.*, 1998). One mechanism that has been proposed to explain the NAO variability and the alternating coherent and incoherent periods is the coupled and uncoupled interaction between the atmosphere and the ocean (e.g. Latif, 1998). Although stochastic processes and variability cannot be totally excluded, if this feature of the NAO is organised, climate forecasts in the Atlantic region and Europe may be enhanced if predictability is increased during coherent active NAO phases (Griffies & Bryan, 1997).

6.9.5 Correlations with the Figarella flood history

The periods of enhanced flooding identified in the Figarella (Table 6.4) appear to some extent to coincide with the periods of low winter (December to March) index values calculated from 1824 to the present day (Figure 6.20). More cyclones from the North Atlantic migrate across the Mediterranean basin during these times of negative NAO anomalies bringing more rain to the region. The flood group D (1824-1832) and E (1840-1851) are coeval with years when alternating winter seasons of low NAO. The late nineteenth century flood groups (F,G,H) can also be broadly associated with the NAO when many of the index values were measured to be below –0.5.

It is difficult to assess the direct influence the North Atlantic atmospheric circulation exerts on the flood frequency in northwest Corsica because of the many other factors, external and inherent in the catchment, that exacerbate or alleviate flooding. It can be assumed, however, that during periods of low NAO there is greater potential for extreme rainfall events and flooding than during periods of high NAO when the storm tracks from the North Atlantic are displaced further north. No dated flood unit evident in the Figarella coincides with prolonged phases of high NAO such as those experienced between 1856-1860, 1895-1898, and for the first two decades of the twentieth century with the exception of 1901 and 1916. However, there are periods of low NAO with no evidence of large floods in the Figarella, especially in the twentieth century.

The extended NAO series (Figure 6.19) shows that the periods of lowest values are coeval with the periods of enhanced flooding in the Mediterranean such as during the latter half of the sixteenth century, and the second half of the nineteenth century. The NAO fluctuates readily from positive to negative phases and so it is quite likely that the large rainfall events transporting the large boulders in the Figarella occur during times of strong negative NAO as Figure 6.17 and Figure 6.18 indicate. It must be highlighted that the NAO is not responsible for all the floods recorded in the Mediterranean area. Large, and often catastrophic floods frequently occur in the Mediterranean due to intensive summer and autumn thunderstorm events (e.g. 21-26 October, 2000, Spain, Appendix XVI).

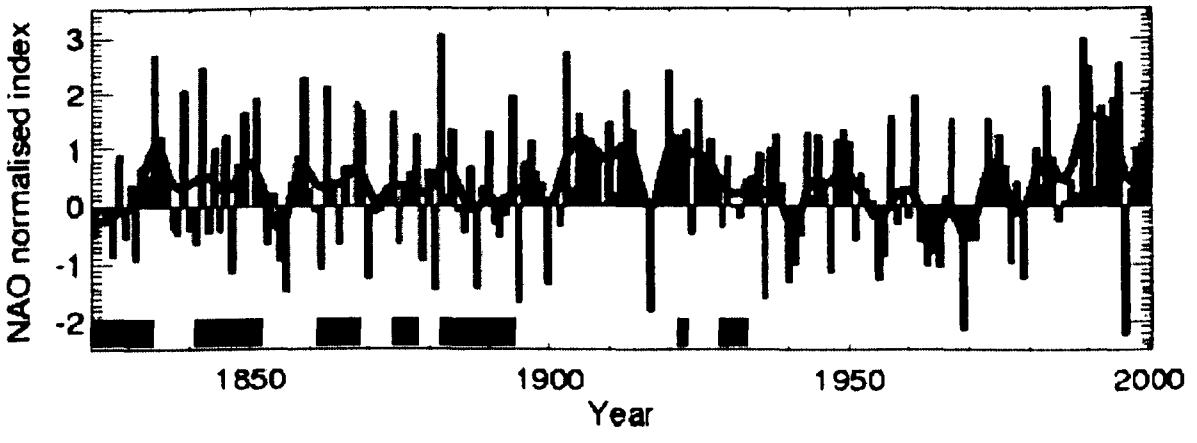

Figure 6.20 The winter NAO index and the identified Figarella flood periods (shaded regions).

6.10 RIVER BEHAVIOUR DURING THE LITTLE ICE AGE

It is difficult to assess the impacts of human activities on flood frequency, flood magnitude and sedimentation independently from the influences of climate change, but this factor needs to be addressed.

6.10.1 Anthropogenic causes

Evidence for human activities during this LIA period in Corsica is poorly documented, and possible impact from land use change is therefore not exactly known. There is evidence of human activity within the Figarella catchment but it appears to be limited, especially in the upper study reach and further upstream where the slopes are very steep. Several areas in the downstream section of the study reach have been cultivated where the slopes are more stable and soil has developed, but currently the terraces lie abandoned (Figure 3.15).

6.10.2 Hydroclimatic conditions

The coarse flood deposits evident on the terrace surfaces (which often exceed 1m in diameter) are likely to have been delivered and deposited during cooler climatic conditions. Bedrock and

hillslopes would have been more vulnerable to mechanical weathering when temperatures were lower during periods of the LIA. Vegetation cover on the slopes would have been sparser than present. An analogue for vegetation in the LIA when temperatures were on average 0.6°C lower (Grove, 1988) could be the modern day vegetation cover of the Figarella catchment slopes at an altitude ~90 m above the study reach (taking the environmental lapse rate to be 6.5°C per 1000 m). Aerial photographs and field observation show that vegetation between 385 to 450 m elevation in the study catchment is mainly scrub, with low lying thickets of beech. No trees colonise the slopes and there are many areas of bare rock and scree slopes. Although the gradient is steeper, it is clear that vegetation cover would be less substantial during cooler periods.

Vegetation cover is also reduced in times of severe aridity, perhaps to a greater extent than in times of cooler temperatures. As previously stated (Chapter 2.4.4.1), the LIA was characterized by high hydroclimatic variability and years of severe aridity were common, with the winter season being most affected (Piervitali & Colancino, 2001). Although extreme conditions varied greatly on a multiyear scale, overall the sixteenth and seventeenth centuries appeared to be drier than the eighteenth and nineteenth centuries (Pfister, 1995; Serre-Bachet *et al.*, 1995; Piervitali & Colacino, 2001). Physical weathering, such as frost shattering would have been prominent during these times of aridity and more marked during cold intervals. The abundant sediment available for transportation would be delivered downstream during the first high intensity or prolonged rainfall event. The competence of the flow would be increased due to the high gradient of the Figarella channel enabling the large boulders to be entrained and transported downstream.

Widespread aggradation could have occurred in the Figarella sometime during the Holocene with the formation of what has been incised and classified as T2 (Figure 6.9). The sedimentological features of the exposed sections (Table 6.3) suggest that material may have been transported down valley by a hyperconcentrated flow. The cobbles and large boulders up to 1.5 m in diameter are unsorted and contain within a matrix supported sandy gravel. It is unlikely that slope wash could have contributed to such a high proportion of fine material within the matrix. There was no organic material within the sections to date the mass deposition. It is unlikely that the alluviation occurred during the LIA, however, as the Figarella must have undergone an intensive incisional phase of about 5 m (Table 6.3) prior to the aggradation of T2. This incison is unlikely over the timescale of the LIA, especially as the deposits on the surface of this terrace date from flood class I (1756, Table 6.4). However, there are several studies in the Mediterranean that have identified alluviation during the LIA. Fuller *et al.* (1998) identify the most recent phase of aggradation in the Guadalope et Mas de las Matas in Spain by luminescence dating as the response to climatic instability relating to the beginning of the LIA. Extensive valley filling and slope accumulation in northeast Spain is also

recognised as a post Medieval phase of deposition which coincides with the onset of the most recent neoglacial (Gutierrez-Elorza & Peb Monne, 1990; Lopez-Aviles, 1998). Increased rates of alluviation over the last 500 years in Crete has also been attributed to climatic controls (Maas, 1998).

6.11 SUMMARY

Lichenometry has proved to be a valuable technique for elucidating the flood history of the Figarella River over the last four centuries or so. However, the linear extrapolation of the calibrated size-age relation to date the earliest flood deposits (sixteenth century) should be regarded tentatively. Nonetheless, the age model indicates that ten distinct periods of enhanced flooding took place over the past 400 years in the Figarella catchment. The intervals of increased flood frequency identified correlate well with cold and wet periods (late 1500s, mid-late 1700s, throughout the 1800s) inferred from secondary evidence and various proxy climate records. Sediment supply was probably increased due to enhanced physical weathering during these times. Increased flooding is evident during periods of severe climatic conditions and also during phases of marked climatic variability as witnessed throughout much of the nineteenth century. This instability is also evident in the behaviour of the river system.

During the Little Ice Age, periods of increased flooding are broadly synchronous throughout the Mediterranean regions and parts of central Europe. The Figarella flood history reported in this study accords well with periods of increased catastrophic flooding identified in the northeast Iberian Peninsula. This suggests that similar forcing factors for increased precipitation are apparent across the western Mediterranean, with the North Atlantic Ocean playing an important role. Cyclonic activity associated with a low North Atlantic Oscillation index enhances the probability of extreme flood events in the western Mediterranean region. An oscillation of eight years is particularly prominent in the North Atlantic ocean–atmospheric circulation.

It is important to establish the natural variability of the climate system over such timescales in order to understand and prepare for climate changes in the future. Investigating the impact of past climatic change on fluvial systems may also aid the management of future changes. Human activities within the catchment may well have exacerbated the response of the river to climatic change but it appears the latter is the overriding control. Anthropogenic activities in the vicinity of the Figarella River appear to have been limited over the past 500 years, although more research is needed on this topic.

7 LATE QUATERNARY RIVER ENVIRONMENTS IN CORSICA: CONTROLS AND CHRONOLOGY

7.1 SYNOPSIS

Detailed discussions of the thesis results are given at the end of Chapters 4, 5 and 6. This discussion chapter draws together the information gained from investigating Corsican river behaviour during the Late Pleistocene and during the more recent Late Holocene period. The records are compared to other terrestrial sequences in the Mediterranean region and any common themes are highlighted. The evaluation of a range of field and laboratory methods for developing the glacial and fluvial chronologies is a major part of this investigation and the benefits of using an integrated approach are emphasized.

7.2 LATE PLEISTOCENE GLACIAL ACTIVITY AND RIVER BEHAVIOUR

There are many allogenic and autogenic factors which can affect river behaviour (Figure 1.2) but determining their form and magnitude of influence can be problematic. The use of a number of chronological controls enables the timing of fluvial activity to be more accurately constrained and a better understanding of the possible causes of river response to be isolated.

7.2.1 Glacial advances

Two exposure ages were established which attribute two moraines in the Taravo and Golo river catchments to cold periods during the Lateglacial period (Chapter 4.5). This study extends upon Conchon's (1975) glacial model by applying an absolute dating method and demonstrating the utility of cosmogenic dating in this environment. Further work is required to construct a complete glacial history and this would enable the moraines dated to the Younger Dryas in this study to be placed within a wider chronological framework for the other glacial deposits preserved in the Corsican landscape. However, encouraging results have been obtained from CND in this study that may provide a catalyst for future work in this field.

Evidence has been presented in Chapter 4 to show that the climatic conditions during the Younger Dryas in Corsica were suitable for glacier growth. Other mountainous regions in the western Mediterranean such as the Apennines also exhibit glacial advances and similar snow lines during this time (e.g. Boenzi & Palmentola, 1997). However, there remains one question, if the so called Mid-Late Würmian glaciers proposed by Conchon (1975, 1986) are dated correctly to the Younger Dryas stadial, at what time were the younger cirque glaciers in Corsica active? While this issue can only be resolved by a more extensive dating programme, it is

worth presenting a brief account of the evidence for post-Pleistocene glacial activity in Southern Europe as this serves to highlight the sensitivity of the region.

Grove (1997) has summarized the history of Holocene glacier variations in the Swiss and Austrian Alps and reports advances between 9.4-9.0, 6.6-6.0, 8.4-8.1, 7.7-7.3, 4.6-4.2, 3.6-3.0 and 0.9-0.8 k radiocarbon years BP. There was a pronounced glacial readvance in the Italian Alps between 3 and 2.5 k years BP, but the maximum Holocene extent was reached between AD 1820-1850, during the Little Ice Age (LIA) (Nesje & Dahl, 2000) when glaciers extended over 2 km beyond their present position (Orombelli & Mason, 1997). The glaciers in the Pyrenees advanced more than 750 m and descended almost 200 m in elevation during the LIA (Nesje & Dahl, 2000). The issue of LIA glacial advancement in Corsica has not been investigated but if there was no evidence of glacial activity during the past millennium, cirque glacier development may have been a result of one of the cold periods recognized during the earlier part of the Holocene (Grove, 1997; Haas, 1998). The pollen record from Lake Creno in central Corsica shows that a sudden decrease of heather and alder was recognized around 7.6 k radiocarbon years BP (Reille *et al.*, 1999) (Chapter 2.4.2). This event which was apparently so strong and so rapid that it is attributed by Reille *et al.* (1999) to anthropogenic activity, although very few signals of human disturbance are identified prior to 7.6 k radiocarbon years BP. In addition, this event is recorded in pollen sequences from another upland site in Corsica, situated more than 20 km away. This demonstrates that the event was not restricted to the Lake Creno site but that it "affected the whole region extending up to all the mountains of the island" (Reille *et al.*, 1999). The timing of this event coincides with a cold period identified in the Alps between 7.7 and 7.3 k radiocarbon years BP (8.2 cal. year BP) which caused glaciers to readvance. Consequently, the reduction in tree pollen in Corsica at this time may have been due to a cooling, rather than an anthropogenic influence. The brevity between climatic change and vegetation response has just recently been highlighted (Allen *et al.*, 1999; Watts *et al.*, 2000; Roucoux *et al.*, 2001), although in contrast, there is no indication of a significant increase in *Artemisia* concentrations at 7.6 k radiocarbon years BP (Figure 2.5).

7.2.2 Glacial chronology

It was highlighted in Chapter 4.8 that the error margins attached to the cosmogenic exposure ages are sufficiently broad to suggest that sample C1 (14.11 ± 1.04 ka), dated to the Older Dryas stadial, may well be attributable to the Younger Dryas like C2 (12.71 ± 0.96 ka), with only 1.39 ka difference between the exposure ages (Table 4.10). The fact that cosmogenic dating techniques are influenced by many more known and unknown factors (Table 4.5) which are likely to underestimate, rather than overestimate the exposure age of the sample has to be addressed. The ages of C1 and C2 could quite feasibly be underestimates, although even with a 30% error margin, the upper exposure age of sample C2 would only be 16.51 ka. An error

margin of +40% would place the upper exposure age of C2 at 18.06 ka, and it could be argued that a global Last Glacial Maximum age could not be ruled out. The need for further research on the production rate of cosmogenic nuclides over time is clear (Chapter 4.4.5).

If the moraine sampled and dated to the Younger Dryas stadial is correct and associated with the T6 deposits (Table 4.2), the preceding glacial advance may be attributable to the Late Würm, perhaps more specifically to the global LGM (Figure 7.1). The deposits concomitant with this advance are at an elevation of 700-1,100 m and are correlated by Conchon (1975, 1986) to the T5 fluvial deposits. Conchon (1986) suggests that these T5 glaciers could be dated to *ca.* 20 ka BP, which is broadly coeval with the LGM stand as proposed above, although it is not clear on what basis this date is obtained. Other mountainous regions within the Mediterranean have glacial deposits preserved from the LGM and are dated to >17.7 ± 0.36 and 22.68 ± 0.63 k radiocarbon years BP in the French and Italian Piedmonts of the Alps (Billard & Orombelli, 1986) and Campo Imperatore in the central Apennines (Giraudi & Frezzotti, 1997), respectively. The deglaciation chronology in the northwest of the Iberian Peninsula developed by Fernandez Mosquera *et al.* (2000) using cosmic-ray produced ^{21}Ne in quartz assigns a glacial polished surface to an exposure age of 22 ± 17 ka.

Attributing the T5 glaciers in Corsica to the LGM is speculative, as is Conchon's correlation with the fluvial deposits. It is not possible without more exposure ages to extend the glacial chronology because:

i) Not all the glacial advances in Corsica during the Pleistocene will have been preserved. Erosion and reworking of sediments by subsequent, more extensive glaciation is a major problem and terminal moraines are rarely present in Corsica and lateral moraines are better preserved in the southern part in the vicinity of Monte Renoso in comparison to the northern region around Monte Cinto and Monte Rotondo (Figure 3.9).

ii) Glacial activity during the Pleistocene may not have been synchronous nor of the same magnitude across the Mediterranean. For example, in northwest Greece, uranium-series ages have shown that the most extensive glaciers were present well before the global LGM (Woodward *et al.*, in press).

iii) The glacial deposits may not necessarily be directly associated with the fluvial deposits. Conchon's (1975, 1986) basis for correlating the glacial and fluvial deposits was on the geomorphic features and weathering characteristics. Therefore the lateral moraines dated by ^{10}Be cosmogenic nuclides in this study may not be related to the T6 fluvial deposits.

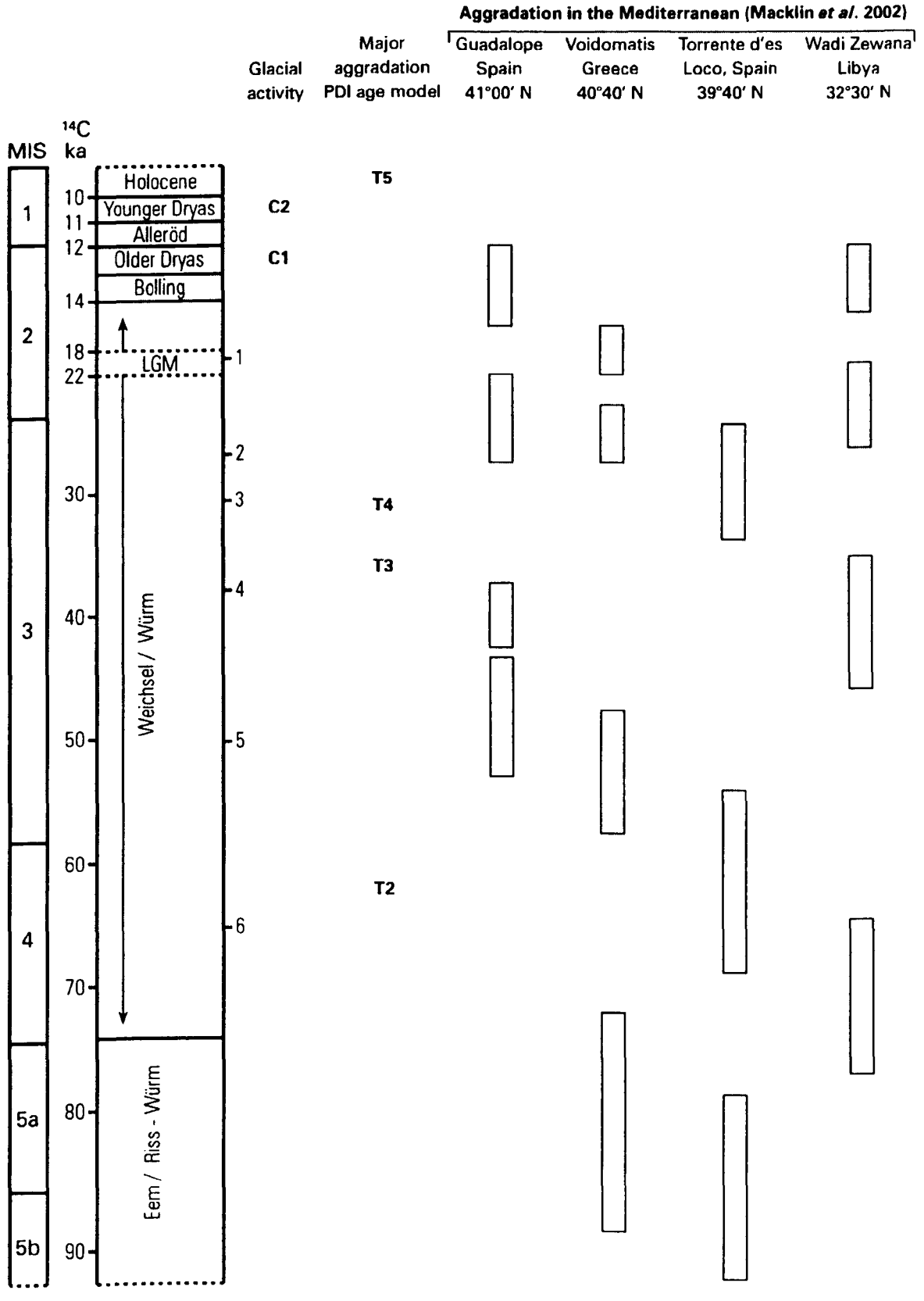

Figure 7.1 The timing of glacial activity in Corsica (established by cosmogenic dating) and major alluviation in the Tavignano catchment (determined by the age model derived from OSL ages and an PDI) in addition to the timing of deposition within other Mediterranean basins (compiled by Macklin *et al.*, 2002).

7.2.3 Late Pleistocene alluviation in the Mediterranean

The age model developed for Late Pleistocene Tavignano alluviation from a combination of pedogenic parameters and OSL dates (Chapter 5.7) appears broadly consistent with the main phases of river aggradation identified across the Mediterranean by Macklin *et al.* (2002) (Figure 2.7, Figure 7.1). However, the resolution of the PDI age model is not sufficient to be certain that the timing of the Tavignano alluviation phases are directly comparable to those identified by Macklin *et al.* (2002) who employ more robust dating controls. In addition, the duration of the alluviation episodes are not constrained within the Tavignano catchment and this poses problems for the assessment of wider patterns of river activity. With these caveats in mind the following section will briefly compare the tentative alluviation age model developed for the Tavignano with the recent ideas of Macklin *et al.* (2002).

The age model suggests that the T6 deposits are Late Holocene in age and correspond to 2 ± 1 ka and the T5 deposits correspond to the Lateglacial/Holocene transition (Figure 7.1). Alluviation during the Lateglacial is also evident in Spain, Greece and Libya with this phase centered on 12.5 ± 1.5 and 13 ± 2 ka (Macklin *et al.*, 2002) (Figure 2.7). One striking difference between the two youngest units is the sedimentology. The alluvial unit T6 clearly shows a change in channel geometry, sediment caliber and depositional style from that of T5 and the older units T2-T4. Unit T6 deposited in the late Holocene contains appreciable thicknesses of fine grained overbank sediments. T2-T5 are more typical of a braided river system where coarse sediments dominate and thick beds of fine grained sediment are rare or absent (Figure 5.6).

The T4 fluvial deposits are dated to around 31 ± 12 ka using the PDI age model (Table 5.14, Figure 5.20). This alluviation phase coincides with others in a number of Mediterranean river basins such as Bergantes and Rio Aguas in Spain and Torrente d'es Coco in Mallorca (e.g. Fuller *et al.*, 1998; Rose & Meng, 1999). The age model suggests that terrace T3 is not significantly older than T4, dated at *ca.* 36 ± 14 ka. Heinrich Event 4 is coeval with this date and confirmation of the cooler climate is provided by the vegetation change to a steppe biome at Lago Grande di Monticchio in Italy (Allen *et al.*, 1999). Mediterranean river activity during this time is characterized by aggradation beginning at 38-39 ka and ending before 30.3 ka, although possibly as early as 34.7 ka (Macklin *et al.*, 2002).

T2, the oldest alluvial terrace examined is ascribed a PDI age model of 62 ± 23 ka and could possibly be a response to Heinrich Event 6 during MIS 4 and dated to *ca.* 66 ka (Bond *et al.*, 1993). This is contemporaneous with a stadial identified in the palaeoenvironmental records in the Mediterranean (e.g. Guiot *et al.*, 1993; Burjachs & Julià, 1994; Allen *et al.*, 1999). It is well documented that MIS 4 (*ca.* 74-58 ka) represented full glacial conditions and a large increase in ice volume in Europe (van Andel & Tzedakis, 1996). Mean temperatures were 12-13°C below present day (Guiot *et al.*, 1989). The lack of vegetation on the hillslopes and the

increased sediment availability would have encouraged river aggradation. The sedimentological characteristics of this unit certainly reflect high energy flows typical of glacial outwash, systematically lacking fine sandy overbank sediments and comprising strata of cobbles and boulders illustrating a braided nature (Figure 5.6). Macklin *et al.* (2002) comment on the small number of alluvial units dated to MIS 4 across the Mediterranean and remark that it unclear as to whether it is due to formation or preservation factors. Alluviation however, appears to be only evident in the smallest drainage basins or those that are affected by glaciation. The enhanced sensitivity of catchments like the Voidomatis in Greece and the Tavignano in Corsica compared to those that are unglaciated perhaps signify a greater response rate of slope/fluvial processes to climatic change (Macklin *et al.*, 2002). Sediment yield is a log linear function of drainage area and elevation which also emphasizes the importance of relatively small and steep catchments for sediment production (Walling & Webb, 1983).

Even though there appears to be a broad agreement with the palaeoenvironmental data and timing of other Mediterranean aggradation events providing some confidence in the PDI (the author is aware of the perils of circularity in this reasoning), the large error margins attached to the ages of the five Tavignano terraces justify great caution when applying this alluviation model without further absolute dating. It is also recognized that not all the units are present in all of the river basins dated by Macklin *et al.* (2002) which suggests preservation is a key issue.

7.2.4 Landscape sensitivity to change

The Tavignano fluvial chronology is not as well constrained as some other Mediterranean river basins (e.g. Macklin *et al.*, 1997; Fuller *et al.*, 1998; Rose *et al.*, 1999; Hamlin *et al.*, 2000), but it has been shown that Late Pleistocene climatic change is likely to have been a strong influence on river behaviour in Corsica. Tectonic activity is relatively limited in Corsica and although there is evidence of some uplift (Chapter 5.3.2), tectonics does not appear to be the dominant factor driving river aggradation and incision phases within the Tavignano catchment. Climate driven base-level change could be a more significant external factor affecting Pleistocene river behaviour with regards to sea-level change through global ice volume (eustatic) variations. Figure 3.7 shows sea-level flucuations between 20 and 80 m have occurred since 100 ka. More detailed sampling, dating and analysis of the Tavignano alluvial units in the lower reaches and of coastal sites are necessary if base-level changes are to be evaluated more quantitatively. Further work is also needed in order to understand the issue regarding complex response within the Tavignano catchment. A diachronous response has been recognized in Mediterranean catchments (e.g. Fuller *et al.*, 1998) with headwater aggradation preceding that in the lower basin, possibly reflecting a sediment wave propagating downstream (Nicholas *et al.*, 1995). Lowland alluviation has also been known to be concomitant with upland incision, which suggests differences in reaction times perhaps due to channel and hillslope variations on the

reach scale (e.g. Macklin *et al.*, 1992). The complex response issue highlights the variability of river activity within individual catchments and demonstrates that on a regional scale differences in river response to environmental change in terms of the timing, nature and magnitude must be expected. Such models are difficult to test, but progress can be achieved with an adequate number of absolute dates from terraces along the river system. Preservation of the units is an important factor here too.

In common with other steepland Mediterranean catchments studied to date, the Tavignano River shows a high sensitivity to environmental change. It has been shown from a number of other Mediterranean catchments that climatic change is one of the dominant controls on river system behaviour, regardless of lithology or tectonic regimes (Macklin *et al.*, 2002). The granitic landscape of Corsica is in contrast to much of the rest of the Mediterranean where granites are rare. Tectonic activity has also been fairly quiescent throughout the Pleistocene in Corsica, unlike parts of southeast Spain for example (e.g. Harvey & Wells, 1987; Mather *et al.*, 1995) (Figure 3.6).

Macklin *et al.* (2002) have demonstrated across the Mediterranean basin similar river responses to climatic change, albeit with some variability in amplitude and duration. It is apparent that Late Pleistocene alluviation occurred mainly during cool, dry stadials when forest or wooded biomes were replaced by steppe vegetation (Macklin *et al.*, 2002). There are a number of reasons why Mediterranean river basins appear to be more sensitive to climatic change on the $10^3 - 10^4$ year timescale than those in central and northern Europe, these include:

i) The Mediterranean was particularly ecologically sensitive during the Late Pleistocene, lying close to the forest/steppe ecotone with northwest Spain, parts of Italy and the western Balkans (Turner & Hannon, 1988) and possibly Corsica being important refuge areas for thermophilous tree taxa. Tree growth would have been sensitive to relatively minor temperature and moisture variations leading to a rapid and significant impact on slope stability and runoff response.

ii) Coupling between hillslopes and channels is one feature that has considerable influence on catchment sensitivity (Brunsden & Thornes, 1979; Harvey, 2001). Steep upland catchments allow for a particularly good slope-channel coupling and a high coarse sediment availability. Coupling is augmented during cooler episodes when vegetation cover is limited and rock breakdown mechanisms are more effective.

iii) Glaciation can be an important influence on downstream alluviation by providing meltwater in the spring and summer months and consequently an additional supply of coarse and fine material to downstream reaches (e.g. Voidomatis, Greece (Lewin *et al.*, 1991); Tavignano, Corsica (this study)). Glaciers can respond rapidly to even modest changes in climate with impacts beyond the glacier margin effecting wholesale changes

in river regimes and sedimentation styles (Woodward *et al.*, 1995; Macklin *et al.*, 1997).

7.3 FLUVIAL RESPONSES TO RECENT ENVIRONMENTAL CHANGES

The preservation of boulder berms and their colonization by lichens on the substrates within the Figarella river reach allowed for the development of a detailed flood history over the past 400 years. Precipitation records, palaeoclimatic data and historical documents available across the Mediterranean were compared to the flood periods identified within northwest Corsica to build up a picture of regional flood history (Chapter 6.8) and to explore potential causal mechanisms (Chapter 6.9).

7.3.1 Regional synchrony

The flood history of the Figarella provides strong evidence to support the argument that climatic change is the dominant control over anthropogenic factors for river behaviour over the past 400 years. The identified periods of enhanced flooding within northwest Corsica appear o show some correlation with a number of other empirical and instrumental records across the Mediterranean (Pfister, 1988; Camuffo & Enzi, 1995; Jones & Bradley, 1995; Barriendos-Vallve & Martin-Vide, 1998) (Figure 7.2). Glacier advances in Switzerland also coincide with episodes of increased magnitude and frequency rainfall events over the past 400 years (Zumbühl *et al.*, 1981). Glacier expansion illustrates an increasingly cold and wet climate, the timing of which is coeval with other climate proxy records in southern Europe (Table 6.7). These periods which include the late sixteenth century, the latter half of the eighteenth century and much of the nineteenth century correspond to the more severe phases of the LIA (1450-1850). As with the response of the Tavignano catchment to long term climatic change, the sensitivity of the Figarella River to decadal and centennial climatic variation is largely controlled by the secondary components of hydrology and vegetation. The overall drop in temperature of *ca.* 1°C and the increased seasonality during the LIA would have reduced the vegetation cover, increased runoff and promoted more rapid rates of mechanical weathering and rock breakdown. Again, it appears that sediment availability and hillslope channel coupling are important factors in river response to climate variability.

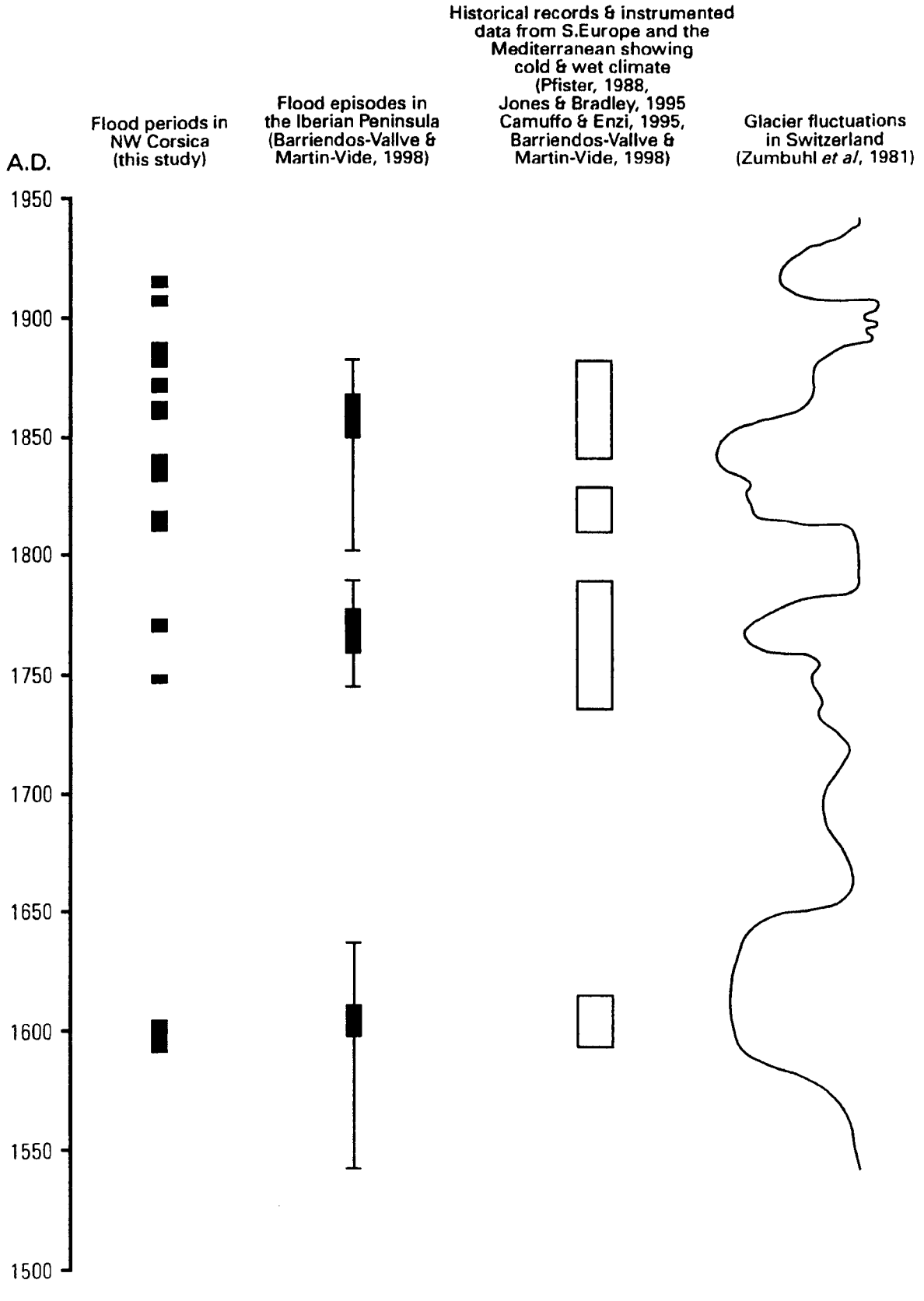

Figure 7.2 The flood history established for the Figarella catchment by lichenometry is coeval with other periods of enhanced precipitation identified in the Mediterranean, historical and instrumented data illustrating cold and wet conditions and glacier fluctuations.

7.3.2 Anthropogenic influence

Numerous studies in the Mediterranean have argued that the primary cause of river basin aggradation during the Late Holocene is attributed to anthropogenic influence (e.g. Wagstaff, 1981; van Andel *et al.*, 1990; Abbott & Valastro, 1995) (Chapter 2.5.2). Few, if any river basins in the Mediterranean are not disturbed by human settlement and agricultural activities, and this is problematic when separating river responses to climate and anthropogenic causes. Deforestation and farming of the land is thought to have been relatively limited in the Figarella catchment and throughout much of Corsica, although there is some evidence on the hillslopes to suggest land use change in the form of terracing (Chapter 3.9, Figure 3.15). The increase in runoff and slope instability as a result of human practices in the area would exacerbate the response of the river to climate change. The partial synchroneity of the Figarella flood intervals with others across the Mediterranean, together with the regional climatic data, suggest that river behaviour in northwest Corsica over the last 450 years has been controlled primarily by climate.

7.3.3 20th century decline in flood magnitude

As the island depopulated towards the beginning of the twentieth century (Chapter 3.9) it is likely that many rural settlements were gradually abandoned, encouraging the regrowth of trees on the slopes, less intensive cultivation practices and a decline in grazing livestock numbers (Grove & Rackham, 2001). Vegetation cover reduces runoff and stabilizes hillslopes, which would in turn reduce slope/channel coupling and thus the sensitivity of the catchment to any environmental change. This may partly explain the decrease in the number of dated flood deposits after 1900, with no evidence of large flood events since 1932. It is reasonable to suggest that the general increase of positive phases of the NAO is also a factor in the declining frequency and magnitude of flooding over the twentieth century (Figure 6.19). The number of rain bearing depressions generating winter storm events over the western Mediterranean would be lower than that with a negative NAO index (Chapter 6.9.5). An apparent decrease in flood frequency and magnitude has also been recognized in Crete since the 1950s (Maas, 1998) and in mainland Greece during the 1900s compared to the previous two centuries (Hamlin, 2000).

7.4 EVALUATING THE CHRONOLOGICAL CONTROLS

The importance of employing dating methods in studies of past fluvial activity has been emphasized throughout this thesis. The following section assesses the radiometric, relative and incremental techniques used in Corsica to develop an understanding of river response to Late Pleistocene and Late Holocene environmental change.

7.4.1 Terrestrial *in situ* cosmogenic nuclide dating

Cosmogenic dating was successfully used on glacial deposits in Corsica to establish exposure ages, where no other method was applicable. The lithology of the two samples from which the radionuclide ^{10}Be was extracted were grandiorite, exhibiting large quartz grains. The other samples collected in the Haut Asco region (Figure 4.2) were rhyolitic and provided far less pure quartz because of the very small crystals, making it difficult to extract the beryllium. Perhaps in future, samples could be taken for *in situ* ^{36}Cl cosmogenic exposure dating, whereby the whole of the rock is used in the preparation and analysis. Of course, supplementary samples should be taken from the same boulders, or at least the same moraines as those dated in this study for cross checking purposes. Additional cosmogenic nuclide exposure ages would allow for a more complete glacial chronology to be developed for Corsica, and would confirm whether there was glacial activity in Corsica during the Younger Dryas, approximately 12 ka. The two cosmogenic exposure ages obtained in Corsica do however show the potential of the technique in such a Mediterranean granitic environment and provides useful calibration points to build on in the future.

With the recognition that terrestrial *in situ* cosmogenic nuclide dating is a valuable tool in geomorphology, the development of cosmogenic preparation laboratories at the University of Edinburgh have just recently been funded. There is hope that AMS analysing facilities at the Scottish University Environmental Research Centre (SUERC) will follow shortly. This will help to promote the technique in the United Kingdom, and in Europe, and make the application of cosmogenic dating more accessible to researchers in this country.

7.4.2 Optical stimulated luminescence (OSL) dating

The samples collected from the Tavignano River alluvial sequence, with the exception of CL1, yielded a much younger age than expected. The geomorphological context and the pedogenic characteristics of the terraces suggest that the age of the oldest unit (T2) extends well into at least MIS 4. Reworking of the sample is one possible explanation, although there is no stratigraphic evidence to suggest that this is the case.

Luminescence dating appears to work better in some environments and contexts than others, such as in northeast Spain (e.g. Fuller *et al.*, 1998) and in the Sudan (Woodward *et al.*, 2001). Rose *et al.* (1999) conducted OSL dating on alluvial terraces in Mallorca and gained good results with the exception of a few profiles where there was evidence of OSL dating inversions. However, the collection and analysis of several samples from within the same alluvial profile is valuable in terms of bracketing the time period of aggradation and identifying anomalies. In practice, because of the analytical costs, few studies achieve this.

With regards to OSL dating along the Tavignano River, it may not be beneficial to collect and process additional samples to those in this study. Alternative absolute chronological controls could be employed instead, although methods are limited to radiocarbon dating (up to 40 ka) and electron spin resonance (ESR) if appropriate materials can be found within the alluvial terraces. The absence of calcretes prevents the use of uranium-series dating.

7.4.3 Relative age dating with pedogenic parameters

The use of a variety of pedogenic parameters to develop a relative age sequence in alluvial environments is well established (e.g. Harden & Taylor, 1983; McFadden & Weldon, 1987; Alonso *et al.*, 1994; Harvey *et al.*, 1995). The combination of colour, clay content and iron oxide concentrations showed good correlation with relative age, although it is more difficult to quantitatively assess the difference in ages between the units. The data obtained were suitable to develop a profile development index (PDI) which was used in conjunction with the OSL dating to create an age model. Limited information was gained from the mineral magnetic property analysis and no contribution was made to the PDI. There are many factors that influence each mineral magnetic parameter. Consequently, interpretation of controlling variables is problematic and several parameters and quotients in this case appeared to contradict one other. Conducting mineralogical analyses to complement the magnetic characterizations may be beneficial in a future study. The origins of the magnetic minerals in a sample can be deduced by examination of their morphology, grain size, chemical composition and their mineral associates (Hounslow & Maher, 1999). Scanning electron microscopy (SEM) can be used in this instance to gain a better understanding of magnetic mineral sources and their causal links with environmental, diagenetic and climatic changes (Hounslow & Maher, 1999).

7.4.4 Lichenometric dating

This incremental dating technique was successfully employed within the Figarella River in northwest Corsica to construct a history of river response to environmental change over the past five centuries. An excellent *Rhizocarpon geographicum* growth curve was constructed for the region which enabled distinctive flood periods to be identified. If discharge or rainfall records were available for the Figarella River then identification of individual precipitation/flood events may have been more easily ascertained. Nevertheless, enhanced periods of flooding within the Figarella catchment were determined which were coeval with those identified in other parts of the western Mediterranean. Cross checking with a second lichen species allowed the technique to be applied with greater confidence. Dendrochronology was also used in conjunction with the lichenometry, and although confirming the relative ages of the terraces on which the boulder berms were deposited, the method did not provide realistic ages of the formations themselves.

Forest clearance, fire and grazing are all factors that are likely to have provided such young ages.

7.5 SUMMARY

Developing a Late Pleistocene glacial and alluvial chronological framework for sites in Corsica has been difficult in view of the dating results discussed above. More *in situ* cosmogenic exposure ages are needed in addition to an alternative absolute dating method to the OSL technique. Furthermore, it is important to appreciate that, in common with many terrestrial records, the glacial and fluvial deposits preserved in Corsica may not represent a complete sequence. This issue of fragmentary evidence further highlights the need for a combined absolute dating approach if accurate comparisons within the wider Mediterranean region are to be made. This study has, however, displayed the successful use of lichenometric dating in constructing a flood history for the Figarella catchment for the past 450 years, and in conjunction with historical records illustrates the influence of climate change on river response.

8 CONCLUSIONS AND FURTHER RESEARCH

8.1 CONCLUSIONS

The river systems of Corsica form valuable archives of environmental change in the western Mediterranean region. The middle and lower reaches of many of the principal rivers contain well preserved sequences of Late Pleistocene and Holocene river terraces and landforms. Pleistocene glacial activity is believed to have contributed to the sediment load forming the alluvial terraces. Cirques carved within the high granite mountains are evident throughout central upland Corsica and lateral moraines from glacial tongues are especially well preserved in the southern region. There is an abundance of evidence for Late Holocene river response to environmental change within some of the smaller steepland river catchments. The characteristic steep gradient and cobble and boulder bed systems contain boulder berms that have been deposited during high magnitude floods. The main conclusions drawn from this investigation of glacial and fluvial deposits in Corsica are presented below.

8.1.1 Towards an improved chronology of glacial activity in Corsica

Good chronological controls are important for developing robust palaeoenvironmental sequences that can be confidently correlated to other continental and marine records. Terrestrial *in-situ* cosmogenic ^{10}Be nuclide dating (CND) is a relatively new technique that has been successfully applied for the first time in the Mediterranean region. The granite lithology of Corsica provided an ideal environment in which to test this absolute dating technique. Two exposure ages of boulders on different moraines were obtained. The ages of 14.09 ± 1.04 ka and 12.70 ± 0.96 ka suggests that the lateral moraines are attributable to the Lateglacial period. The exposure ages coincide with the Older-Dryas and Younger-Dryas coolings respectively - intervals noted in many Mediterranean palaeoclimatic records. It is possible that both moraines are attributable to the Younger Dryas stadial which was the more intense cooling period. Alternatively, the older moraine could be associated with the LGM. The high ^{10}Be counts during the AMS analysis provide confidence in the accuracy of the results. It is also significant to point out that glacial activity took place during the Lateglacial in other parts of the Mediterranean. Support for this interpretation was also gained from the simple snowpack model based on present day climatic conditions in Corsica and proxy temperature and precipitation reductions for the Younger Dryas. However, it is also clear that more samples are needed from these and other sites for CND to confirm that glaciers were present in Corsica during the Lateglacial period.

8.1.2 Late Pleistocene alluviation and pedogenic weathering within the Tavignano catchment

The optically stimulated luminescence dating method employed to determine the timing of the Tavignano River fluvial sequence consistently underestimated the ages of each of the terrace units. Both the geomorphic context and weathering characteristics suggested a much older sequence. The redness, clay content and iron concentrations of the terrace soil profiles provided a robust relative age sequence, effectively characterizing the weathering in the units. The three soil development parameters were used as part of an integrated approach for developing a highly successful profile development index, unique to this study. In conjunction with the OSL dating, the ages of the Tavignano units were estimated (T2, 62 ± 23 ka; T3, 36 ±14 ka; T4, 31 ± 12 ka; T5, 10 ± 5; T6, 2 ± 1 ka) using a simple model. However, the data were semi-quantitative with large error margins. Nonetheless, the periods of major aggradation identified by this age-model along the Tavignano River appear to show a broad correlation with major alluviation phases in other Mediterranean regions. It is important to point out that additional absolute dating controls are needed to test this model and constrain the timing of aggradation more precisely.

The existing geochronology of the Tavignano fluvial sequence is not robust enough to enable causal mechanisms of Late Pleistocene river behaviour to be established, although it is thought that climatic change has exerted a strong influence on long-term river activity. Tectonic movements in Corsica throughout the late Quaternary were limited and are not believed to be a dominant forcing mechanism for aggradation or incision. Other studies have shown that the timing of major aggradation phases across the Mediterranean region coincides with cooler climatic conditions.

8.1.3 River response to decadal-centennial scale environmental change in the Figarella catchment

The North Atlantic Ocean plays an important role in Mediterranean climate on an annual to decadal timescale. Over the past few decades, enhanced flood frequency and flood magnitude across the western Mediterranean appears to be coeval with a strongly negative winter North Atlantic Oscillation Index value which is attributed to increased cyclonic activity. Five day storm events in northeast Spain (1990-1985) correlate with strong negative winter NAO phases approximately every 8 years. This periodicity is concomitant with the duration of an oscillation identified as a long term feature in the North Atlantic climate system, suggesting that natural climate variability on this timescale has not been significantly obscured in the records by anthropogenic signals such as global warming.

Lichenometric dating of coarse flood deposits in the Figarella basin in northwest Corsica was highly successful in establishing the timing of flood periods over an historical timescale. The principal lichen species used to provide the age control was *Rhizocarpon geographicum* and the

growth rate calculated for the region was 0.27 mm yr^{-1} with an r^2 value of > 0.85. At least ten distinct periods of enhanced flooding took place over the past five centuries. Flooding was particularly prominent during the late 1500s, mid-late 1700s and throughout the 1800s in the Figarella catchment. These intervals during the Little Ice Age have been shown to be particularly cold and wet by numerous climate proxy records and historical documents. Sediment availability is likely to have been high during these times due to increased mechanical weathering primarily through frost action, especially at high elevations and on northerly aspects. Reduced vegetation cover as a result of cooler temperature would have promoted rapid runoff, increasing flashiness and flood. Anthropogenic activity may have influenced the sediment load and flow regime through land-use change (e.g. increased deforestation, cultivation and grazing) although the extent cannot be easily quantified. The apparent synchrony of flood events across the Mediterranean region during the Little Ice Age is persuasive evidence to suggest that climate variability is the overriding control on flood frequency.

Lichenometry proved to be a valuable incremental dating technique in this environment of sufficient resolution to confidently link climate change to river behaviour. Dendrochronology was not so useful as a complimentary technique in this case, but it was not needed due to the success of the lichenometric dating. The use of a second lichen species and growth curve provided a valuable cross check on the method.

8.2 RECOMMENDATIONS FOR FUTURE WORK

The need for more absolute ages to constrain the timing of glacial and fluvial activity in Corsica has been emphasized throughout this investigation. The two cosmogenic nuclide exposure ages obtained in this study have clearly demonstrated the potential of the technique and provide a stepping-stone for future dating of glacial deposits in Corsica and other mountainous Mediterranean environments where other suitable lithologies are present. Alternative dating methods for the alluvial units of the Tavignano River should be considered and further research on the potential for OSL dating would be beneficial (e.g. single-grain dating). The distance transported and the turbidity of flood waters are just two factors affecting sediment zeroing and are issues which could be investigated further to help refine the OSL technique. An alternative to absolute dating techniques would be the identification of tephras in soil profiles. Corsica is close to the Italian volcanic provinces and many tephras are present in the Tyrrhenian Sea. Tephra layers derived from the same volcanic event provide time-parallel markers in sedimentary sequences and serve as important tie-lines among terrestrial, marine and ice-core records (e.g. Lowe, 2001).

Further investigation of Quaternary tectonic activity and sea-level change in Corsica is necessary in order to fully assess their impact on river behaviour. More detailed studies of the coastal plain sequences are needed in addition to good chronological controls. Net incision

rates can also be estimated to provide a more detailed history of fluvial activity. It may then be possible to identify with greater confidence the long-term causal factors associated with major changes in river behaviour. Examination of the lithological composition of clasts within the Tavignano alluvial units and identification of the upstream sediment sources may allow for a better understanding of the extent to which glacial activity influenced fluvial processes during the Late Pleistocene. Sediment provenance in this context has been successfully applied in the Pindus Mountains of northwest Greece (e.g. Lewin *et al.*, 1991; Woodward *et al.*, 1992).

Future research should also involve the collection of high resolution climate-proxy records within Corsica. Palynological and lacustrine data could be obtained from the many mountain lakes on the island to provide a tighter environmental change framework. Coleoptera and other such valuable indicators of temperature change could also be studied in Corsica and this may resolve some of the issues relating to glacier development during the Lateglacial. The coastal plain and the off-shore regions contain sequences and records that extend back beyond the Lateglacial and these may offer long term records of fluvial activity.

With regards to future work on river response to environmental change over a historical timescale, more steepland mountain catchments need to be investigated. Additional studies in Spain and Italy for example will enable the timing of enhanced flood frequency across the western Mediterranean over the past four centuries to be compared and controls of climate variability to be more clearly evaluated. Studying responses to past climate change in this manner provides valuable empirical data for model calibration and may lead to improved predictions of future change. Specific to Corsica, other drainage basins exhibiting similar characteristics to the Figarella catchment and Little Ice Age boulder berms could be investigated. Analysis of local daily rainfall records in Corsica (these were not available for the Figarella) could also be useful in terms of identifying individual heavy precipitation events which correlate to the age of the coarse flood deposits preserved on the valley floors. In addition, the nature of the links between the North Atlantic Oscillation index and intense precipitation in Corsica over the last 150 years could be explored. A further need concerns the better understanding of the timing and activity of land-use change in the Figarella catchment and other Mediterranean steepland study areas in order to evaluate the anthropogenic component of increased flood frequency over the last four centuries. It is appreciated however, that land use history is very difficult to reconstruct in many environments (including the U.K.) even where good documentary records are available.

An extension to the study involving the Figarella catchment could include the radiocarbon dating of the terrace surfaces on which the boulder berms were deposited, providing suitable material could be obtained. The coarse sedimentology of the units suggests that high energy flows were responsible for their formation. Establishing the terrace ages would provide an insight into river behaviour during earlier parts of the Holocene period (perhaps when human

populations were sparse) which could then be compared to other Mediterranean regions. As with all investigations of river response to environmental change, whatever the temporal or spatial scale, it can be argued that it is the development of a robust chronology which is central to improving our understanding.

BIBLIOGRAPHY

Abal'yan, T.S., Mukhin, V.M. and Polunin, A.Ya. 1980. On glacial nourishment and possibilities of long-term prediction of the mountain river's runoff with vast glacierization of the catchment areas. In: The Data of Glaciological Studies. Discussion, N39, Moscow, 42-49.

Abbott, J.T. and Valastro, S. Jnr. 1995. The Holocene alluvial records of the chorai of Metapontum, Basilicata and Croton, Calabria, Italy. In: Lewin, J., Macklin, M.G., Woodward, J.C. (Eds), Mediterranean Quaternary River Environments. Balkema, Rotterdam, 195-205.

Adams, J., Maslin, M., Thimas, E. 1999. Sudden climate transitions during the Quaternary. Progress in Physical Geography, 23, 1, 1-36.

Ahnert, F. 1998. Introduction to Geomorphology. Arnold, London, John Wiley, New York.

Aitken, M.J. 1985. Thermoluminescence dating. Academic Press, London and New York.

Aitken, M.J. 1998. An Introduction to Optical Dating: The Dating of Quaternary Sediments by the Use of Photo-Stimulated Luminescence. Oxford University Press.

Aitken, M.J. 1992. Optical dating. Quaternary Science Reviews, 11, 127-131.

Ajmone Marson, F., Bain, D.C. and Duthie, D.M.L. 1988a. Parent material uniformity and degree of weathering in a soil chronosequence, northwestern Italy. Catena, 15, 507-517.

Ajmone Marson, F., Barberis, E. and Arduino, E. 1988b. A soil chronosequence in northwestern Italy: Morphological, physical and chemical characteristics. Geoderma, 42, 51-64.

Alexander, R.W., Harvey, A.M., Calvo, A., James, P.A. and Cerda, A. 1994. Natural stabilization mechanisms on badland slopes: Tabernas, Almeria, Spain. In: Millington, A.C. and Pye, K. (Eds), Environmental Change in Drylands: Biogeographical and Geomorphological Perspectives. John Wiley and Sons, Chichester, 85-111.

Allen, H.D. 2001. Mediterranean Ecogeography. Prentice Hall, Harlow.

Allen, J.R.M., Brand, U., Brauer, A., Hubbertens, H.W., Huntley, B., Keller, J., Kraml, M., Mackensen, A., Mingram, J., Negendank, J.F.W, Nowaczyk, N.R., Oberhansli, H., Watts, W.A., Wulf, S. and Zolitschka, B. 1999. Rapid environmental changes in southern Europe during the last glacial period. Nature, 400, 740-743.

Allen, J.R.M., Huntley, B and Watts, W.A. 1996. The vegetation and climate of northwest Iberia over the last 14,000 yr. Journal of Quaternary Science, 11, 125-147.

Alley, R.B. and Clark, P.U. 1999. The deglaciation of the northern hemisphere: a global perspective. Annual Review of Earth Planetary Sciences, 27, 149-182.

Alley, R.B., Shuman, C.A., Meese, D.A., Gow, A.J., Taylor, K.C., Grootes, P.M., White, J.W.C., Ram, M., Waddington, E.D., Mayewski, P.A. and Zielinski, G.A. 1993. Abrupt increase in Greenland snow accumulation at the end of the Younger Dryas event. Nature, 362, 527-529.

Aloisi, J.C., Monaco, A., Planchais, N., Thommeret, J. and Thommeret, Y. 1978. The Holocene transgression in the Golfe du Lion, Southwestern France: Paleogeographic and paleobotanical evolution. Geogr. Phys. Quat., 32, 2, 145-162.

Alonso, A. and Garzón, G. 1994. Quaternary evolution of a meandering gravel bed river in central Spain. Terra Nova, 6, 465-475.

Alonso, P., Sierra, C., Ortega, E. and Dorronsoro, C. 1994. Soil development indices of soils developed on fluvial terraces (Penaranda de Bracamonte, Salamanca, Spain). Catena, 23, 295-308.

Ammann, B. and Lotter, A.F. 1989. Late-glacial radiocarbon- and palynostratigraphy on the Swiss plateau. Boreas, 18, 109-126.

Amorosi, A., Farina, M., Severi, P., Preti, D., Caporale, L. and Di Dio, G. 1996. Genetically related alluvial deposits across active fault zones: an example of alluvial fan-terrace correlation from the upper Quaternary of the southern Po Basin, Italy. Sedimentary Geology, 102, 275-295.

Andrieu, V., Eicher, U. and Reille, M. 1993. The end of the last Pleniglacial in the Pyrenees (France): pollen analytical, isotopic and radiometric data. Comptes Rendus de l'Academie des Sciences, Paris Serie II, 316, 245-250.

Anthony, E. Y. and Poths, J. 1992. ^{3}He surface exposure dating and its implications for magma evolution in the Portrillo volcanic field, Rio Grande Rift, New Mexico, USA. Geochimica et Cosmochmica Acta, 56, 4105-4108.

Appenzeller, C., Stocker, T.F. and Anklin, M. 1998. North Atlantic Oscillation dynamics recorded in Greenland ice cores. Science, 282, 446-449.

Arduino, E., Barberis, E., Carraro, F. and Forno, M.G. 1984. Estimating relative ages from iron-oxide/total-iron ratios of soils in western Po Valley, Italy. Geoderma, 33, 39-52.

Arenillas, M., Cantarino, I., Martìnez, R., Martìnez de Pisòn, E. and Pedrero, A. 1991. Los glaciares del Pirineo español. Revista de Obras Pùblilcas, 3, 9-19.

Armstrong, R.A. 1974. The descriptive ecology of saxicolous lichens in Wales. Journal of Ecology, 62, 33-45.

Arnaud-Fassetta, G. and Provansal, M. 1999. High frequency variations of water flux and sediment discharge during the Little Ice Age (1586-1735 AD) in the Rhône Delta (Mediterranean France). Relationship to the catchment basin. Hydrobiologia, 410, 241-250.

Asioli, A., Trincardi, F., Lowe, J.J., Ariztegui, D., Langone, L. and Oldfield, F. 2001. Sub-millennial scale climatic oscillations in the central Adriatic during the Lateglacial: palaeoceanographic implications. Quaternary Science Reviews, 20, 1201-1221.

Bailey, G.N., Lewin, J., Macklin, M.G. and Woodward, J.C. 1990. The "Older Fill" of the Voidomatis valley Northwest Greece and its relationship to the Palaeolithic archaeology and glacial history of the region. Journal of Archaeological Science, 17, 145-150.

Bailey, G., Turner, C., Woodward, J., Macklin, M. and Lewin, J. 1997. In Bailey, G.N. (Ed), Klithi: Palaeolithic settlement and Quaternary landscapes in northwest Greece, Volume 1. McDonald Institute, Cambridge, 321-345.

Bailiff, I.K. 1992. Luminescence dating of alluvial deposits. In: Needham, S. and Macklin, M.G. (Eds), Alluvial Archaeology in Britain, Oxbow Monograph 27, Oxford, Oxbow Press, 27-35.

Ballais, J.L. 1995. Alluvial Holocene terraces in eastern Maghreb: climate and anthropogenic controls. In: Lewin, J., Macklin, M.G., Woodward, J.C. (Eds.), Mediterranean Quaternary River Environments. Balkema, Rotterdam, 183-194.

Ballais, J.-L. 1998. The South of France and Corsica. In: Conacher, A.J. and Sala, M. (Eds), Land degradation in Mediterranean environments of the world; nature and extent, causes and solutions. John Wiley and Sons Ltd.

Bárcena, M.A., Cach, I., Abrantes, F., Sierro, F.J., Grimalt, J.O. and Flores, J.A. 2001. Paleoproductivity variations related to climatic conditions in the Alboran Sea (western Mediterranean) during the last glacial-interglacial transition: the diatom record. Palaeogeography, Palaeoclimatology, Palaeoecology, 167, 3-4, 337-357.

Bard, E., Hamelin, B., Arnold, M., Montaggioni, L., Cabioch, G., Faure, G. and Rougerie, F. 1996. Deglacial sea-level record form Tahiti corals and the timing of global meltwater discharge. Nature, 382, 241-244.

Bard, E., Hamelin, B. and Fairbanks, R.G. 1990. U-Th ages obtained by mass spectrometry in corals from Barbados – sea level during the past 130,000 years. Nature, 346, 456-459.

Bard E., Rostek, F., Turon, J.L. and Gendreau, S. 2000. Hydrological impact of Heinrich Events in the Subtropical Northeast Atlantic. Science, 289, 1321-1324.

Barker, G.W. and Hunt, C.O. 1995. Quaternary valley floor erosion and alluviation in the Bifferno Valley, Molise, Italy: the role of tectonics, climate, sea level change, and human activity. In: Lewin, J., Macklin, M.G. and Woodward, J.C. (Eds), Mediterranean Quaternary River Environments. Balkema, Rotterdam.

Barlow, L.K., White, J.W.C., Barry, R.G., Rogers, J.C. and Grootes, P.M. 1993. The North Atlantic oscillation signature in deuterium and deuterium excess signals in the Greenland Ice Sheet Project 2 ice core, 1840-1970. Geophysical Research Letters, 20, 24, 2901-2904.

Barriendos Vallve, M. and Martin-Vide, J. 1998. Secular climatic oscillations as indicated by catastrophic floods in the Spanish Mediterranean coastal area (14th-19th Centuries). Climatic Change, 38, 473-491.

Barron, E. and Pollard, D. High resolution climate simulations of oxygen isotope stage 3 in Europe. Quaternary Research, 58, 3, 296-309.

Bassi, G., Sabadini, R. and Rebaï, S. 1997. Modern tectonic regime in the Tyrrhenian area: observations and models. Geophysical Journal International, 129, 330-346.

Bateman, M.D. 2000. Quartz optical dating report for CL1. Unpublished report, Sheffield Centre for International Drylands Research (SCIDR).

Bateman, M.D. and Catt, J.A. 1996. An absolute chronology for the raised beach deposits at Sewerby, E. Yorkshire, U.K. Journal of Quaternary Science, 11, 389-395.

Beccaluva, L., Brotzu, P., Macciotta, G., Morbidelli, L., Serri, G. and Traversa, G. 1989. In: Boriani, A., Bonafede, M., Piccardo, G.B. and Vali, G.B. (Eds), The Lithosphere in Italy. Advances in Earth Science Research. Academia Nazionale dei Lincei, 229-248.

Beer, J. 2000. Long-term indirect indices of solar variability. Space Science Reviews, 94, 53-66.

Beer, J., Raisbeck, G.M. and Yiou, F. 1991. The variations of ^{10}Be and solar activity. In: Sonett, C.P. et al. (Eds), The Sun In Time. University of Arizona, Tucson, USA, 343-359.

Beer, J., Siegentaler, U., Bonani, G., Finkel, R.C., Oeschger, H., Suter, M and Wölfli, W. 1988. Information on past solar activity and geomagnetism from ^{10}Be in the Camp Century ice core. Nature, 331, 675-679.

Benedict, J.B. 1967. Recent Glacial History of an alpine area in the Colorado Front Range, U.S.A. I. Establishing a lichen growth curve. Journal of Glaciology, 6, 48, 817-832.

Benito, G. Machado, M.J. and Perez-Gonzalez, A. 1996. Climate change and flood sensitivity in Spain. In: Branson, J., Brown, A.G. and Gregory, K.J. (Eds), Global Continental Changes: the Context of Palaeohydrology. Geological Society Special Publications, 115, 85-98.

Bennett, K.D., Tzedakis, P.C. and Willis, K.J. 1991. Quaternary refugia of north European trees. Journal of Biogeography, 18, 103-115.

Berger, G.W. 1996. Progress in luminescence dating methods for Quaternary sediments. In: Rutter, N.W. and Catto, N.R. (Eds), Dating Methods for Quaternary Deposits. Geological Association of Canada, 1-23.

Berger W.H. and Jansen, E. 1995. Younger Dryas episode: Ice collapse and superfjord heat pump. In: Troelstra, S.R., van Hinte, J.E. and Ganssen, G.M. (Eds), The Younger Dryas. North Holland, Amsterdam, 61-105.

Beschel, R.E. 1961. Dating rock surfaces by lichen growth and its application to glaciology and physiography (lichenometry). In Raasch, G.O (Ed), Geology of the Arctic 2. Toronto, University of Toronto Press, 1044-1062.

Bierman, P.R. 1994. Using in situ produced cosmogenic isotopes to estimate rates of landscape evolution: A review from the geomorphic perspective. Journal of Geophysical Research, 99, B7, 13885-13896.

Bierman, P.R. and Gillespie, A.R. 1991. The evolution of granitic landforms, field observations and cosmogenic insights. Geological Society of America, Abstracts with Programs, 23, 5, 89.

Bierman, P.R., Gillespie, A.R. and Caffee, M.W. 1995. Cosmogenic ages for earthquake recurrence, intervals and debris flow fan deposition, Owens Valley, California. Science, 270, 447-450.

Bierman, P.R., Marsella, K.A., Patterson, C., Thompson Davis, P. and Caffee, M. 1999. Mid-Pleistocene cosmogenic minimum-age limits for pre-Wisconsian glacial surfaces in southwestern Minnesota and southern Baffin Island: a multiple approach. Geomorphology, 27, 25-39.

Bigg, G.R. 1994. An ocean general circulation model view of the glacial Mediterranean thermohaline circulation. Palaeoceanography, 9, 5, 705-722.

Billard, A. and Orombelli, G. 1986. Quaternary glaciaitons in the French and Italian Piedmonts of the Alps. Quaternary Science Reviews, 5, 407-411.

Bilzi, A.F. and Ciolkosz, E.J. 1977. A field morphology rating scale for evaluating pedological development. Soil Science, 124, 45-48.

Bintliff, J.L. 1976. The plain of Western Macedonia and the Neolithic site of Nea Nikomedeia. Proceedings of the Prehistoric Society, 42, 241-262.

Bintliff, J.L. 1977. Natural Environment and Human Settlement in Prehistoric Greece. British Archaeological Report Supplementary Series, 28. BAR, Oxford.

Birkeland, P.W. 1974. Pedology, Weathering and Geomorphological Research. Oxford University Press, New York.

Birkeland, P.W. 1982. Subdivision of Holocene glacial deposits, Ben Ohau Range, New Zealand using relative-dating methods. Geological Society of America Bulletin, 93, 433-449.

Birkeland, P.W. 1984. Holocene soil chronofunctions, Southern Alps, New Zealand. Geoderma, 34, 115-134.

Birkeland, P.W. 1999. Soils and Geomorphology. Third edition. Oxford University Press, New York.

Birkeland, P.W. 1990. Soil-geomorphic research – a selective overview. Geomorphology, 3, 207-224.

Birman, J.H. 1968. Glacial reconnaissance in Turkey. Geological Society of America Bulletin, 79, 1009-1026.

Blum, M.D. 1990. Climatic and eustatic controls on the Gulf Coastal Plain fluvial sedimentation: an example from the Late Quaternary of the Colorado River, Texas. In: Armentrout, J.M. and Perkins, B.F. (Eds), Sequence Stratigraphy as an Exploration Tool: Concepts and Practices in the Gulf Coast. Gulf Coast Section of the Society of Economic Palaeontologists and Mineralogists Foundation, Proceeding of the 11th Annual Research Conference, 71-83.

Blum, M.D. and Törnqvist, T.E. 2000. Fluvial responses to climate and sea-level change: a review and look forward. Sedimentology, 47, 1, 2-48.

Blume, H.P. and Schwertmann, U. 1969. Genetic evaluation of profile distribution of aluminium, iron and manganese oxides. Soil Science Society of America Proceedings, 33, 438-444.

Bockheim, J.G. 1980. Solution and use of chronofunctions in studying soil development. Geoderma, 24, 71-85.

Boenzi, F. and Palmentola, G.B. 1997. Glacial features and snow-line trend during the last glacial age in the Southern Apennines (Italy) and on the Albanian and Greek mountains. Zeitschrift fur Geomorphologie N.F. 41, 21-29.

Bond, G. and 13 others. 1992. Evidence for massive discharge if icebergs into the North Atlantic ocean during the last glacial period. Nature, 360, 245-249.

Bond, G.C., Broecker, W., Johnsen, S., McManus, J., Labeyrie, L., Jouzel, J. and Bonani, G. 1993. Correlations between climate records from North Atlantic sediments and Greenland ice. Nature, 365, 143-147.

Bond, G.C., Heinrich, H., Broecker, W., Labeyrie, L., McManus, J., Andrews, J., Huon, S., Jantschik, R., Clasen, S., Simet, C., Tedesco, K., Klas, M., Bnani, G. and Ivy, S. 1992. Evidence for massive discharges of ice bergs into the North Atlantic Ocean during the last glacial period. Nature, 360, 245-249.

Bond, G., Kromer, B., Beer, J., Muscheler, R., Evans, M.N., Showers, W., Hoffmann, S., Lotti-Bond, R., Hajdas, I. and Bonani, G. 2001. Persistent solar influence on North Atlantic climate during the Holocene. Science, 294, 2130-2136.

Bond, G.C., Showers, W., Cheseby, M., Lotti, R., Almasi, P., deMenocal, P., Priore, P., Cullen, H., Hajdas, I. and Bonani, G. 1997. A pervasive millennial-scale cycle in North Atlantic Holocene and glacial climates. Science, 278, 1257-1265.

Borchard, G. and Hill, R.L. 1985. Smectitic pedogenesis and late Holocene tectonism along the Raymond Fault, San Marino, California. In: Weide, D.L. (Ed.), Soils and Quaternary Geology of the Southwestern United States. Geological Survey of America Special Paper, 203.

Borovikova, L.N., Denisov, Y.M., Trofimova, E.B. and Shentsis. 1972. Matematicheskoye modelirovanie protessa stoka gornukh rek (On mathematical modelling of the mountain rivers' runoff). Lenigrad, Hydrometeoizdat, 152.

Botter-Jensen, L. 1998. Luminescence techniques: instrumentation and methods. Radiation Measurements, 27, 5-6, 749-768.

Bradley, R.S., and Jones, P.D. (Eds). 1995. Climate since A.D. 1500. Routledge, London 1-16.

Braithwaite, R.J. 1977. Temperature and glacier ablation - a parametric approach. Ph.D. Thesis, McGill University.

Braithwaite, R.J. 1981. On glacier energy balance, ablation and air temperature. Journal of Glaciology, 27, 381-391.

Braithwaite, R.J. 1995. Positive degree-day factors for ablation on the Greenland ice sheet studies by energy-balance modelling. Journal of Glaciology, 41, 153-160.

Brázdil, R., Glaser, R., Pfister, C., Dobrovolny, Antoine, J., Barriendos, M., Camuffo.D., Deutsch, M., Enzi, S., Guidoboni, E., Kotyza, O. and Rodrigo, F.S. 1999. Flood events of selected European rivers in the sixteenth century, 239-285.

Briffa, K.R., Bartholin, T.S., Eckstein, D., Jones, P.D., Karlén, W., Schweingruber, F.H. and Zetterberg, P. 1990. A 1,400 year tree-ring record of summer temperatures in Fennoscandia. Nature, 346, 434-439.

Briffa, K.R., Jones, P.D., Vogel, R.B., Scheingruber, F.H., Balillie, M.G.L., Shiyatov, S.G. and Vaganov, E.A. 1999. European tree rings and climate in the 16th century. Climatic Change, 43, 151-168.

Broecker, W.S. 1997. Paleocean circulation during the last deglaciation; a bipolar seasaw? Paleoceanography, 13, 119-121.

Broecker, W.S. and Denton, G. 1989. The role of ocean-atmosphere reorganisation in glacial cycles. Geochimica et Costmochimica Acta, 53, 2465-2501.

Brook, E.J., Brown, E.T., Kurz, M.D., Ackert, R.P., Raisbeck, G.M. and Yiou, F. 1995. Constraints on age, erosion and uplift of Neogene glacial deposits in the Transantarctic Mountains using in situ cosmogenic ^{10}Be and ^{26}Al. Geology, 23, 1063-1066.

Brook, E.J. and Kurz, M.D. 1993. Surface-exposure chronology using in situ cosmogenic ^{3}He in Antarctic quartz sandstone boulders. Quaternary Research, 39, 1-10.

Brook, E.J., Kurz, M.D., Ackert, R.P., Denton, G.H. and Brown, E.T. 1993. Chronology of Taylor Glacier advances in the Arena Valley, Antarctica, using in situ cosmogenic ^{3}He and ^{10}Be. Quaternary Research, 39, 11-23.

Brown, A.G. 1998. Fluvial evidence of the Medieval warm period and the Late Medieval climatic deterioration in Europe. In: Benito, G., Baker, V.R. and Gregory, K.J. (Eds), Palaeohydrology and Environmental Change. Chichester, United Kingdom, Wiley, 43-52.

Brown, E.T., Brook, E.J., Raisbeck, G.M., Yiou, F. and Kurz, M.D. 1992. Effective attenuation lengths of cosmic rays producing ^{10}Be and ^{26}Al in quartz: Implications for exposure age dating. Geophysical Research Letters, 19, 369-372.

Brown, E.T., Edmond, J.M., Raisbeck, G.M., Yiou, F., Kurz, M.D. and Brook, E. 1991. Examination of surface exposure ages of Antarctic moraines using in situ produced ^{10}Be and ^{26}Al. Geochimica et Cosmochimica Acta, 55, 2269-2283.

Brown, E.T., Trull, T.W., Jean-Baptiste, P., Raisbeck, G., Bourlès, D., Yiou, F. and Marty, B. 2000. Determination of cosmogenic production rates of ^{10}Be, ^{3}He and ^{3}H in water. Nuclear Instruments and Methods of Physics Research B, 172, 873-883.

Brunet, C., Monie, P., Jolivet, L. and Cadet, J.P. 2000. Migration of compression and extension in the Tyrrhenian Sea, insights from Ar-40/Ar-39 ages on micas along a transect from Corsica to Tuscany. Tectonophysics, 321, 1, 127-155.

Brunetti, M., Buffoni, L., Maugeri, M. and Nanni, T. 2000. Precipitation intensity trends in northern Italy from 1865 to 1996. Theoretical and Applied Climatology, 20, 1017-1031.

Brunetti, M., Colacino, M., Maugeri, M and Nanni, T. 2001. Trends in the daily intensity of precipitation in Italy from 1951-1996. International Journal of Climatology, 21, 299-316.

Brunsden, D. and Thornes, J.B. 1979. Landscape sensitivity and change. Transactions of the Institute of British Geographers, New Series, 4, 463-484.

Buffoni, L., Maugeri, M., Nanni, T. 1999. Precipitation in Italy from 1833 to 1966. Theoretical and Applied Climatology, 63, 33-40.

Bull, W.B. 1979. Threshold of critical power in streams. Bulletin of the Geological Society of America, 90, 453-464.

Bull, W.B. 1988. Floods, degradation and aggradation. In: Baker, V.R., Kochel, R.C. and Patton, P.C. (Eds), Flood Geomorphology. John Wiley, New York, 157-165.

Bull, W.B. 1991. Geomorphic Responses to Climatic Change. Oxford University Press, Oxford.

Burbank, D.W., Leland, J., Fielding, E., Anderson, R.S., Brozovic, N., Reid, M.R. and Duncan, C. 1996. Bedrock incision, rock uplift and threshold hill slopes in the Northwest Himalayas. Nature, 379, 505-510.

Burgueño, A. 1980. Diversos aspectos climatológicos de la lluvia en Barcelona. Tesina de llicenciatura, Facultat de Física, Universitat de Barcelona.

Burjachs, F. and Juliá, R. 1994. Abrupt climatic changes during the last interglaciation based on pollen analysis of the Abric Romani, Catalonia, Spain. Quaternary Research, 42, 308-315.

Busacca, A.J. 1987. Pedogenesis of a chronsequence in the Sacramento Valley, California, California USA. I. Application of soil development index. Geoderma, 41, 123-148.

Butzer, K.W. 1971. Environment and archaeology: an ecological approach to prehistory. Aldine Pub. Co.

Butzer, K.W. 1980. Holocene alluvial sequence: problems of dating and correlation. In: Cullingford, R.A., Davidson, D.A. and Lewin, J. (Eds), Timescales in Geomorphology. John Wiley, New York, 131-142.

Cacho, I., Grimalt, J.O., Canals, M., Sbaffi, L., Shackleton, N.J., Schonfeld, J. and Zahn, R. 2001. Variability of the western Mediterranean Sea surface temperature during the last 25,000 years and its connection with the Northern Hemisphere climatic changes. Paleoceanography, 16, 1, 40-52.

Cacho, I., Grimalt, J.O., Pelejero, C., Canals, M., Sierro, F.J., Flores, J.A. and Shackleton, N.J. 1999. Dansgaard-Oeschger and Heinrich event imprints in the Alboran Sea paleotemperatures. Paleoceanography, 14, 698-705.

Campbell, I.D., Campbell, C., Apps, M.J., Rutter, N.W. and Bush, A.B.G. 1998. Late Holocene ~1500 yr climatic periodicities and their implications. Geology, 26, 5, 471-473.

Camuffo, D. and Enzi, S. 1995. Reconstructing the climate of northern Italy from archive sources. In: Bradley, R.S., and Jones, P.D. (Eds), Climate since A.D. 1500. Routledge, London, 143-154.

Camuffo, D., Secco, C., Brimblecombe, P and Martin-Vide, J. 2000. Sea storms in the Adriatic Sea and the western Mediterranean during the last millennium. Climatic Change, 46, 209-223.

Carmigani, L., Decandia, F.A., Disperati, L., Fantozzi, P.L., Lazzarotto, A., Liotta, D. and Oggiano, G. 1995. Relationships between the Tertiary structural evolution of the Sardinia-Corsica-Provençal domain and the Northern Apennines. Terra Nova, 7, 128-137.

Castagnoli, G., Albrecht, A., Beer, J., Bonino, G., Shen, C., Callegari, E., Taricco, C., Dittrich-Hannen, B., Kubik, P., Suter, M. and Zhu, G.M. 1995. Evidence for enhanced ^{10}Be deposition on Mediterranean sediment 35 kyr BP. Geophysical Research Letters, 22, 707-710.

Castagnoli, G.C., Bonino, G., Taricco, C. and Lehman, B. 1998. Cosmogenic isotopes and geomagnetic signals in a Mediterranean Sea sediment at 35 000 y BP. Il Nuovo Cimento, 21C, 2, 243-246.

Catt, J.A. 1986. Soils and Quaternary Geology: A Handbook for Field Scientists. Clarendon Press, Oxford.

Cayre, O., Lancelot, Y., Vincent, E. and Hall, M.A. 1999. Paleoceanographic reconstructions from planktonic foraminifera off the Iberian Margin: Temperature, salinity and Heinrich Events. Paleoceanography, 14, 384-396.

Cerling, T.E. 1990. Dating geomorphologic surfaces using cosmogenic ^{3}He. Quaternary Research, 33, 148-156.

Cerling, T.E. and Craig, H. 1994. Geomorphology and in-situ cosmogenic isotopes. Annual Review of Earth Planetary Science, 22, 273-317.

Cerling, T.E., Poreda, R.J. and Rathburn, S.L. 1994. Cosmogenic ^{3}He and ^{21}Ne age of the Big Lost River Flood, Snake River Plain, Idaho. Geology, 22, 227-230.

Cerling, T.E., Webb, R.H., Poreda, R.J., Rigby, A.D. and Melis, T.S. 1999. Cosmogenic He-3 ages and frequency of late Holocene debris flows from Prospect Canyon, Grand Canyon, USA. Geomorphology, 27, 1-2, 93-111.

Chadwick, O.A., Hall, R.D. and Phillips, F.M. 1997. Chronology of Pleistocene glacial advances in the central Rocky Mountains. Geological Society of America Bulletin, 109, 11, 1443-1452.

Chadwyck and Healey, 1992. World Climate Disk, Global Climatic Change Data (on CD-ROM). Chadwyck and Healey Ltd, Cambridge.

Chappell, J. and Shackleton, N.J. 1986. Oxygen isotopes and sea level. Nature, 324, 137-140.

Chen, J.H., Curran, H.A., White, B. and Wasserburg, G.J. 1991. Precise chronology of the last interglacial period: ^{234}U/^{230}Th Data from fossil coral reefs in the Bahamas. Bulletin of the Geological Society of America, 103, 82-97.

Chorley, R.J. 1962. Geomorphology and general systems theory. Unites States Geological Survey Professional Paper, 500B.

Church, M., Kellerhals, R. and Day, T.J. 1989. Regional clastic sediment yield in British Colombia. Canadian Journal of Earth Science, 26, 31-45.

Church, M. and Ryder, J.M. 1972. Paraglacial sedimentation: a consideration of fluvial processes conditioned by glaciation. Geological Society of America Bulletin, 83, 3059-3072.

Clapp, E.M., Bierman, P.R., Schick, A.P., Lekach, J., Enzel, Y. and Caffee, M. 2000. Sediment yield exceeds sediment production in arid region drainage basins. Geology, 28, 11, 995-998.

Clapperton, C. 1995. Fluctuations of local glaciers at the termination of the Pleistocene: 18-8 ka BP. Quaternary International, 28, 41-50.

Clark, D., Bierman, P.R. and Larsen, P. 1995. Improving in situ cosmogenic chronometers. Quaternary Research, 44, 366-376.

Clark, P.U. and Bartlein, P.J. 1995. Correlation of the Late Pleistocene glaciation on the western United States with North Atlantic Heinrich events. Geology, 23, 483-486.

Clark, P.U., Marshall, S.J., Clarke, G.K.C., Hostetler, S.W., Licciardi, J.M. and Teller, J.T. 2001. Freshwater forcing of abrupt climate change during the last glaciation. Science, 293, 283-287.

Clarke, M.L. 1996. IRSL dating of sands: Bleaching characterstic at deposition inferred from the use of single aliquots. Radiation Measurements, 26, 4, 611-620.

COHMAP Members. 1988. Climatic changes of the last 18,000 years: observations and model simulations. Science, 241, 1043-1052.

Collier, R.E.L., Leeder, M.R. and Jackson, J.A. 1995. Quaternary drainage development, sediment fluxes and extensional tectonics in Greece. In: Lewin, J., Macklin, M.G., Woodward, J.C. (Eds), Mediterranean Quaternary River Environments. Balkema, Rotterdam, 31-44.

Collier, R.E.L., Leeder, M.R., Trout, M., Ferentinos, G., Lyberis, E. and Papatheodoeou, G. 2000. High sediment yields and cool, wet winters: Test of last glacial paleoclimates in the northern Mediterranean. Geology, 28, 11, 999-1002.

Colls, A.E. 1999. Optical dating of fluvial sediments from the Loire Valley, France. Unpublished M.Sc Thesis, University of Oxford, Oxford.

Colls, A.E., Stokes, S., Blum, M.D. and Straffin, E. 2001. Age limits on the Late Quaternary evolution of the upper Loire River. Quaternary Science Reviews, 20, 743-750.

Combourieu-Nebout, N., Paterne, M., Turon, J.-L., Siani, G. 1998. A high resolution record of the last deglaciaiton in the central Mediterranean Sea: Palaeovegetation and palaeohydrological evolution. Quaternary Science Reviews, 17, 4-5, 303-317.

Conacher, A.J. and Sala, M. (Eds). 1998. Land Degradation in Mediterranean Environments of the World. Wiley.

Conchon, O. 1975. Les formations quaternaires de type continental en Corse orientale: Thèse, L'Université de Paris VI.

Conchon, O. 1977. Les glaciations quaternaires dans le Centre-Sud de la Corse. Comparison avec la Corse du Nord et les regions perimediterraneennes: Bull. Soc. France, XIX, 5, 1041-1045.

Conchon, O. 1978. Quaternary studies in Corsica (France). Quaternary Research, 9, 41-53.

Conchon, O. 1982. The Last Glaciation in Corsica: International Geological Correlation Programme. Quaternary Glaciations in the Quaternary: A field Guide.

Conchon, O. 1986. Quaternary glaciations in Corsica. Quaternary Science Reviews, 5, 429-432.

Conchon, O. 1988. Paléogéographie et paléoclimatologie de las Corse au Quaternaire. Chronolgie des événements. Bull. Soc. Géol. France, 8, 4, 587-594.

Conchon, O. & Gauthier, A. 1985. Phenomenes naturels exceptionnels en Corse: Interet pur l'etude geologique de la periode Quaternaire. Sciences Naturelles, 142-165.

Cook, E.R., D'Arrigo, R.D. and Briffa, K.R. 1998. A reconstruction of the North Atlantic Oscillation using tree-ring chronologies from North America and Europe. Holocene, 8, 9-17.

Craig, H. and Poreda, R.J. 1986. Cosmogenic ^{3}He in terrestrial rocks: The summit lavas of Maui. Proceedings of the National Academy of Science, USA, 83, 1970-1974.

Cullen, H.M., D'Arrigo, R.D., Cook, E.R. and Mann, M.E. 2001. Multiproxy reconstructions of the North Atlantic Oscillation. Paleoceanography, 16, 1, 27-39.

Dansgaard, W., Johnson, S.J., Clausen, H.B., Dahl-Jensen, D., Gundenstrup, N.S., Hammer, C.U., Hvidberg, C.S., Steffensen, J.P. and Sveinbjörnsdóttir, A.E. 1993. Evidence for general instability of past climate from a 250-kyr ice-core record. Nature, 364, 218-220.

Dansgaard, W., White, J.W.C., and Johnsen, S.J. 1989. The abrupt termination of the Younger Dryas climate event. Nature, 339, 532-534.

D'Arrigo, R.D., Cook, E.R., Jacoby, G.C. and Briffa, K.R. 1993. NAO and sea surface temperature signatures in tree-ring records from the North Atlantic sector. Quaternary Science Reviews, 12, 431-440.

Davidson, D.A. 1980. Erosion in Greece during the First and Second Millenia B.C. In: Cullingford, R.A. and Davidson, D.A. (Eds), Timescales in Geomorphology. New York, John Wiley, 143-158.

Davis, R. and Schaeffer, O.A. 1955. Chlorine – 36 in nature: Ann. N.Y. Acad.Sci.,62, 105-122.

de Beaulieu, J-L., Andrieu, V., Ponel, P., Reille, M. and Lowe, J.J. 1994. The Weichselian Late-glacial in southwestern Europe (Iberian Peninsula, Pyrenees, Massif Central, northern Apennines). Journal of Quaternary Science, 9, 101-107.

de Beaulieu, J-L., Pons, A and Reille, M. 1985. Recherches pollenanalytiques sur l'histoire de la végétation de la bordure nord du Massif de Cantal (Massif Central, France). Pollen et Spores, 24, 251-300.

de Beaulieu, J-L. and Reille, M. 1984. A long upper Pleistocene pollen record from Les Echets, near Lyon, France. Boreas, 13, 2, 111-132.

de Beaulieu J-L. and Reille, M. 1992. The last climatic cycle at la Grande Pile (Vosages, France) a new pollen profile. Quaternary Science Reviews, 11, 431-438.

de Raparaz, A. 1990. La culture en terrasses, expression de la petite paysannerie mediterranéenne traditionelle. Méditerranée, 71, 23-29.

Dearing, J. 1999. Magnetic susceptibility. In: Walden, J., Oldfield, F. and Smith. J. (Eds), Environmental magnetism: A practical guide. Quaternary Research Association, Technical Guide 6, 35-63.

Dearing, J.A., Bird, P.M., Dann, R.J.L. and Benjamin, S.F. 1997. Secondary ferrimagnetic minerals in Welsh soils: a comparison of mineral magnetic detection methods and implications for mineral formation. Geophysical Journal International, 130, 727-736.

Dearing, J.A., Dann, R.J.L., Hay, K., Lees, J.A., Loveland, P.J., Maher, B.A. and O'Grady, K. 1996a. Frequency-dependent susceptibility measurements of environmental materials. Geophysical Journal International, 124, 228-240.

Dearing, J.A., Hay, K.L., Baban, S.M.J., Huddleston, A.S., Wellington, E.M.H. and Loveland, P.J. 1996b. Magnetic susceptibility of soil: an evaluation of conflicting theories using a national data set. Geophysical Journal International 127, 728-734.

Delworth, T., Manabe, S. and Stouffer, R.J. 1993. Interdecadal variability of the thermohaline circulation in a coupled ocean-atmosphere model. Journal of Climatology, 6, 1993-2011.

Delworth, T.L., Manabe, S. and Stouffer, R.J. 1997. Multidecadal climate variability in the Greenland Sea and surrounding regions: A coupled model simulation. Geophysical Research Letters, 24, 257-260.

Demitrack, A. 1986. The Late Quaternary Geologic History of the Larissa Plain, Thessaly, Greece: Tectonic, Climatic and Human Impact on the landscape. Ph.D. dissertation, Stanford University, CA, Ann Arbor, Michigan: University Microfilms.

Denton, G.H. and Hendy, C.H. 1994. Younger Dryas age advance of Franz-Josef Glacier in the Southern Alps of New Zealand. Science, 264, 1434-1437.

Desilets, D. and Zreda, M. 2001. On scaling cosmogenic nuclide production rates for altitude and latitude using cosmic-ray measurements. Earth and Planetary Science Letters, 193, 213-225.

Devereux, C.M. 1983. Recent erosion and sedimentation in southern Portugal. Unpublished PhD thesis, University of London.

Dewey, J.F., Pitman III, W.C., Ryan, W.B.F. and Bonnin, J. 1973. Plate tectonics and the evolution of the Alpine system. Geological Society of America Bulletin, 84, 3137-3180 .

D'Orefice, M. Pecci, M., Smiraglia, C. and Ventura, R. 2000. Retreat of Mediterranean glaciers since the Little Ice Age: Case study of Ghiacciaio del Calderone, Central Apennines, Italy. Arctic and Alpine Research, 32, 2, 197-201.

Dorronsoro, C. and Alonso, P. 1994. Chronosequence in Almar River fluvial-terrace soil. Soil Science Society og America Journal, 58, 3, 910-925.

Doswell III, C.A., Ramis, C., Romero, R. and Alonso, S. 1998. A diagnostic study of three heavy precipitation episodes in the western Mediterranean region. Weather Forecast, 13, 102-124

Dubar, M. 1987. Donneés nouvelles sur la transgression Holocène dans le région de Nice (France). Bull. Soc. Géol. France, 8, 3, 1, 195-198.

Duller, G.A.T. 1991. Equivalent dose determination of single aliquots. Nuclear Tracks and Radiation Measurements, 18, 371-378.

Duller, G.A.T. 1995. Luminescence dating of sediments using single aliquots: methods and applications. Radiation Measurements, 24, 3, 217-226.

Duller, G.A.T. 1996. Recent developments in luminescence dating of Quaternary sediments. Progress in Physical Geography, 20, 2, 127-145.

Dunai, T.J. 2000. Scaling factors for production rates of in situ produced cosmogenic nuclides: a critical reevaluation. Earth and Planetary Science Letters, 176, 157-169.

Dunai, T.J. 2001. Influence of secular variation of the geomagnetic field on production rates of in situ produced cosmogenic nuclides. Earth and Planetary Science Letters, 193, 197-212.

Duplessy, J.C., Labeyrie, L., Arnold, M., Paterne, M., Duprat, J. and Vanweering, T.C.E. 1992. Changes in surface salinity of the North Atlantic Ocean during the last deglaciation. Nature, 358, 6848, 724-727.

Easton, R.M. 1994. Lichens and Rocks: A Review. Geoscience Canada, 21-2, 59-76.

Eddy, J.A. 1977. Climate and the changing Sun. Climatic Change, 1, 2, 173-190.

Egal, E. 1992. Structures and tectonic evolution of the external zone of Alpine Corsica. Journal of Structural Geology, 14, 1215-1228.

Ely, L.L. 1997. Response of extreme floods in the southwestern United States to climatic variations in the late Holocene. Geomorphology, 19, 3-4, 175-201.

Evenson, E., Gosse, J. and Klein, J. 1993. Application of in situ produced cosmogenic nuclide exposure ages to reconstruct glacial histories at the Pinedale type locality, Wyoming. Geological Society of American Abstracts with Programs, 25, 6, 308.

Evenson, E.B., Klein, J., Lawn, B., Middleton, R. and Gosse, J. 1994. Glacial chronology of the Wind River Mountains from measurements of cosmogenic radionuclides in boulders. Geological Society of American Abstracts with Programs, 26, A-511.

Fabel, D. and Harbor, J. 1999. The use of in-situ produced cosmogenic radionuclides in glaciology amd glacial geomorphology. Annals of Glaciology, 28, 103-110.

Fawcett, P.J., Ágústsdóttir, A.M., Alley, R.B. and Shuman, C.A. 1997. The Younger Dryas termination and North Atlantic deep water formation: insight from climate model simulations and Greenland ice cores. Paleoceanography, 12, 23-38.

Felis, T., Pätzold, J., Loya, Y., Fine, M., Nawar, A.H. and Wefer, G. 2000. A coral oxygen isotope record from the northern Red Sea documenting NAO, ENSO, and North Pacific teleconnections on Middle East climate variability since the year 1750. Paleoceanography, 15, 6, 679-694

Ferguson, R.I. 1993. Understanding braiding processes in gravel-bed rivers: progress and unsolved problems. In: Bristow, C.S. and Best, J.L. (Eds), Braided Rivers, Geological Society of London, Special Publication, 75, 73-88.

Fernandez Mosquera, D., Marti, K., Vidal Romani, J.R. and Weigel, A. 2000. Late Pleistocene deglaciation chronology in the NW of the Iberian Peninsula using cosmic-ray produced ^{21}Ne in quartz. Nuclear Instruments and Methods in Physics Research B, 172, 832-837.

Ferrandini, J., Bethoux, N., Gauthier, A., Frechet, J., Thouvenot, F. and Fotaine, C. 1994. Première tentative d'étude sismotectonique de la Corse à partir des données d'un reséau sismologique régional et de la campagne, SISBALIG II, C.R. Acad. Sci. Paris, 319, 705-712.

Finke, E.A.W. 1988. Landscape Evolution of the Argive Plain, Greece: Paleoecology, Holocene Depositional History and Coastline Changes. Ph.D dissertation, Stanfors University, CA, Ann Arbor: University Microfilms.

Flemming, N.C. 1969. Archaeological Evidence for Eustatic Change of Sea Level and Earth Movements in the Western Mediterranean during the last 2000 years. The Geological Society of America, Special Paper 109.

Flocas, A.A. 1988. Frontal depressions over the Mediterranean Sea and central Southern Europe. Méditerranée, 66, 4, 43-52.

Florschütz, F., Menendez Amor, J. and Wijmstra, T.A. 1971. Palynology of a thick Quaternary succession in southern Spain. Palaeogeography, Palaeoclimatology, Palaeoecology, 10, 233-264.

Folland, C.K. 1983. Regional-scale interannual variability of climate - a northwest European perspective. Meteorological Magazine, 112, 163-183.

Follieri, M., Giardini, M., Magri, D. and Sadori, L. 1988. 250 000 year pollen record from Valle di Castiglione (Roma). Pollen et Spores, 30, 329-356.

Follieri, M., Giardini, M., Magri, D. and Sadori, L. 1998. Palynostratigraphy of the last glacial period in the volcanic region of central Italy. Quaternary International, 47/48, 3-20.

Font Tullot, I. 1988. Historia del Clima de España . Instituto Nacional de Meteorologia, Madrid.

Frank, M. 2000. Comparison of cosmogenic radionuclide production and geomagnetic field intensity over the last 200 000 years. Philosophical Transactions of the Royal Society of London, A358, 1089, 1107.

Frank, M., Schwarz, B., Baumann, S., Kubik, P.W., Suter, M. and Mangini, A. 1997. A 200 kyr record of cosmogenic radionuclide production rate and geomagnetic field intensity from Be-10 in globally stacked deep sea sediments. Earth and Planetary Science Letters, 149, 1-4, 121-129.

Friedman, G.M. and Sanders, J.E. 1978. Principles of Sedimentology. Wiley, New York.

Friedrich, M., Kromer, B., Kaiser, K.F., Spurk, M., Hughen, K.A. and Johnsen, S.J. 2001. High-resolution climate signals in the Bølling-Allerød Interstadial (Greenland Interstadial 1) as reflected in European tree-ring chronologies compared to marine varves and ice-core records. Quaternary Science Reviews, 20, 1223-1232.

Frogley, M.R., Griffiths, H.I. and Heaton, T.H.E. 2001. Historical biogeography and Late Quaternary environmental change of Lake Pamvotis, Ioannina (north-western Greece): evidence from ostracods. Journal of Biogeography, 28, 6, 745-756.

Frostick, L.E. and Reid, I. 1989. Climatic versus tectonic controls of fan sequences: lessons from the Dead Sea Israel. Journal of the Geological Society, London, 146, 527-538.

Fuller, I.C., Macklin, M.G., Lewin, J., Passmore, D.G., Wintle, A.G. 1998. River response to high-frequency climate oscillations in southern Europe over the past 200 k.y. Geology, 26, 3, 275-278.

Fuller, I.C., Macklin, M.G., Passmore, D.G., Brewer, P.A., Lewin, J., Wintle, A.G. 1996. Geochronologies and environmental records of Quaternary fluvial sequences in the Guadalope basin, northeast Spain, based on luminesence dating. In: Branson, J., Brown, A.G., Gregory, K.J. (Eds), Global continental changes: the context of palaeohydrology. Geological Society (London) Special Publication 115, 99-120.

Fuller, I.C., Wintle, A.G. and Duller, G.A.T. 1994. Test of the partial bleach methodology as applied to the infra-red stimulated luminescence of an alluvial sediment from the Danube. Quaternary Geochronology (Quaternary Science Reviews) 13, 539-544.

Gale, S.J. and Hoare, P.G. 1997. The glacial history of the northwest Picos de Europa of northern Spain. Zeitschrift fur Geomorphologie, N.F. 41, 81-96.

Galloway, R.B. 1996. Equivalent dose determination using only one aliquot: alternative analysis of data obtained from Infra red stimulation of feldspars. Radiation Measurements, 26, 103-106.

Gallup, C.D., Edwards, R.L. and Johnson, R.G. 1994. The timing of high sea levels over the past 200,000 years. Science, 263, 796-800.

Gellatly, A.F, Grove J.M., Bücher, A., Latham, R. and Whalley, W.B. 1995. Recent historical fluctuations of the Glacier du Taillon, Pyrenees. Physical Geography, 15, 399-413.

Gellatly, A.F., Smiraglia, C., Grove, J.M. and Latham, R. 1994. Recent variations of Ghiacciaio del Calderone, Abruzzi, Italy. Journal of Glaciology, 40, 136, 486-490.

Ghil, M. and Vautard, R. 1991. Interdecadal oscillations and the warming trend in global temperature time series. Nature, 350, 324-327.

Giraudi, C. and Frezzotti, M. 1997. Late Pleistocene glacial events in the Central Apennines, Italy. Quaternary Research, 48, 280-290.

Gosse, J.C. and Phillips, F.M. 2001. Terrestrial in situ cosmogenic nuclides: theory and application. Quaternary Science Reviews, 20, 1475-1560.

Gosse, J.C., Grant, D.R., Klein, J. and Lawn, B. 1995. Precise cosmogenic 10-Be measurements in western North America: a support for a global Younger Dryas cooling event. Geology, 23, 877-880.

Gosse, J.C., Klein, J., Evenson, E.B., Lawn, B. and Middleton, R. 1995. Beryllium-10 dating of the duration and retreat of the Last Pinedale Glacial Sequence. Science, 268, 1329-1333.

Goudi, A., Anderson, M., Burt, T., Lewin, J., Richards, K., Whalley, B. and Worsley, P. 1990. Geomorphological Techniques. Second Edition. British Geomorphological Research Group Publication, Unwin Hyman Ltd, London.

Graf, T., Kohl, C.P., Marti, K. and Nishiizumi, K. 1991. Cosmic ray produced neon in Antarctic rocks. Geophysical Research Letters, 18, 203-6.

Gran, S.E., Matmon, A., Bierman, P.R., Enzel, Y. and Caffee, M. 1999. Evidence for rapid, Holocene displacement on the Nahef East normal fault, northern Israel; a cosmogenic Cl-36 approach. Abstracts with Programs, Geological Society of America, 31, 7, 301-012.

Granger, D.E., Kirchner, J.W. and Finkel, R.C. 1997. Quaternary downcutting rate of the New River, Virginia measured from differential decay of cosmogenic ^{26}Al and ^{10}Be in cave deposited alluvium. Geology, 25, 107-110.

Griffies, S.M. and Bryan, K. 1997. Predictability of North Atlantic multidecadal climate variability. Science, 275, 5297, 181-184.

Grootes, P.M., Stuiver, M., White, J.W.C., Johnsen, S., and Jouzel, J. 1993. Comparison of oxygen isotope records from the GISP2 and GRIP Greenland ice cores. Nature, 366, 552-554.

Gross, M.G. 1971. In: Carver, E.D. (Ed), Procedures in Sedimentary Petrology. Wiley, New York.

Grove, A.T. 1997. Classics in physical geography. Progress in Physical Geograpahy, 21, 251-256.

Grove, A.T. 2001. The "Little Ice Age" and its geomorphological consequences in Mediterranean Europe. Climatic Change, 48, 121-136.

Grove, A.T. and Rackham, O. 2001. The Nature of Mediterranean Europe: an Ecological History. Yale, U.P.

Grove, J.M. 1988. The Little Ice Age. Meuthen and Co. Ltd.

Gualtieri, L. Glushkova, O. and Brigham-Grette, J. 2000. Evidence for restricted ice extent during the last glacial maximum in the Koryak Mountains of Chukotka, far eastern Russia. Geological Society of America Bulletin, 112, 7, 1106-1118.

Guiot, J. 1990. Methodology of the last climatic cycle reconstruction from pollen data. Palaeogeography, Palaeoclimatology and Palaeoecology, 80, 46-69.

Guiot, J., Beaulieu, J.L., Cheddadi, R., David, F., Ponel, P. and Reille, M. 1993. The climate in western Europe during the last Glacial/Interglacial cycle derived from pollen and insect remains. Palaeogeography, Palaeoclimatology, Palaeoecology, 103, 73-93.

Guiot J., Beaulieu, J.L. de, Pons, A. and Reille, M. 1989. A 140,000-year climatic reconstruction from two European pollen records. Nature, 338, 309-313.

Guiot, J., Torre, F., Jolly, D., Peyron, O., Boreaux, J.J. and Cheddadi, R. 2000. Inverse vegetation modeling by Monte Carlo sampling to reconstruct palaeoclimates under changed precipitation seasonality and CO_2 conditions: application to glacial climate in the Mediterranean region. Ecological Modelling, 127, 2-3, 119-40.

Guitérrez-Elorza, M. and Peña Monne, J.L. 1990. Upper Holocnee climatic change and geomorphological processes on slopes and infilled valleys from archaeological dating (NE Spain). In: Imeson, A.C. and DeGroot, R.S. (Eds), Landscape Ecological Impact of Climatic Change on the Mediterranean Region. Universities of Wegeningen, Utrecht and Amsterdam, 1-18.

Haas, J-N., Richoz, I, Tinner, W. and Wick, L. 1998. Synchronous Holocene climatic oscillations recorded on the Swiss Plateau and at timberline in the Alps. The Holocene 8, 3, 301-309.

Hall, A. and Stouffer, R.J. 2001. An abrupt climate event in a coupled ocean-atmosphere simulation without external forcing. Nature, 409, 171-174.

Hallet, B., Hunter, L. and Bogen, J. 1996. Rates of erosion and sediment evacuation by glaciers: A review of field data and their implications. Global and Planetary Change, 12, 213-235.

Hallet, B. and Putkonen, J. 1994. Surface dating of dynamic landforms: Young boulders on aging moraines. Science, 265, 937-940.

Hamlin, R. 2000. Environmental change and catastrophic flooding in the Voidomatis and Aoos basins, northwest Greece. Unpublished Ph.D Thesis, University of Leeds.

Hamlin, R.H.B., Woodward, J.C., Black, S., Macklin, M.G. 2000. Sediment fingerprinting as a tool for interpreting long-term river activity: the Voidomatis basin, NW Greece. In: Foster, I.D.L. (Ed), Tracers in Geomorphology. John Wiley and Sons, Chichester, 473-501.

Hancock, G.S., Anderson, R.S., Chadwick, O.A. and Finkel, R.C. 1999. Dating fluvial terraces with ^{10}Be and ^{26}Al profiles: application to the Wind River, Wyoming. Geomorphology, 27, 41-60.

Harden, J.W. 1982. A quantitative index of soil development from field descriptions: Examples from a chronosequence in central California. Geoderma, 28, 1-28.

Harden, J.W. 1987. Soils developed in granitic alluvium near Merced, California. U.S. Geological Survey Bulletin, 1590-A, 65 .

Harden, J.W. 1988. Genetic interpretations of elemental and chemical differences in a soil chronosequence, California. Geoderma, 43, 179-193.

Harden, J.W. and Taylor, E.M. 1983. A quantitative comparison of soil development in four climatic regimes. Quaternary Research, 20, 342-359.

Harrison, S.P. and Digerfeldt, G. 1993. European lakes as palaeohydrological and palaeoclimatic indicators. Quaternary Science Reviews, 12, 233-248.

Harrison, S.P., Yu, G. and Tarasov, P.E. 1996. The Late Quaternary lake-level record from northern Eurasia. Quaternary Research, 45, 138-159.

Harvey, A.M. 1996. The role of alluvial fans in the mountain fluvial systems of southeast Spain: implications of climatic change. Earth Surface Processes and Landforms, 21, 543-553.

Harvey, A.M. 2001. Coupling between hillslopes and channels in upland fluvial systems; implications for landscape sensitivity, illustrated from the Howgill Fells, Northwest England. Catena, 42, 2-4, 225-250.

Harvey, A. M., Alexander R.W. and James, P.A. 1984. Lichens, soil development and the age of Holocene valley floor landforms: Howgill Fells, Cumbria. Geografiska Annaler, 66A, 353-366.

Harvey, A.M., Miller, S.Y and Wells, S.G. 1995. Quaternary soil and river terrace sequences in the Aguas/Feos river systems: Sorbas basin, southeast Spain. In: Lewin, J., Macklin, M.G., Woodward, J.C (Eds), Mediterranean Quaternary River Environments. Balkema, Rotterdam, 263-281.

Harvey, A.M. and Wells, S.G. 1987. Response of Quaternary fluvial systems to differential epeirogenic uplift: Aguas and Feos river systems, southeast Spain. Geology, 15, 689-693.

Hays, J.D., Imbrie, J. and Shackleton, N.J. 1976. Variations in the earth's orbit: pacemaker of the ice ages. Science, 194, 1121-1132.

Heinrich, H. 1988. Origin and consequences of cycling ice rafting in the northwest Atlantic Ocean during the past 130,000 years. Quaternary Research, 29, 142-152.

Hérail, G., Hubschman, J. and Jalut, G. 1996. Quaternary glaciation in the French Pyrenees. Quaternary Science Reviews, 5, 397-402.

Higgitt, S.R., Oldfield, F. and Appleby, P.G. 1999. Appendix 1, Magnetic properties and their interpretation. The record of land use change and soil erosion in the late Holocene sediments of the Petit Lac d-Annecy, eastern France. The Holocene, 1, 14-28.

Higgs, E.S. and Vita Finzi, C. 1966. The climate, environment and industries of Stone Age Greece: Part II. Prehistoric Society Proceedings, 32, 1-29.

Higgs, E.S., Vita-Finzi, C., Harris, D.R. and Fagg, A.E. 1967. The climate, environment and industries of Stone Age Greece, part III. Proceedings of the Prehistoric Society, 33, 1-29.

Hoelzle, M. and Haeberli, W. 1999. World Glacier Inventory. World Glacier Monitoring Service and National Snow and Ice Data Centre, World Data Center fro Glaciology, Boulder, CO., Digital Media.

Holzhauser, H. and Zumbühl, H.J. 1996. The history of the Lower Grindlewald Glacier during the last 2800 years - paleosols, fossil wood and historical pictorial records - new results. Zeitschrift fur Geomorphologie, NF, 104, 95-127.

Holzhauser, H. and Zumbühl, H.J. 1999. Glacier fluctuations in the western Swiss and French Alps in the 16th century. Climatic Change, 43, 223-237.

Hong, D.G., Galloway, R.B. and Hashimoto, T. 2000. Additative dose single and multiple aliquot methods of equivalent dose determination compared for quartz luminescence stimulated by green light. Japanese Journal of Applied Physics, 39, 4209-4216.

Hounslow, M. and Maher, B.A. 1999. Laboratory procedures for quantitative extraction and analysis of magnetic minerals from sediments. In: Walden, J., Oldfield, F. and Smith. J. (Eds), Environmental magnetism: A practical guide. Quaternary Research Association, Technical Guide 6, 139-185.

Hughen, K.A., Overpeck, J.T., Peterson, L.C. and Trumbore, S. 1996. Rapid climate changes in the tropical Atlantic region during the last deglaciation. Nature, 380, 51-54.

Hunt, C.O. and Gilbertson, D.D. 1995. Human activity, landscape change and valley alluviation in the Feccia Valley, Tuscany, Italy. In: Lewin, J., Macklin, M.G., Woodward, J.C. (Eds.), Mediterranean Quaternary River Environments. Balkema, Rotterdam, 167-176

Huntley, B. and Birks, H.J.B. 1983. An Atlas of Past and Present Pollen Maps for Europe: 0-13,000 Years Ago. Cambridge, CUP

Huntley, B. and Prentice, I.C. 1993. Holocene vegetation and climates of Europe. In: Wright, H.E. *et al.* (Eds), Global Climates since the Last Glacial Maximum. University of Minnesota Press, Minneapolis, 569.

Huntley, D.J., Godfrey-Smith, D.I. and Thewalt, M.L.W. 1985. Optical dating of sediments. Nature, 313, 105-107.

Hurrell, J.W. 1995. Decadal trends in the North Atlantic Oscillation: Regional temperatures and precipitation. Science, 269, 676-679.

Hurrell, J.W. 1996. Influence of variations in extratropical wintertime teleconnections on Northern Hemisphere temperature. Geophysical Research Letters, 23, 665-668.

Hurrell, J.W. 2001. The North Atlantic Oscillation. Science, 291, 603-605.

Hurrell, J.W. and van Loon, H. 1997. Decadal variaitons in climate associated with the North Atlantic oscillation. Climatic Change, 36, 301-326.

Hurst, V.J. 1977. Visual estimation of iron in saprolite. Geological Society of America Bulletin, 88, 174-176.

Innes, J.L. 1983. Lichenometric dating of debris-flow deposits in the Scottish Highlands. Earth Surface Processes and Landforms, 8, 579-588.

Innes, J.L. 1984. The optimal sample size in lichenometric studies. Arctic and Alpine Research, 16, 233-244.

Innes, J.L. 1985. An examination of some factors affecting the largest lichenometrics on a substrate. Arctic and Alpine Research, 17, 98-106.

Innes, J.L. 1988. Use of lichens in dating. In: Galun, M. (Ed), Handbook of lichenology, CRC Press, Baton, Rouge, 75-92.

Ivy-Ochs, S. 1996. The dating of rock surfaces using in situ produced ^{10}Be, ^{26}Al and ^{36}Cl, with examples from Antartica and the Swiss Alps. Unpublished Ph.D. Thesis, ETH No. 11763, Swiss Federal Institute of Technology Zürich.

Ivy-Ochs, S., Schlüchter, C., Kubik, P.W. and Denton, G.H. 1999. Moraine exposure dates imply synchronous Younger Dryas glacier advances in the European Alps and in the Southern Alps of New Zealand. Geografiska Annaler Series A-Physical Geography, 81, 2, 313-323.

Ivy-Ochs, S., Schlüchter, C., Kubik, P.W., Synal, H-A., Beer, J. and Kerschner, H. 1996. The exposure age of an Egesen moraine at Julier Pass, Witzerland, measured with the cosmogenic radionuclides ^{10}Be, ^{26}Al and ^{36}Cl. Eclogae Geologicae Helvetiae, 89, 1049-1063.

Jalut, G., Amat, A.E., Bonnet, L., Gauquelin, T. and Fontugne, M. 2000. Holocene climatic changes in the Western Mediterranean, from south-east France to south-east Spain. Palaeogeography, Palaeoclimatology, Palaeoecology, 160, 255-290.

Jalut, G., Monserrat Marti, J., Fontugne, M., Delibiras, G., Vilaplana, J.M. and Julia, R. 1992. Glacial to Interglacial vegetation changes in the northern and southern Pyrénées. Quaternary Science Reviews, 11, 449-480.

James, P.A. and Chester, D.K. 1995. Soils of Quaternary river sediments in the Algarve. In: Lewin, J., Macklin, M.G., Woodward, J.C. (Eds.), Mediterranean Quaternary River Environments. Balkema, Rotterdam, 245-262.

Jansa, A., Genoves, A., Campins, J. and Picornell, M.A. 1995. Mediterranean cyclones and Alpine heavy-rain flood events, MAP Newsletter, 3, 35-37.

Jenny, H. 1941. Factors of soil formation. McGraw-Hill, New York.

Jenny, H. 1980. The soil resource-origin and behaviour. Springer-Verlag, New York.

Jóhannesson, T., Sigurosson, O., Laumann, T. and Kennett, M. 1993. Degree-day glacier mass balance modelling with applications to glacier in Iceland and Norway. Reykjavik, Orkustofnun. Nordic Hydrological Programme Report 33.

Johnsen, S.J., Clausen, H.B., Dansgaard, W., Fuhrer, K., Gundestrup, N., Hammer, C.U., Iverson, P., Jouzel, J., Stauffer, B. and Steffensen, J.P. 1992. Irregular glacial interstadials recorded in a Greenland ice core. Nature, 359, 6393, 311-313.

Johnsen, S.J., Dahl-Jensen, D., Gundestrup, N., Steffensen, P., Clausen, H., Miller, H., Masson-Delmotte, V., Sveinbjörnsdottir, A.E. and White, J. Oxygen isotope and palaeotemperature records from six Greenland ice-core stations: Camp Century, Dye-3, GRIP, GISP2, Renland and NorthGRIP. Journal of Quaternary Science, 16, 4, 299-307.

Johnson, D.L. and Stegner -Watson, D. 1987. Evolution model of pedogenesis. Soil Science, 143, 349-366.

Jolivet, L., Daniel. J-M. and Fournier, M. 1991. Geometry and kinematics of extension in Alpine Corsica. Earth and Planetary Science Letters, 104, 278-291.

Jolivet, L. and Faccenna, C. 2000. Mediterranean extension and the Africa-Eurasia collision. Tectonics, 19, 6, 1095-1106.

Jones, P.D. and Bradley, R.S. 1995. Climatic variations in the longest instrumental records. In: Bradley, R.S. and Jones, P.D. (Eds), Climate since A.D. 1500. Routledge, 246-268.

Jones, P.D., Jónsson, T. and Wheeler, D. 1997. Extension to the North Atlantic Oscillation using early instrumental pressure observations from Gibraltar and south-west Iceland. International Journal of Climatology, 17, 1433-1450.

Jones, P.D., Osborn, T. and Briffa, K.R. 2001. The evolution of climate over the last millennium. Science, 292, 662-667.

Jones, S.J., Frostrick, L.E. and Astin, T.R. 1999. Climatic and tectonic controls on fluvial incision and aggradation in the Spanish Pyrenees. Journal of the Geological Society, London, 156, 761-769.

Jouzel, J., Barkov, N.I, Barnola, J.M., Bender, M., Chapellaz, J., Genton, C., Kotlyakov, V.M., Lipenkov, V., Lorius, C., Petit, J.R., Raynaud, D., Raisbeck, G., Ritz, C., Sowers, T., Stievenard, M., Yiou, F. and Yiou, P. 1993. Extending the Vostock ice-core record of palaeoclimate to the penultimate glacial period. Nature, 364, 407-411.

Jull, A. J., Wilson, G., Burr, G., Toolin, L. J. and Donahue, D. J. 1992. Measurements of cosmogenic ^{14}C produced by spallation in high-altitude rocks. Radiocarbon, 34, 737-744.

Kallel, N., Paterne, M., Labeyrie, L., Duplessy, J-C. and Arnold, M. 1997. Temperature and salinity records in the Tyrrhenian Sea during the last 18,000 years. Palaeogeography, Palaeoclimatology, Palaeoecology, 135, 97-108.

Kasser, P. 1959. Der Einfluss von Gletscherrückgang und Gletschervostoss auf den Wasserhaushalt. Wasser-und Energiewirschaft, 51, 155-168.

Keigwin, L., Curry, W.B., Lehman, S.J.and Johnsen, S. 1994. The role of the deep ocean in North Atlantic climate change between 70 and 130 kyr ago. Nature, 371, 323-329.

Kiden, P. and Tornqvist, T.E. 1998. Can river terrace flights be used to quantify Quaternary tectonic uplift rates? Journal of Quaternary Science, 13, 6, 573-574.

Kindler, P., Davaud, E. and Strasser, A. 1997. Tyrrhenain coastal deposits from Sardinia (Italy): a petrographic record of high sea levels and shifting climate belts during the last interglacial (isotopic substage 5e). Palaeogeography, Palaeoclimatology, Palaeoecology, 133, 1-25.

King, G., Sturdy, D. and Bailey, G. 1997. The tectonic background to the Epirus landscape. In: Bailey, G.N. (Ed), Klithi: Palaeolithic Settlement and Quaternary Landscape in Northwest Greece. Volume 2: Klithi in its local and regional setting, McDonald Institute, 541-558

Knighton, D. 1998. Fluvial Forms and Processes: A New Perspective. Arnold.

Knox, J.C. 1984. Fluvial responses to small scale climatic changes. In: Costa J.E. and Fleisher P.J. (Eds), Developments and Application of Geomorphology, Springer-Verlag, 318-342.

Knox, J.C. 1987. Historical valley floor sedimentation in the Upper Mississippi Valley. Annals of the Association of American Geographers, 77, 224-244.

Knox, J.C. 1993. Large increases in flood magnitude in response to modest changes in climate. Nature, 361, 430-432.

Knox, J.C. 1995. Fluvial systems since 20,000 years BP. In: Gregory, K.J., Starkel, L. and Baker, V.R. (Eds), Global Continental Palaeohydrology. Chichester, Wiley, 87-108.

Knuepfer, P.L.K. 1988. Estimating ages of late Quaternary stream terraces from analaysis of weathering rinds and soils. Geological Scociety of America Bulletin, 100, 1224-1236.

Kochel, R.C. 1988. Geomorphic impact of large floods: review and new perspectives on magnitude and frequency. In: Baker , V.R, Kochel, R.C. and Patton, P.C. (eds) , Flood Geomorphology. New York. Wiley Inter-science, 169-187.

Kohl, C.P. and Nishiizumi, K. 1992. Chemical isolation of quartz for measurement of in situ produced cosmogenic nuclides. Geochimica et Cosmochimica Acta, 56, 3583-87.

Kraft, J.C., Aschenbrenner, S.E. and Rapp, G. 1977. Palaeogeogaphic reconstructions of coastal Aegean archaeological sites. Sciewnce, 195, 942-947.

Kraft, J.C., Rapp, G. and Aschenbrenner, S.E. 1975. Holocene palaeogeography of the coastal plain of the Gulf of Messenia, Greece, and its relationship to archaeological setting and coastal change. Bulletin of the Geological Society of America, 86, 1191-1208.

Kubik, P.W., Ivy-Ochs, S., Masarik, J., Frank, M. and Schlüchter, C. 1998. ^{10}Be and ^{26}Al production rates deduced from an instantaneous event within the dendro-calibration curve, the landslide of Köfels, Ötz Valley, Austria. Earth and Planetary Science Letters, 161, 231-241.

Kukla, G., Heller, F., Lui, X.M. and Meybeck, M. 1988. Pleistocene climates in China dated by magnetic susceptibility. Geology, 16, 811-814.

Kurz, M.D. 1986. Cosmogenic helium in a terrestrial igneous rock. Nature, 320, 435-439.

Kurz, M.D. and Brook, E.J. 1994. Surface exposure dating with cosmogenic nuclides. In: Beck, C. (Ed), Dating in Exposed and Surface Contexts. University of New Mexico Press, Albuquerque, USA, 139-159.

Kurz, M.D., Colodner, D., Trull, T.W., Moore, R and O'Brien, K. 1990. Cosmic ray exposure dating with in situ produced cosmogenic ^{3}He: Results from young Hawaiian lava flows. Earth and Planetary Science Letters, 97, 177-189.

Kutzbach, J.E and Guetter, P.J. 1986. The influence of changing orbital parameters and surface boundary conditions on climate simulations for the past 18,000 years. Journal of Atmospheric Science 43, 1726-1759.

Kuzucuoglu, C. 1995. River response to tectonics with examples form the northwestern Anatolia, Turkey. In: Lewin, J., Macklin, M.G., Woodward, J.C. (Eds.), Mediterranean Quaternary River Environments. Balkema, Rotterdam, 45-53

Labeyrie, J., Lalou, C., Monaco, A. and Thommeret, J. 1976. Chronologie des niveaux eustatiques sur la côte du Roussillon de 33 000 ans BP a nos jours. C.R. Acad. Sci., D, 282, 349-352.

Laborel, J., Morhange, C., Lafont, R., Le Campion, J., Laborel-Deguen, F. and Sartoretto, S. 1994. Biological evidence of sea-level rise during the last 4500 years on the rocky coasts of continental southwestern France and Corsica. Marine Geology, 120, 203-223.

Lal, D. and Peters, B. 1967. Cosmic ray produced radioactivity on earth in: Handbuch der Physik, Vol.XLVI/2. Springer, Berlin, 551-612.

Lal, D. 1988. In situ produced cosmogenic isotopes in terrestrial rocks. Annual Review of Earth and Planetary Science, 16, 355-388.

Lal, D. 1991. Cosmic ray labeling of erosion surfaces and in situ nuclide production rates and erosion model. Earth and Planetary Science Letters, 104, 424-439.

Lal, D. 1998. Cosmic ray produced isotopes in terrestrial systems. Proc. Indian. Acad. Sci. (Earth Planet. Sci.), 107, 4, 241-249.

Lamb, H.H. 1977. Climate Present, Past and Future, Volume 2. Methuen, London.

Lambeck, K. and Bard, E. 2000. Sea-level change along the French Mediterranean coast for the past 30 000 years. Earth and Planetary Science Letters, 175, 203-222.

Lanci, L., Hirt, A.M., Lowrie, W., Lotter, A.F., Lemcke, G. and Sturm, M. 1999. Mineral-magnetic record of Late Quaternary climatic changes in a high Alpine Lake. Earth and Planetary Science Letters, 170, 49-59.

Lang, A. 1994. Infra-red stimualted luminescnece dating of Holocene reworked silty sediments. Quaternary Geochronology. Quaternary Science Reviews, 13, 525-528.

Lao, Y., Anderson, R.F., Broecker, W.S., Trumbore, S.E., Hofman, H.J. and Wölfli, W. 1992. Increased production of cosmogenic Be-10 during the Last Glacial Maximum. Nature, 357, 6379, 576-578.

Latif, M., Anderson, D., Barnett, T., Cane, M., Kleeman, R., Leetmaa, A., O'Brien, J., Rosati, A. and Schneider, E. 1998. A review of the predictability and prediction of ENSO. Journal of Geophysical Research, C, 103, 7, 14375-14393.

Laumann, T. and Reeh, N. 1993. Sensitivity to climate change of the mass balance of glaciers in southern Norway. Journal of Glaciology, 39, 656-665.

Leland, J. Reid, M.R., Burbank, D.W., Finkel, R. and Caffee, M. 1998. Incision and differential bedrock uplift along the Indus River near Nanga Parbat, Pakistan Himalaya, from Be-10 and Al-26 exposure age dating of bedrock straths. Earth and Planetary Science Letters, 154, 1-4, 93-107.

Leeder, M.R. 1993. Tectonic controls upon drainage basin development, river channel migration and alluvial architecture: implications for hydrocarbon reservoir development and characterization. In: North, C.P. and Prosser, D.J. (Eds) Characterization of Fluvial and Section Reservoirs. Geological Society of London, Special Publication, 73, 7-22.

Leopold, L.B. and Langbein, W.B. 1962. The concept of entropy in landscape evolution. United States Geological Survey Professional Paper, 500A.

Lewin, J. 1995. The impact of Quaternary tectonic activity on river behaviour. In: Lewin, J., Macklin, M.G., Woodward, J.C (Eds), Mediterranean Quaternary River Environments. Balkema, Rotterdam, 29-30.

Lewin, J., Macklin M.G., Woodward, J.C. 1991. Late Quaternary fluvial sedimentation in the Voidomatis basin, Epirus, northwest Greece. Quaternary Research, 35, 103-115.

Lewin, J., Macklin, M.G. and Woodward, J.C. (Eds), 1995a. Mediterranean Quaternary River Environments. Balkema, Rotterdam.

Lewin, J., Macklin, M.G., Woodward, J.C. 1995b. Mediterranean Quaternary river environments - some future research needs. In: Lewin, J., Macklin, M.G., Woodward, J.C (Eds), Mediterranean Quaternary River Environments. Balkema, Rotterdam, 283-284.

L'Homer, A., Bazile, F., Thommeret, J. and Thommeret, Y. 1981. Principales étapes de l'édification du delta du Rhone de 7000 BP à nos jours; variations du niveau marin. Oceanis, 7, 4, 389-408.

Libby, W.F. 1952. Radiocarbon dating. University of Chicago Press, Chicago.

Litt, T., Brauer, A., Goslar, T., Merkt, J., Balaga, K., Müller, H., Ralska-Jasiewiczowa, M., Stebich, M., Nedendank, J.F.W. 2001. Correlation and synchronisation of Lateglacial continental sequences in northern central Europe based on annually laminated lacustrine sediments. Quaternary Science Reviews, 20, 11, 1233-1249.

Llasat, M-C. and Rodriguez, R. 1997. Towards a regionalization of extreme rainfall events in the Mediterranean area. In: Gustard, E. et al. (Eds), Friend '97 – Regional Hydrology: Concepts and Models for Sustainable Water Resource Management (Proceedings of the Postojna, Slovenia, Conference, September-October 1997). IAHS Publication, 246, 215-222.

López-Avilés, A., Ashworth, P.J., Macklin, M.G. 1998. Floods and Quaternary sedimentation style in a bedrock-controlled reach of the Bergantes River, Ebro basin, northeast Spain. In: Benito, G., Baker, V.R., Gregory, K.J. (Eds.), Palaeohydrology and Environmental Change. John Wiley and Sons: Chichester, 181-196.

Lowe, J.J. 1992. Lateglacial and early Holocene lake sediments from the northern Apennines, Italy-pollen stratigraphy and radiocarbon dating. Boreas, 21, 193-208.

Lowe, J.J. 2001. Abrupt climatic changes in Europe during the last glacial-interglacial transition: the potential for testing hypotheses on the synchroneity of climatic events using tephrochronology. Global and Planetary Change, 30, 73-84.

Lowe, J.J. and Walker, M.J.C. 1997. Reconstructing Quaternary Environments, second edition.

Lowe, J.J. and Watson, C. 1993. Lateglacial and early Holocene pollen stratigraphy of the northern Apennines, Italy. Quaternary Science Reviews, 12, 727-738.

Luterbacher, J., Schmutz, C., Gyalistras, D., Xoplaki, E. and Wanner, H. 1999. Reconstruction of monthly NAO and EU indices back to 1675. Geophysical Research Letters, 26, 2745-2748.

Maas, G.S. 1998. River response to Quaternary environmental change, southwestern Crete, Greece. Unpublished Ph.D. Thesis, University of Leeds.

Maas, G.S. and Macklin, M.G. 2002. The impact of recent climate change on flooding and sediment supply within a Mediterranean mountain catchment, southwestern Crete, Greece. Earth Surface Processes and Landforms, 27, 10, 1087-1105.

Maas, G.S., Macklin M.G. and Kirkby, M.J. 1998. Late Pleistocene and Holocene river development in Mediterranean steepland environments, south-west Crete, Greece. In: Benito, G., Baker, V.R. and Gregory, K.J. (Eds), Palaeohydrology and Environmental Change. Chichester, United Kingdom, Wiley, 153-166.

Macklin, M.G. 1986. Channel and floodplain metamorphosis in the River Nent, Cumberland. In: Macklin M.G. and Rose J. (Eds) Quaternary river landforms and sediments in the northern Pennines, England; Field Guide: Newcastle, England. British Geomorphological Research Group/Quaternary Research Association, 19-33.

Macklin, M.G. 1995. Geochronology, correlation and controls of Quaternary river erosion and sedimentation. In: Lewin, J., Macklin, M.G., Woodward, J.C (Eds), Mediterranean Quaternary River Environments. Balkema, Rotterdam, 179-181.

Macklin, M.G., Fuller I.C., Lewin, J., Mass, G.S., Passmore, D.G., Rose, J., Woodward, J.C., Black, S., Hamlin, R.H.B. and Rowan, J.S. 2002. Correlation of fluvial sequences in the Mediterranean basin over the last interglacial-glacial cycle and their relationship to climate change. Quaternary Science Reviews, 21, 14-15, 1633-1641.

Macklin, M.G., Lewin, J. and Woodward, J.C. 1995. Quaternary fluvial systems in the Mediterranean basin. In: Lewin, J., Macklin, M.G. and Woodward, J.C. (Eds), Mediterranean Quaternary River Environments. Balkema, Rotterdam, 1-25.

Macklin, M.G., Lewin, J., Woodward, J.C. 1997. Quaternary river sedimentary sequences of the Voidomatis Basin. In: Bailey, G.N. (Ed), Klithi: Palaeolithic settlement and Quaternary landscapes in northwest Greece. Volume 2: Klithi in its Local and Regional Setting. McDonald Institute for Archaeologcial Research, Cambridge, 347-359.

Macklin, M.G. and Passmore, D.G. 1995. Pleistocene environmental change in the Guadalope basin, northeast Spain: fluvial and archaeological records. In: Lewin, J., Macklin, M.G., Woodward, J.C. (Eds), Mediterranean Quaternary River Environments. Balkema: Rotterdam, 103-113.

Macklin, M.G., Rumsby B.T. and Heap, T. 1992. Flood alluviation and entrenchment: Holocene valley-floor development and transformation in the British uplands. Geological Society of America Bulletin, 104, 631-643.

Maddy, D., Green, C.P. and Bridgland, D.R. 2000. Crustal uplift in southern England: Evidence from the river terrace records. Geomorphology, 33, 167-182.

Maddy, D., Macklin, M.G. and Woodward, J.C. 2001. Fluvial archives of environmental change. In: Maddy, D., Macklin, M.G. and Woodward, J.C (Eds), River Basin Sediment Systems: Archives of Environmental Change. A.A. Balkema, 3-18.

Mahaney, W.C. 1998. Dating Methods: Progress in Physical Geography, 22, 1, 114-120.

Maher, B.A. 1986. Characterisation of soils by mineral magnetic measurements. Physics of the Earth and Planetary Interiors, 42, 76-92.

Maher, B.A. 1988. Magnetic properties of some synthetic sub-micron magnetites. Geophysical Journal of the Royal Astronomical Society, 94, 83-96.

Maher, B.A. 1998. Magnetic properties of modern soils and Quaternary loessic paleosols: paleoclimatic implications. Palaeogeography, Palaeoclimatology Palaeoecology, 137, 1-2, 25-54.

Maher, B.A., Thompson, R. and Zhou, L.P. 1994. Spatial and temporal reconstructions of changes in the Asian palaeomonsoon: a new mineral magnetic approach. Earth and Planetary Science Letters, 125, 461-471.

Maheras, P. 1988. Changes in precipitation conditions in the western Mediterranean over the last century. Journal of Climatology, 8, 179-189.

Maheras, P., Balafoutis, C. and Vafiadis, M. 1992. Precipitation in the central Mediterranean during the last century. Theoretical and Applied Climatology, 45, 3, 209-216.

Maheras, P., Flocas, H.A., Patrikas, I. and Anagnostopoulou, C. 2001. A 40 year objective climatology of surface cyclones in the Mediterranean region: Spatial and temporal distribution. International Journal of Climatology, 21, 1, 109-130.

Malinverno, A., and Ryan, W.B.F. 1986. Extension in the Tyrrhenian Sea and shortening of the Apennines as result of arc migration driven by sinking of the lithosphere. Tectonics, 5, 227-245.

Manabe, S. and Stouffer, R.J. 1988. Two stable equilibria of a coupled ocean-atmosphere model. Journal of Climate, 1, 841-866.

Manabe, S. and Stouffer, R.J. 1997. Simulation of abrupt climate changes induced by freshwater input to the North Atlantic Ocean. Nature, 378, 165-167.

Mangerud, J., Andersen, S.T., Bergluna, B.E. and Donner, J.J. 1974. Quaternary stratigraphy of Norden, a proposal for terminology and classification. Boreas, 3, 109-128.

Manley, G. 1974. Central England temperatures: monthly means 1659-1973. Quarterly Journal of the Royal Meteorological Society, 100, 389-405.

Markewich, H.W., Pavich, M.J., Mausbach, M.J., Hall, R.L., Johnson, R.G. and Hearn, P.P. 1987. Age relations between soils and geology in the Coastal Plain of Georgia and Virginia. U.S. Geological Survey Bulletin, 1589-A.

Marsella, K.A, Bierman, P.R., Davis, P.T., and Caffee, M.W. 2000. Cosmogenic Be-10 and Al-26 ages for the Last Glacial Maximum, eastern Baffin Island, Arctic Canada. Geological Society of America Bulletin, 112, 8, 1296-1312.

Marti, K. and Craig, H. 1987. Cosmic-ray produced neon and helium in the summit lavas of Maui. Nature, 325, 335-337.

Martin-Vide, J. and Vallve, M.B. 1995. The use of rogation ceremony records in climatic reconstruction – a case study from Catalonia (Spain). Climatic Change, 30, 2, 201-221.

Martinson, D.G., Pisias, N.G., Hays, J.D., Imbrie, J., Moore, T.C.Jr. and Shackleton, N.J. 1987. Age dating and the orbital theory of the ice ages: development of a high resolution 0 to 300,000 year chronostratigraphy. Quaternary Research, 27, 1-29.

Masarik, J. and Beer, J. 1999. Simulation of particle fluxes and cosmogenic nuclides production in the Earth's atmosphere. Journal of Geophysical Research, 104, 12,099, 13,112..

Masarik, J. and Reedy, R.C. 1995. Terrestrial cosmogenic-nuclide production systematics calculated from numerical simulations. Earth and Planetary Science Letters, 136, 381-396.

Mather, A.E. 2000. Adjustment of a drainage network to capture induced base-level change: an example from the Sorbas Basin, SE Spain. Geomorphology, 34, 3-4, 271-289.

Mather, A.E., Silva, P.G., Goy, J.L., Harvey, A.M. and Zazo, C. 1995. Tectonics versus climate: an example from Late Quaternary aggradation and dissectional sequences on the Mula basin, southeast Spain. In: Lewin, J., Macklin, M.G., Woodward, J.C. (Eds), Mediterranean Quaternary River Environments. Balkema: Rotterdam, 77-87.

Matthews, J.A. 1974. Families of lichenometric dating curves from the Storbreen gletschervorfeld, Jotunheimen, Norway. Norsk Geografisk Tidsskrift, 28, 215-235.

Matthews, J.A. 1975. Experiments on the reproducibility and reliability of lichenometric dates, Storbreen gletschervofeld, Jotenheim, Norway. Norsk Geografisk Tidsskrift, 29, 97-109.

Mauquoy, D., van Geel, B., Blaauw, M. and van der Plicht, J. 2002. Evidence from northwest European bogs shows 'Little Ice Age' climatic changes driven by variations in solar activity. Holocene, 12, 1, 1-6.

Mayewski, P.A., Meeker, L.D., Twickler, M.S., Whitlow, S., Yang, Q., Lyons, W.B. and Prentice, M. 1997. Major features and forcing of high-latitude Northern Hemisphere atmospheric circulation using a 110 000-year long glaciochemical series. Journal of Geophysical Research 102, 26345-26365.

McFadden, L.D. and Hendricks, D.M. 1985. Changes in the content and composition of pedogenic iron oxyhydroxides in a chronosequence of soils in Southern California. Quaternary Research, 23, 189-204.

McFadden, L.D. and Weldon, R.J. 1987. Rates and processes of soil development on Quaternary terraces in Cajon Pass, California. Geological Society of America Bulletin, 98, 280-293.

McKeague, J.A. and Day, J.H. 1966. Dithionite and oxalate-extractable Fe and Al as aids in differentiating various classes of soils. Canadian Journal of Soil Science, 46, 13-22.

McManus, J.F., Bond, G.C., Broecker, W.S., Johnsen, S., Labeyrie, L. and Higgins, S. 1994. High resolution climate records from the North Atlantic during the last interglacial. Nature, 371, 326-329.

Meese, D.A., Gow, A.J., Grootes, P., Mayewski, P.A., Ram, M., Stuiver, M., Taylor, K.C., Waddington, E.D. and Zielinski, G.A. 1994. The accumulation record from the GISP2 Core as an indicator of climate change thghout the Holocene. Science, 266, 1680-1682.

Meese, D.A., Gow, A.J., Alley, R.B., Zielinski, G.A., Grootes, P.M., Ram, M., Taylor, K.C., Mayewski, P.A., Bolzan, J.F. 1997. The Greenland Ice Sheet Project 2 depth-age scale: methods and results. Journal of Geophysical Research – Oceans, 102, C12, 26411-16423.

Mehra, O.P and Jackson, M.L. 1960. Iron oxide removal from soils and clays by a dithionite-citrate system buffered with sodium bicarbonate. Seventh National Conference on Clays and Clay Minerals, 317-327.

Mejdahl, V. and Bøtter-Jensen, L. 1994. Luminescence dating of sediments using a new technique based on single-aliquot measurements. Quaternary Geochronology, Quarternary Science Reviews, 13, 551-554.

Mejdahl, V., BotterJensen, L. 1997. Experience with the SARA OSL method. Radiation Measurements, 27, 2, 291-294.

Merrett S.P. and Macklin, M.G. 1999. Historic river response to extreme flooding in the Yorkshire Dales, northern England. In: Brown, A.G. and Quine, T.A. (Eds), Fluvial Processes and Environmental Change. Chichester, United Kingdom, Wiley, 345-360.

Messerli, B. 1967. Die Eiszeitliche und die gegenwartige vergletscherung im Mittelmeeraum. Geographica Helvetica, 22, 105-228.

Messerli, B. 1980. Mountain glaciers in the Mediterranean and in Africa. In: World Glacier Inventory Workshop. IAHS-AISH Publication, 126, 197-211.

Miall, A.D. 1996. The geology of fluvial deposits: sedimentary facies, basin analysis and petroleum geology. Springer-Verlag Inc., Berlin.

Middleton, R. and Klein, J. 1987 . ^{26}Al: measurement and applications: Philosophical Transactions of the Royal Society of London, A323, 121-43.

Miller, G.H. 1973. Late Quaternary glacial and climatic history of Northern Cumberland Peninsula, east Baffin Island, N.W.T., Canada. Quaternary Research, 3, 561-583.

Montserrat, J.M. 1992. Evolución glaciar y postglaciar del clima y la vegetación en lavertiente sur del Pirineo. Estudio palinológico. Monograffias del Instituto Pirenaico de Ecologia, 6, 147.

Morrison, R.B. 1978. Quaternary soil stratigraphy concepts, methods and problems. In: Mahaney, W.C. (Ed), Quaternary Soils. Geo Abstracts Ltd., University of East Anglia, Norwich, England, 77-108.

Moses, T., Kiladis, G.N., Diaz, H.F. and Barry, R.G. 1987. Characteristics and frequency of reversals in mean sea level pressure in the North Atlantic sector and their relationship to long term temperature trends. Journal of Climatology, 7, 13-30.

Muhs, D.R. 1982. A soil chronosequence on Quaternary marine terraces, San Clemente Island, California. Geoderma, 28, 357-283.

Murray, A.S. 1996. Developments in optically stimulated luminescence and photo-transferred thermoluminescence dating of young sediments: Application to a 2000-year sequence of flood deposits. Geochimica et Cosmochimica Acta, 60, 4, 565-576.

Murray, A.S., Roberts, R.G. and Wintle, A.G. 1997. Equivalent dose measurememnt using a single-aliquot of quartz. Radiation Measurements, 27, 171-184.

Murray, A.S. and Wintle, A.G. 2000. Luminescence dating of quartz using an improved single aliquot regenerative-dose protocol. Radiation Measurements, 32, 57-73.

Nanson, G.C. and Knighton, A.D. 1996. Anabranching rivers: their cause, character and classification. Earth Surface Processes and Landforms, 21, 217-39.

Narcisi, B. 2001. Palaeoenvironmental and palaeoclimatic implications of the Late Quaternary sediment record of Vico volcanic lake (central Italy). Journal of Quaternary Science, 16, 3, 245-255.

Narcisi, B., Anselmi, B., Catalano, F., Dai Pra, G. and Magri, G. 1992. Lithostratigraphy of the 250 000 year record of lacustrine sediments from the Valle Di Castiglione Crater, Roma. Quaternary Science Reviews, 11, 353-362.

Nemec, W. and Postma, G. 1993. Quaternary alluvial fans in southwestern Crete: sedimentation processes and geomorphic evolution. In: Marzo, M. and Puigdefabregas, C. (Eds), Alluvial Sedimentation. International Association of. Sedimentologists, Special Publication, 17, 235-276.

Nesteroff, W.D. 1984. Etude de quelqúes grès de plage du sud de la Corse datations ^{14}C et implications néotectoniques pour le bloc Corso-Sarde. In: Le Beach-rock. Travaux de la Maison de L'Orient, Lyon, 8, 99-111.

Nesje, A. and Dahl, S.O. 2000. Glaciers and Environmental Change. Key issues in environmental change. Arnold Publishers, London.

Newson, M.D. 1997. Land, Water and Development: Sustainable management of river basin systems. Routledge, London & New York.

Nicholas, A.P., Ashworth, P. J., Kirkby, M.J., Macklin, M.G. and Murray, T. 1995. Large-scale fluctuations and fluvial sediment transport rates and storage volumes. Progress in Physical Geography, 19, 500-519.

Nishiizumi, K., Klein, J., Middleton, R. and Craig, H. 1991a. Cosmogenic ^{10}Be, ^{26}Al and ^{3}He in olivine from Maui lavas. Earth Planetary Science Letters, 98, 263-266.

Nishiizumi, K., Kohl, C.P., Arnold, J.R., Dorn, R.I., Klein, J., Fink, D. and Middleton, R. 1991b. Cosmic ray produces ^{10}Be and ^{26}Al in Antarctic rocks: Exposure and erosion history. Earth Planetary Science Letters, 104, 440-454.

Nishiizumi, K., Kohl, C.P., Arnold, J.R., Dorn, R.I., Klein, J., Fink, D., Middleton, R. and Lal, D. 1993. Role of in situ cosmogenic nuclides ^{10}Be and ^{26}Al in the study of diverse geomorphic processes. Earth Surface Processes and Landforms, 18, 407-425.

Nishiizumi, K., Kohl, C.P., Shoemaker, E.M., Arnold, J.R., Klein, J., Fink, D. and Middleton, R. 1991c. In situ Be-10 and Al-26 exposure ages at Meteor Crater, Arizona. Geochimica et Cosmochimica Acta, 55, 2699-2703.

Nishiizumi, K., Winterer, E.L., Kohl, C.P., Klein, J., Middleton, R., Lal, D. and Arnold, J.R. 1989. Cosmic ray production rates of ^{10}Be and ^{26}Al in quartz from glacially polished rocks. Journal of Geophysical Research, 94, B12, 17907-17915.

O'Brien, S.R., Mayewski, A., Meeker, L.D., Meese, D.A., Twickler, M.S. and Whitlow, S.I. 1996. Complexity of Holocene climate as reconstructed from a Grenland ice core. Science, 270, 1962-1964.

Orombelli G. and Mason, P. 1997. Holocene glacier fluctuations in the Italian Alpine region, In: Frenzel, B (Ed) Glacier fluctuations during the Holocene. European Palaeoclimate and Man, 16, 59-65.
Osborn, T.J., Briffa, K.R., Tett, S.F.B., Jones, P.D. and Trigo, R.M. 1999. Evaluation of the North Atlantic Oscillation as simulated by a coupled climate model. Climate Dynamics, 15, 685-702.

Palutikof, J.P., Conte, M., Casimiro Mendes, J., Goodess, C.M. and Espirito Santo, F. 1996. Climate and climatic change. In: Brandt, C.J. and Thornes, J.B. (Eds), Mediterranean Desertification and Land Use. John Wiley, New York, 43-86.

Pappalardo, M. 1999. Remarks upon the present-day condition of the glaciers in the Italian Maritime Alps. Geografia Fisica e Dinamica Quaternaria, 22, 79-82.

Pardé, M. 1955. Fleuves et Rivières, 3rd edn, Colin, Paris.

Parfitt, R.L. and Childs, C.W. 1988. Estimation of forms of Fe and Al: A review, and analysis of contrasting soils by dissolution and Moesbauer methods. Australian Journal of Soil Research, 26, 121-144.

Parry, V.L. 1999. Relative age dating of a Quaternary Aluvial Sequence of the Tavignano River, Corsica. Unpublished MSc dissertation, University of Leeds.

Pasquale, V., Verdoya, M., Chiozzi, P. and Ranalli, G. 1997. Rheology and seismotectonic regime in the northern central Mediterranean. Tectonophysics, 270, 239-257.

Paterne, M., Guichard, F., Labeyrie, J., Gillot, P.Y. and Duplessy, J.C. 1986. Tyrrhenian sea tephrachronology of the oxygen isotopes record for the past 60,000 years. Marine Geology, 72, 259-285.

Paterne, M., Kallel, N., Labeyrie, L.D., Vautravers, M., Duplessey, J.C., Rossingnol-Strick, M., Cortijo, E., Arnold, M. and Fontugne, M. 1999. Hydrological relationship between the North Atlantic Ocean and the Mediterranean Sea during the past 15-75 kyr. Paleoceanography, 14, 626-638.

Paterson, W.S.B. 1994. The Physics of Glaciers. Third edition. Elsevier Science, Amsterdam.

Pavese, M.P., Banzon, V., Colacino, M., Gregori, G.P. and Pasqua, M. 1995. Three historical data series on floods and anomalous climatic events in Italy. In: Bradley, R.S., and Jones, P.D. (Eds), Climate since A.D. 1500. Routledge, London, 155-170.

Pedley, M. and Frostick, L.E. 1999. Unravelling tectonic and climatic signals in sedimentary successions: an introduction. Journal of the Geological Society, London, 156, 747.

Peñalba, M.C., Arnold, M., Guiot, J., Duplessy, J-C. and de Beaulieu, J-L. 1997. Termination of the Last Glaciation in the Iberian Peninsula inferred from the pollen sequence of Quintanar de la Sierra. Quaternary Research, 48, 205-214.

Penck, A. and Brückner, E. 1909. Die Alpen im Eiszeitalter. Tauchnitz, Leipzig.

Pérez-Obiol and Julià, R. 1994. Climatic change on the Iberian Peninsula recorded in a 30,000 yr pollen record from Lake Banyoles. Quaternary Research, 41, 91-98.

Peyron, O., Guiot, J, Cheddadi, R., Tarasov, P., Reille, M., de Beaulieu, J.L., Bottema, S. and Andrieu, V. 1998. Climatic reconstruction in Europe for 18 000 yr B.P. from pollen data. Quaternary Research, 49, 183-196.

Pfister, C. 1988. Variations in Spring-Summer Climate of Central Europe from the High Middle Ages to 1850. In: Wanner, H. and Siegenthaler, U. (Eds), Long and Short-term variability of Climate. Springer, Berlin, 57-82.

Pfister, C. 1992. Five Centuries of Little Ice Age Climate in Western Europe. In: Mikami, T. (Ed), Proceedings of the International Symposium on the Little Ice Age. Department of Geography, Toyko Metropolitan University, Tokyo, 208-212.

Pfister, C. 1995. Monthly temperature and precipitation in central Europe from 1525-1979: quantifying documentary evidence on weather and its effects. In: Bradley, R.S., and Jones, P.D. (Eds), Climate since A.D. 1500. Routledge, London, 118-142.

Pfister, C., Brazdil, R., Glaser, R., Barriendos, M., Camuffo, D., Deutsch, M., Dobrovolny, P., Enzi, S., Guidoboni, E., Kotyza, O., Militzer, S., Racz, L., Rodrigo, F.S. 1999. Documentary evidence on climate in sixteenth-century Europe. Climatic Change, 43, 1, 55-110.

Phillips, F.M. and Zreda, M.G. 1992. Late Quaternary glacial history of the Sierra Nevada from cosmogenic ^{36}Cl dating of moraines at Bishop Creek: EOS Transactions, AGU, 73,186.

Phillips, F.M., Zreda, M.G., Benson, L.V., Plummer, M.A., Elmore, D. and Sharma, P. 1996. Chronology for fluctuations in late Pleistocene Sierra Nevada glaciers and lakes. Science, 274, 749-751.

Phillips, F.M., Zreda, M.G., Elmore, D. and Sharma, P. 1996. A reevaluation of cosmogenic ^{36}Cl production rates in terrestrial rocks. Geophysical Research Letters, 23, 949-952.

Phillips, F.M., Zreda, M.G., Gosse, J.C., Klein, J., Evenson, E.B., Hall, R.D., Chadwick, D.A. and Sharma, P. 1997. Cosmogenic ^{3}He and ^{10}Be ages of Quaternary glacial and fluvial deposits of the Wind River Range, Wyoming. Geological Society of America Bulletin, 109, 11, 1453-1463.

Phillips, F.M., Zreda, M.G., Smith, S.M., Elmore D., Kubik P.W. 1991. Age and geomorphic history of Meteor Crater, Arizona, from cosmogenic ^{36}Cl and ^{14}C in rock varnish. Geochimica et Cosmochimica Acta, 55, 2695-2698.

Phillips, F.M., Zreda, M.G., Smith, S.S., Elmore D., Kubik P.W., Sharma, P. 1990. Cosmogenic chlorine-36 chronology for glacial deposits at Bloody Canyon, eastern Sierra Nevada. Science, 248, 1529-1532.

Piervitali, E. and Colacino, M. 2001. Evidence of drought in western Sicily during the period 1565-1915 from Liturgical offices. Climatic Change, 49, 225-238.

Piervitali, E., Colacino, M. and Conte, M. 1997. Signals of climatic change in the central-western Mediterranean basin. Theoretical and Applied Climatology, 58, 211-219.

Piervitali, E., Colacino, M and Conte, M. 1998. Rainfall over the Central-Western Mediterranean basin in the period 1951-1995. Part 1: precipitation trends. Il Nuovo Cimento, 21 C, 3, 331-344.

Piervitali, E., Conte, M. and Colancino, M. 1999. Rainfall over the Central-Western Mediterranean basin in the period 1951-1995. Part II: Precipitation scenarios. Il Nuovo Cimento, 22, 5, 649-661.

Pirazzoli, P.A. 1976. Sea-level variations in the northwest Mediterranean during Roman Times. Science, 194, 519-521.

Pirazzoli, P.A. 1991. World Atlas of Holocene Sea Level Changes. Elsevier Oceanography Series 58, Elsevier.

Plaut, G., Ghil, M, and Vautard, R. 1995. Interannual and interdecadal variability in 335 years of central England temperatures. Science, 268, 710-713.

Poesen, J.W.A. and Hooke J.M. 1997. Erosion, flooding and channel management in Mediterranean environments of southern Europe. Progress in Physical Geography, 21, 2, 157-199.

Ponel, P. and Coope, G.R. 1990. Lateglacial and early Flandrian Coleoptera from La Taphanel, Massif-Central, France: climatic and ecological implications. Journal of Quaternary Science, 5, 235-249.

Ponel, P. and Lowe, J.J. 1992. Coleopteran, pollen and radiocarbon evidence from the Prato Spilla 'D' succession, N Italy. Comptes Rendus de l'Academie de Sciences, Paris, Serie II, 315, 1425-1431.

Pons, A. Beaulieu, J.L. de, Guiot, J. and Reille, M. 1987. The Younger Dryas in southwestern Europe: an abrupt climatic change as evidenced from pollen records. In: Berger, W.H. and Labeyrie, L.D. (Eds), Abrupt Climatic Change: Evidence and Implications. Reidel, Dordrecht, 195-208.

Pons, A. and Reille, M. 1988. The Holocene and Upper Pleistocene pollen record from Padul (Granada, Spain): A new study. Palaeogeography, Palaeoclimatology, Palaeoecology, 66, 23-263.

Pope, R.J.J. 2000. The application of mineral magnetic and extractable iron (Fed) analysis for differentiating and relatively dating fan surfaces in central Greece. Geomorphology, 32, 57-67.

Pope, K.O. and van Andel, T.H. 1984. Late Quaternary alluviation and soil formation in the southern Argolid: its history, causes and archaeological implications. Journal of Archaeological Science, 11, 281-306.

Poreda, R. and Cerling, T. 1992. Cosmogenic neon in recent lavas from the western United States. Geophysical Research Letters, 19, 1863-1866.

Porter, S.C. 1981. Lichenometric studies in the Cascade Range of Washington: establishment of Rhizocarpon geographicum growth curves at Mount Rainer. Arctic and Alpine Research, 13, 11-23.

Porter, S.C. and Orombelli, G. 1982. Late-Glacial ice advances in the western Italian Alps. Boreas, 11, 125-140.

Prentice, I.C., Guiot, J. and Harrison, S. 1992. Mediterranean vegetation, lake levels and palaeoclimate at the Last Glacial Maximum. Nature, 360, 658-660.

Pye, K. 1983. Red beds. In: Goudie, A.S. and Pye, K. (Eds), Chemical Sediments and Geomorphology. Academic Press, London, 227-263.

Qian, B., Corte-Real, J. and Xu, H. 2000. Is the North Atlantic Oscillation the most important atmospheric pattern for precipitation in Europe? Journal of Geophysical Research, 105, D9, 11901-11910.

Quadrelli R., Pavan, V. and Molteni, F. 2001. Wintertime variability of Mediterranean precipitation and its links with large-scale circulation anomalies. Climate Dynamics, 17, 5-6, 457-466.

Raisbeck, G.M., Yiou, F. and Bourles, D. 1985. Evidence for an increase in cosmogenic ^{10}Be during a geomagnetic reversal. Nature, 315, 315-317.

Raisbeck, G.M., Yiou, F., Bourles, D., Lorius, C., Jouzel, J. and Barkov, N.I. 1987. Evidence for two intervals of enhanced ^{10}Be deposition in Antarctic ice during the last glacial period. Nature, 326, 273-276.

Ramil-Rego, P., Guitian, M.A.R., Sobrino, C.M., Gomez-Orellana, L. 2000. Some considerations about the postglacial history and recent distribution of Fagus sylvatica in the NW Iberian Peninsula. Folia Geobotanica, 35, 3, 241-271.

Ramis, C., Llasat, M.C., Genovés, A. and Jansá, A. 1994. The October, 1987 floods in Catalonia: synoptic and mesoscale mechanisms. Meteorological Applications, 1, 337-350.

Ramrath, A., Zolitschka, B., Wulf, S. and Negendank, J.F.W. 1999. Late Pleistocene climatic variations as recorded in two Italian maar lakes (Lago di Mezzano, Lago di Monticchio). Quaternary Science Reviews, 18, 977-992.

Rebaï, S., Philip, H. and Taboada, A. 1992. Modern tectonic stress field in the Mediterranean region: evidence for variation in stress directions at different scales. Geophysical Journal International, 110, 106-140.

Reddaway, J.M. and Bigg, G.R. 1996. Climatic change over the Mediterranean and links to the more general atmospheric circulation. International Journal of Climatology, 16, 6, 651-662.

Reedy, R.C. 1987. Nuclide production by primary cosmic-ray protons. Journal of Geophysical Research, 92, E697-E702.

Reedy, R.C., Arnold, J.R. and Lal, D. 1983. Cosmic ray record in solar system matter. Annual Reviews of Earth Planetary Science, 33, 505-37.

Reedy, R.C., Nishiizumi, K. and Arnold, J.R. 1990. Solar cosmic rays: fluxes and reaction cross sections. Lunar and Planetary Conference XX, Houston, 890-891.

Reedy, R.C., Tuniz, C. and Fink, D. 1994. Report on the workshop on production rates of terrestrial in-situ –produced cosmogenic nuclides. Nuclear Instruments and Methods in Physics Research, B 92, 1-4, 335-339.

Reid, G.C. 1997. Solar forcing of global climate change since the mid-17th century. Climatic Change, 37, 2, 391-405.

Reille, M. 1975. Contribution pollenanalytique à l'histoire tardiglaciaire et holocène de la végétation de la montagne corse, Thèse Doct. Etat, Marseille.

Reille, M. 1993a. New pollen-analytical researches at Freychinede, Ariege, Pyrenees, France. Dissertationes Botanicae, 196, 377-386.

Reille, M. 1993b. The Lateglacial-Holocene interface in a site of southern Europe on the Atlantic coast: La Moura (Pyrenees Atlantiques, France). Comptes Rendus Academie des Sciences Paris, 316, 463-468.

Reille, M. and Andrieu, V. 1995. The late Pleistocene and Holocene in the Lourdes Basin. Western Pyrenees, France: New pollen analytical and chronological data. Vegetation History and Archaeobotany, 4, 1-21.

Reille, M., Beaulieu, J.-L. de, Svobodova, H., Andrieu-Ponel, V. and Goeury, C. 2000. Pollen analytical biostratigraphy of the last five climatic cycles from a long continental sequence from the Velay region (Massif Central, France). Journal of Quaternary Science, 15, 665-685.

Reille, M., Gamisans, J., Andrieu-Ponel, V. and de Beaulieu, J.-L. 1999. The Holocene at Lac de Creno, Corsica, France: a key site for the whole island. New Phytologist, 141, 291-307.

Reille, M., Gamisans, J., Beaulieu, J.L. de, and Andrieu, V. 1997. The late-glacial at Lac de Creno (Corsica, France): a key site in the western Mediterranean basin. New Phytologist, 135, 547-559.

Reille, M. and Lowe, J.J. 1993. A re-evaluation of the vegetation history of the eastern Pyrenees (France) from the end of the last glacial to the present. Quaternary Science Reviews, 12, 47-77.

Reneau, S.L. 2000. Stream incision and terrace development in Frijoles Canyon, Bandelier National Monumnet, New Mexico, and the influence of lithology and climate. Geomorphology, 32, 171-193.

Renssen, H. and Isarin, R.F.B. 1998. Surface temperature in NW Europe during the Younger Dryas: AGCM simulation compared with temperature reconstructions. Climate Dynamics, 14, 33-44.

Renssen, H., Isarin, R.F.B., Jacob, D., Podzun, R. and Vandenberghe, J. 2001. Simulation of the Younger Dryas climate in Europe using a regional climate model nested in an AGCM: preliminary results. Global and Planetary Change, 30, 41-57.

Repka, J.L., Anderson, R.S. and Finkel, R.C. 1997. Cosmogenic dating of fluvial terraces, Fremont River, Utah. Earth and Planetary Science Letters, 152, 59-73.

Rind, D. and Overpeck, J. 1993. Hypothesized causes of decade-to-century-scale climate variability: climate model results. Quaternary Science Reviews, 12, 357-374.

Rind, D., Peteet, D., Broecker, W., McIntyre, A. and Ruddiman, W. 1986. The impact of cold North Atlantic sea surface temperatures on climate implications for the Younger Dryas cooling (11-10 k). Climate Dynamics, 1, 3-33.

Roberts, N. and Wright, H.E. Jr. 1993. Vegetational, lake level and climatic history of the Near East and southwestern Asia. In: Wright, H.E. Jr, Kutzbach, J.E., Web III, T., Ruddiman, W.F., Street-Perrott, F.A. and Bartlein, P.J. (Eds), Global Climates since the Last Glacial Maximum. Minneapolis, Minnesota, 194-220.

Roberts, N. 1995. Climatic forcing of alluvial fan regimes during the Late Quaternary in the Knya basin, south central Turkey. In: Lewin, J., Macklin, M.G., Woodward, J.C. (Eds), Mediterranean Quaternary River Environments. Balkema, Rotterdam, 207-218.

Roberts, N. 1998. The Holocene. An Environmental History. Second edition. Oxford, Blackwell.

Roberts, R.G. 1997. Luminescence dating in archaeology: From origins to optical. Radiation Measurements, 27, 5-6, 819-892.

Robock, A. 2000. Volcanic eruptions and climate. Reviews of Geophysics, 38, 2, 191-219.

Rodwell, M.J., Rowell, D.P. and Folland, C.K. 1999. Oceanic forcing of the wintertime North Atlantic oscillation and European climate. Nature, 398, 320-323.

Rogers, J.C. 1984. The association between the North Atlantic Oscillation and the Southern Oscillation in the Northern Hemisphere. Monthly Weather Reviews, 112, 1999-2015.

Rogers, J.C. 1990. Patterns of low frequency monthly sea level pressure variability (1899-1986) and associated wave cyclone frequencies. Journal of Climatology, 1364-1379.

Rohling, E.J., Hayes, A., De Rijk, S., Kroon, D., Zachariasse, W.J. and Eisma, D. 1998. Abrupt cold spells in the northwest Mediterranean . Paleoceanography, 13, 316-322.

Romero, R., Guijarro, J.A., Ramis, C. and Alonso, S. 1998. A 30-year (1964-1993) daily rainfall data base for the Spanish Mediterrnaean regions: first exploratory study. International Journal of Climatology, 18, 541-560.

Rose. J. and Meng, X. 1999. River activity in small catchments over the last 140 ka, North-east Mallorca, Spain. In: Brown, A.G. and Quine, T.A. (Eds), Fluvial Processes and Environmental Change. Chichester, Wiley, 91-102.

Rose, J., Meng, X. and Watson, C. 1999. Palaeoclimate and palaeoenvironmental responses in the western Mediterranean over the last 140 ka: evidence from Mallorca Spain. Journal of the Geological Society, London, 156, 435-448.

Rose, J. Turner, C., Coope, G.R., Bryan, M.D. 1980. Channel changes in a lowland river catchment over the last 13,000 years. In: Cullingford, R.A., Davidson, D.A., Lewin, J. (Eds.), Timescales in Geomorphology. John Wiley and Sons, Chichester, 91-102.

Ross, G.J. and Wang, C. 1993. Extractable Al, Fe, Mn and Si. In: Carter, M.R. (Ed), Soil Sampling and Methods of Analysis. Canadian Society of Soil Science, Lewis Publishers, 239-246.

Rossingnol-Strick, M. and Planchais, N. 1989. Climate patterns revealed by pollen and oxygen isotope records of a tyrrhenian sea core. Nature, 342, 413-416.

Roucoux, K.H., Shackleton, N.J., Arbreu, L. de, Schönfeld, J and Tzedakis, P.C. 2001. Combined marine proxy and pollen analyses reveal rapid Iberian vegetation response to North Atlantic millenial-scale climate oscillations. Quaternary Research, 56, 128-132.

Rowan, J.S., Black, S., Macklin, M.G., Tabner, B.J. and Dore, J. 2000. Quaternary environmental change in Cyrenaica evidenced by U-Th, ESR and OSL dating of coastal alluvial fan sequences. Libyan Studies, 31, 5-16.

Ruddiman, W.F. and McIntyre, A. 1981. The North Atlantic Ocean during the last deglaciation. Palaeogeography, Palaeoclimatology, Palaeoecology, 35, 145-214.

Rumsby, B. and Macklin, M.G. 1996. River response to the last neoglacial (the 'Little Ice Age') in northern, western and central Europe. In: Branson, J., Brown, A.G. and Gregory, K.J. (Eds), Global Continental Changes: the Context of Palaeohydrology. Geological Society Special Publications, 115, 217-234.

Saïd, S. and Gégout, J.C. 2000. Using the age of the oldest woody specimen for studying post-pasture successions in Corsica (Mediterranean island). Acta Oecologica, 21, 3, 193-201.

Sartoretto, S., Verlaque, M. and Laborel, J. 1996. Age of settlement and accumulation rate of submarine "coralligène" (-10 to –60 m) of the northwestern Mediterranean Sea; relation to Holocene rise in sea level. Marine Geology, 130, 317-331.

Sanchez Goni, M.F., Cacho, I.., Turon, J-L., Guiot, J., Sierro, F.J., Peypouquet, J-P., Grimalt, J.O. and Shackleton, N.J. 2002. Synchroneity between marine and terrestrial responses to millennial scale climatic variability during the last glacial period in the Mediterranean region. Climate Dynamics, 19, 95-105.

Scalenghe, R., Zanini, E. and Nielsen, D.R. 2000. Modeling soil development in a post-incisive chronosequence. Soil Science, technical articles, 165, 6, 455-462.

Schlesinger, M.E. and Ramankutty, N. 1994. An oscillation in the global climate system of period 65-70 years. Nature, 367, 723-726.

Schmutz, C., Luterbacher, J., Gyalistras, D., Xoplaki, E. and Wanner, H. 2000. Can we trust prosy-based NAO index reconstructions? Geophysical Research Letters, 27, 8, 1135-1138.

Schöwiese, C.D. and Rapp, J. 1997. Climate Trend Atlas of Europe based on observations 1891-1990. Kluwer Academic Publishers, Dordrecht.

Schulte, L. and Julia, R. 2001. A Quaternary soil chronosequence of Southeastern Spain. Zeitschrift fur Geomorphologie, 45, 2, 145-158.

Schumm, S.A. 1973. Geomorphic thresholds and the complex response of drainage systems. In: Morisawa, M. (Ed), Fluvial Geomorphology. State University of New York, Binghampton, 473-485.

Schumm, S.A. 1977. The Fluvial System. New York, John Wiley and Sons.

Schumm, S.A. and Lichty, R.W. 1965. Time, space and causality in geomorphology. American Journal of Science, 263, 110-119.

Schwertmann, U. 1993. Relations between iron oxides, soil colour, and soil formation. Soil Science Society of America, Special Publication, 31, 51-69.

Schwertmann, U. and Taylor, R.M. 1989. Iron oxides. In: Dixon, J.B. and Weed, S.B. (Eds), Minerals in soil environments. Soil Science Society of America Book Series, 1, 379-437.

Serre-Bachet, F., Guiot, J. and Tessier, L. 1995. Dendroclimatic evidence from southwestern Europe and northwestern Africa. In: Bradley, R.S., and Jones, P.D. (Eds), Climate since A.D. 1500. Routledge, London, 349-365.

Shabalova, M.V. and Weber, S.L. 1999. Patterns of temperature variability on mutlidecadal to centennial timescales. Journal of Geophysical Research, 104, D24, 31023-31041.

Shackleton, N.J., Hall, M.A., and Vincent, E. 2000. Phase relationships between millennial-scale events 64,000-24,000 years ago. Paleoceanography, 15, 6, 565-569.

Sharma, K.K., Gu, Z.Y., Lal, D., Caffee, M.W. and Southon, J. 1998. Late Quaternary morphotectonic evolution of the upper Indus Valley profile; A cosmogenic radionuclide study of river polished surfaces. Current Science, 75, 366-371.

Sharma, P. and Middleton, R. 1989. Radiogenic production of ^{10}Be and ^{26}Al in uranium and thorium ores: Implications for studying terrestrial samples containing low levels of ^{10}Be and ^{26}Al. Geochimica Cosmochimica Acta, 53, 709-716.

Sheldrick, B.H. and McKeague, J.A. 1975. A comparison of extractable Fe and Al data using methods followed in the U.S.A. and Canada. Canadian journal of soil science, 55, 77-78.

Shepard, M.K., Arvidson, R.E., Caffee, M., Finkel, R. and Harris, L. 1995. Cosmogenic exposure ages of basalt flows: Lunar Crater volcanic field, Nevada. Geology, 23, 21-24.

Siame, L.L., Bourlès, D.L., Sébrier, M., Bellier, O., Castano, J.C., Araujo, M., Perezz, M., Raisbeck, G.M. and Yiou, F. 1997. Cosmogenic dating ranging from 20 to 700 ka of a series of alluvial fan surfaces affected by the El Tigre fault, Argentina. Geology, 25, 11, 975-978.

Simi, P. 1964. Le climat de la Corse. Minst. Ed. Nat., Com. Trav. hist. scientis. Bull. Sect. Géogr., Paris. Impr. Nat. T LXXVI, 1-22

Simón, M., Sanchez, S. and Garci, I. 2000. Soil-landscape evolution on a Mediterranean high mountain. Catena, 39, 3, 211-231.

Simonson, R.W. 1978. A multiple-process model of soil genesis. In Mahaney, W.C. (Ed.), Quaternary soils, 1-25. Geo Abstracts Ltd., University of East Anglia, Norwich, England.

Singer C, Shulmeister J, McLea B. 1998. Evidence against a significant Younger Dryas cooling event in New Zealand. Science 281, 5378, 812-814.

Singer, M.J., FGine, P., Verosub, K.L. and Chadwick, O.A. 1992. Time dependence of magnetic susceptibility of soil chronosequences on the Californian coast. Quaternary Research, 37, 323-332.

Singh, P. and Kumar, N. 1996. Determination of snowmelt factor in the Himalyan region. Hydrological Sciences Journal, 41, 301-310.

Singh, P and Singh, V.P. 2001. Snow and Glacier Hydrology. Water Science and Technology Library, Volume 37. Kluwer Academic Publishers, Dordrecht.

Smith, K. and Ward, R. 1998. Floods: Physical Processes and Human Impacts. John Wiley & Sons, Chichester.

Smith, A.G. and Woodcock, N.H. 1982. Tectonic synthesis of the Alpine- Mediterranean region: a review. In: Berckhemer, H., Hsü, K. (Eds), Alpine-Mediterranean Geodynamics, Geodynamics Series volume 7., American Geophysical Union/ Geological Society of America, 15-38.

Smith, G.W., Nance, R.D. and Genes, A.N. 1997. Quaternary glacial history of Mount Olympus, Greece. GSA Bulletin, 109, 7, 809-824.

Soil Survey Division Staff. 1993. Soil Survey Manual, U.S. Dept. Agri. Handbook, 18, 437.

Starkel, L. 1991. Long-distance correlation of fluvial events in the Temperate Zone: In: Starkel, L., Gregory, K.J., Thornes, J.B. (Eds), Temperate Palaeohydrology: Fluvial Processes in the Temperate zone during the last 15,000 years. Wiley, Chichester, 473-495.

Staudacher, T. and Allégre, C.J. 1991. Cosmogenic neon in ultramafic nodules from Asia and in quartzite from Antarctica. Earth Planetary Science Letters, 106, 87-102.

Staudacher, T. and Allégre, C.J. 1993. Ages of the second caldera of Piton de la Fournaise volcano (Réunion) determined by cosmic ray produced ^{3}He and ^{21}Ne. Earth and Planetary Science Letters, 119, 395-404.

Stein, R., Nam, S.I., Grobe, H. and Hubberten, H. 1996. Late Quaternary glacial history and short-term ice-rafted debris fluctuations along the East Greenland continental margin. In: Andrews, J.T., Austin, W.E.N., Bergsten, H., and Jennings, A.E. (Eds), Late Quaternary palaeooceanography of the North Atlantic margins. Geological Society Special Publication, 111, 135-151.

Stocker, T.F. and Mysak, L.A. 1992. Climatic fluctuations on the century time scale: a review of high-resolution proxy data and possible mechanisms. Climatic Change, 20, 227-250.

Stocker, T.F. & Wright, D.G. 1996. Rapid changes in ocean circulation and atmospheric carbon. Paleoceanography, 11, 6, 773-795.

Stokes, S. 1992. Optical dating of young (modern) sediments using quartz: results from a selection of depositional environments. Quaternary Science Reviews, 11, 153-159.

Stuiver, M. 1980. Solar variability and climatic change during the current millennium. Nature, 286, 868-871.

Stuiver, M. and Grootes, P.M. 2000. GISP2 oxygen isotope ratios. Quaternary Research, 53, 277-284

Sumner, G., Homar, V. and Ramis, C. 2001. Precipitation seasonality in eastern and southern coastal Spain. International Journal of Climatology, 21, 219-247.

Swanson, T., Caffee, M., Finkel, R., Harris, L., Southon, J., Zreda, M. and Phillips, F. 1993. Establishment of new production parameters for chlorine-36 dating based on the deglaciation history of Whidbey Island, Washington. Geological Society of America Abstract with Programs, 25, A-461.

Taylor, K.C., Alley, R.B., Doyle, G.A., Grootes, P.M., Mayewski, P.A., lamorey, G.W., White, J.W.C. and Barlow, L.K. 1993. The 'flickering switch' of the late Pleistocene climate change. Nature, 361, 432-436.

Taylor, K.C., Mayewski, P.A., Alley, R.B., Brook, E.J., Gow, A.J., Grootes, P.M., Meese, D.A., Saltzman, E.S., Severinghaus, J.P., Twickler, M.S., White, J.W.C., Whitlow, S. and Zielinski, G.A. 1997. The Holocene-Younger Dryas transition recorded at Summit, Greenland. Nature, 278, 825-827.

Thompson, L.G., Mosley-Thompson, E., Dansgaard, W. and Grootes, P.M. 1986. The Little Ice Age as recorded in the stratigraphy of the tropical Quelccaya ice cap. Science, 234, 361-364.

Thompson, R. and Maher, B.A. 1995. Age models, sediment fluxes and paleoclimatic reconstructions for the Chinese loess and palaeosol sequences. Geophysical Journal International, 123, 611-622.

Thompson, R. and Oldfield, F. 1986. Environmental Magnetism. Allen and Unwin.

Thouveny, N., Beaulieu, J.C. de, Bonifay, E., Creer, K.M., Guiot, J., icole, M., Johnsen, S., Jouzel, J., Reille, M., Williams, T. and Williamson, D. 1994. Climate variations in Europe over the past 140 kyr deduced from rock magnetism. Nature, 371, 503-506.

Torrent, J., Schwertmann, U. and Schulze, D.G. 1980. Iron oxide mineralogy of two river terrace sequences in Spain. Geoderma, 23, 191-208.

Torrent, J., Schwertmann, U., Fechter, H. and Alferez, F. 1983. Quantitative relationship between soil colour and hematite content. Soil Science, 136, 354-358.

Trigo, I.F., Davies, T.D. and Bigg, G.R. 2000. Decline in Mediterranean rainfall caused by weakening of Mediterranean cyclones. Geophysical Research Letters, 27, 18, 2913-2916.

Turner, C., Hannon, G.E. 1988. Vegetational evidence for the Late Quaternary climatic changes in southwest Europe in relation to the influence of the North Atlantic Ocean. Philiosophical Transactions of the Royal Society, B 3318, 451-485.

Tzedakis, P.C. 1993. Long term tree populations in northwest Greece through multiple Quaternary climatic cycles. Nature, 364, 437-440.

Tzedakis, P.C., Andrieu, V., de Beaulieu, J.L., Birks, H.J.B., Crowhurst, S., Follieri, M., Hooghiemstra, H., Magri, D., Reille, M., Sadori, L., Shackleton, N.J. and Wijmstra, T.A. 2001. Establishing a terrestrial chronological framework as a basis for biostratigraphical comparisons. Quaternary Science Reviews, 20, 1583-1592.

Tzedakis, P.C., Andrieu, V., de Beaulieu, J.L., Crowhurst, S., Follieri, M., Hooghiemstra, H., Magri, D., Reille, M., Sadori, L., Shackleton, N.J. and Wijmstra, T.A. 1997. Comparison of terrestrial and marine records of changinf climate of the last 500,000 years. Earth and Planetary Science Letters, 150, 1-2, 171-176.

Valero-Garcés, B., Zeroual, E. and Kelts, K. 1998. Arid phases in the Western Mediterranean region during the Lat Glacial cycle reconstructed from lacustrine records. In: Benito, G., Baker, V.R. and Gregory, K.J. (Eds), Palaeohydrology and Environmental Change. Chichester, United Kingdom, Wiley, 67-80.

van Andel, T.H. 1998. Middle and Upper Palaeolithic environments and the calibration of ^{14}C dates beyond 10,000 BP. Antiquity, 72, 27-33.

van Andel, T.H., Runnels, C.N. and Pope, K.O. 1986. Five thousand years of land use and abuse in the southern Argloid, Greece. Hesperia, 55, 103-128.

van Andel, T.H. and Tzedakis, P.C. 1996. Palaeolithic landscapes of Europe and environs, 150,000-25,000 years ago: an overview. Quaternary Science Reviews, 15, 481-500.

van Andel, T. H., Zangger, E. and Demitrack, A. 1990. Land use and soil erosion in Prehistoric and Historical Greece. Journal of Field Archaeology, 17, 379-396.

van Andel, T.H., Zangger, E. and Perissoratis, C. 1990b. Quaternary transgressive/regressive cycles in the Gulf of Argos, Greece. Quaternary Research, 34, 317-329.

Vita-Finzi, C. 1969. The Mediterranean Valleys: Geological changes in historical times. Cambridge, Cambridge University Press.

Von Grafenstein, U., Erlenkauser, H., Brauer, A., Jouzel, J., Johnsen, S.J. 1999. A mid-European decadal isotope-climate record from 15,500 to 5,000 years BP. Science, 284, 1654-1657.

Waelbroeck, C., Duplessy, J.C., Michel, E., Labeyrie, L., Paillard, D. and Duprat, J. 2001. The timing of the last deglaciaiton in North Atlantic climate records. Nature, 412, 6848, 724-727.

Wagstaff., J.M. 1981. Buried assumptions: some problems with the interpretation of the "Younger Fill" raised by recent data from Greece. Journal of Archaeological Science, 8, 167-177.

Wainwright , J. 1996. Hillslope response to extreme strom events: The example of the Vaison-La0Romaine Event. In: Anderson, M.G. and Brooks, S.M. (Eds), Advances in Hillslope Processes, Volume 2. John Wiley & SOnsm Chichester, 997-1026.

Walden, J. 1999. Remanence measurements. In: Walden, J., Oldfield, F. and Smith. J. (Eds), Environmental Magnetism: A practical guide. Quaternary Research Association, Technical Guide 6, 63-89.

Walling, D.E. and Webb, B.W. 1983. Patterns of Sediment Yield. In: Gregory, K.J. (Ed), Background to Palaeohydrology. Chichester, Wiley, 69-100.

Watts, W.A. 1985. A long pollen record from Laghi di Monticchio, southern Italy: a preliminary account. Journal of the Geographical Society, 142, 491-499.

Watts, W.A. 1986. Stages of climatic changes from full glacial to Holocene in northwest Spain, southern France and Italy: a comparison of the Atlantic coast and the Mediterranean Basin. In: Ghazi, A. and Fantechi, R. (Eds), Current Issues in Climate Research, Reidel, Dordrecht, D., 101-112.

Watts, W.A., Allen, J.R.M. and Huntley, B. 2000. Palaeoecology of three interstadial events during oxygen-isotope Stage 3 and 4: A lacustrine record from Lago Grande di Monticchio, southern Italy. Palaeogeography, Palaeoclimatology and Palaeoecology, 155, 83-93.

Watts, W.A., Allen, J.R.M., Huntley, B. and Fritz, S.C. 1996. Vegetation history and climate of the last 15,000 years at Laghi di Monticchio, Southern Italy. Quaternary Science Reviews, 15, 113-132.

Webber, P.J. and Andrews, J.T. 1973. Lichenometry: A commentary. Arctic and Alpine Research, 5, 4, 295-302.

Wentworth, C.K. 1922. A scale of grade and class terms for clastic sediments. Journal of Geology, 30, 377-392.

White, J.C.W., Barlow, L.K., Fisher, D., Grootes, P.M., Jouzel, J., Johnsen, S.J., Stuiver, M. Clausen, H.B. 1997. The climate signal in the stable isotopes of snow from Summit, Greenland; results of comparisons with modern climate observations. Journal of Geophysical Research, C, 102, 12, 26,425-26,439.

Wigley, T.M.L. 1992. Future climate of the Mediterranean Basin with particular emphasis on changes in precipitation. IN: Jefic, L., Millman, J.D. and Sestini, G. (Eds), Climatic Change and the Mediterranean. Edward Arnold, London, 15-44.

Wigley, T.M.L. and Farmer, G. 1982. Climate of the eastern Mediterranean and the Near East. In Bintliff, J.L. and van Zeist, W. (Eds), Palaeoclimates, Palaeoenvironments and Human Communities in the Eastern Mediterranean Region in the Late Prehistory B.A.R. International Series 133, Oxford, British Archaeological Reports, 3-37.

Wijmstra, T.A. 1969. Palynology of the first 30 metres of a 120 m deep section in northern Greece. Acta Botanica Neerlandica, 18, 511-527.

Willis, K.J. 1994. The vegetational history of the Balkans. Quaternary Science Reviews, 13, 769-788.

Willis, K.J., Rudner, E. and Sümegi, P. 2000. The full Glacial forests of central and southeastern Europe. Quaternary Research, 53, 203-213.

Winograd, I.J., Coplen T.B., Landwehr, J.M., Riggs, A.C., Ludwig, K.R., Szabo, B.J., Kolesar, P.T. and Revesz, K.M. 1992. Continuous 500,000-year climate record from vein calcite in Devils Hole, Nevada Science, 258, 255-260.

Winograd, I.J., Landwehr, J.M., Ludwig, K.R., Coplein, T.B. and Riggs, A.C. 1997. Duration and structure of the past four Interglaciations. Quaternary Research, 48, 141-154.

Wintel, A.G. 1977. Detailed study of a thermoluminescent mineral exhibiting anomalous fading. Journal of Luminescence, 15, 385-393.

Wintle, A.G. 1991. Luminescence dating. In: Smart, P.L. and Frances, P.D. (Eds), Quaternary Dating Methods – A Users Guide. Quaternary Research Association Technical Guide 4, Cambridge, 108-127.

Wintle, A.G. 1998. Luminescence dating: laboratory procedures and protocols. Radaition Measurements 27, 5-6, 769-817.

Wintle, A.G. and Murray, A.S. 1999. Luminescence sensitivity changes in quartz. Radiation Measurements, 30, 107-118.

Woillard, G.M. 1978. Grande Pile peat bog: a continuous pollen record for the last 140 000 years. Quaternary Research, 9, 1-21.

Woillard, G.M. and Mook, W.G. 1982. Carbon-14 dates at Grande Pile: Correlation of land and sea chronologies. Science, 215, 8,159-161.

Woo, M.K. and Fitzharris, B.B. 1992. Reconstruction of mass balance variations for Franz Josef Glacier, New Zealand, 1913-1989. Arctic Alpine Research, 24, 281-290.

Woodward, J.C. 1990. Late Quaternary sedimentary environments in the Voidomatis basin, northwest Greece, unpublished Ph.D., University of Cambridge.

Woodward, J.C. 1995. Patterns and erosion and suspended sediment yield in the Mediterranean river basins. In: Foster, I.D.L., Gurnell, A.M., and Webb, B.E. (Eds), Sediment and Water Quality in River Catchments. Wiley, Chichester, 365-389.

Woodward, J.C., Lewin, J. and Macklin, M.G. 1992. Alluvial sediment sources in a glaciated catchment: the Voidomatis Basin, Northwest Greece. Earth Surface Processes and Landforms, 17, 205-216.

Woodward. J.C., Lewin, J., Macklin, M.G. 1995. Glaciation, river behaviour and the Palaeolithic settlement of upland northwest Greece. In: Lewin, J., Macklin, M.G., Woodward, J.C. (Eds), Mediterranean Quaternary River Environments. Balkema, Rotterdam, 115-129.

Woodward, J.C., Macklin, M.G., Lewin, J. 1994. Pedogenic weathering and relative-age dating of Quaternary alluvial sediments in the Pindus Mountains of northwest Greece. In: Robinson, D.A., Williams, R.B.G. (Eds), Rock Weathering and Landforms Evolution. Wiley, Chichester, 259-283.

Woodward, J.C. Macklin, M.G. and Smith, G.R. in press. Pleistocene glaciation in the mountains of Greece. In: Ehlers, J. and Gibbard, P.L. (Eds), Quaternary Glaciations - Extent and Chronology. Part I: Europe. Amsterdam, Elsevier.

Woodward, J.C., Macklin, M.G. and Welsby, D.A. 2001. The Holocene fluvial sedimentary record and alluvial geoarchaeology in the Nile Valley of Northern Sudan. In: Maddy, D.R., Macklin, M.G. and Woodward, J.C. (Eds), River Basin Sediment Systems: Archives of Environmental Change. Balkema, Rotterdam, 327-355.

Yokoyama, Y., Reyss, J. and Guichard, F. 1977. Production of radionuclides by cosmic rays at mountain altitudes. Earth and Planetary Science Letters, 36, 44-50.

Yoshida, S. 1962. Hydrometeorological study on snowmelt. Journal of Meterological Research, 14, 879-899.

Yu, L. and Oldfield, F. 1993. Quantitative sediment source ascription using magnetic measurements in a reservoir-catchments system near Nijar, S.E. Spain. Earth Surface Processes and Landforms, 18, 441-454.

Zehfuss, P.H., Bierman, P.R., Gillespie, A.R., Burke, R.M. and Caffee, M.W. 2001. Slip rates on the Fish Springs fault, Owens Valley, California, deduced from cosmogenic Be-10 and Al-26 and soil development on fan surfaces. Geological Society of America Bulletin, 113, 2, 241-255.

Zreda, M.G. and Noller, J.S. 1998. Ages of prehistoric earthquakes revealed by cosmogenic chlorine-36 in a bedrock fault scarp at Hebgen Lake. Science, 282, 5391, 1097-1099.

Zreda. M.G. and Phillips, F.M. 1995. Insights into alpine moraine development from cosmogenic ^{36}Cl buildup dating. Geomorphology, 14, 149-156.

Zreda, M.G., Phillips, F.M. and Elmore, D. 1994. Cosmogenic ^{36}Cl accumulation in unstable landforms 2. Simulations and measurements on eroding moraines. Water Resources Research, 30, 3127-3136.

Zreda, M.G., Phillips, F.M., Kubik, P.W., Sharma, P. and Elmore, D. 1991. Cosmogenic ^{36}Cl dating of a young basaltic eruption complex, Lathrop Wells, Nevada. Geology, 21, 57-60.

Zreda, M.G, Phillips, F.M., Kubik, P.W., Sharma, P. and Elmore, D. 1993. Cosmogenic Cl-36 of a young basaltic eruption complex, Lathrop Wells, Nevada. Geology, 21, 1, 57-60.

Zumbühl, H., Budmiger, G. and Haeberli, W. 1981. Historical documents. In: Switzerland and Her Glaciers. Kummerly and Frey, Berne, 48-69.

APPENDIX I

Sample preparation for *in-situ* ^{10}Be cosmogenic nuclide dating - laboratory notes

1. **Rock grinding and crushing**
2. **Isolation and dissolving of quartz**
3. **Fuming**
4. **Taking an aliquot**
5. **Iron extraction**
6. **Precipitation**
7. **Cation exchange**
8. **Precipitation**
9. **Drying and baking**
10. **Target pressing**

1. Rock grinding and crushing

- It is important to thoroughly clean the equipment to avoid contamination.
- The thickness of the rock was recorded before being crushed. A jaw crusher was used to break the rock up into manageable sizes, and a smaller machine to crush to 2 mm size. The sample was then sieved and the 0.5-1mm fraction and the 1-2 mm fraction separated and bagged. Crushed samples should be monominerallic if possible.
- Sieving is a good way to reduce bias if not dissolving all of the crushed material, but it should ideally be placed repeatedly in a splitter, or mixed by using the paper corner folding method. However, Masarik and Reedy (1995) suggest that there is not an exponential relationship of production rate with depth in the first few cm or so, perhaps reducing the importance of mixing.
- A Franz separator could be used 3-4 times at this stage to remove the mafic minerals. Alternatively, heavy liquid mineral separation can be conducted to remove any magnetic fines. This leads to a purer quartz sample.

2. Isolation and dissolving of quartz

- Crushed rock was rinsed (50-70 g), and placed in a plastic 1 litre beaker with 50 ml of 40% hydrofluoric acid (HF) and 0.5 l of distilled water and agitated on a shaker table for ~24 hours. The material was rinsed thoroughly and the fines were discarded. The HF step was repeated 5-6 times or until all the other minerals had dissolved. The sample was dried on a hotplate at 60-70°C for several hours and using a microscope, the remaining feldspars (white, opaque), epidote (green) and muscovite grains were removed. Any black specks from the crushing machine were also removed. The purer the quartz, the better.
- Repeated digestion of the sample with HF isolates the quartz but also totally decontaminates the material from atmospheric ^{10}Be. Because meteoric Be is only absorbed on the surface of the quartz structure, even after one HF leaching step it is completely removed (Ivy-Ochs, 1999, PSI report) (unlike pyroxene).
- The quartz sample was weighed and placed in a Savillex PFA teflon beaker together with the Be carrier (ICP standard ^{9}Be $(NO_3)_2$ solution 1 mg/ml or 1000 ppm) which was measured by an Eppindorf autopipette. A blank was also prepared (just the carrier was added). Amount of carrier depends on the age of the sample and the weight of quartz to be dissolved. The sample should have at least 10x the carrier (~$5x10^{-13}$). AMS has a sensitivity of 10^{-15} to 10^{-11}. Ideally the amount of carrier added should be 0.4 or 0.5 ml, but 0.35 ml is acceptable if there is limited pure quartz (it is just more difficult to find the Be in the blank sample as the beaker has to be rinsed thoroughly before every extraction). Samples C1 and C2 had 0.35ml of carrier added. The weight was also recorded before the Be solution evaporated (0.35 ml = 0.35 g) as the auto pipette was not always exact. Nitric acid (69%HNO_3) was used to rinse the sides of the beaker where the Be carrier had been added. N.B. Be is toxic. Do not spill.
- Concentrated 48%HF was added to cover the quartz, and the beaker swirled. Samples were left on a hotplate at 80°C to dissolve. The HF was continually topped up so the sample did not dry out. If the HF effervesced violently, a little pure water was put in it to calm it. Samples on the hotplates should always have a protective cover over them and all this should be conducted in the fume cupboard. The sample blank should be treated similarly to the samples (so add a little HF, although this is not essential). Pure water was added so the blank did not evaporate. There is no problem if the sample dries completely when left overnight however, even if there appears to be nothing in the beaker. Be does not evaporate off at such low temperatures.
- 5 g of quartz usually dissolves a day on average, but samples C1 and C2 only took 6 days in total. Silicon is dissolved and removed as volatile silicon tetrafluoride (SiF_4).

3. **Fuming**

- Next procedure included adding several ml of concentrated nitric acid to the samples and fuming until nearly dry on a hotplate of 80-90°C. This was repeated an additional 2 times with nitric acid and another 3 times with concentrated hydrochloric acid. With sample C1, fuming was undertaken 8 times altogether, 4 HNO_3, 3 HCL and one inbetween with half HNO3 and half HCL. If the HCL step is conducted before the sample is ready (if not transparent), and nitric acid is added, 3 fumings of HNO_3 have to be repeated before the HCL step again. Samples C1 and C2 seemed to have some sort of white salts/precipitate forming. This could have been calcium fluoride. Ideally all the fluoride should be fumed off as SiF_4. Sometimes there are problems with column overloading when the cation exchange is employed if there is a lot of fluoride (calcium/aluminium) in the sample.
- The samples were a bright yellow/orange colour when nitric/hydrochloric was added. This is indicative of a high iron content. C1>C2.

4. **Taking an aliquot**

- The nearly dry samples (no moving moisture) were taken and hydrochloric acid was added to lower the pH. The sides of the beakers were rinsed with HCL to ensure the Be did not remain stuck to the sides. Using a clean pipette an aliquot was taken and placed in a 100ml round flask. The undissolved material / precipitate / zircon specks were carefully avoided and kept in a small sample pot. The beakers were thoroughly rinsed with pure water (x3 at least) and the flask is filled up to 100ml. It was then shaken vigorously. If the solution is not clear it should be left for 20-30 minutes, or longer so that the solids settle. C2 was slightly foggy so it was left to settle for 20 minutes. Transferred ~4ml into small tube for Al ICP-AES measurement (future reference). The tube and lid was rinsed and dried thoroughly. The beaker was rinsed to remove any left junk, and the remaining solution poured back. The flask was rinsed with a little HCL and pure water. The sample solution was then placed back on the hotplate to evaporate down.

5. **Iron extraction**

- N.B. Extraction of iron can be conducted before or after the cation exchange column.
- A 20ml drip tube was filled with 10ml resin (Analytical Grade Anion Exchange Resin, AG 1-X8 Resin, 50-100*mesh, Chloride form (500g) Catalogue 140-1431. *or 100-200 mesh, smaller granules – remove Fe more efficiently?, either are fine). The resin needs to be wet so it can be pipetted into the tube, so pure water was added to the jar of resin, and 10ml of solid resin used (let water drain through). The resin was rinsed by eluting i) 50 ml H_20, ii) 50ml 1 molar HCL, iii) 50 ml 4.5 molar HCL and iv) 100 ml 9 molar HCL. If the column has been used previously, precede the cleaning step with 100ml 1 molar HCL. Using H_20 immediately after the Fe extraction would result in precipitation of $Fe(OH)_3$. The cleaning procedure can be done using made up 1, 4.5 and 9 molar HCL solutions from concentrated HCL; it does not have to be exact.
- The samples were taken up in 2-3ml of 9 molar HCL. Everything should have dissolved. The solution should be clear, if not, add a little more HCL. The sample was pipetted onto the anion resin and collected in a small bottle. Rinsed the beaker with 4-5ml of 9 molar HCL. Added 20 ml of 9N HCL and collected it in the beaker and poured the bottle contents back into the beaker. Rinsed bottle with a little acid and water. Repeated for the blank. Placed samples back on the hotplate (100°C). Kept temperature below 120°C as aluminium fluoride evaporates at 180°C. Cleaned and filled the columns with several ml of 9N HCL and used a stopper to ensure the resin did not dry out.
- The iron is removed from the sample and left on the column in the form of $FeCl_4^-$.

6. **Precipitation**

- Dryish sample was saturated and all was dissolved with a few ml of concentrated HCL so a clear liquid was formed. This was transferred to a 10 ml small tube. The beaker was thoroughly rinsed with pure water and a little acid by continuously squirting with a pipette around the sides of the beaker. No more than 7-8ml can be used to rinse with though as ammonium has to be added.
- 25-30 drops of NH_4OH was added to increase the pH, although the amount varies according to how much HCL was used to rinse the beaker. The optimum pH for beryllium and aluminium hydroxides to be precipitated is 8, but 7-9 is O.K. (Ochs & Ivy-Ochs, 1998). A lid was placed on the tube and the sample shaken well. Precipitation of the hydroxides should be clearly evident. The pH was tested on the lid (white section should go pale pink – if dark pink, add a little HCL and if white, add several more drops of ammonium). The sample was shaken well and left overnight. The more the sample is shaken the better, and the longer the sample is left the better this unlocks and releases the Boron.

- Centrifuged the samples, 4000 r.p.m. for about 15 min. Poured off the liquid into another tube and saved. Shot in fresh water to ¾ full and shook well so that it was evenly mixed. Centrifuged again, and poured the supernatant off again and kept. Squirted a few ml of HCL into the sample tube and poured back into own beaker. Rinsed the tube thoroughly (x4-5 times) with acid and pure water. Cooked until almost dry so there was no moving moisture.

7. Cation exchange

- Cation Exchange Resin, AG 50W-X8, 100-200 mesh, Hydrogen form (500g) (Catalogue, 142-1441 – Bio-Rad Labs). Measured volume of column (up to 5-10 cm from top), marked, placed a small bit of quartz wool at the bottom end and checked with water that it did not block. The columns were filled up to the mark with the resin (solid) and the water was drained through. Cleaned the resin by draining through 3 column volumes of i) 9 molar HCL, ii) 4.5 molar HCL and iii) 1 molar HCL (made up HCL to the specific concentrations).
- Took up the sample in 1-2 ml of 1 molar HCL (exact concentration: C(HCL) = 1mol/1 1N, 1.09970 Titrisol for 1000ml) after it had cooled down, and swirled it. Sample should be clear. Add a little more HCL if it is foggy. Loaded onto the column gradually and collected it in a bottle.
- 10 column volumes of exact 1N HCL was passed through the column. The first 2 volumes (Vorlauf) were collected in a bottle. Some of this amount was used to rinse the beaker out. The 3-10 volumes were captured in the beaker. The beryllium is generally extracted from the cation column during the 4-7th column volume in the form of $BeCl^{+1}$.
- The Al can start to be eluted during the 9-10^{th} column volume, but usually the Al is extracted by draining 4.5 N HCL through. 3 column volumes of 4.5N HCL were collected in a bottle. Aluminium is eluted as Al^{+3}.
- The beaker contents (3-10 column volumes) containing the $BeCl^{+1}$ were cooked down to dryness at 140°C (turned down to 110°C overnight). If there appears to be a lot of white precipitate when dry, it is preferable to elute the sample again through the cation exchange column, so as to obtain a purer Beryllium sample. (A purer Be sample will lead to a more accurate AMS measurement with lower errors). Again the vorlauf amount is retained in a bottle and the 3-10 column volumes collected in the beaker. For samples C1 and C2, 2 columns were conducted. Both samples seemed to have a lot of white precipitate when dry, inferring other elements may have been eluted with the beryllium. The 1-3 column volumes of Al were again collected in a bottle using 4.5N HCL.

8. Precipitation

- After the samples were dry, they were taken up in 2-3ml of 1N HCL (exact concentration) and placed in a centrifuge tube. The beaker was rinsed thoroughly as before for the previous precipitation stage with a little concentrated HCL and pure water. Ammonium was added and the tubes were shaken well. The pH was tested to ensure it was 8 and the samples were left overnight before being centrifuged (4000 r.p.m., 15 min). There should be a lot less precipitation evident than that before the cation exchange column procedure.
- The sample solution containing the aluminium (first Al elute) was placed into its own beaker after the Be sample had been precipitated and it was also cooked down until dry and then precipitated.
- The Be blank sample was treated in the same way. With only 0.35ml of Be carrier it is difficult to see it /not to lose it. It is suggested that maybe an Al carrier should be added also (Ivy-Ochs, p.c.) to the blank. However with the sample blank prepared with C1 and C2 (April 2000), the Be hydroxides during the precipitation stage were clearly evident. Rinsing the beakers thoroughly to ensure the Be is not stuck to the sides is essential at all stages.
- The Be samples, Al samples and the blank were centrifuged after being left overnight and the supernatant was decanted. Pure water was squirted in up to ¾ in the tube after the first centrifuge, and vigorously shaken to ensure the precipitant was evenly mixed.

9. Drying and baking

- Dust sprayed everything to minimise the influence of Boron- the quartz tray and the sample holders, and the pipettes and drew a diagram as to which sample was where on the tray.
- Air was gently exuded into the precipitate with a drop of water to ease it away from the tube sides. It was taken up in the pipette and placed in the sample holder (tiegel) – a small a volume as possible. It does not matter if not all the sample is placed in, although with the Be, the more the better, as there is a limited amount. If the holder is full and there is still a lot of sample left, centrifuge again and wait for sample to dry down a little and pipette the remaining amount into holder.

- The samples must not dry too quickly – they must not bubble and splash out and contaminate. The hotplate was set on 80°C and the samples were left to dry. Samples C1 and C2 were left overnight and were dry the next morning (~24 h).
- Placed lids on the tiegels and the quartz tray lid and baked the samples in the muffle furnace at 950°C for 2h 25m. The furnace is a source of Boron, so it is important that the lids are on.

10. Target pressing

- The samples were cooled and they were pressed in a target with copper powder (for conductivity during measurement). In a laminar flow cupboard, the samples were ground, the sides were scraped, and mixed with copper powder. The proportion of copper is not important, but generally, 4-5x copper is used to sample. The sample mixture is compacted in the target until the hole is completely filled. A mask is used when dealing with Be, as the powder can be poisonous if inhaled. All the instruments must be rinsed with alcohol, and a different spoon used for each sample and one for the copper powder to avoid any cross contamination. Samples were labelled on the copper disc and noted in the file.

APPENDIX II

Correction factor for mountain shielding to calculate cosmogenic nuclide exposure ages

Mountain shielding for samples C1 and C2, to be used in conjunction with Equation 4.2. The latitude and longitude correction is obtained by Lal's (1991) polynomial equation and the thickness of the sample by Equation 4.3.

Sample C1 Mt Giovanni, N 42 00' 08, alt. 1,200 m		Sample C2 Col de Vergio, N 42 18' 47, alt. 1,220 m	
Orientation (degrees)	Angle ($\tan^{-1}$)	Orientation (degrees)	Angle ($\tan^{-1}$)
0-7	3.68	0-5	3.33
7-12	3.62	5-9	2.9
12-18	5.96	9-13	5.57
18-30	9.73	13-19	6.52
30-46	11.46	19-25	8.09
46-55	12.37	25-32	8.37
55-80	15.16	32-42	7.62
80-98	11.92	42-54	6.69
98-105	6.74	54-58	7.74
105-112	5.03	58-66	6.39
112-118	4.61	66-72	6.24
118-124	6.2	72-78	5.59
124-134	5.56	78-83	2.34
134-144	4.76	83-91	4.21
144-155	2.31	91-100	7.21
190-198	6.94	147-158	12.12
198-217	9.46	158-174	15.33
217-229	10.87	174-190	15.42
229-244	20.56	190-205	14.04
244-269	19.52	205-215	11.98
269-290	19.29	215-225	10.62
290-310	21.21	225-239	13.5
		239-260	24.01
		260-290	20.14
		290-310	15.05

APPENDIX III

Snowpack model, based on present day conditions in Corsica and proxy climate data for the Younger Dryas cooling

Elev (m)	Jan.	Feb.	Mar.	Apr.	May.	June	July	Aug.	Sep.	Oct.	Nov.	Dec
Temperature (°C) (based on the 1951-1985 monthly average for Ajaccio (World Climate Disk) and the ELR of 6.5°C/km)												
0	7.9	8.6	10.1	12.3	15.8	19.5	22.0	22.0	19.8	16.0	12.0	9.2
165	6.8	7.5	9.0	11.2	14.7	18.4	20.9	20.9	18.7	14.9	10.9	8.1
470	4.8	5.5	7.0	9.2	12.7	16.4	18.9	18.9	16.7	12.9	8.9	6.1
600	4.0	4.7	6.2	8.4	11.9	15.6	18.1	18.1	15.9	12.1	8.1	5.3
740	3.1	3.8	5.3	7.5	11.0	14.7	17.2	17.2	15.0	11.2	7.2	4.4
950	1.7	2.4	3.9	6.1	9.6	13.3	15.8	15.8	13.6	9.8	5.8	3.0
1260	-0.3	0.4	1.9	4.1	7.6	11.3	13.8	13.8	11.6	7.8	3.8	1.0
1500	-1.9	-1.2	0.4	2.6	6.1	9.8	12.3	12.3	10.1	6.3	2.3	-0.6
1750	-3.5	-2.8	-1.3	0.9	4.4	8.1	10.6	10.6	8.4	4.6	0.6	-2.2
2000	-5.1	-4.4	-2.9	-0.7	2.8	6.5	9.0	9.0	6.8	3.0	-1.0	-3.8
2250	-6.7	-6.0	-4.5	-2.3	1.2	4.9	7.4	7.4	5.2	1.4	-2.6	-5.4
2500	-8.4	-7.7	-6.2	-4.0	-0.4	3.3	5.8	5.8	3.6	-0.3	-4.3	-7.1
2750	-10.0	-9.3	-7.8	-5.6	-2.1	1.6	4.1	4.1	1.9	-1.9	-5.9	-8.7
Rainfall (mm) (based on the 1951-1985 monthly average for Ajaccio (World Climate Disk) and the percentage increase in rainfall with elevation calculated from interpolating Figures 2.8 & 2.12)												
0	77.08	70.39	60.29	46.66	46.61	22.33	9.90	20.10	45.40	83.74	95.64	82.35
165	77.69	70.96	60.78	47.04	46.98	22.50	9.98	20.26	45.77	84.41	96.41	83.00
470	103.57	94.59	81.02	62.70	62.63	30.00	13.30	27.00	61.01	112.52	128.51	110.64
600	131.94	120.50	103.21	79.88	79.79	38.22	16.95	34.40	77.72	143.35	163.72	140.96
740	150.41	137.37	117.66	91.06	90.96	43.57	19.32	39.22	88.60	163.42	186.65	160.70
950	163.95	149.74	128.25	99.26	99.14	47.49	21.06	42.75	96.58	178.13	203.44	175.16
1260	184.94	168.90	144.67	111.96	111.83	53.57	23.75	48.22	108.94	200.93	229.48	197.58

After year 5, permanent snow is evident at an elevation of 2,716 m. Below this altitude, snow cover is only present part of the year. Refer to the following tables.

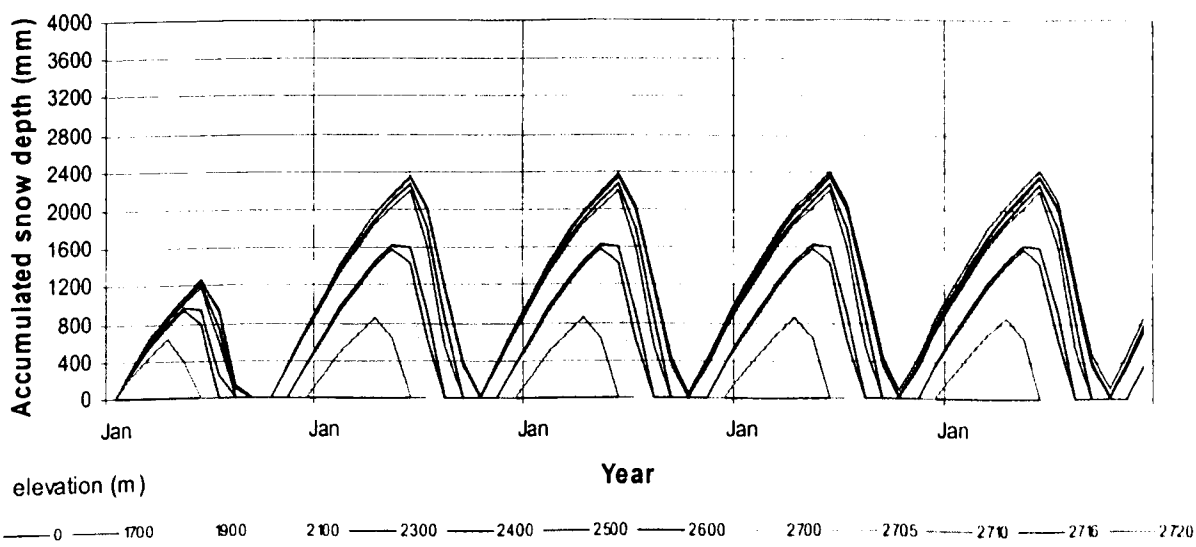

Rate of accumulation and ablation of snow varies with elevation which influences the net total (e.g. Yr 5)

Rate of accumulation of snow

Elevation	Jan	Feb	Mar	Apr	May	Jun	Jul	Aug	Sep	Oct	Nov	Dec
0	0.00	0.00	0.00	0.00	0.00	0.00	0.00	0.00	0.00	0.00	0.00	0.00
1700	234.65	214.83	178.47	0.00	0.00	0.00	0.00	0.00	0.00	0.00	0.00	239.92
1900	253.18	231.83	192.37	149.39	0.00	0.00	0.00	0.00	0.00	0.00	301.10	258.45
2100	271.72	248.82	206.28	160.21	0.00	0.00	0.00	0.00	0.00	0.00	322.73	276.99
2300	290.26	265.81	220.18	171.02	0.00	0.00	0.00	0.00	0.00	0.00	344.36	295.53
2400	299.53	274.31	227.13	176.43	0.00	0.00	0.00	0.00	0.00	0.00	355.17	304.80
2500	308.80	282.80	234.08	181.83	181.78	0.00	0.00	0.00	0.00	334.77	365.98	314.07
2600	318.07	291.30	241.04	187.24	187.19	0.00	0.00	0.00	0.00	344.81	376.80	323.33
2700	327.33	299.80	247.99	192.65	192.59	0.00	0.00	0.00	0.00	354.86	387.61	332.60
2705	327.80	300.22	248.34	192.92	192.86	0.00	0.00	0.00	0.00	355.36	388.15	333.07
2710	328.26	300.65	248.68	193.19	193.13	0.00	0.00	0.00	0.00	355.86	388.69	333.53
2716	328.82	301.16	249.10	193.51	193.46	0.00	0.00	0.00	0.00	356.46	389.34	334.09
2720	329.19	301.50	249.38	193.73	193.67	0.00	0.00	0.00	0.00	356.86	389.77	334.46

Rate of ablation

Jan	Feb	Mar	Apr	May	Jun	Jul	Aug	Sep	Oct	Nov	Dec
1477.9	1450.6	1879.7	2220.2	2930.8	3514.1	4093.6	4094.1	3561.9	2979.7	2166.2	1706.9
0.0	0.0	0.0	231.2	875.5	1525.1	2038.3	2038.8	1572.9	924.4	177.2	0.0
0.0	0.0	0.0	0.0	633.7	1291.1	1796.5	1797.0	1338.9	682.6	0.0	0.0
0.0	0.0	0.0	0.0	391.9	1057.1	1554.7	1555.2	1104.9	440.8	0.0	0.0
0.0	0.0	0.0	0.0	150.1	823.1	1312.9	1313.4	870.9	199.0	0.0	0.0
0.0	0.0	0.0	0.0	29.2	706.1	1192.0	1192.5	753.9	78.1	0.0	0.0
0.0	0.0	0.0	0.0	0.0	589.1	1071.1	1071.6	636.9	0.0	0.0	0.0
0.0	0.0	0.0	0.0	0.0	472.1	950.2	950.7	519.9	0.0	0.0	0.0
0.0	0.0	0.0	0.0	0.0	355.1	829.3	829.8	402.9	0.0	0.0	0.0
0.0	0.0	0.0	0.0	0.0	349.3	823.2	823.8	397.1	0.0	0.0	0.0
0.0	0.0	0.0	0.0	0.0	343.4	817.2	817.7	391.2	0.0	0.0	0.0
0.0	0.0	0.0	0.0	0.0	336.4	810.0	810.5	384.2	0.0	0.0	0.0
0.0	0.0	0.0	0.0	0.0	331.7	805.1	805.6	379.5	0.0	0.0	0.0

Year 5 of the model

Jan	Feb	Mar	Apr	May	Jun	Jul	Aug	Sep	Oct	Nov	Dec
0.0	0.0	0.0	0.0	0.0	0.0	0.0	0.0	0.0	0.0	0.0	0.0
239.9	474.6	689.4	867.9	636.7	0.0	0.0	0.0	0.0	0.0	0.0	0.0
559.6	812.7	1044.6	1236.9	1386.3	752.6	0.0	0.0	0.0	0.0	0.0	301.1
599.7	871.4	1120.3	1326.5	1486.7	1094.8	37.7	0.0	0.0	0.0	0.0	322.7
639.9	930.1	1196.0	1416.1	1587.2	1437.0	613.9	0.0	0.0	0.0	0.0	344.4
660.0	959.5	1233.8	1460.9	1637.4	1608.1	902.0	0.0	0.0	0.0	0.0	355.2
1014.8	1323.6	1606.4	1840.5	2022.3	2204.1	1615.0	543.9	0.0	0.0	334.8	700.8
1044.9	1363.0	1654.3	1895.3	2082.6	2269.8	1797.7	847.5	0.0	0.0	344.8	721.6
1075.1	1402.4	1702.2	1950.2	2142.8	2335.4	1980.3	1151.0	321.2	0.0	354.9	742.5
1076.6	1404.4	1704.6	1952.9	2145.8	2338.7	1989.4	1166.2	342.4	0.0	355.4	743.5
1078.1	1406.3	1707.0	1955.7	2148.9	2342.0	1998.6	1181.4	363.6	0.0	355.9	744.6
1094.5	1423.4	1724.5	1973.6	2167.1	2360.6	2024.2	1214.2	403.8	19.5	376.0	765.3
1160.7	1489.9	1791.4	2040.8	2234.5	2428.2	2096.5	1291.3	485.7	106.2	463.0	852.8

N.B. With present conditions, snow is present at 1,700 m in May but not in June
Permanent snow is evident at an elevation of 2,716 m

APPENDIX IV

Methodology for analysing soil properties

1. **Redness rating**
2. **Particle size**
3. **Organic matter (%)**
4. **Calcium carbonate (%)**
5. **Pedogenic oxyhydroxides (Fe_d)**
6. **Pedogenic oxyhydroxides (Fe_o)**

1. Redness rating (Torrent *et al.*, 1983)

- Sieve the samples to < 2mm fraction
- Rub soil particles on white paper and use Munsell chart to classify colour through a hue, value and chroma value
- Redness rating = (10-hue)* (chroma/value)

2. Particle size

- Sieve the samples to the <2 mm fraction.
- Run a control sample through the Coulter® LS™ 230 counter to determine the optimum quantity of calgon to produce the greatest dispersant of particles in the clay fraction.
    - Add soil sample direct to the Coulter Counter.
    - Make a paste with 1 g of soil and a small volume of 5% Calgon.
    - Repeat with 100, 150 and 250 ml 5% Calgon.
- Conduct the particle size analysis using the best results from above (150 ml 5% calgon).
- Add 150 ml 5% Clagon to 1 g of soil and place on a horizontal shaker for 24 hours.
- Rinse the Coulter® LS™ 230 at 100% pump speed for 3 minutes, and measure for background and loading. Calibrate with standard GIS garnet.
- Run each sample three times for 90 seconds each using Polarisation Intensity Differential Scatter (PIDS) (to measure particle sizes <0.4 μm) and Fraunhofer.
- The composition of sand (< 2000 – 63 μm), silt (<63 – 2 μm) and clay (< 2 μm) of each sample is expressed as a percentage.

3. Organic matter (%) (Gross, 1971)

- Oven dry for 24 hours at 105°C and place in a dessicator to cool.
- Place a weighed amount of soil in a crucible and heat in a furnace for 24 hours at 550°C.
- Remove, place in dessicator to cool and reweigh.
- % organic matter = $\frac{\text{(final soil weight + crucible) * 100}}{\text{initial soil weight + crucible}}$

4. Calcium carbonate (%) (Gross, 1971), conducted by Parry (1999)

- Add 10-20 ml of the HCL (5%) to a weighed quantity of air dried soil moistened with distilled water.
- Stir the solution until the effervescence ceases.
- Rinse the sample with distilled water and carefully pippet off.
- Air dry the soil and reweigh.
- % $CaCO_3$ = $\frac{\text{(final soil weight + crucible) * 100}}{\text{initial soil weight + crucible}}$

5. Total pedogenetic iron (Fe_d). Dithionite-Citrate method (Soil conservation service, U.S. Department of Agriculture, 1972) (Ross & Wang, 1993).

This treatment is particularly useful for dissolving the "free" (nonsilicate) Fe in soils (Ross & Wang, 1993). The overnight shaking procedure is simpler than the dithionite-citrate-bicarbonate method of Mehra & Jackson (1960) and it gives closely similar results (Sheldrick & McKeague, 1975).

All labware was thoroughly cleaned in 0.5 M nitric acid overnight and rinsed with dionised water before conducting the Pedogenic oxyhydroxide iron experiments. Labware reused during the procedures was also cleaned in this way to ensure no cross contamination. Polished water (no ions) was used to rinse the glassware in which the solutions from the reagents listed below were made.

APPENDIX IV continued

Reagents

Sodium hydrosulphite (dithionite), $Na_2S_2O_4$
Sodium citrate ($Na_3C_6H_5O_7 \cdot 2H_2O$), 0.68 M (200 g/l)
Certified atomic absorption standards, + 1%

- Weigh 0.5 g of soil, ground to pass a 35-mesh (500 μm) sieve, into a 30 ml plastic centrifuge tube.
- Add 25 ml of the sodium citrate solution.
- Add 0.4 g of dithionite.
- Stopper tightly and shake in an end-over-end shaker overnight.
- Remove stoppers and centrifuge for 20 min at 510 x g. Filter extracts containing suspended material.
- Prepare standard solutions for Fe by atomic absorption/ICP in a matrix of the extracting solution .
- If it is necessary to dilute the extracts, either dilute them with the extracting solution or prepare standards containing the same concentration of extracting solution as the diluted extracts.
- % Fe = $\frac{\mu g/ml \text{ in final solution} * \text{extractant (ml)} * \text{dilution} * 100}{\text{sample weight (mg)} * 1000}$

6. Paracrystalline and organically complexed iron (Fe_o). Acid ammonium oxalate method (McKeague & Day, 1966) (Ross & Wang, 1993). Fe_o determiniation.

The oxalate procedure is used to remove the sesquioxide weathering products from soils. Schwertmann (1959) showed that it could beused to estimate noncrystalline and poorly crystaline Fe in soils.

Reagents

A Oxalate solution $(NH_4)_2\ C_2O_4 \cdot H_2O$, 0.2 M (28.3 g/l)
B Oxalic acid solution ($H_2C_2O_4 \cdot 2H_2O$), 0.2 M (25.2 g/l)
Mix 700 ml of A and 535 ml of B, check pH and adjust to pH 3.0 by adding either A or B

- Weigh 0.250 g of soil, ground to pass a 100-mesh (150 μm) sieve, into a 15 ml test tube.
- Add 10 ml of the acid oxalate solution and stopper the tube tightly.
- Place the tubes in an end-over-end shaker and shake for 4 h (the extraction has to be conducted in the dark).
- Centrifuge the tubes for 20 min at 510 x g, decant the supernatant into a suitable container and analyse within a few days.
- Determine Fe by atomic absorption/ICP, following standard procedures (see Fe_d methodology).
- % Fe = $\frac{\mu g/ml \text{ in final solution} * \text{extractant (ml)} * \text{dilution} * 100}{\text{sample weight (mg)} * 10}$

APPENDIX V

Redness rating

Based on Munsell colour charts

Profile/ Lab. No.	Depth (cm)	Hue		Value	Chroma	Colour	Torrent *et al.*, 1983
T2							
1	0-30	7.5	YR	5	6	Brown	3.00
2	30-60	5	YR	4	6	Yellowish red	7.50
3	60-80	5	YR	5	8	Yellowish red	8.00
4	80-120	5	YR	5	8	Yellowish red	8.00
5	120-150	5	YR	5	8	Yellowish red	8.00
6	150-230	5	YR	6	8	Reddish yellow	6.67
7	230-380	7.5	YR	6	6	Reddish yellow	2.50
8	380-410	7.5	YR	6	6	Reddish yellow	2.50
T3							
9	0-20	7.5	YR	6	6	Reddish yellow	2.50
10	20-40	7.5	YR	5	6	Strong brown	3.00
11	40-60	5	YR	4	6	Yellowish red	7.50
12	60-80	5	YR	5	8	Yellowish red	8.00
13	80-100	5	YR	5	8	Yellowish red	8.00
14	100-120	5	YR	4	6	Yellowish red	7.50
15	120-140	5	YR	4	6	Yellowish red	7.50
16	140-160	5	YR	5	8	Yellowish red	8.00
17	160-180	5	YR	4	4	Reddish brown	5.00
18	180-200	7.5	YR	6	8	Reddish yellow	3.33
T4							
19	0-20	7.5	YR	4	6	Strong brown	3.75
20	20-40	5	YR	6	8	Reddish yellow	6.67
21	40-60	5	YR	5	8	Yellowish red	8.00
22	60-80	5	YR	6	8	Reddish yellow	6.67
23	80-100	5	YR	7	8	Reddish yellow	5.71
24	100-120	5	YR	6	6	Reddish yellow	5.00
25	120-140	7.5	YR	6	6	Reddish yellow	2.50
26	140-160	7.5	YR	4	6	Strong brown	3.75
27	160-180	7.5	YR	6	6	Reddish yellow	2.50
T5							
28	0-20	7.5	YR	4	2	Brown	1.25
29	20-40	7.5	YR	4	2	Brown	1.25
30	40-60	7.5	YR	4	3	Brown	1.88
31	60-80	7.5	YR	5	6	Strong brown	3.00
32	80-100	7.5	YR	5	6	Strong brown	3.00
33	100-120	7.5	YR	5	4	Brown	2.00
34	120-140	7.5	YR	5	4	Brown	2.00
35	140-160	7.5	YR	4	4	Brown	2.50
36	160-180	7.5	YR	5	2	Brown	1.00
37	180-200	7.5	YR	4	2	Brown	1.25
T6							
38	0-24	10	YR	6	3	pale brown	0.00
39	24-43	7.5	YR	6	4	light brown	1.67
40	43-56	7.5	YR	6	3	light brown	1.25

APPENDIX V continued

Profile/ Lab. No.	Depth (cm)	Hue		Value	Chroma	Colour	Torrent *et al.*, 1983
41	56-76	7.5	YR	6	2	pinkish grey	0.83
42	76-92	10	YR	6	2	light brownish grey	0.00
43	92-105	7.5	YR	7	2	pinkish grey	0.71
44	105-120	10	YR	6	1	grey	0.00
45	120-133	10	YR	6	2	light brownish grey	0.00
46	1333-147	10	YR	6	1	grey	0.00
47	147-156	10	YR	6	1	grey	0.00
48	156-170	10	YR	6	2	light brownish grey	0.00

N.B. Torrent et al., 1983 redness index (10-H) x Chroma/Value, where H is the number that precedes the YR of the hue designation.

APPENDIX VI

Particle size, Organic carbon and Calcium carbonate analysis

		Parry (1999)	Particle size (%)		
Profile/ Lab. No.	Orqanic carbon (%)	Calcium carbonate (%)	Sand (>63-<2000 µm)	Silt (>2-<63 µm)	Clay (<2 µm)
T2					
1	3.1	1.0	8.5	78.9	12.6
2	1.9	0.8	4.3	70.4	25.3
3	3.6	1.0	6.8	73.4	19.8
4	10.4	0.6	3.7	60.9	35.4
5	3.9	0.4	6.0	73.6	20.4
6	4.9	0.3	3.9	70.5	25.6
7	3.7	0.5	4.2	75.4	20.4
8	3.3	0.4	10.7	78.7	10.6
T3					
9	2.8	1.0	8.2	75.4	16.4
10	3.0	0.2	8.0	71.5	20.5
11	4.2	0.2	5.1	67.5	27.4
12	7.2	0.4	4.7	63.1	32.2
13	3.8	1.0	5.1	68.5	26.4
14	3.4	0.2	4.8	79.8	15.4
15	4.3	0.8	6.0	74.6	19.4
16	4.0	0.6	15.1	69.3	15.6
17	3.9	0.8	12.2	70.4	17.4
18	3.6	0.8	18.4	67.8	13.8
T4					
19	4.9	0.5	13.0	70.5	16.5
20	3.8	0.3	6.1	76.1	17.8
21	3.2	1.0	8.1	61.5	30.4
22	3.0	0.9	8.3	70.3	21.4
23	2.7	1.3	10.6	63.7	25.7
24	2.8	0.9	17.5	60.9	21.6
25	2.9	1.4	27.7	58.4	13.9
26	2.6	0.9	29.9	57.7	12.4
27	2.4	1.0	27.6	62.8	9.6
T5					
28	6.2	2.4	63.9	30.5	5.6
29	5.2	1.4	49.6	41.5	8.9
30	3	1.9	50.4	36.9	12.7
31	2.3	1.8	54.6	35.8	9.6
32	1.4	1.2	47.6	40.6	11.8
33	2.3	1.8	45.7	45.8	8.5
34	3.4	2.0	60.5	31.9	7.6
35	2.2	2.2	58.1	34.7	7.2
36	1.8	2.1	53.5	40.2	6.3
37	2.3	1.2	58.0	37.8	4.2
T6					
38	3.6	1.7	64.2	32.6	3.2
39	4.8	3.2	61.4	34.1	4.5
40	3.5	2.9	71.4	24.9	3.7
41	2.9	1.8	68.2	27.6	4.2
42	2.8	2.5	56.2	40.5	3.3
43	2.2	2.2	54.9	41.7	3.4
44	2.5	9	62.3	34.6	3.1
45	2.8	11.4	59.4	37.8	2.8
46	2.1	9.6	61.3	35.8	2.9
47	2	7.7	53.3	43.6	3.1
48	1.6	4.4	60.6	36.4	3
Duplicates					
3	3.6	No data	10.5	60.1	29.4
3	3.8	No data	12.6	65.3	22.1 [a]
8	3.5	No data	6.8	83.4	9.8
8	3.4	No data	12.4	71.4	16.2 [a]

[a] samples were sonicated over night

APPENDIX VII

Pedogenic oxyhydroxide iron content

The ICP spectrometer was calibrated with a multi element standard and three other standards (2.5, 5, 10 ppm) made up from the extraction mixture.

Profile/ Lab. No.	Fe_d determination			Fe_o determination		
	Mass	Concentration	% Fe_d	Mass	Concentration	% Fe_o
T2						
1	0.5067	112.5	0.555	0.263	18.89	0.072
2	0.5017	68.28	0.340	0.2627	13.29	0.051
3	0.5272	174.2	0.826	0.2577	18.21	0.071
4	0.5296	451.9	2.133	0.2628	29.19	0.111
5	0.5212	270.4	1.297	0.252	53.47	0.212
6	0.5092	277.9	1.364	0.2512	20.37	0.081
7	0.5062	177.9	0.879	0.2687	7.222	0.027
8	0.5104	123.1	0.603	0.2565	12.1	0.047
T3						
9	0.5142	145	0.705	0.254	33.18	0.131
10	0.5034	284.1	1.411	0.2521	46.7	0.185
11	0.5153	421.8	2.046	0.2542	43.92	0.173
12	0.5102	516.8	2.532	0.261	47.67	0.183
13	0.5112	493.3	2.412	0.2532	29.29	0.116
14	0.5152	450.2	2.185	0.2606	31.77	0.122
15	0.53	480.8	2.268	0.2655	31.39	0.118
16	0.5234	420.3	2.008	0.2564	44.32	0.173
17	0.5256	455.5	2.167	0.2622	54.24	0.207
18	0.5071	438.3	2.161	0.250	51.86	0.207
T4						
19	0.5475	457.7	2.090	0.2613	30.13	0.115
20	0.5285	466.5	2.207	0.2557	30.73	0.120
21	0.5142	416.5	2.025	0.2573	28.69	0.112
22	0.505	363	1.797	0.2493	24.23	0.097
23	0.5036	338.1	1.678	0.2502	23.15	0.093
24	0.5325	379.7	1.783	0.2683	25.08	0.093
25	0.5355	356.6	1.665	0.2618	23.27	0.089
26	0.5579	379.8	1.702	0.269	25.21	0.094
27	0.5104	312.5	1.531	0.255	29.98	0.118
T5						
28	0.5365	258.7	1.205	0.2576	97.11	0.377
29	0.5383	256.1	1.189	0.28548	102.8	0.360
30	0.5261	254.5	1.209	0.2517	104.4	0.415
31	0.5077	228.3	1.124	0.254	90.86	0.358
32	0.5078	190	0.935	0.2516	75.65	0.301
33	0.5177	285.3	1.378	0.2515	66.81	0.266
34	0.5067	385.3	1.901	0.2539	169.8	0.669
35	0.5119	316.1	1.544	0.2498	130.3	0.522
36	0.5151	261.8	1.271	0.256	78.79	0.308
37	0.505	410.6	2.033	0.257	163.6	0.637
T6						
38	0.5243	149	0.710	0.2554	48.52	0.190
39	0.5162	160.2	0.776	0.2564	51.03	0.199
40	0.5157	327.2	1.586	0.2579	51.32	0.199
41	0.5133	140.2	0.683	0.2609	50.66	0.194
42	0.5308	307.5	1.448	0.2597	51.17	0.197

APPENDIX VII continued

Profile/ Lab. No.	Fe_d determination			Fe_o determination		
	Mass	Concentration	% Fe_d	Mass	Concentration	% Fe_o
43	0.5279	129	0.611	0.2661	48.71	0.183
44	0.5074	120.2	0.592	0.252	43.23	0.172
45	0.5086	124.6	0.612	0.2569	38.53	0.150
46	0.5095	109.1	0.535	0.2565	31.53	0.123
47	0.5211	120.2	0.577	0.2529	31.96	0.126
48	0.5259	127.9	0.608	0.2547	43.10	0.169
Duplicates						
3	0.5342	174.2	0.815	0.2695	18.77	0.070
15	0.5093	459.8	2.257	0.2515	29.53	0.117
29	0.520	244.5	1.175	0.2524	104.1	0.412
41	0.5142	137.6	0.669	0.2510	46.52	0.185
Blanks						
A			0.605			0.1376
B			0.00			0.1243
C			0.00			0.0472

APPENDIX VIII

Mineral Magnetic Properties

Lab. No.	χlf	χhf	χfd%	χarm	IRM 10 mT	IRM 20 mT	IRM 50 mT	IRM 100 mT	IRM 300 mT	SIRM 1000 mT
	$x10^{-8} m^3kg^{-1}$				$x10^{-5} Am^2kg^{-1}$					
T2										
1	13.7	12.7	7.1	51.9	6.5	20.1	47.1	58.6	76.9	86.8
2	14.4	13.5	6.3	40.9	7.1	21.6	45.0	74.3	92.6	101.2
3	23.6	22.6	4.0	79.5	9.0	26.8	53.2	73.3	79.8	90.7
4	28.4	27.5	3.2	77.5	8.0	21.6	43.9	52.3	58.8	69.1
5	20.5	18.8	8.3	45.8	11.5	33.3	51.8	58.1	63.7	71.7
6	25.5	24.5	3.7	63.5	12.0	26.2	46.2	54.0	63.2	63.5
7	25.2	24.3	3.8	88.6	12.2	26.2	49.4	64.1	73.4	79.8
8	22.5	21.6	4.3	51.5	8.8	19.4	37.3	47.3	55.2	60.4
	22.5	**21.6**	**4.3**	**51.5**	**8.8**	**19.4**	**37.3**	**47.3**	**55.2**	**60.4**
T3										
9	49.2	48.4	1.6	167.4	11.6	52.3	203.8	299.5	359.0	442.0
10	58.1	56.6	2.6	183.9	15.9	66.9	250.5	365.3	468.5	558.1
11	61.7	59.0	4.4	158.5	10.0	48.5	253.7	397.0	600.2	723.5
12	62.8	58.2	7.3	117.6	17.9	52.1	250.3	395.9	556.6	657.5
13	75.5	73.6	2.6	122.8	23.9	72.9	330.0	598.6	846.0	1059.7
14	93.5	92.1	1.5	132.4	30.6	92.7	454.7	774.7	1034.3	1328.2
15	106.9	105.9	0.9	177.3	31.0	104.2	626.8	1214.2	1721.3	1913.5
16	73.0	72.2	1.0	133.0	25.5	90.6	495.2	871.3	1163.1	1339.1
17	144.9	142.8	1.5	198.1	48.0	152.6	753.2	1323.4	1930.1	2304.1
18	103.6	101.5	2.0	149.7	30.2	100.4	574.2	1157.3	1678.0	2014.8
	103.2	**99.4**	**3.7**	**66.2**	**23.9**	**15.9**	**267.6**	**459.9**	**287.8**	**1174.3**
T4										
19	238.7	219.2	8.2	1008.3	174.3	629.3	1324.7	1499.5	1753.1	2007.7
20	171.4	158.9	7.3	567.9	41.2	209.6	911.6	1504.8	1933.2	2091.4
21	192.8	183.0	5.1	592.5	55.8	241.2	1165.4	2441.2	3449.2	3889.9
22	242.9	234.9	3.3	637.1	58.4	309.0	1682.0	4028.0	5810.0	6355.8
23	179.1	173.0	3.5	457.3	45.1	228.4	1270.3	2384.5	3572.2	3672.2
24	308.2	297.9	3.3	801.6	258.6	648.7	2270.9	4574.9	6564.5	7062.3
25	196.8	189.7	3.6	443.0	41.9	255.8	1365.1	2743.8	4175.5	4593.1
26	156.5	151.5	3.2	380.9	116.6	309.7	998.4	1759.4	2462.1	3593.2
27	124.2	118.1	4.9	291.7	25.9	138.1	724.4	1294.7	1979.6	2175.7
	119.6	**116.6**	**2.5**	**128.1**	**47.3**	**135.7**	**493.3**	**1026.3**	**1156.8**	**1221.1**
T5										
28	186.4	177.5	4.8	603.7	77.4	233.4	976.8	1465.9	1896.2	2231.8
29	213.6	205.9	3.6	584.7	100.6	292.4	1285.8	2032.7	2523.4	2954.1
30	171.3	165.5	3.4	354.4	91.1	250.8	877.8	1399.3	1728.8	2219.4
31	162.8	159.0	2.3	265.8	67.9	241.0	964.8	1464.5	1890.0	2197.7
32	262.2	258.8	1.3	400.5	112.9	393.1	1712.4	2518.0	3221.9	3728.5
33	167.0	163.8	1.9	225.0	64.5	234.8	1078.8	1598.4	2143.0	2515.4
34	142.2	139.3	2.0	232.6	63.2	229.0	1042.8	1706.8	2247.6	2593.1
35	147.5	145.6	1.3	190.3	76.8	204.6	896.4	1370.3	1882.4	2215.5
36	238.7	235.9	1.2	324.6	172.5	584.9	1361.9	2258.3	2647.8	3437.3
37	226.6	223.0	1.6	247.6	135.8	327.4	1322.7	1863.9	2368.2	2708.8
	183.8	**179.9**	**2.1**	**163.8**	**160.6**	**166.1**	**1154.8**	**130.3**	**349.5**	**578.3**

APPENDIX XVIII continued

Lab. No.	χlf	χhf	χfd%	χarm	IRM 10 mT	IRM 20 mT	IRM 50 mT	IRM 100 mT	IRM 300 mT	SIRM 1000 mT
	$x10^{-8}$ m^3kg^{-1}				$x10^{-5}$ Am^2kg^{-1}					
T6										
38	104.1	99.2	4.7	267.7	58.7	167.0	588.4	812.7	957.5	1120.0
39	106.8	102.2	4.3	287.2	63.4	181.3	641.9	869.9	986.6	1184.3
40	107.6	102.2	5.0	296.9	59.7	183.9	631.6	854.6	1029.9	1153.5
41	101.5	97.1	4.3	249.9	52.3	163.2	565.0	737.4	883.0	1049.7
42	92.8	89.2	3.9	213.1	49.7	151.7	528.9	710.2	858.0	987.5
43	83.2	80.3	3.5	187.3	62.4	166.6	543.9	734.7	815.0	991.9
44	85.9	83.5	2.8	204.7	51.1	129.9	540.3	691.7	866.1	1006.9
45	86.1	82.7	3.9	217.2	68.4	179.3	571.7	757.3	898.5	1037.2
46	94.4	91.9	2.6	217.6	59.6	193.0	647.1	882.4	1045.7	1208.2
47	119.6	117.6	1.6	245.4	69.0	227.4	774.8	1075.3	1297.0	1461.1
48	145.7	143.5	1.5	242.7	88.9	262.8	865.5	1203.7	1426.7	1606.2
	145.7	**143.5**	**1.5**	**242.7**	**88.9**	**262.8**	**865.5**	**1203.7**	**1426.7**	**1606.2**
Duplicates				[b]						
3				77.4		25.3			74.8	
				81.2		27.9			86.3	
15				176.4		102.2			1699.3	
				183.1		112.9			1712.3	
29				577.6		267.9			2526.3	
				586.3		296.3			2588.3	
41				247.4		160.9			880.6	
				248.5		179.3			923.2	

N.B. bold values indicate least altered material

[b] duplicates measured as ARM and converted to χarm

Lab. No.	SIRM/χ ($x10^3Am^{-1}$)	SIRM/ARM (Am^2kg^{-1})	χarm/SIRM ($x10^{-3}$mA)	Soft IRM ($x10^{-5}Am^2kg^{-1}$)	Hard IRM ($x10^{-5}Am^2kg^{-1}$)
T2					
1	6.3	26.2	0.60	20.1	9.87
2	7.0	38.9	0.40	21.6	8.56
3	3.8	17.9	0.88	26.8	10.88
4	2.4	14.0	1.12	21.6	10.28
5	3.5	24.6	0.64	33.3	7.96
6	2.5	15.7	1.00	26.2	0.31
7	3.2	14.2	1.11	26.2	6.42
8	2.7	18.4	0.85	19.4	5.21
	2.7	**18.4**	**0.85**	**19.4**	**5.21**
T3					
9	9.0	41.5	0.38	52.3	82.98
10	9.6	47.7	0.33	66.9	89.69
11	11.7	71.7	0.22	48.5	123.36
12	10.5	87.9	0.18	52.1	100.93
13	14.0	135.5	0.12	72.9	213.71
14	14.2	157.6	0.10	92.7	293.95
15	17.9	169.6	0.09	104.2	192.23
16	18.4	158.1	0.10	90.6	176.06
17	15.9	182.7	0.09	152.6	373.98
18	19.4	211.4	0.07	100.4	336.74
	11.4	**278.6**	**0.06**	**15.9**	**228.8**

APPENDIX VIII continued

Lab. No.	SIRM/χ ($x10^3 Am^{-1}$)	SIRM/ARM (Am^2kg^{-1})	χarm/SIRM ($x10^{-3}mA$)	Soft IRM ($x10^{-5}Am^2kg^{-1}$)	Hard IRM ($x10^{-5}Am^2kg^{-1}$)
T4					
19	8.4	31.3	0.50	629.3	254.62
20	12.2	57.9	0.27	209.6	158.15
21	20.2	103.1	0.15	241.2	440.72
22	26.2	156.7	0.10	309.0	545.86
23	20.5	126.1	0.12	228.4	100.05
24	22.9	138.4	0.11	648.7	497.84
25	23.3	162.9	0.10	255.8	417.61
26	23.0	148.2	0.11	309.7	1131.11
27	17.5	117.2	0.13	138.1	196.09
	10.2	**144.7**	**0.10**	**135.7**	**1027.4**
T5					
28	12.0	58.1	0.27	233.4	335.57
29	13.8	79.4	0.20	292.4	430.65
30	13.0	98.4	0.16	250.8	490.64
31	13.5	129.9	0.12	241.0	307.68
32	14.2	146.3	0.11	393.1	506.54
33	15.1	175.6	0.09	234.8	372.41
34	18.2	175.1	0.09	229.0	345.51
35	15.0	182.9	0.09	204.6	333.14
36	14.4	166.3	0.09	584.9	789.53
37	12.0	171.9	0.09	327.4	340.63
	3.2	**55.5**	**0.28**	**166.1**	**228.8**
T6					
38	10.8	65.7	0.24	167.0	162.51
39	11.1	64.8	0.24	181.3	197.63
40	10.7	61.0	0.26	183.9	123.59
41	10.3	66.0	0.24	163.2	166.71
42	10.6	72.8	0.22	151.7	129.54
43	11.9	83.2	0.19	166.6	176.90
44	11.7	77.3	0.20	129.9	140.83
45	12.1	75.0	0.21	179.3	138.70
46	12.8	87.2	0.18	193.0	162.50
47	12.2	93.5	0.17	227.4	164.09
48	11.0	104.0	0.15	262.8	179.50
	11.0	**104.0**	**0.15**	**262.8**	**179.5**

N.B. bold values indicate the least altered material

APPENDIX IX

Sedimentological classes

Grain size scales used for sedimentary logging in the field, based on Wentworth (1922) and Friedman & Sanders (1978).

Size	Class term
>256 mm	Boulder
64-256 mm	Cobble
4-64 mm	Pebble
2-4 mm	Granule
0.5-2 mm	Coarse sand
250-500 microns	Medium Sand
63-250 microns	Fine sand
2-63 microns	Silt
<2	Clay

APPENDIX X

Soil characteristics of the Tavignano River profiles

There was difficulty distinguishing many of the soil properties in the field, such as structure and texture as the profiles predominantly comprise matrix supported cobble and boulders beds. The horizon boundaries were also not very distinctive, so only a simple classification has been presented (from Soil Survey Division Staff, 1993).

Terrace T2

Horizon	Depth (cm)	Sedimentology	Average clast size (> 2 mm) and shape	Colour (Dry)	Notes
E	0-30	Fine sand		7.5YR5/6	Bleached layer
Bt1	30-60	Granule/pebble	4 mm Sub-angular	5YR4/6	
Bt2	60-75	Silt and fine sand		5YR5/8	Rubified
Bt3	75-110	Granule/pebble	4 mm Sub-angular	5YR5/8	Clay aggregates
Bt4	110-130	Coarse sand/fine gravel		5YR5/8	Indurated
Bt5	130-215	Sandy matrix with cobbles and boulders (30%)	50 mm Sub-rounded	5YR5/8	Mixture of sizes: 60% 30-50 mm 30% 50-150 mm 10% 150-300 mm
Bt6	215-415	Sandy gravel		7.5YR6/6	Upwards fining CL8 collected
Bw1	415-460	Sandy matrix with cobbles (40%)	80 mm Rounded	7.5YR5/6	Stratified, uniform size
Bw2	460-500	Fine-medium sand		7.5YR6/6	
Bw3	500-600	Sand/gravel matrix with cobbles and boulders (30%)	200 mm Sub-rounded	7.5YR6/6	

Terrace T3

Horizon	Depth (cm)	Sedimentology	Average clast size (> 2mm) and shape	Colour (Dry)	Notes
Ap	0-30 mm	Medium sand		7.5YR6/6	+ Colluvial material?
Bt1	30-200	Matrix supported cobbles (20%)	100 mm Angular	5YR4/6	
Bt2	200-375	Cobbles and pebbles within a sandy matrix (30%)	60 mm Sub-angular	5YR4/4	Imbrication, upwards fining
Bw1	375-640	Matrix supported cobbles (5%)	70 mm Rounded	7.5YR4/6	Upwards fining
Bw2	640-720	Granules and pebbles in coarse sand (30%)	4 mm Sub-angular	7.5YR4/6	Upwards fining
C1	720-750	Medium/fine sand		7.5YR6/6	C1.2 collected
C2	750-900	Cobbles and boulders in a sand/fine gravel matrix (15%)	120 mm Sub-rounded	7.5YR6/6	Slight imbrication

APPENDIX X continued
Terrace T4

Horizon	Depth (cm)	Sedimentology	Average clast size (>2 mm) and shape	Colour (Dry)	Notes
Bt1	0-95	Coarse gravels supported in a silt matrix (20%)	50 mm Sub-rounded	5YR6/8	Slightly weathered
Bt2	95-175	Gravel matrix, even mixture of cobbles and boulders (30%)	150 mm Rounded	5YR6/6	Clast supported in places
Cu	175-195	Silt/sand lens		7.5YR6/3	Varies laterally 25-30 cm in thickness
R	195-300	Bedrock			Schist

Terrace T5

Horizon	Depth (cm)	Sedimentology	Average clast size (> 2 mm) and shape	Colour (Dry)	Notes
	0-60	Coarse sand, fine gravel matrix with pebbles and cobbles (10%)	80 mm Sub-angular	7.5YR4/2	
Bt	60-150	Coarse sand matrix with cobbles (20%)	100 mm Sub-rounded	7.5YR5/6	Slight upwards fining
Bw	150-190	Granules in a sand/silt matrix (5%)	3 mm Sub-angular	7.5YR4/2	
Cu1	190-225	Coarse sand/fine gravel matrix with cobbles and boulders (20%)	250 mm Angular	7.5YR5/2	
Cu2	225-275	Granules in a silt matrix (30%)	4 mm Angular	7.5YR5/2	Stratified
Cu3	275-400	Cobbles and boulders in sandy matrix (15%)	150 mm Rounded	7.5YR5/2	Imbricated

Terrace T6 (No horizons have developed)

Horizon	Depth (cm)	Sedimentology	Average clast size (> 2mm) and shape	Colour (Dry)	Notes
	0-24	Silt with some fine sand		10YR6/3	Stratified
	24-43	Silt with some sand		7.5YR6/4	
	43-55	Silt with some sand		7.5YR6/3	
	55-76	Silt with trace amounts of sand		7.5YR6/2	Stratified
	76-92	Silt and fine sand		10YR6/2	Stratified
	92-105	Silty sand		7.5YR7/2	
	105-120	Silty fine sand		10YR6/1	
	120-133	Silt with some fine sand		10YR6/2	Stratified
	133-147	Silt with some sand		10YR6/1	Stratified
	147-156	Fine/medium sand with some silt		10YR6/1	
	156-170	Sandy gravel member	< 4mm	10YR6/2	

APPENDIX XI

Quartz Optical Stimulated Luminescence dating

Conducted at the Sheffield Centre for International Drylands (SCIDR) under the supervision of Dr Mark Bateman

1. **Preparation**
2. **Sieving**
3. **Heavy mineral separation**
4. **Etching with HF**

1. Preparation

- The sediment at the ends of the tube were discarded (~1 inch) to ensure that the analysed material is that which has not been exposed to light during sampling.
- The sample was extruded from the tube (~100g, about up to 150 ml mark on a 300 ml beaker) and placed in a labelled beaker.
- Sample was pre treated with hydrochloric acid (1 M HCL) until all reaction ceased. This ensured that all carbonates had dissolved.
- The sample was washed and the fines were discaded (stir and settle for 30 section and decant supernatant)
- Sample was pre treated with hydrogen peroxide (H_2O_2, 40%) to remove all the organic matter present in the sample.
- The sample was washed.

2. Sieving

- Sieved the sample under running water so that particles between 90 and 250 μm were retained.
- The sample was sieved through a nest to obtain the fraction with the smallest size variation but the maximum sample. Samples CL2, 7 were sieved through 90-180 and fraction retained. CL4, 6 and 8 were sieved through 90-180 and then 90-125. (Particle size analysis on a dry sample (<1 mm) was undertaken prior to the sieving to gain an idea of the optimum fraction to sieve).
- The sieves were cleaned thoroughly in an ultrasonic bath to ensure no cross contamination.
- The samples were oven dried (30°C).

3. Heavy mineral separation

- Heavy mineral separation was conducted. Poured ~150 ml sodium polytungstate (Na pt) in a measuring cylinder and with deionised water and reduced the density / specific gravity to 2.7 g/cm^3 (quartz is ~2.64).
- Poured the Na pt equally into boiling tubes (4) and added the OSL sample.
- Placed in an ultrasonic bath for 3-4 mins to mix well
- Centrifuged for 8 mins at 1200 rpm to separate the light and heavy minerals.
- Samples had a relatively large proportion of heavy minerals. CL6 and CL8 separated well and had a greater lighter mineral fraction than CL2 and CL4.
- Froze Na pt around the heavy minerals (those that sank to the bottom of the tube) with liquid nitrogen – frozen layer between the heavy and the light fractions.
- Poured off the unfrozen light fraction into labelled buchner funnel filled with fast filter paper (no. 1) and with the aid of a vaccum pump, sucked Na pt off.
- Samples were washed thoroughly with water through the buchner funnel. Meths was used to ensure all Na pt residues were rinsed off (IMS goes white if Na pt still present).
- All Na pt was recycled.
- The samples were placed in the oven overnight to dry.

4. Etching with HF

- The dried samples were taken off the filter paper and placed back in the beakers. Solid white Na pt specks visible in the sample were removed to minimise the reaction with the hydrofluoric acid.
- Dispensed 30 ml of hydrofluoric acid into each beaker and left to etch for an hour.
- The samples were then diluted with deionised water and rinsed thoroughly, 3 or 4 times.
- Hydrochloric acid was then pored over the sample in the beakers and left for an hour.
- Sample were rinsed and dried in the often
- Samples were then dry sieved through a 90 μm sieve and the >90 retained.

APPENDIX XII

Soil Moisture for OSL dating

The samples were weighed then placed in a 110°C oven for 24 hours and reweighed.

Sample	Crucible	Crucible weight	Wet weight	Total	Dry weight	Loss	Wet weight (%)
CL1	37A	123.44	57.06	176.97	53.53	3.53	6.186
CL2	38A	115.63	72.08	184.19	68.56	3.52	4.883
CL3	36A	104.18	75.86	177.19	73.01	2.85	3.757
CL4	35A	111.59	80.78	187.66	76.07	4.71	5.831
CL5	34A	98.99	85.78	179.67	80.68	5.10	5.945
CL6	30A	111.12	90.07	197.33	86.21	3.86	4.286
CL7	12A	114.45	98.52	204.92	90.47	8.05	8.171
CL8	19A	106.59	77.09	178.20	71.61	5.48	7.109

APPENDIX XIII

OSL analysis

CL2	Shfd01001		
Aliquot	Nat. Acq OSL (cts/s)	Palaeodose (Gy)	Error
1	8702	73.48	8.03
2	10982	99.36	12.35
3	3272	73.99	10.04
4	4725	76.51	10.07
5	4710	88.78	15.54
6	12567	70.94	5.1
7	16535	94.32	7.48
8	3877	79.47	14.08
9	2935	57.78	9.07
10	2650	46.89	6.33
11	5377	62.08	7.37
12	14555	67.28	5.04
13	3147	54.09	7.33
14	4595	59.60	6.86

CL4	Shfd01002		
Aliquot	Nat. Acq OSL (cts/s)	Palaeodose (Gy)	Error
1	4732	18.48	1.51
2	4722	18.09	1.1
3	6245	18.72	1.14
4	5252	18.72	1.11
5	5280	18.52	1.06
6	5122	16.67	1.5
7	5690	20.75	1.12
8	8067	16.78	1.57
9	4747	18.86	1.27
10	5575	18.94	1.25
11	5822	18.19	1.3
12	6420	18.97	1.03
13	6347	17.98	1.31
14	4567	21.31	1.73
15	5870	21.24	1.22
16	4180	20.22	1.73
17	4550	19.13	1.31

APPENDIX XII continued

CL6	Shfd01003		
Aliquot	Nat. Acq OSL (cts/s)	Palaeodose (Gy)	Error
1	2872	13.02	151
2	1912	12.65	1.1
3	1352	12.65	1.14
4	1370	12.65	1.11
5	3687	9.61	1.06
6	2307	18.66	1.5
7	1100	14.24	1.12
8	2487	11.22	1.57
9	2525	14.45	1.27
10	3057	18.03	1.25

CL8	Shfd01004		
Aliquot	Nat. Acq OSL (cts/s)	Palaeodose (Gy)	Error
1	81387	114.79	14.69
2	112692	102.67	6.93
3	122155	109.94	8.63
4	73755	79.34	7.72
5	129930	93.19	5.94
6	80937	97	9.76
7	102955	91.57	5.91
8	144835	181.18	33.25
9	103942	91.97	4.84
10	133160	84.18	4.19
11	127620	94.24	5.08
12	122100	85.03	4.18
13	104547	83.47	4.86
14	118712	115.59	10.44
15	98795	99.36	8.92
16	99682	93.66	10.22
17	231630	92.8	3.24
18	107765	110.26	9.16
19	107047	89.45	14.74
20	85895	108.11	5.96
21	98245	99.12	6.88
22	81702	73.44	7.34
23	69335	66.16	10.92
24	92715	87.73	12.24
25	101002	71.19	3.9
26	151500	87.07	6.81
27	126227	80.46	5.56
28	109365	77.94	4.5
29	112947	90.25	6.95
30	106307	63.37	3.37
31	113507	68.41	4.43
32	106792	88.66	3.97
33	92660	89.19	7.81

APPENDIX XIV

Constructing a lichen age-size curve

Five of the largest lichens colonising the substrate surface (gravestone) were measured to obtain an average. In the situation whereby there were less than five suitable lichens to measure, the average of those recorded were taken (>3).

Rhizocarpon geographicum

Location	Date	Lichen size (mm)	Average	Standard deviation
Belgodore	1900	38, 38, 38, 37, 34	37.00	1.73
	1975	14, 13, 12, 10, 10	11.80	1.79
Calenzana	1941	18, 18, 18, 17, 17	17.60	0.55
	1942	16, 15, 14	15.00	1.00
Calvi	1908	34, 31, 29, 28, 23	29.00	4.06
	1912	28, 26, 26, 26, 24	26.00	1.41
	1933	15, 14, 14, 14, 13	14.00	0.71
	1975	10, 9.5, 9, 9, 9	9.30	0.45
	1976	14, 13, 12.5, 11, 11	12.30	1.30
Occhitana	1921	27, 23, 20	23.33	3.51
Spelatona	1953	16, 15, 15, 14, 13	14.60	1.14
St. P. Chapel	1948	20, 19, 19, 17	18.75	1.26
	1974	11.5, 11.5, 9, 9	10.25	1.44
Ville de Paraso	1908	26, 26, 25, 24	25.25	0.96
	1935	20, 19, 19, 19, 18	19.00	0.71

Lecanora rupicola

Location	Date	Lichen size (mm)	Average	Standard deviation
Algajola	1961	55, 55, 50, 50, 45	51.00	4.18
Belgadore	1963	48, 47, 44, 43, 41	44.60	2.88
Calenzana	1925	63, 51	57.00	8.49
	1928	69, 62, 55, 50, 48	56.80	8.70
	1934	65, 61, 59, 57, 55	59.40	3.85
	1945	41, 36, 34	37.00	3.61
	1947	55, 50, 40	48.33	7.64
	1973	33, 32, 32, 32, 31	32.00	0.71
	1981	19, 18, 18, 17, 16	17.60	1.14
Calvi	1891	107, 103, 103, 99	103.00	3.27
	1910	129, 120, 115, 96, 90	110.00	16.45
	1954	52, 51, 50, 48	50.25	1.71
	1960	47, 46, 46, 43, 35	43.40	4.93
	1975	23, 21, 21, 19, 19	20.60	1.67
	1978	25, 22, 22, 21.5, 21	22.30	1.57
Ille Rousse	1929	96, 86, 86, 81, 72	84.20	8.73
	1941	67, 64, 63, 62, 57	62.60	3.65
	1965	40, 40, 39, 39, 37	39.00	1.22
	1966	42, 39, 36, 34, 34	37.00	3.46
	1980	22, 21, 20, 19, 19	20.20	1.30
Moncale	1959	52, 51, 51, 50	51.00	0.82
	1976	35, 33, 32, 30, 29	31.80	2.39
Spelatona	1946	62, 53, 50, 49, 47	52.20	5.89
	1953	57, 55, 51, 50, 50	52.60	3.21
	1983	29, 21, 21, 20, 20	22.20	4.19
Zilla	1978	26, 24, 21, 21, 20	22.40	2.51

APPENDIX XV

Figarella River boulder berm lichen measurements

The five largest lichens colonising the coarse flood deposits in the Figarella catchment (Figure 6.9)

Site	Lichen size (mm)	Average	Standard deviation	Age of substrate [a] (yrs)
A	49, 48, 43, 43, 41	44.80	3.49	156.66
B	49, 46, 46, 45, 38	44.80	4.09	156.66
C	46, 33, 32, 28, 27	33.20	7.60	113.37
D	25, 24, 24, 23 ,23	23.80	0.84	78.30
E	33, 33, 32, 31, 29	31.60	1.67	107.40
F	23, 21, 21, 20, 20	21.00	1.26	67.85
G	53, 49, 46, 46, 45	47.80	3.27	167.85
	172, 168, 160, 154,154	**161.60**	**8.17**	**169.19**
H	24, 22, 22, 22, 21	22.20	1.10	72.33
I	38, 37, 34, 33, 31	34.60	2.88	118.60
	119, 110, 110, 109, 109	**111.40**	**6.36**	**115.16**
J	38, 37, 35, 33, 30	34.60	3.21	118.60
K	65, 61, 60, 60, 58	60.80	2.65	216.36
L	52, 49, 48, 42, 37	45.60	6.02	159.64
	162, 152, 148	**154.0**	**7.21**	**165.75**
M	58, 51, 50, 46, 45	50.00	5.15	176.06
N	38, 38, 36, 36, 33	36.20	2.05	124.57
O	42, 41, 40, 39, 38	40.00	1.58	138.75
P	46, 39, 38, 37, 32	38.40	5.03	132.78
Q	49, 48, 41, 40, 36	42.80	5.54	149.19
R	74, 68, 66, 65, 61	68.25	4.03	244.16
S	140, 125, 113, 110, 100	117.60	15.37	428.30
T	39, 38, 36, 35, 35	36.60	1.82	126.06
U	41, 40, 39, 39, 38	39.60	0.89	137.25
V	65, 63, 62, 60, 58	61.60	2.70	219.34
W	44, 42, 37, 35, 34	38.40	4.39	132.78
X	38, 36, 35, 35, 35	35.80	1.41	123.08
Y	48, 46, 44, 42, 40	44.00	3.16	153.67
Z	190, 110, 99, 80, 78	111.40	45.92	405.16
AA	**275, 168, 141**	**194.67**	**70.87**	**204.78**

[a] Calculated using the size-age relationship shown in Figure 6.7, 0.268 $mmyr^{-1}$ for RZ and 0.9291 $mmyr^{-1}$ for **LR** (in bold).

APPENDIX XVI

Recent floods in the western Mediterranean

Source: http://www.inm.es/MEDEX/Data/Selection_cases.htm

Date	Countries affected	Severe weather: SW = strong wind HP = heavy ppt	Societal impacts
4-6 Nov. 1997	Portugal (PO) (S. Alentejo) Spain (SP) France (FR) (Med. Coast, Cevennes, Alps)	HP, SW (FR) 287 mm/24 h (S. Alps) 500 mm/24 h (Cevennes) 150 mm/24 h (SP) 80 mm/6 hr (PO) Wind > 35 m/s (FR)	Floods (FR, SP, PO) Casualties (FR, SP, PO) Material losses. 4
24-26 Mar. 1998	Tunisia (Northeast) (TU) Greece (GR)	SW, HP Wind 30 m/s (TU) (Athens & W. GR) 140 mm/24 h (GR) Depression over Corsica moved east	Flood (GR) Disruption of Athens airport, electric power poles destruction.
20-22 Sep. 1999	Portugal (Northwest) Italy (IT)	HP > 160 mm/24 h (PO, IT)	
6-9 Nov. 1999	Spain (West Med., Bal. Isl) Italy Croatia (CR) Greece (E. contin.)	SW, HP Severe Bora (45 m/s) strong winds West Med. Strong lee cyclone, heavy ppt (GR) 70-90 mm/24 h IT and	Floods (GR, IT) Problems with electric power system (CR), serious traffic interruptions (CR), sig. wave height ~ 7.5 m West Med., risk for navigation, railway interruptions (IT). Storm surge, N. Adriatic.
11-14 Nov. 1999	Spain France Italy (Sardinia)	HP, SW (FR) 197 mm/24 h (SP) 600 mm/36 h (FR, Lezignan) 100 mm/1 h and 376 mm/48 h (Sardinia) Continued heavy ppt and windstorm in S FR	Serious floods (Sardinia, FR) 30 casualties (FR) 1000 M Euros loss (FR)
21-26 Oct. 2000	Spain (Catal., SE of Aragon, N. Valencian comm..)	HP 600 mm/48 h >300 mm/24 h (Catal. Upper level cutoff cyclone, surface cyclone SE of Iberian Peninsula)	Serious flash floods, 8 casualties in Catal. and landslides in other parts of Spain. Many building and roads affected and damaged.
5-6 Nov. 2000	France Italy	SW, HP (FR, IT) 150 mm/24 h (Monte Carlo) V. strong winds near coasts	Floods 7.5 m swell (FR coast) Material losses
25-31 Dec. 2000	Spain (Catal.) Italy (Sardinia) Tunisia (TU)	SW 50 m/s (Kasserine, TU) > 35 m/s (SP) 7 days of rain (IT) 3 cyclones, 1 deep cyclone	Local floods, intense wind and rough seas (Sardinia) 8 casualties (avalanches in the Pyrenees) Building damage (TU)

APPENDIX XVII

Five day storm events in Barcelona

53 five day storm events (> mean + 1 standard deviation) between 1900 and 1985 (422 in total). Data provided by Burgueño (1980).

Date	Precipitation total (mm)	Date	Precipitation total (mm)
January 19, 1903	83.9	November 5, 1962	164.1
September 28, 1907	83.4	November 6, 1962	164.5
September 29, 1907	85.4	November 7, 1962	107.41
May 8, 1915	89.0	January 18, 1963	90.1
May 9, 1915	84.8	January 19, 1963	90.3
April 6, 1916	83.15	January 20, 1963	100.6
February 7, 1917	104.8	September 13, 1963	168.6
February 8, 1917	108.7	September 14, 1963	135.4
February 9, 1917	90.6	September 15, 1963	110.2
October 23, 1918	100.8	April 4, 1969	117.6
February 23, 1921	113.45	April 5, 1969	138.9
November 26, 1921	146.7	April 6, 1969	148.8
November 27, 1921	142.4	April 7, 1969	86.7
March 13, 1931	153.7	October 20, 1969	127
March 14, 1931	145.0	October 9, 1970	83.8
December 16, 1932	82.5	October 10, 1970	85.1
November 3, 1934	101.91	December 4, 1971	149.1
November 4, 1934	102.71	December 5, 1971	149
November 5, 1934	100.61	May 18, 1977	99.8
October 5, 1937	128.0	February 17, 1982	144.4
December 14, 1943	111.9	February 18, 1982	100.5
January 14, 1945	94.6	November 7, 1983	196.8
October 3, 1951	246.0	November 8, 1983	233.5
October 4, 1951	217.9	November 16, 1983	91.4
September 26, 1953	157.7	March 15, 1984	131.3
May 16, 1954	107.8	May 16, 1984	82.1
May 17, 1954	104.4		